The regulation of gene expression in sulphate reducing bacteria

by

Ian Thomas Cadby



A thesis submitted to the University of Birmingham
for the degree of DOCTOR OF PHILOSOPHY

School of Biosciences
College of Life and Environmental Sciences
University of Birmingham
January 2014

UNIVERSITY OF
BIRMINGHAM

University of Birmingham Research Archive

e-theses repository

This unpublished thesis/dissertation is copyright of the author and/or third parties. The intellectual property rights of the author or third parties in respect of this work are as defined by The Copyright Designs and Patents Act 1988 or as modified by any successor legislation.

Any use made of information contained in this thesis/dissertation must be in accordance with that legislation and must be properly acknowledged. Further distribution or reproduction in any format is prohibited without the permission of the copyright holder.

Acknowledgements

Firstly I must thank my supervisor Prof Jeff Cole for accepting me into his group and for his guidance throughout the project. I must thank Dr Angeliki Marietou for her assistance during the early stages of my project. I would also like to thank Prof Steve Busby for helping direct my research, as well as my current boss Dr Andy Lovering for his extreme patience!

I feel honoured to have known the late great Prof Harry Smith. His cheerful disposition and encouragement (not to mention post lab meeting ales) were very, very welcome – particularly during some of the more difficult times. Special thanks go to Dr Dave Lee, Dr Doug Browning and Dr Kerry Hollands for their willingness to share their knowledge and expertise. I would also like to express my gratitude to: Dr Derrick Squire; Dr David Chismon; Dr Mohammed Shahidul Islam; Dr Jack Bryant; Dr Laura Rowley; Dr Patchuarawin Ruanto; Dr Sudesh Mohan; Dr Yanina Sevastsyanovich; Dr Amanda Hopper; Dr Claire Wingrove; Lenny Zaffaroni; Dr Masha Tutukina and Matthew Faulkner, thank you for your help, friendship and encouragement!

I consider myself very lucky to have had a large family cheering me on throughout my PhD. Thanks go to Ma and Pops, all the Cadby clan and to the Thomas family for their love, support and unwavering faith in me.

Finally, I would like to acknowledge those closest to me during the four years in lab G7. I can't think of a better person to have shared the time with than my special buddy Dr Jack Bryant, who started his PhD at the same time as me. Jack and I would celebrate success or commiserate failure with equal gusto at the staff bar – a tradition that I am happy to say has outlived our PhD years! My close friends Dr Claire Wingrove and Dr Amanda Hopper welcomed me into the Cole lab and helped me through some of the tougher times – usually by providing a warm smile and lending an ear (thanks Claire) or by poor quality singing (thanks Amanda). My oldest friend Dr Oliver Durrant was always a phone call away and, having been through the PhD experience some years ahead of me, always had an ear for my worries and helpful advice for my problems.

Last (and most importantly) I want to thank my wife Hannah. She has sat through presentation rehearsals, proof-read reports and, particularly during my final year, been a "science widow" (partners of PhD students will know what this means) - all to support me. If my viva performance were a true reflection of the love and encouragement she has given throughout the PhD then there would be no corrections.

Abstract

Desulfovibrio desulfuricans ATCC27774 can use both nitrate and sulphate as terminal electron acceptors for growth. Contrary to expectations, the less favourable terminal electron acceptor, sulphate, is utilised preferentially. It has been proposed that the *nap* gene cluster of *D. desulfuricans*, which encodes nitrate reduction, is regulated at the transcription level by both sulphate repression and nitrate induction. Transcription factors of the CRP/FNR family have been implicated in this regulation.

At the start of this study a bioinformatic analysis identified five CRP-homologues in *D. desulfuricans*, two of which, HcpR and HcpR2, were predicted to bind discrete regulatory motifs and influence the transcription of *nap*, *hcpR* and the gene for the hybrid cluster protein, *hcp*. Physiological and qRT-PCR experiments revealed that expression of *hcpR* is induced in the presence of nitrite whereas expression of *hcpR2* is constitutive. Furthermore, tolerance to nitrosative stress can be pre-induced by exposure to nitrite.

In electromobility shift and footprinting assays, HcpR bound to CRP-like DNA targets upstream of the *nap* and *hcpR* operons: HcpR2 bound to a different target upstream of *hcp*. HcpR was shown to heterolgously affect transcription at CRP-regulated promoters in an *Escherichia coli* host. The pET expression system was used to overproduce HcpR, the recombinant protein was purified and western analysis with a rabbit anti-HcpR antiserum revealed that nitric oxide is the inducer of HcpR synthesis. Once induced, significant levels of HcpR persisted in the absence of effector for many generations.

The results suggest that the primary function of HcpR is auto-regulation of the *hcpR* operon. This transcription unit includes genes similar to *nimA* and *wrbA* and their expression is believed to be essential for protecting *D. desulfuricans* against nitrosative stress. Contrary to the predictions of the bioinformatic analysis, expression of *nap* did not correlate with *hcpR* levels. An alternative hypothesis is proposed in which *nap* and *nrf* are primarily regulated by a sigma-54-dependent mechanism.

Table of contents

Abstract i
Table of contents ii
List of figures vi
List of tables ix
List of abbreviations x
Chapter 1: Introduction 1
1.1 Introduction 2
1.2 Sulphate reducing prokaryotes 3
1.3 The sulphate reduction pathway 6
Overview of the sulphate reduction pathway 6
Activation of sulphate by Sat 7
The reduction of APS to sulphite 8
The reduction of sulphite to sulphide 9
1.4 The electron transport chain of SRB 10
Electron transport to the sulphate reduction pathway 10
Auxiliary electron transfer proteins in SRB 13
1.5 Production of ATP by SRB 14
Substrate level phosphorylation 16
Formate cycling 16
Hydrogen cycling 17
1.6 Nitrate reduction by *E. coli* 17
1.7 Periplasmic nitrate reductase 19
1.8 Nitrite reductases 22
1.9 Nitric oxide and reactive nitrogen species 25
1.10 Protection against nitrosative stress 26
1.11 Protection against oxidative stress 29
1.12 The nitrate-sulphate diauxie of *D. desulfuricans* 31
1.13 The paradigm of diauxie: carbon source utilisation by *Escherichia coli* 33
1.14 Transcription regulation by CRP 36
CRP: regulation by an allosteric effector 36
The DNA targets of CRP 41
Activation and repression of transcription by CRP 41
The *Escherichia coli* CRP regulon 44
Adaption to anaerobic growth by FNR 45
1.15 Transcription regulators implicated in nitrate-nitrite dependent growth of *E. coli.* 47
1.16 Aims and objectives 50

Chapter 2: Materials and Methods 52
2.1 Growth of bacteria 53
Growth of *D. desulfuricans* 53
Growth of *E. coli* 54
Plasmids 54
Preparation of competent cells 58
Transformation of *E. coli* with plasmid DNA 58
Preparation of nitric oxide saturated water 59
2.2 Purification of DNA 59
Purification of gDNA 59
Purification of plasmid DNA 59
Purification of PCR products and linear DNA fragments 61
Phenol-chloroform extraction and ethanol precipitation of DNA 61
2.3 Analysis and manipulation of DNA 62
Polymerase Chain Reaction (PCR) 62
DNA restriction digests, modifications and ligations 64
Agarose gel electrophoresis of DNA 64
Polyacrylamide gel electrophoresis of DNA 65
Cloning of DNA fragments into vectors 65
DNA Sequencing 66
2.4 RNA techniques 66
Purification of RNA 66
Reverse transcription reactions (RT-PCR) 67
Quantitative PCR (qPCR) 67
Primers for qPCR 68
2.5 Protein techniques 68
SDS-PAGE of protein samples 68
Protein purification 71
Polyclonal anti-HcpR antibody production 72
Measuring HcpR levels using western blot analysis 72
TPTZ assay 74
mPEG-mal labelling of proteins 74
2.6 DNA binding assays 75
Electroelution of DNA 75
Electromobility shift assays (EMSAs) 75
DNaseI footprinting assays 77
2.7 β-galactosidase assays 78
2.8 Measurements of terminal electron acceptor concentrations 79
Quantification of terminal electron acceptors in growth medium 79
Nitrite reductase activity assay 81
2.9 Computational techniques 82

P values 82
Bioinformatics 82
Chapter 3: Results: An *in silico* analysis of nitrate metabolism and the CRP family proteins of *Desulfovibrio desulfuricans* 83
3.1 Introduction 84
3.2 Conserved *nap* gene clusters and their regulatory motifs in *Desulfovibrio* species 85
3.3 Identification of CRP/FNR family proteins of *D. desulfuricans* 89
3.4 CooA proteins in *Desulfovibrio* 93
3.5 Two unidentified CRP/FNR homologues from *D. desulfuricans* 99
Ddes_1411, Ddes_2092 and their homologues 99
Potential DNA targets for Ddes_1411 and Ddes_2092-like regulators 104
3.6 HcpR from *D. desulfuricans* 109
DNA recognition by HcpR 109
The *D. desulfuricans* HcpR locus 112
The HcpR regulon 114
Modulation of HcpR activity 121
3.7 Regulation of nitrosative stress response in *D. desulfuricans* by HcpR2 124
HcpR2 is distinct from the HcpR proteins of other *Desulfovibrio* species 124
DNA recognition by HcpR2 127
The HcpR2 regulon 130
3.8 Genes potentially related to nitrate-nitrite reduction and nitrosative stress in *D. desulfuricans* 132
3.9 Discussion 136
Chapter 4: Results: Growth and gene expression profiles of *D. desulfuricans* in response to different terminal electron acceptors 145
4.1 Introduction 146
4.2 Growth of *D. desulfuricans* in the presence of individual terminal electron acceptors 147
4.3 Terminal electron acceptor selection by *D. desulfuricans* 150
The effects of sulphate and sulphite upon nitrate and nitrite reduction 150
The effects of nitrite and nitrate upon reduction of sulphate and sulphite 153
4.4 Induction of nitrite reduction and resistance to nitrosative stress 155
4.5 Transcription of the nitrate-nitrite and sulphate-sulphite pathways 157
Expression of *napC* and *nrfA* in response to different terminal electron acceptors 159
Expression of *sat*, *apsB*, *dsrA*, *qmoB* and *dsrJ* in response to different terminal electron acceptors 161
4.6 Transcript abundances of *hcpR*, *hcpR2* and key regulon members 162
Differential expression of *hcpR* and *hcpR2* 162
The expression of cytochromes and *hcp* in response to different terminal electron acceptors 165
4.7 Discussion 168
Sulphate and sulphite reduction by *D. desulfuricans* 168

Nitrite reduction by *D. desulfuricans* 170
Nitrate reduction by *D. desulfuricans* 172
Nitrate and nitrite responsive genes *ssc* and *hcp* 173
Regulation of *hcpR* and *hcpR2* 174
Chapter 5: Results: Characterisation of HcpR and HcpR2 177
5.1 Introduction 178
5.2 Overexpression and purification of HcpR 179
5.3 DNA binding of HcpR at the *nap* promoter 183
5.4 DNA binding by HcpR in the presence of effector molecules 185
5.5 Identification of HcpR DNA target sites 189
5.6 The influence of HcpR on transcription in *E. coli* 192
5.7 HcpR expression in response to terminal electron acceptors 201
5.8 The effect of exogenous nitric oxide upon HcpR expression 206
5.9 The cysteines of HcpR: potential nitric oxide sensors 210
5.10 The transcriptional partners of *hcpR* 214
5.11 Differential expression at the *hcp* locus 219
5.12 Overexpression and purification of HcpR2 223
5.13 Sequence specific DNA binding by HcpR2 228
5.14 Discussion 230
Chapter 6: Discussion: The regulation of gene expression in response to terminal electron acceptors and nitrosative stress 235
6.1 Introduction 236
6.2 HcpR proteins: insights from other studies 236
6.3 An assessment of DNA binding by HcpR 239
6.4 Potential roles for the transcriptional partners of *hcpR* 243
6.5 Potential roles for the transcriptional partner of *hcp*: *ylbA* 246
6.6 Auto-regulation of the *hcpR* operon 247
6.7 Regulation of *hcp* by HcpR2 252
6.8 Regulation of genes responsible for sulphate reduction 256
6.9 Regulation of genes responsible for nitrate reduction 257
A model of *nap* regulation by HcpR 257
An alternative model of *nap* regulation by sigma-54 259
Regulation of nitrite reductase 267
6.9 HcpR proteins and the environment 268
6.10 Final conclusions 271
References 273

List of figures

Figure 1.1: The flow of electrons from the periplasm to the sulphate reduction pathway via membrane associated respiratory complexes 12
Figure 1.2: ATP production in Gram-negative SRB by substrate-level phosphoryation, formate cycling and hydrogen cycling 15
Figure 1.3: Models of electron flow to NapA in *D. desulfuricans.* 24
Figure 1.4: Overview of the regulation of adenylate cyclase activity and the uptake of non-PTS sugars by the PEP-PTS. 35
Figure 1.5: The crystal structure of the cAMP-CRP-DNA complex 38
Figure 1.6: The binding of the allosteric effector cAMP to CRP causes a conformational change 40
Figure 1.7: Overview of the regulation of transcription by CRP 42
Figure 3.1 Nap gene clusters of *Desulfovibrio* and related bacteria 86
Figure 3.2 CRP-like sites upstream of the *nap* gene clusters of *Desulfovibrio* and related bacteria 88
Figure 3.3: Generalised work scheme for *in silico* analysis of CRP/FNR homologues 92
Figure 3.4: The DNA recognition helices of *Desulfovibrio* CooA proteins and *Rhodospirillum rubrum* CooA, and the genomic context of *Desulfovibrio* CooA proteins 95
Figure 3.5: Multiple alignment of CooA proteins 98
Figure 3.6: The genomic contexts of the genes encoding Ddes_2092, Ddes_1411 and homologues 102
Figure 3.7: The DNA recognition helices and putative DNA binding sites of Ddes_2092, Ddes_1411 and their homologues 106
Figure 3.8: The DNA recognition helices of *D. desulfuricans* HcpR, *E. coli* CRP and FNR 111
Figure 3.9: Comparison of the *hcpR* loci of *D. vulgaris*, *Desulfovibrio* G20 and *D. desulfuricans* 113
Figure 3.10: Genomic context of *hcpR* and *hcp* in the sulphate reducing bacteria *Desulfovibrio* sp. 3_1_syn3, *Desulfovibrio* sp. 6_1_46AFAA and *Desulfovibrio desulfuricans* 120
Figure 3.11: Multiple alignment of selected HcpR proteins 123
Figure 3.12: Hypothetical three-dimensional structure of HcpR from *Desulfovibrio desulfuricans* 125
Figure 3.13: Identification of a putative consensus DNA binding site for HcpR2-type CRP regulators 129
Figure 3.14: the putative HcpR2 regulon of *D. desulfuricans* 131
Figure 3.15: The promoter proximal DNA sequences of *sat* and *aps* of *D. desulfuricans* ... 139
Figure 3.16: The promoter proximal DNA sequences of *nrf* and *nap* of *D. desulfuricans* ... 140
Figure 3.17: The promoter proximal DNA sequences of Ddes_1825 and Ddes_1828 of *D. desulfuricans* 143

Figure 4.1: The effects of different terminal electron acceptors upon growth of *D. desulfuricans* 148
Figure 4.2: The effects of sulphate and sulphite on growth and nitrate and nitrite reduction by *D. desulfuricans* 152
Figure 4.3: The effects of nitrate and nitrite on growth and sulphate and sulphite reduction by *D. desulfuricans* 154
Figure 4.4: The effects of culture pre-treatment upon nitrite-dependent growth 156
Figure 4.5: Nitrite reduction rates of nitrate or sulphate adapted *D. desulfuricans* 158
Figure 4.6: RT-qPCR of genes involved in nitrate and nitrite reduction in *D. desulfuricans* 160
Figure 4.7: RT-qPCR of genes involved in the sulphate reduction pathway in *D. desulfuricans* 162
Figure 4.8: RT-qPCR of genes encoding HcpR proteins in *D. desulfuricans* 164
Figure 4.9: RT-qPCR of genes encoding periplasmic cyctochromes in *D. desulfuricans* 166
Figure 4.10: RT-qPCR of *hcp* in *D. desulfuricans* 167
Figure 5.1: Overexpression of recombinant HcpR in *E. coli*. 180
Figure 5.2: Purification of recombinant HcpR overexpressed in *E. coli*. 182
Figure 5.3: Comparison between the DNA binding affinities of HcpR and CRP for the *nap* promoter fragment in the presence of cAMP 184
Figure 5.4: The effects of differing cAMP concentrations upon DNA binding by HcpR 186
Figure 5.5: The effect of *D. desulfuricans* protein-free extracts upon DNA binding by CRP and HcpR 188
Figure 5.6: EMSA of truncated copies of the *nap* promoter with HcpR 190
Figure 5.7: Measuring HcpR binding to the p*nap* DNA fragment by DNaseI footprinting assays 191
Figure 5.8: Binding of HcpR to the *D. desulfuricans* Ddes_1825, *sat, aprAB* and *hcpR* promoter fragments 193
Figure 5.9: The effects of HcpR expression upon transcription from CRP regulated promoters in *E. coli* in the presence and absence of CRP 196
Figure 5.10: The effects of anaerobic growth upon HcpR-dependent repression of the p*galΔ4* promoter 198
Figure 5.11: The effects of CRP and HcpR upon transcription from *D. desulfuricans* promoters 200
Figure 5.12: Detection of HcpR by western blot using anti-HcpR antibodies 202
Figure 5.13: HcpR expression in the presence of nitrate, sulphate, sulphite and thiosulphate 204
Figure 5.14: The effects of nitrite and HcpR pre-induction on HcpR synthesis 205
Figure 5.15: Growth of *D. desulfuricans* and HcpR synthesis in the presence of exogenous nitric oxide 209
Figure 5.16: qRT-PCR analysis of *hcpR, nrf, nap* and *split soret* expression in response to nitric oxide treatment 211

Figure 5.17: The effects of reducing or oxidising agents upon HcpR conformation and DNA binding activity 213
Figure 5.18 : Transcript mapping of the *hcpR* locus 217
Figure 5.19: qRT-PCR analysis of *hcpr2*, *hcp* and *dfx* expression in response to nitric oxide 220
Figure 5.20: Transcript mapping of the *hcpR2* locus 222
Figure 5.21: Overexpression of recombinant HcpR2 in *E. coli* strain BL21* 224
Figure 5.22: Purification of recombinant HcpR2 227
Figure 5.23: *In vitro* DNA binding activity of HcpR2 229
Figure 6.1: Hierarchical ranking of HcpR target sites tested by EMSA 241
Figure 6.2: Nitric oxide dependent regulation of the *hcpR* operon 250
Figure 6.3: Regulation of *hcp and dfx-rbo-roo* by HcpR2 254
Figure 6.4: Model of *nap* regulation dependent upon dual activation by HcpR and a NarL-NarP-like regulator with sigma-70 RNAP 261
Figure 6.5: Sigma-54 elements at the *nap* and *nrf* promoters 264
Figure 6.6: A model of *nap* regulation by sigma-54 266

List of tables

Table 2.1 Strains used in this study..... 55
Table 2.2 Plasmids used in this study 56
Table 2.3 Primers used in this study 63
Table 2.4 qRT-PCR primers used in this study 69
Table 3.1 Identities of CRP/FNR homologues from selected *Desulfovibrio* species 90
Table 3.2 A putative regulon for regulators Ddes_2092 and Ddes_1441 108
Table 3.3 candidate binding sites for HcpR upstream of *D. desulfuricans* core regulon members 115
Table 3.4 Novel HcpR regulon members in *D. desulfuricans* 117

List of abbreviations

AAA+	ATPase associated with various cellular activities domain
APS	Adenosine 5'-phosphosulphate
ADP	Adenosine diphosphate
AMP	Adenosine monophosphate
ATP	Adenosine triphosphate
cAMP	Cyclic adenosine monophosphate
Carb	Carbenicillin
Chlor	Chloramphenicol
CIP	Calf intestinal alkaline phosphatase
CoA	Coenzyme A
C-terminus	Carboxyl terminus
DMSO	Dimethylsulfoxide
DNA	Deoxyribonucleic acid
dNTP	Deoxynucloside triphosphate
EDTA	Ethylene diaminetetraacetic acid
EMSA	Electromobility shift assay
FAD	Flavin adenine dinucleotide
GAF	cGMP phosphodiesterase adenylate cyclase FhlA
GTP	Guanosine triphosphate
HPLC	High pressure liquid chromatography
IPTG	Isopropyl-β-D-1-thiogalactopyranoside
Kan	Kanamycin
LB	Lennox broth
mPEG-mal	Methoxypolyethylene glycol maleimide
NA	Nutrient agar
NADPH	Nicotinamide adenine dinucleotide phosphate (reduced)
NAD^+	Nicotinamide adenine dinucleotide
NO	Nitric oxide
N-terminus	Amino terminus
OD	Optical density
ONPG	Orthonitrophenyl-β-D-galactopyranoside
PCR	Polymerase chain reaction
Pi	Phosphate

PPi	Pyrophosphate
RNA	Ribonucleic acid
RNAP	RNA polymerase
RNS	Reactive nitrogen species
ROS	Reactive oxygen species
SDS	Sodium dodecyl sulphate
SRB	Sulphate reducing bacteria
SRP	Sulphate reducing bacterium
PAGE	Polyacrylamide gel electrophoresis
TBE	Tris-borate-ethylene diaminetetraacetic acid
TCA	Tricarboxylic acid
TEMED	*N*,*N*,*N*′,*N*′-Tetramethylethylenediamine
TMAO	Trimethylamine (*N*-oxide)
UV	Ultra violet

Chapter 1

Introduction

1.1 Introduction

The sulphate reducing bacteria (SRB) are defined by their ability to utilise sulphate as a terminal electron acceptor for growth. Generally regarded as strict anaerobes, SRB are ubiquitous in anoxic or oxygen limited environments and are major contributors to the global cycling of carbon and sulphate (Muyzer & Stams, 2008). The assumed involvement of SRB in human bowel diseases, the corrosion of metals, and their ability to occupy seemingly adverse environmental niches has encouraged interest from researchers. Although SRB are able to utilise alternative terminal electron acceptors to sulphate, dissimilatory nitrate reduction by the group is relatively uncommon (Moura *et al.*, 1997). *Desulfovibrio desulfuricans* ATCC27774 is an example of a SRB that is able to reduce both sulphate and nitrate.

Nitrate and sulphate are reduced by *D. desulfuricans*, not simultaneously, but in a hierarchical manner akin to carbon source utilisation by *Escherichia coli* (Baumann Denk, 1950). Sulphate is utilised before nitrate despite nitrate yielding higher cell densities and more rapid growth rates compared to sulphate (Marietou *et al.*, 2008; Marietou, 2009). This phenomenon contradicts the dogma that bacteria will utilise the thermodynamically most favourable growth substrates first when a selection is available. Thus, the sulphate-nitrate diauxie of *D. desulfuricans* is seemingly degenerate as no obvious advantage is conferred to the bacterium. The mechanism underpinning this diauxie is unknown. In *E. coli* many genes encoding proteins necessary for carbon metabolism are regulated by the cAMP receptor protein, CRP. Previous studies have suggested that HcpR, a homologue of CRP, might regulate expression of the nitrate reductase genes of *D. desulfuricans* and also genes encoding the proteins of the sulphate

reduction pathway in other *Desulfovibrio* species (Marietou *et al.*, 2009; Rodionov *et al.*, 2004; Rodionov *et al.*, 2005).

This chapter will begin with an introduction to the enzymes that permit SRB to reduce sulphate for the purpose of energy generation and also those responsible for periplasmic nitrate and nitrite reduction by *E. coli*. Nitrate and nitrite reduction yields toxic side-products that can damage intracellular components. Furthermore, incomplete oxygen reduction can also generate toxic side products. The enzymes necessary for anaerobiosis and sulphate reduction in SRB are particularly sensitive to these stresses and so the mechanisms by which bacteria defend themselves against these damages are described. The details of the sulphate-nitrate diauxie of *D. desulfuricans* will be reviewed and, for comparison, the textbook example of glucose-lactose diauxie in *E. coli* will be described. CRP, which plays a crucial role in regulating the transcription of operons specific to carbon source utilisation by *E. coli*, will be discussed as will the network of transcription regulators that control expression of genes necessary for nitrate and nitrite dependent growth in *E. coli*. Finally, a summary of the aims and objectives of this study will be provided.

1.2 Sulphate reducing prokaryotes

SRB are part of a larger group, the sulphate reducing prokaryotes (SRP). The SRP include members from the bacterial phyla *Firmicutes* (*Clostrdia), Nitrospiriae (Nitrospira), Proteobacteria (δ-proteobacteria)* and the archeael phylum *Euryarchaeota (Archaeoglobus)* (Fauque & Barton, 2012). The genomes of SRP encode the enzymes necessary for catalysing the reduction of sulphate, which is a multistep process. Most of the enzymes of the sulphate reduction pathway have high levels of similarity to the

enzymes of the sulphur oxidation pathway encoded in the genomes of microbes that are reliant upon sulphur oxidation for energy (Meyer & Kuever, 2008). The oxidation of sulphur and the reduction of sulphate by microbes are ancient processes derived from a time when atmospheric oxygen levels were low. It is believed that at that time, approximately 3.4 billion years ago, sulphur oxidising phototrophic prokaryotes formed microbial mats and that the favourable conditions within these mats led to the evolution of the SRP (Shen *et al.*, 2001).

Although SRP are regarded as anaerobes, some members are able to tolerate near atmospheric levels of oxygen (Cypionka, 2000; Lobo *et al.*, 2007). Their ubiquitous nature and ability to utilise carbon containing molecules and sulphate for growth directly link them to the global cycling of sulphur and carbon (Muyzer & Stams, 2008). The end product of sulphate reduction, sulphide, has the potent smell of rotten eggs and is easily identifiable (Postgate, 1984). SRPs have been isolated from a wide range of environments including soils, fresh water, marine and estuarine sediments, deep sea vents, spoiled foods, sewage plants, human and animal digestive tracts, symbionts, ground water and a gold mine (Gibson, 1990; Zhou *et al.*, 2011). These habitats represent great versatility and adaptation within the group.

SRB are an attractive target for research. The microbial induced corrosion of iron or steel is extremely costly to industry. Biofilms of mixed bacteria adhere to these metal surfaces and their metabolic activities form an anaerobic environment that favours the proliferation of SRB (Hamilton, 2003; Hamilton, 1995). The localised proliferation of SRB leads to electrochemical corrosion and chemical dissolution of the iron surface by production of sulphide and the utilisation of iron as an electron donor for sulphate

reduction (Vourdouw, 1995; Muyzer & Stams, 2008). SRB also cause the souring of petroleum reserves (Vourdouw, 2011). Hydrogen sulphide is toxic, primarily due to its high affinity for the iron groups of proteins, and hydrogen sulphide poisoning is quoted as the leading cause of deaths to operatives in livestock operations (Evans, 1967; Predicala *et al.*, 2008).

SRB, being common in the human gut, have been implicated in a range of bowel diseases such as ulcerative colitis, irritable bowel syndrome and Crohn's disease (Jia *et al.*, 2012, Rowan *et al.*, 2009; Macfarlane *et al.*, 2009). Disequilibrium of the intestinal microbiome and increased production of hydrogen sulphide in the gut are believed to be involved in these conditions. However, whether SRB in the gut are a causative agent, an exacerbating factor, or a marker of these diseases remains unknown (Fava & Danese, 2011).

Some species of SRB are able to reduce toxic heavy metal ions and represent a potential tool for bioremediation applications. The reduction of these metals results in decreased solubility and precipitation (Lovley, 1995). Precipitated metals represent less of a biological hazard. Specific examples of bioremediation trials using SRB include the reduction, precipitation and subsequent removal of uranium (VI) and chromate (VI) from contaminated waters and the processing of acid mine drainage (Lovley & Phillips, 1992; Lovley & Phillips, 1994; Natarajan, 2008). SRB have also been used to metabolise nitroaromatic compounds such as explosives and pesticides from contaminated soils (Boopathy, 2009). SRB have also been used to recover platinum from spent catalytic converters from the automotive industry (Yong *et al.*, 2003).

1.3 The sulphate reduction pathway

Overview of the sulphate reduction pathway

Sulphur is essential for life being a component of the amino acids cysteine and methionine. Sulphur is abundant in the environment in the form of the sulphate ion. However, sulphate is not easily utilised by life-forms since it may be described as being biologically inert (Bradley *et al.* 2009). Indeed, for sulphate to be used by organisms, either as a building block for biological molecules (assimilatory sulphate reduction) or as a terminal electron acceptor in heterotrophic metabolism (dissimilatory sulphate reduction), it must first be subjected to an activation step. Sulphate is activated by adenylation, the transferral of AMP from ATP to sulphate. This process is catalysed by sulphate adenylyltransferases, Sat, also known as ATP sulphurylases, ATPS. The end products of sulphate adenylation are adenosine-5'-phosphosulphate (APS) and inorganic pyrophosphate (PPi):

$$ATP + SO_4^{2-} \leftrightarrow PPi + APS \ (\Delta G = +46 \text{ kJ/mol})$$

This reaction is thermodynamically unfavourable and therefore relies upon the hydrolysis of PPi by inorganic pyrophosphatase to pull the reaction to completion:

$$PPi + H_2O \rightarrow 2Pi \ (\Delta G = -22 \text{ kJ/mol})$$

The high-energy APS produced by sulphate adenylation is amenable to reduction in the subsequent step of the dissimilatory reduction pathway. APS is hydrolysed and reduced to sulphite and AMP by APS reductase, Apr:

$$APS + (H_2)\ 2e^- \leftrightarrow SO_3^{2-} + AMP\ (\Delta G = -69\ kJ/mol)$$

Finally, sulphite is reduced to sulphide by dissimilatory sulphite reductases, dSiR or Dsr:

$$SO_3^{2-} + (3H_2)\ 6e^- \leftrightarrow S^{2-} + (3H_2O)\ (\Delta G = -174\ kJ/mol)$$

Since two ATP equivalents are invested in the pathway, with two phosphates being displaced from ATP during the activation step, sulphate reduction represents a heavy burden for organisms dependent upon this terminal electron acceptor. Furthermore, organisms that generate phospho-APS (PAPS) in the assimilatory sulphate reduction pathway must invest an additional ATP for this phosphorylation step.

The dissimilatory reduction of sulphate is coupled to the oxidation of growth substrates such as lactate, ethanol or hydrogen. The reduction of one mole of sulphate provides electrons sufficient for the oxidation of two moles lactate which in turn generate two moles of ATP by substrate-level phosphorylation. Thus, the ATP requirement for sulphate reduction and the ATP yield from lactate oxidation balance (Postgate, 1984). Therefore, SRB must possess additional mechanisms for generating energy.

Activation of sulphate by Sat

Sat enzymes are ubiquitous, being found in all domains of life, and can catalyse the adenylation of sulphate for either assimilatory or dissimilatory pathways. The structures of Sat enzymes are varied with those crystallised being multimeric complexes. Sat enzymes that have been characterised to date include homodimeric, homohexameric and heteromultimeric structures (Yu *et al.*, 2007; Taguchi *et al.*, 2004; Beynon *et al.*, 2007; Ullrich *et al.*, 2001; MacRae *et al.*, 2001; Mougous *et al.*, 2006). Additionally, Sat

monomers are variable in terms of their domain architecture. For example, some Sats include APS kinase domains and some contain a further domain with pyrophosphatase activity (Bradley *et al.*, 2009).

A conserved feature of Sat enzymes is the presence of an active site that can accommodate both ATP and the sulphate ion. The active site, which contains highly conserved Asp, Arg and Glu residues for substrate co-ordination, is pocket-like in structure and is proximal to a mobile loop region which regulates enzyme activity (Yu *et al.*, 2007; Beynon *et al.*, 2001; Taguchi *et al.*, 2004). The loop folds over the pocket when substrate is bound forming the active conformation and then flips up in the inactive conformation allowing release of reaction products (Yu *et al.*, 2007; Beynon *et al.*, 2001; Taguchi *et al.*, 2004). Movement of the loop may be regulated by allosteric effector molecules and the active site can be occupied by competitive inhibitors (Gay *et al.*, 2009; Ullrich & Huber., 2001). The Sat enzymes of *D. desulfuricans* and *D. gigas* are predicted to be similar to the zinc binding Sat of *T. thermophilus* HB8 with conserved cysteine residues for the coordination of zinc ions that are believed to confer structural stability to the enzyme (Yu *et al.*, 2008; Taguchi *et al.*, 2004).

The reduction of APS to sulphite

Apr, the enzyme that reduces APS to sulphite, is found in a wide range of organisms. In some organisms, such as *E. coli*, APS is phosphorylated to PAPS prior to reduction by Apr as part of the assimilatory sulphate reduction pathway. However, for SRB utilising sulphate in the dissimilatory sulphate reduction pathway the substrate for Apr is APS.

Apr enzymes are heteromultimeric complexes containing α and β subunits that are encoded by the *aprBA* operon. The α subunit contains an FAD cofactor proximal to the

enzyme active site and the β subunit contains two [4Fe-4S] iron-sulphur clusters (Chiang *et al.*, 2009). The smaller β subunit associates with the α subunit via a long tail domain (Chiang *et al.*, 2009). Like Sat, Apr adopts active and inactive conformations. In *D. gigas,* active Apr exists as a heterodimer with electrons for APS reduction presumably being passed from the [4Fe-4S] clusters to the FAD cofactor that is in close proximity to the substrate binding channel (Chiang *et al.*, 2009; Fang *et al.*, 2011). The inactive form of *D. gigas* Apr is a hexamer made up of six αβ heterodimers. In the hexamer the positioning of each heterodimer in the structure is such that the substrate binding channel is occluded by its neighbour resulting in a lack of activity in this conformation. AMP acts as an allosteric effector of Apr, triggering the dissociation of the hexamer into functionally active dimers. Thus, it has been proposed that the activity of Apr from *D. gigas* is regulated by the sensing of APS or AMP (Chiang *et al.*, 2009; Fang *et al.*, 2011).

The reduction of sulphite to sulphide

The final stage of the dissimilatory sulphate reduction pathway, the six electron reduction of sulphite to sulphide, is catalysed by dSiR enzymes. dSiRs are typically heterotetramers comprised of two α and two β subunits, encoded for by the *dsrAB* operon. Variants of this arrangement are known with additional subunits γ and δ contributing to the complex in some organisms (Crane & Getzoff, 1996).

DsrA and DsrB in *A. fulgidus* exist as a complex of two heterodimers with each heterodimer possessing an active site (Schiffer *et al.*, 2008). The heterotetramer contains four siroheme rings coupled to [4Fe-4S] iron-sulphur clusters and four [4Fe-4S] clusters. It has been suggested that half of the siroheme-[4Fe-4S] groups are directly

involved in catalysis with the remainder contributing to electron transport to the catalytic groups (Schiffer *et al*., 2008). Indeed, in the DsrAB heterotetramer of *D. vulgaris* the two structural siroheme-[4Fe-4S] groups are replaced with two sirohydrochlorin groups (Oliveira *et al.*, 2008). Different routes for electrons to be shuttled to the catalytic sites have been proposed with electrons being relayed via the [4Fe-4S] clusters to the catalytic siroheme-[4Fe-4S] groups (Schiffer *et al*., 2008).

The *D. vulgaris* Dsr complex includes γ subunits, encoded by the *dsrC* gene. These associate with the $\alpha_2\beta_2$ unit by fitting into a cleft between the α and β subunits (Oliveira *et al.*, 2008). The C-terminus of γ can cross-link with residues of the substrate binding site in a manner that would be inhibitory to sulphite reduction (Oliveira *et al.*, 2008). It has been proposed that the γ subunit has a helix-turn-helix motif that is capable of binding to DNA sites. Indeed, the DsrC protein of *Allochromatium vinosum*, a sulphur oxidising bacterium, can bind to a near palindromic sequence the *dsrA* promoter region *in vitro*, presumably DsrC influences transcription of the *dsrAB* operon (Grimm *et al.*, 2010).

1.4 The electron transport chain of SRB

Electron transport to the sulphate reduction pathway

The electrons necessary for the reduction of APS and sulphite are derived from the oxidation of substrates such as lactate, ethanol or hydrogen. Hydrogen is oxidised in the periplasm by a consortium of hydrogenases. However, since the reduction of APS and sulphite occurs within the cytoplasm, a network of electron transporting proteins must exist for the translocation of these electrons. Unfortunately, the electron transport chain

of SRB has only been partially characterised and the exact nature of how electrons are transported from electron donors to APS and sulphite remains unknown. The components of the chain that have been studied are summarised in Figure 1.1.

Recently, the Qrc complex of *D. vulgaris* Hildenborough was purified and characterised (Venceslau *et al.*, 2010). The QrcABCD complex is composed of four protein subunits: a six *c*-type haem containing subunit, a single [3Fe-4S] iron-sulphur cluster containing subunit, a four [4Fe-4S] iron-sulphur cluster containing subunit, and an integral membrane associating subunit that anchors the complex to the cytoplasmic membrane (Venceslau *et al,*, 2010). Qrc is a menaquinone reductase with a binding site for quinone proximal to the [3Fe-4S] cluster. Electrons for reduction of the quinone pool come from the periplasmic oxidation of formate or hydrogen via a pool of c_3-type haem containing proteins in the periplasm (Venceslau *et al.*, 2010).

Another respiratory complex conserved amongst *Desulfovibrio* species is the QmoABC complex. This complex was purified from *D. desulfuricans* and is composed of three different subunits containing two *b*-type haems, two FAD cofactors, a single [3Fe-4S] iron-sulphur cluster and four [4Fe-4S] iron-sulphur clusters (Pires *et al.*, 2003). QmoA and QmoB are located within the cytoplasm and contain FAD and [4Fe-4S] clusters, whereas QmoC associates with the membrane and contains haem groups and also iron-sulphur clusters (Pires *et al.*, 2003). Involvement in the respiratory chain was first shown by the ability of a menaquinone analogue to reduce both haem groups of the complex (Pires *et al.*, 2003). The co-localisation of the *qmoABC* and *aprBA* operons suggested that the Qmo complex is responsible for presenting electrons to Apr. Deletion mutants of the *qmoABC* operon in *D. vulgaris* Hildenborough have been constructed.

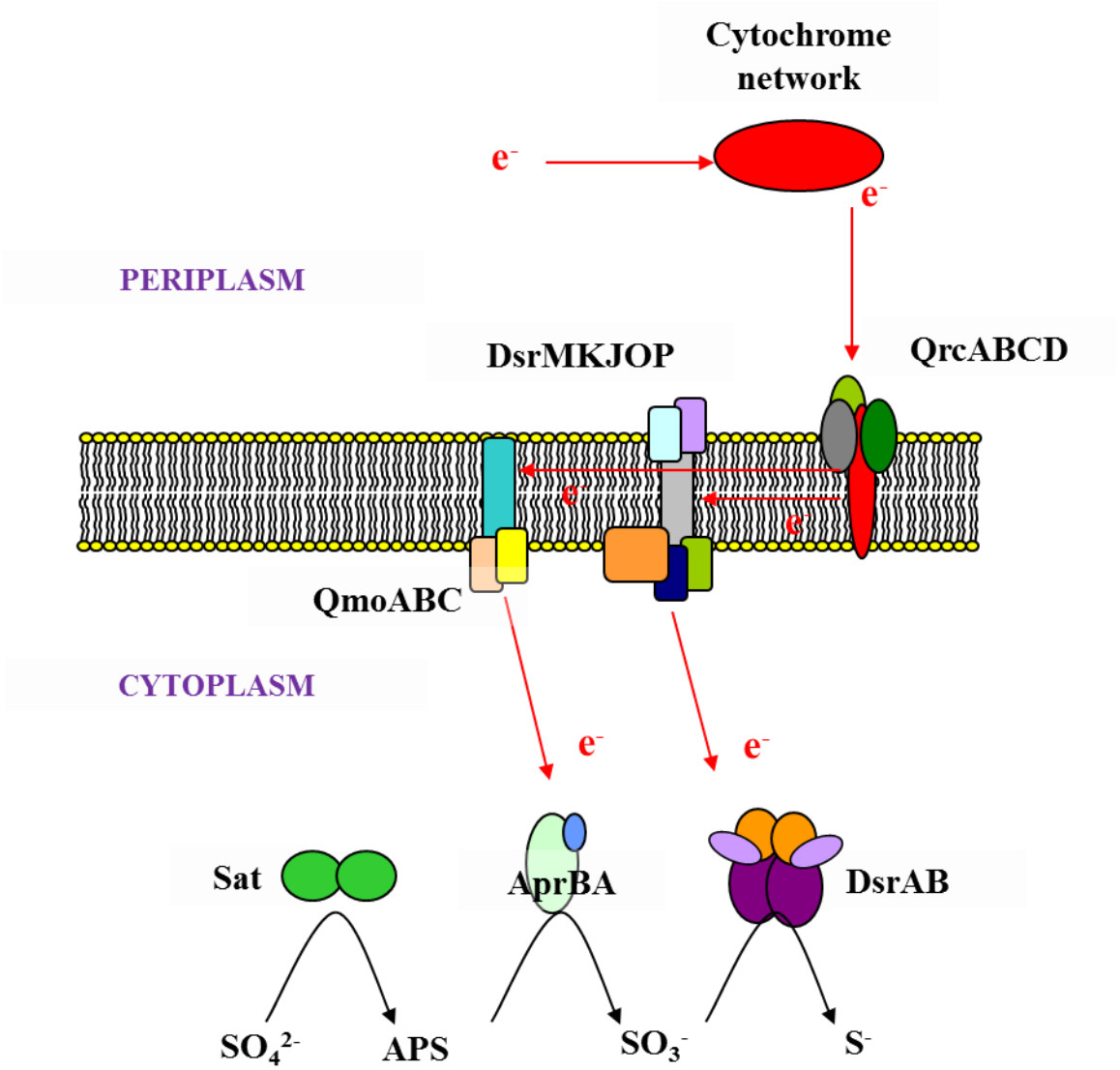


Figure 1.1: The flow of electrons from the periplasm to the sulphate reduction pathway via membrane associated respiratory complexes. Red arrows indicate electron (e^-) migrations. Electrons are believed to be relayed from periplasmic cytochromes to the membrane bound respiratory complexes and then to Apr and Dsr in the cytoplasm.

The resultant strains are unable to grow on sulphate as the sole terminal electron acceptor but are able to grow in the presence of sulphite (Zane *et al.*, 2010). This suggests that QmoABC functions as part of the sulphate respiratory chain in *Desulfovibrio* and also that the Qmo complex oxidises the menaquinol pool, providing electrons for APS reduction. Thus, Qrc and Qmo may be regarded as forming a redox loop cycling the quinone pool.

Another respiratory complex, DsrMKJOP, from *D. desulfuricans* has been purified and characterised. This complex, like Qmo and Qrc, contains multiple subunits with cofactors including *c*-type haems, *b*-type haems and iron-sulphur clusters (Pires *et al.*, 2006). Similar to Qmo, reduction of some of the haem groups may be achieved with a menaquinone analogue and also the *dsrMKJOP* operon is co-localised with the *dsrAB* operon, thus the DsrMKJOP complex is assumed to have a role in the transport of electrons to DsrAB (Pires *et al.*, 2006). However, the precise function of the DsrMKJOP complex is yet to be proven and it has also been speculated that Dsr could directly transport electrons from the periplasm to the cytoplasm.

Auxiliary electron transfer proteins in SRB

There is an assortment of different cytochromes in *Desulfovibrio* species that are believed to be involved in electron transfer chains. The split-soret cytochrome c, Ssc, is named after its characteristic reduced absorbance spectrum which has an unusual ‘shoulder’ adjacent to the soret band at 424 nm (Liu *et al.*, 1988). Ssc is present in *D. desulfuricans* grown on either sulphate or nitrate but since levels of Ssc are elevated in the presence of nitrate it has been suggested that it has a role in nitrate-specific growth (Liu *et al.*, 1988; Abreu *et al.*, 2003; da Silva *et al.*, 2012). Ssc does not have any nitrate

or nitrite reductase activity but was recently shown to be rapidly reduced by the formate dehydrogenase complex, FdhABC. The current proposal is that Ssc is an electron donor for the Nap complex (da Silva *et al.*, 2012).

The tetrahaem type I cytochrome *c*, TpIc_3, is common throughout SRB and is believed to transport electrons from dehydrogenases in the periplasm to the Qrc complex which in turn relay these electrons to the components of the sulphate reduction pathway (da Silva *et al.*, 2012; Venceslau *et al.*, 2011). The nine haem cytochrome Nhc is a membrane bound cytochrome complex that lacks a cytoplasmic domain and as such is believed to be involved in electron transport between the quinol/quinone pool and the periplasm. Nhc has been reported to receive electrons from periplasmic hydrogenases via TpIc_3, directly from these hydrogenases and also directly from FdhABC (da Silva *et al.*, 2012). The network of cytochromes responsible for electron transfer in *Desulfovibrio* species requires further characterisation.

1.5 Production of ATP by SRB

SRB are able to utilize a range of different electron donors including lactate, acetate, ethanol, methanol, butanol, butyrate, malate, propanol, succinate and hydrogen may also be utilised (Liamleam *et al.*, 2007). SRB must be thrifty with cellular resources in order to yield ATP whilst utilising the energetically costly terminal electron acceptor, sulphate. Thus, a number of pathways and models for ATP generation have been proposed for the Gram-negative SRB (reviewed in Keller & Wall, 2011). An overview of three of these processes is given in Figure 1.2.

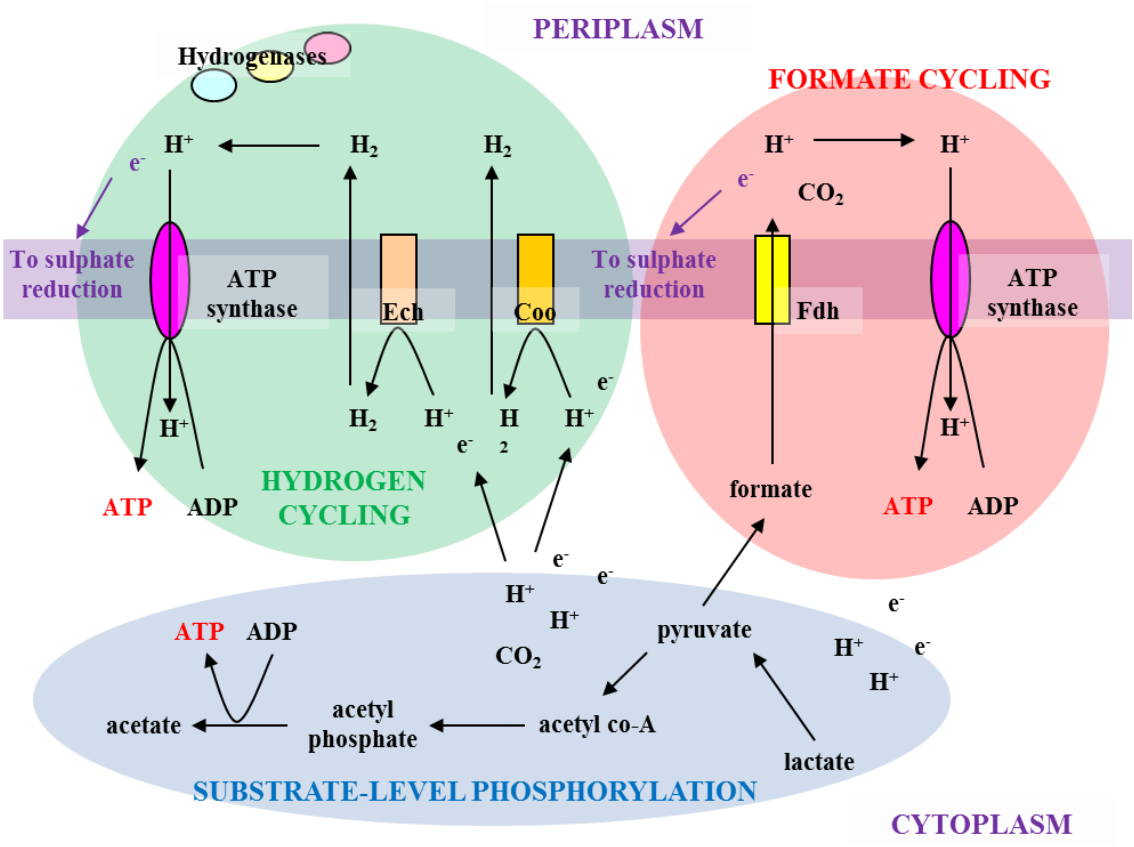


Figure 1.2: ATP production in Gram-negative SRB by substrate-level phosphoryation, formate cycling and hydrogen cycling. Three models of energy conservation by SRB have been proposed to support growth while utilising sulphate as a terminal electron acceptor. Refer to the text for details.

Substrate level phosphorylation

ATP can be synthesised from the oxidation of lactate by substrate-level phosphorylation. In the cytoplasm, lactate is oxidised to pyruvate by lactate dehydrogenase. Pyruvate is then oxidised by a pyruvate:ferredoxin oxidoreductase and the resulting acetyl-CoA is subsequently converted to acetyl-phosphate by the phosphate acetyl transferase. Finally, acetyl-phosphate is dephosphorylated to acetate by acetate kinase with the phosphate group being transferred to ADP yielding ATP (Keller & Wall, 2011). Each mole of lactate oxidised yields a mole of ATP by substrate-level phosphorylation. The pathway also yields CO_2, $4e^-$ and $4H^+$. These additional products are crucial for energy conservation by *Desulfovibrio*. Furthermore, an intermediate of this pathway, pyruvate, can be oxidised by an alternative pathway that generates ATP.

Formate cycling

Pyruvate generated from lactate oxidation can be oxidised to formate by pyruvate-formate lyase. Formate is then transported into the periplasm and oxidised to CO_2 by the formate dehydrogenase, Fdh (da Silva *et al.*, 2011). Electrons from this oxidation are used to reduce either the cytochrome c_3 pool or the menaquinone pool from which they may be shuttled through membrane bound complexes. Protons are also produced by this oxidation step. These protons contribute to the generation of an electrochemical gradient that drives ATP synthesis by the membrane bound enzyme, ATP synthase, as H^+ passes from the periplasm into the cytoplasm. Although this example of formate cycling uses lactate, growth of *Desulfovibrio* in medium containing formate or hydrogen as the electron donor induced much higher rates of Fdh activity (da Silva, 2011).

Hydrogen cycling

The final model of ATP generation in *Desulfovibrio* discussed here, hydrogen cycling, was first proposed by Odom & Peck (1981). As already mentioned, the oxidation of lactate in the cytoplasm generates protons and electrons. Cytoplasmic hydrogenases such as Ech and Coo convert these protons and electrons to hydrogen that can freely diffuse across the cytoplasmic membrane into the periplasm (Zhou *et al.*, 2011). Once in the periplasm, hydrogen may be converted to protons and electrons by various hydrogenases such as the Hyn1 [NiFe], Hyd [FeFe] or Hys [NiFeSe] (Venceslau *et al.*, 2010). As with formate cycling, the electrons produced may be transferred to the cytochrome c_3 pool or to the menaquinone pool and the membrane bound complexes. Again, the presence of protons in the periplasm contributes to the generation of an electrochemical gradient and drives ATP synthesis by ATP synthase. Should growth be on hydrogen as the electron donor instead of lactate then a proton motive force can be generated without the need for the cytoplasmic hydrogenases (Zhou *et al.*, 2011). Thus, a variety of pathways have been proposed to explain how *Desulfovibrio* yields ATP whilst reducing sulphate.

1.6 Nitrate reduction by *E. coli*

Nitrate is the preferred terminal electron acceptor of *E. coli* under anaerobic conditions. The reduction of nitrate to ammonia proceeds by two sequential reductions. First, nitrate reductases catalyse the two electron reduction of nitrate to nitrite:

$$NO_3^- + 2H^+ + 2e^- \rightarrow NO_2^- + H_2O$$

Bacterial nitrate reductases are categorised according to their function and location within the cell. The active sites of most nitrate reductases, both prokaryotic and eukaryotic, contain a molybdenum cofactor although there are exceptions to this rule (Moreno-Vivián *et al.,* 1999; Richardson *et al.*, 2001; Antipov *et al.*, 1998; Afshar *et al.*, 1998). Nitrate can be reduced in *E. coli* by three distinct nitrate reductases and the resulting nitrite can be reduced to ammonia by two distinct nitrite reductases. Each of these components of the nitrate reduction pathway display different affinities for their respective substrate and interact with other cellular components. Thus, by having multiple routes to ammonification *E. coli* is well equipped for a range of different conditions. In turn, the genes encoding these different reductases are under the regulatory control of multiple transcription factors allowing exquisite control over nitrate reduction via alternative pathways.

Respiratory nitrate reductases (Nar) are found associated with the cytoplasmic membrane. These protein complexes are comprised of electron transporting subunits and a catalytic subunit with its active site orientated towards the cytoplasm. Electrons for the reduction of nitrate are donated from the quinol pool and are transported by electron transporting subunits to the catalytic subunit. This also results in the pumping of two protons across the cytoplasmic membrane and so the oxidation of the quinol pool and the reduction of nitrate form a redox loop that creates a proton motive force for the synthesis of ATP (Richardson & Watmough, 1999).

The *E. coli* NarGHJI system is a membrane bound respiratory nitrate reductase. NarGHJI forms a respiratory chain, via the quinol pool, with formate dehydrogenase N in the periplasm (Mitchell, 1976). NarJ functions as a chaperone for the catalytic

subunit, NarG, by aiding insertion of the Mo cofactor (Blasco *et al*., 1998). NarH relays electrons from the transmembrane unit, NarI, to NarG and these three subunits complex together as a heterotrimer (Bertero *et al*., 2003). Expression of NarGHJI is maximal when nitrate concentrations are high (Wang *et al*., 1999). The second respiratory nitrate reductase complex of *E. coli*, NarZYWV is also a cytoplasmic enzyme that is associated with the membrane. This system is analogous to the NarGHJI system and the two have similar activities (Blasco *et al*., 1990). However, NarZYWV is expressed independently of nitrate and oxygen concentrations and is instead primarily regulated by growth phase, being up-regulated in stationary phase (Wang *et al.*, 1999).

The third *E. coli* nitrate reductase complex, NapFDAGHBC, is referred to as the periplasmic nitrate reductase due to its periplasmic location. Nap has a higher affinity for nitrate than its membrane-bound counterparts, leading to the assumption that the Nap and Nar systems provide efficient nitrate reductase activity in the presence of varied nitrate concentrations with Nap being responsible for the scavenging of low concentrations of nitrate (Potter *et al.*, 1999; Cole, 1996). Nitrate reduction by *D. desulfuricans* is reported to occur solely in the periplasm (Marietou *et al.*, 2009; Marietou, 2008).

1.7 Periplasmic nitrate reductase

Nap enzymes contain multiple subunits each with distinct functions. The *E. coli* Nap complex is the best understood example. It is made up of seven different subunits encoded for by the *napFDAGHBC* operon although there are many different combinations of subunits in other bacteria that also include other Nap subunits not encoded in the *E. coli* genome.

In *E. coli*, *D. desulfuricans*, *R. sphaeroides* and *Cupriavidus necator* the catalytic subunit, NapA, contains one [4Fe-4S] iron-sulphur cluster and one Mo-bis-molybdopterin guanidine dinucleotide (Mo-bis-MGD) cofactor (Jepson *et al.*, 2006; Dias *et al.*, 1999; Arnoux *et al.*, 2003; Coelho *et al.*, 2011). Crystal structures reveal that NapA has multiple domains and a signal peptide that is cleaved on export to the periplasm. The active site of NapA is funnel-like in appearance with the Mo-bis-MGD cofactor located in the pit of this funnel. The [4Fe-4S] cluster and one of the MGD moieties are in close association with each other facilitating the relay of electrons to the active site (Jepson *et al.*, 2006; Dias *et al.*, 1999).

NapA associates with NapB in organisms that encode this subunit and the affinity with which this association forms is variable (Arnoux *et al.*, 2003; Jepson *et al.*, 2006). NapB, which is small in comparison with NapA, has extended N- and C-terminus regions with the remainder of the protein forming a globular domain. These extended terminus regions mediate the association with NapA that has been likened to an embrace (Coelho *et al.*, 2011). NapB contains two *c*-type heme groups in close proximity to each other with one heme being proximal to the [4Fe-4S] cluster of NapA. A tyrosine residue occupies the space between this heme and the [4Fe-4S] cluster and is believed to be the bridge between NapB and NapA for electron migration to the Mo-bis MGD cofactor via the [4Fe-4S] cluster (Coelho *et al.*, 2011; Jepson *et al.*, 2006). This tyrosine is conserved in the NapA proteins of *E. coli* and *R. sphaeriodes* but is absent from *D. desulfuricans* NapA (Coelho *et al.*, 2011).

Electrons are relayed to NapB from other electron transfer proteins, such as NapC. NapC is a membrane-bound tetraheme cytochrome *c*, thought to catalyse quinol

oxidation and relay electrons to the NapAB complex (Cartron *et al.*, 2002). The membrane-bound complex of NapG and NapH, which are iron-sulphur binding proteins, are believed to be functionally equivalent to NapC (Brondijk *et al.*, 2004).

The partitioning of proteins into the periplasm requires targeted passage of the proteins across the cytoplasmic membrane. Thus, the Nap subunits require a specific transport system into the periplasm. The *E. coli* NapD subunit is found in the cytoplasm rather than in the periplasm yet is strictly required for periplasmic nitrate reduction (Potter & Cole, 1999). The NapD monomer is cylindrical in shape with α helices and β sheets arranged so that one face of the protein is covered in α helices and the other is covered in β sheets (Maillard *et al.*, 2007). The β sheet surface of the protein is responsible for binding to the twin-arginine signal peptide of NapA and exporting it to the periplasm. A crystal structure of NapD binding to a portion of NapA is available, an α helix of the NapA signal peptide fits into a groove in the β sheet surface of NapD, but a full article detailing this interaction is still pending (Minailiuc *et al.*, 2008).

The function of NapF is yet to be conclusively proven, but it has been shown to reside within the cytoplasm associated with the inner membrane and interacts with both NapA and NapD. It is suggested that its role in *E. coli* and in *Wolinella succinogenes* is in assisting the maturation of NapA, possibly being involved in cofactor insertion into NapA (Nilavongse *et al.* 2006; Kern & Simon, 2009).

The *napCMADGH* gene cluster of *D. desulfuricans* differs from that of *E. coli* most strikingly in its lack of NapB and NapF subunits and in its inclusion of a NapM subunit (Marietou *et al.*, 2005). This NapM subunit is believed to be a tetra-haem cytochrome *c* that is transported into the periplasm. Attempts to purify and characterise NapM have so

far been unsuccessful (da Silva *et al.*, 2011). In models of electron flow to NapA in *D. desulfuricans* NapM has been proposed to function in one of three ways. NapM either relays electrons to NapA from both NapC and NapGH, from NapC alone, or to function as an electron donor for NapA independently of NapC or NapGH (Figure 1.3) (Marietou, 2009).

1.8 Nitrite reductases

Following the reduction of nitrate to nitrite in dissimilatory pathways, nitrite is reduced to ammonia or nitric oxide by several different enzymes. This reduction step requires six electrons:

$$NO_2^- + 8H^+ + 6e^- \rightarrow NH_4^+ + 2H_2O$$

The NADH-dependent cytoplasmic nitrite reductase, NirBD of *E. coli*, does not contribute directly to the generation of a PMF and is believed to be primarily responsible for nitrite detoxification (Wang & Gunsalus, 2000). NirB is the catalytic subunit of the enzyme with NirD assuming a structural role in the complex. NirB contains a sirohaem prosthetic group and nitrite reduction by the complex is dependent upon NADH. Regulation of *nirBD* is complex with multiple transcription factors influencing transcription from the *nirB* promoter (Browning *et al.*, 2005). Expression of *nirB* is stimulated by anaerobiosis and the presence of nitrate or nitrite (Wang & Gunsalus, 2000; Tyson *et al.*, 1993). Also encoded at the *nirBD* locus are genes for NirC, a nitrite transporter, and CysG, a sirohaem synthase.

The second *E. coli* nitrite reductase, NrfABCD, is located in the periplasm associated with the cytoplasmic membrane and functions in a respiratory chain with formate

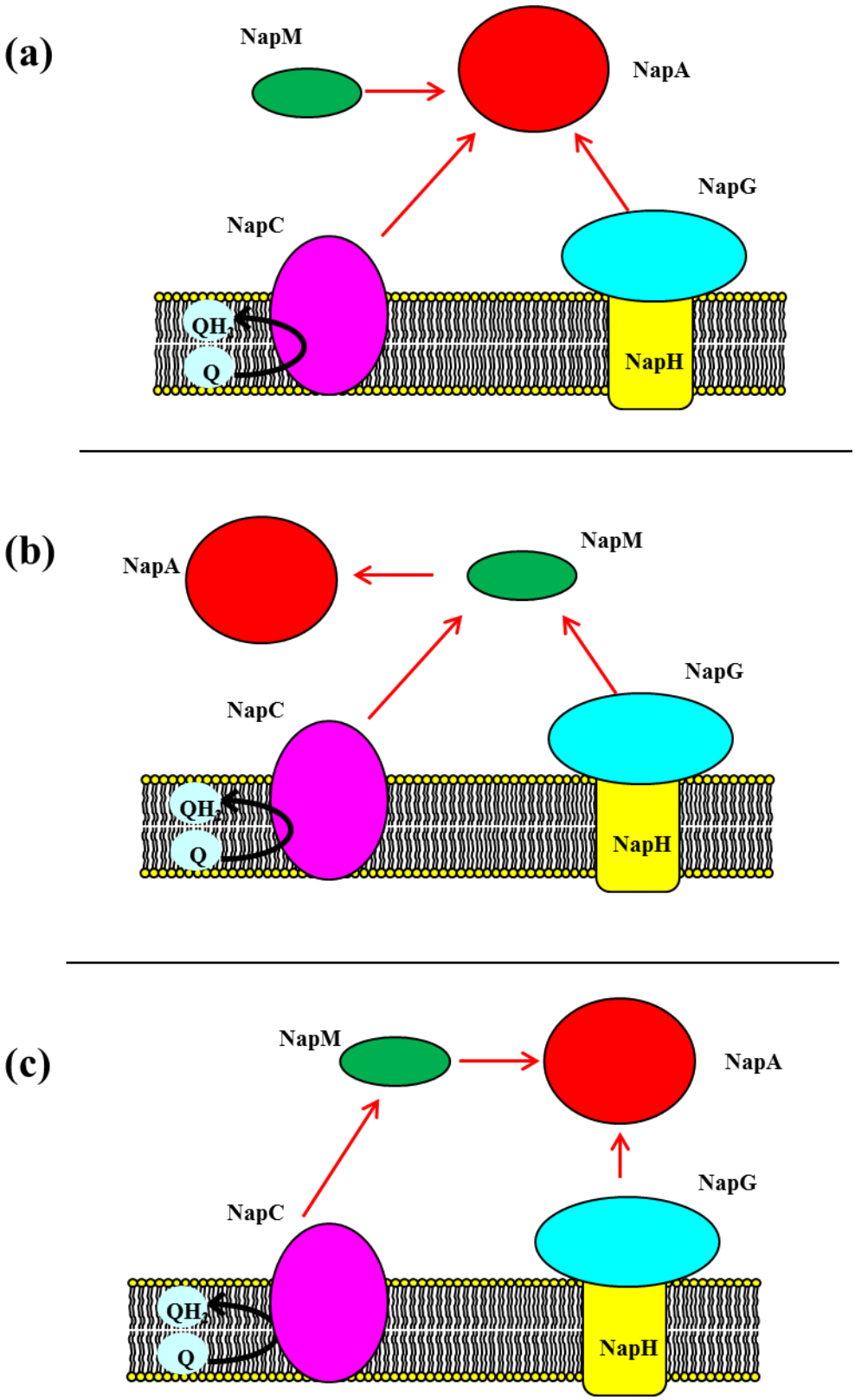

(a)
NapM
NapA
NapG
NapC
QH2
Q
NapH
(b)
NapA
NapM
NapG
NapC
QH2
Q
NapH
(c)
NapM
NapA
NapG
NapC
QH2
Q
NapH

Figure 1.3: Models of electron flow to NapA in *D. desulfuricans.* Marietou (2009) proposed three models for electron flow to NapA in the NapB independent system of *D. desulfuricans*. (a) Electrons are transferred directly to NapA from the NapM, NapC or NapGH subunits. (b) NapM serves as an adapter for NapA by receiving electrons from the NapC and NapGH subunits and then relaying them to the catalytic subunit. (c) NapM functions as a link between NapC and NapA with NapGH transferring electrons to NapA independently of NapM. Red arrows indicate electron migrations. Figure adapted from Marietou (2009).

dehydrogenases (Motteram *et al.*, 1981; Darwin *et al.*, 1993). NrfA and NrfB are both pentahaem *c*-type cytochromes and form a complex (Bamford *et al.*, 2002). NrfC and D are associated with the membrane and are believed to shuttle electrons from the quinol pool to the catalytic complex (Lockwood *et al.*, 2011). NrfA confers sufficient nitric oxide reductase activity that a *nrfA* deletion mutant shows significant sensitivity to nitric oxide (Poock *et al.*, 2002). In *D. desulfuricans* and many other bacteria the Nrf system is encoded by the *nrfHA* operon. These two subunits form a heterotrimeric complex of two NrfA subunits and a single NrfH (Almeida *et al*., 2003). NrfH is a tetra haem cytochrome with a transmembrane domain and a soluble domain. The transmembrane domain contains a single haem that is believed to oxidise the quinol pool passing electrons to the NrfA subuints via the three haem groups of the soluble domain (Almeida *et al*., 2003).

1.9 Nitric oxide and reactive nitrogen species

Bacteria, particularly those able to reduce nitrate and nitrite, are likely to encounter nitric oxide (NO) and reactive nitrogen species (RNS). A non-exhaustive list of RNS includes peroxynitrate (O_2NOO^-), peroxynitrite ($ONOO^-$), hydroxylamine (NH_2OH), nitrogen monoxide ($^{\bullet}NO$), nitroxyl (NO^-) and dinitrogen trioxide (N_2O_3) (Hill *et al.*, 2010). RNS are produced from chemical reactions in the environment and also as a product of metabolism (Vine & Cole, 2011a). The microbial ammonification pathway generates nitric oxide and RNS as side products and nitric oxide is produced as an intermediate in the denitrifrication pathway (Zumft, 1997). Bacteria are prone to exogenous nitric oxide sources since nitric oxide is a diffusible molecule. Bacteria that

reside within animal hosts will be at even greater risk of exposure due to the fact that nitric oxide is employed as a potent antimicrobial by the host innate immune system.

Various enzymes of the nitrate reduction pathway have been implicated in the generation of nitric oxide and RNS. Nrf, Nir and NarGHJI have each been described as significant sources of NO under different growth conditions (Weiss, 2006; Corker & Poole, 2003; Ji & Hollocher, 1988; Vine *et al.*, 2011). Although there are some discrepancies in the literature, it is generally accepted that NarG activity towards nitrite represents the predominant source of NO generation in *E. coli* (Vine & Cole, 2011a). The genomes of eukaryotes and some bacteria encode NO synthases that produce NO from arginine (Gusarov *et al.*, 2009).

NO and RNS are toxic to bacteria. NO reacts with proteins, typically resulting in loss of enzyme function. The protein components of the citric acid cycle are recognised as being sensitive to NO and RNS (Gardner *et al.*, 1997; Richardson *et al.*, 2011). RNS react with proteins causing nitrosation or nitration. Nitrosation results in the addition of a nitroso (-NO) group to a protein whereas nitration results in the addition of a nitro ($-NO_2$) group (Hill *et al.*, 2010). When nitric oxide reacts with a transition metal the damage is termed nitrosylation. RNS are also damaging to DNA, causing deamination or nitration of bases. The DNA damage caused by RNS must be repaired to prevent the accumulation of mutations.

1.10 Protection against nitrosative stress

Bacteria have evolved complex mechanisms for detoxifying nitric oxide and RNS. The genome of *E. coli* encodes three identified nitric oxide detoxifying enzymes (Vine &

Cole, 2011b). The flavohemoglobin, Hmp, functions as a dioxygenase of nitric oxide in aerobic conditions and a low activity nitric oxide reductase in anaerobic conditions (Gardner & Gardner, 2002). Flavohemoglobins contain both a flavin and a heme group and are believed to have a conserved function providing nitric oxide protection under aerobic conditions (Gardner, 2012; Forrester & Foster, 2012). In a recent model of Hmp activity, oxygen associates with the ferrous, Fe^{2+}, iron of the haem group and reacts with nitric oxide yielding nitrate and oxidising the iron group to the ferric, Fe^{3+}, state. The ferrous state is then restored by the FAD group using electrons donated from NADH (Forrester & Foster, 2012).

In contrast with Hmp, the flavorubredoxin, NorV, functions as a high affinity nitric oxide reductase under anaerobic conditions (Gomes *et al*., 2002). The aerobic activity of Hmp complements the anaerobic activity of NorV to provide significant protection against nitric oxide in different conditions (Gardner & Gardner, 2002; Gardner *et al.*¸2002; Vine & Cole, 2011). NorV includes domains for the binding of flavin, diiron and an iron-sulphur cluster. The *norV* gene is co-transcribed with *norW*, which encodes the cognate reductase of NorV. Electrons for the reduction of nitric oxide are relayed from NADH to NorV via NorW (Vincente *et al*., 2006). The third identified nitric oxide detoxifying enzyme of *E. coli* is NrfA. In addition to its nitrite reductase activity NrfA is able to reduce nitric oxide and hydroxylamine (Poock *et al.*, 2002; van Wonderen *et al.*, 2008). Owing to its periplasmic location, NrfA complements NorV which resides within the cytoplasm (van Wonderen *et al.*, 2008). Recent articles by Vine & Cole (2011a & 2011b) highlighted how no single enzyme complex can be attributed to nitric oxide detoxification of *E. coli* and that unidentified pathways to nitric oxide detoxification must exist in this bacterium.

In addition to enzymes responsible for the direct detoxification and reduction of nitric oxide there are a host of additional proteins that are believed to be implicated in coping with the side effects of nitric oxide or RNS exposure. YtfE, a di-iron containing protein, is implicated in the repair of protein iron-sulfur clusters damaged by nitrosative stress (Justino *et al.* 2006; Todorovic *et al.,* 2008; Vine *et al.,* 2010). The hybrid cluster protein, Hcp, has also been implicated in the response to nitric oxide and nitrosative stress although its exact role remains unclear. Hcp contains two iron-sulphur clusters: a [4Fe-4S] cluster and a novel, 'hybrid', [4Fe-2S-2O] cluster (Arendsen *et al.,* 1998). In *E. coli* the *hcp* gene is co-localised with *hcr* which encodes the cognate reductase of Hcp. Hcr, which contains an FAD and [2Fe-2S] cluster, reduces Hcp with electrons donated from NADH (van den Berg *et al.*, 2000). The *hcp* gene is annotated as encoding a hydroxylamine reductase. Activity towards hydroxylamine has been recorded for Hcp, however, it is generally accepted that this is not the native substrate of Hcp (Vine & Cole, 2011). The PhD thesis work of Vine (2012) provides evidence that *E. coli* Hcp does not function as a nitric oxide reductase but that Hcp and YtfE work synergistically to repair protein damage caused by nitric oxide.

The genome of *D. vulgaris* Hildenborough encodes two *hcp* genes that are each co-localised with *roo* genes (Johnston *et al.,* 2009). Recently it was proposed that the Hcp proteins of *D. vugaris* Hildenborough protect the electron transport chains necessary for nitrite reduction during times of nitrosative stress by removing RNS (Yurkiw *et al.*, 2012). Each Hcp protein seems to exert its effects upon specific respiratory chains with Hcp1 and Hcp2 protecting electron flow from lactate and hydrogen, respectively (Yurkiw *et al.*, 2012). These observations seem to support the suggestion by Vine (2012) that Hcp functions in repair pathways. The expression of *hcp*, *hcr*, *ytfE*, *hmp*,

norVW, *nrfA*, and the nitrate-nitrite reductases of *E. coli* are regulated at the transcription level being up-regulated under certain conditions.

1.11 Protection against oxidative stress

Reactive oxygen species (ROS) can damage bacteria in similar ways to RNS. ROS include the superoxide radical (O_2^-), hydrogen peroxide (H_2O_2) and the hydroxyl radical (HO^-), which are toxic due to their ability to react with a range of different cellular molecules. Furthermore, molecular oxygen can damage components of the sulphate reduction pathway and auxiliary enzymes (Brioukhanov *et al.*, 2010). Thus, *Desulfovibrio* species, being anaerobic bacteria, are equipped with a host of defence mechanisms for protecting themselves and their sensitive respiratory chains from the damaging effects of oxygen and ROS.

Desulfoferredoxin, Dfx, was initially identified in *D. desulfuricans* grown in the presence of nitrate (Moura *et al.*, 1990). This protein functions as a superoxide reductase and was shown to complement a superoxide dismutase deficient, *sodA-sodB*, mutant of *E. coli* (Liochev & Fridovich, 1997; Lombard *et al.*, 2000). Indeed, a Dfx mutant of *D. vulgaris* exhibited increased sensitivity to oxygen (Voordouw *et al.*, 1998).

The gene encoding Dfx is co-localised with a gene encoding a rubredoxin, Rd, and it was suggested that Rd could function as an electron donor for Dfx, thus Dfx is also known as rubredoxin oxidoreductase, Rbo (Brumlik & Vourdoow, 1989). A recent review of superoxide reductases highlighted that the expression of *dfx* seems to be constitutive in some bacteria and regulated in response to oxygen in others (Pinto *et al.*, 2010). Dfx has been linked to survival of *D. desulfuricans* in the presence of near-

atmospheric concentrations of oxygen but since the activity of Dfx does not seem to be significantly induced by exposure to these conditions it is assumed that the expression of Dfx could be constitutive in this bacterium (Lobo *et al.*, 2007).

In SRB that lack Dfx, superoxide reductase activity is provided by two other proteins. Neelaredoxin, Nlr and desulforedoxin, Dx, from *D. gigas* are non-haem iron containing proteins that are believed to form a functional couple equivalent to Dfx (Chen *et al.*, 1994; Ascenso *et al.*, 2000; Auchère *et al.*, 2006). Additionally, the Rd of *D. gigas* has been demonstrated to be involved in reduction of molecular oxygen to water (Chen *et al*., 1993; Gomes *et al*., 1997).

In some SRB there exists an enzyme pathway that catalyses the reduction of molecular oxygen to water in the cytoplasm whilst also generating energy from substrate level phosphorylation**.** In this pathway NADH is reduced by an NADH:rubredoxin oxidoreductase. Electrons are relayed via rubredoxin, Rd, to rubredoxin:oxygen oxidoreductase, Roo, which catalyses the reduction of molecular oxygen (Frazão *et al.*, 2000). Furthermore, some SRB possess a periplasmic oxygen reductase that involves a cytochrome *c* containing enzyme (Baumgarten *et al.*, 2001)**.** Thus, similar to nitric oxide reductases in *E. coli*, there are oxygen reductases in SRB that have distinct functional roles. The membrane-bound cytochrome *bd* complex also functions as an oxygen reductase in SRB (Dolla *et al.*, 2006). Additionally, there are a host of other enzymes also believed to be involved in oxygen stress in SRB including rubrerythrins, Rbr, and nygerythrins, Ngr (Figueiredo *et al.*, 2012). Many of the genes encoding these ROS stress response proteins in SRB are believed to be controlled by the transcription factor PerR (Rodionov *et al.*, 2004; Rodionov *et al.*, 2005).

1.12 The nitrate-sulphate diauxie of *D. desulfuricans*

Escherichia coli is able to grow on a variety of carbon sources and will select certain carbohydrates over others. Growth on media containing both glucose and lactose would be glucose-dependent first before lactose-dependent growth proceeds. This selection results in a characteristic growth profile consisting of two phases and is called diauxie. In being equipped to select certain carbon sources preferentially *E. coli* is able to respond to and take advantage of transient changes in its environment.

The *Desulfovibrio* species *D. desulfuricans, D. desulfuricans* C4S and *D. desulfuricans* FBA 20a are able to reduce nitrate as an alternative terminal electron acceptor to sulphate (Marietou *et al.*, 2005; Voordouw, 1995; Pietzsch *et al.*, 2003). Other *Desulfovibrio* species that can reduce nitrate for growth are *D. fulfuralis, D. profundus, D. oxamicus, D. simplex* and *D. termitidis* (Moura et al., 2007). Nitrate is reduced by these SRB by ammonification pathways (Seitz & Cypionka, 1986).

Diauxic growth is also observed when *D. desulfuricans* is grown in a medium containing a limited supply of sulphate and nitrate (Marietou *et al.*, 2009). Sulphate is eliminated from the growth medium by *D. desulfuricans* before nitrate consumption begins. Although growth is more rapid and higher yields of biomass are obtained during growth on nitrate, in media containing both sulphate and nitrate, sulphate is utilised preferentially (Marietou *et al.*, 2009). Sulphate is a thermodynamically less favourable terminal electron acceptor to nitrate, its reduction requires ATP therefore this diauxie does not seem to provide any obvious advantage to *D. desulfuricans* (Marietou, 2009). Since it is assumed that when more than one terminal electron acceptor is available in the environment bacteria will use the thermodynamically most favourable one first, the

mechanism behind this seemingly degenerate sulphate-nitrate diauxie is of interest (Zinoni *et al.*, 1984).

With respect to nitrate, sulphate and nitrite availability, the expression of *dsrAB* and *nrfHA* is reported as being constitutive whereas *napC* expression is subject to nitrate induction and repression by sulphate (Marietou *et al.,* 2009). Thus, nitrate reduction in *D. desulfuricans* is regulated at the transcriptional level. Also, nitrate reduction is subject to inhibition and/or repression by hydrogen sulphide, the end product of sulphate reduction and so the sulphate-nitrate diauxie of *D. desulfuricans* is only witnessed in cultures where sulphide is continually eliminated from the growth medium (Marietou *et al.,* 2009; Dalsgaard & Bak, 1994).

How this nitrate-sulphate diauxie functions is unknown. The presence of inverted repeat DNA sequences, similar to those targeted by CRP from *E. coli,* upstream of the *napCMADGH* transcription start site led to the proposal that a CRP homologue might, at least in part, be responsible for this diauxie (Marietou *et al.,* 2009). The *in silico* analyses by Rodionov *et al.* identified a putative CRP homologue in some SRB that is predicted to bind DNA sequences similar to those targeted by CRP (Rodionov *et al.*, 2004; Rodionov *et al.*, 2005). This regulator, named HcpR, is believed to be responsible for regulating expression of *hcp, sat* and *aprBA* in *D. vulgaris* and *Desulfovibrio* G20. These research articles pre-dated the publication of the *D. desulfuricans* genome sequence and so whether *D. desulfuricans* encodes an HcpR protein was unknown. However, if an HcpR or CRP protein were present in *D. desulfuricans* it would represent an obvious candidate for controlling the sulphate-nitrate diauxie of *D. desulfuricans* by modulating expression of *nap* (Marietou *et al.,* 2009).

Interestingly, and in a clear parallel with this hypothetical model, CRP plays a crucial role in regulating operons specific to carbon source utilisation by *E. coli*. Thus, in contemplating the sulphate-nitrate diauxie of *D. desulfuricans* it is worthwhile to consider the glucose-lactose diauxie of *E. coli* and transcription regulation by CRP.

1.13 The paradigm of diauxie: carbon source utilisation by *Escherichia coli*

The phenomenon of diauxie was discovered by Jacques Monod and represents a major breakthrough in our understanding of how bacteria adapt to their surroundings (Monod, 1966). In assessing any other diauxie it is prudent to consider this paradigm, which is actually a combination of three inter-linked processes: catabolite repression, inducer exclusion and transient repression.

Catabolite repression, also known as the glucose-effect, is the process of glucose inhibiting the expression of genes necessary for the utilisation of other, less preferable, carbon sources when both are present in the growth medium. This repression effect by glucose is so profound that the addition of glucose to cultures readily utilising an alternative carbon source causes growth upon that carbon source to cease and switch to glucose utilisation. This switch is known as transient repression. Glucose also inhibits the uptake of other, less preferable, carbon sources in a process termed inducer exclusion.

Central to these processes is the activity of the phosphoenolpyruvate (PEP) carbohydrate phosphotransferase system (PTS), which is responsible for the transport of

carbohydrates into the cell. Carbohydrates are concomitantly phosphorylated during uptake by the PEP-PTS (Figure 1.4). This phosphate group, derived from PEP, is relayed through a series of proteins to PEP-PTS carbohydrate-specific enzyme complexes (EII complexes), which are responsible for the uptake of specific carbohydrates. The $EIIABC^{Glc}$ complex is specific for the uptake of glucose. Phosphate is relayed to the membrane-spanning $EIIBC^{Glc}$ components of the complex. When present in the environment, glucose is transported into the cell by $EIIBC^{Glc}$ and is simultaneously phosphorylated to glucose-6-phosphate.

Crucial to carbohydrate diauxie is the ability of $EIIA^{Glc}$ and phospho-$EIIA^{Glc}$ to interact with components of other carbohydrate uptake systems and influence their activities. $EIIA^{Glc}$ has an inhibitory effect upon the PTS-independent uptake systems, whereas phospho-$EIIA^{Glc}$ activates the enzyme adenylate cyclase, which converts ATP to cyclic-AMP (cAMP). Thus, in the presence of glucose the flow of phosphate through the PEP-PTS system will be sustained and the dephosphorylated form of $EIIA^{Glc}$ will be predominant. In turn, the uptake of PTS-independent sugars will be inhibited. In an absence of glucose a traffic-jam scenario occurs where phosphate cannot be passed to glucose and so the components of the PEP-PTS system will become phosphorylated. The inhibitory effects of dephosphorylated $EIIA^{Glc}$ upon PTS-independent uptake systems will now be relinquished so other sugars, such as lactose, may be imported. Furthermore, phospho-$EIIA^{Glc}$ will stimulate cAMP production (reviewed by Postma, 2000).

Thus, the levels or ratio of $EIIA^{Glc}$ and phospho-$EIIA^{Glc}$, which are in part dictated by the rate of glucose uptake and phosphorylation, have distinct physiological effects. The

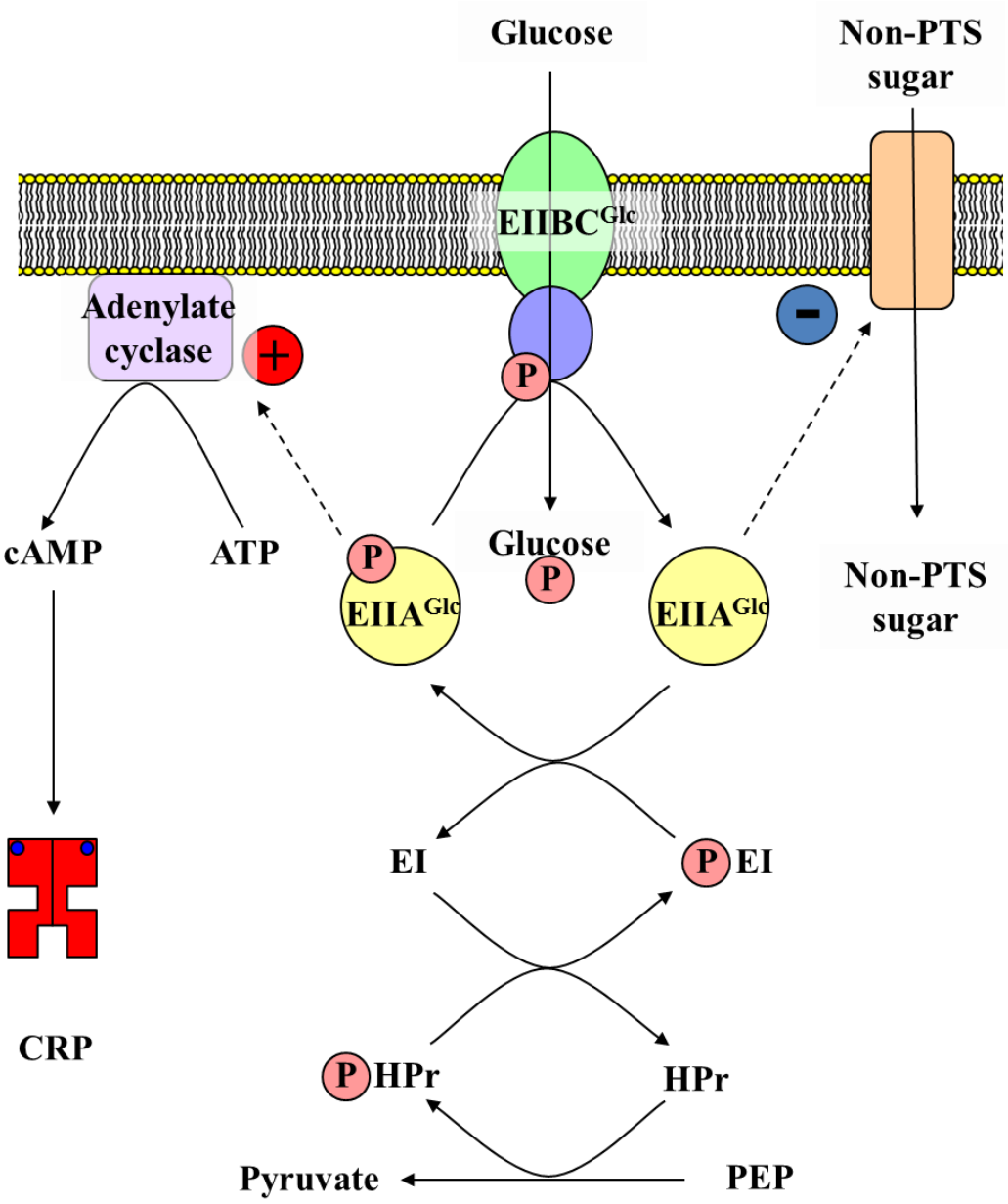


Figure 1.4: Overview of the regulation of adenylate cyclase activity and the uptake of non-PTS sugars by the PEP-PTS. Figure adapted from Postma, 2000. Phosphate is relayed to carbohydrate-specific complexes by a series of proteins. $EIIA^{Glc}$ and Phospho-$EIIA^{Glc}$ have different activities resulting in the inhibition of alternative carbohydrate uptake when glucose is present and induction of adenylate cyclase activity when glucose is absent. For details refer to the text.

intracellular levels of cAMP and PTS-independent sugars have profound effects upon gene expression. Intracellular lactose is sensed by the *lac* repressor transcription factor which leads to de-repression of the lactose utilisation (*lac*) operon. cAMP is the allosteric effector molecule of the global transcription regulator, CRP. Its presence stimulates DNA binding activity by CRP which has a positive effect upon the transcription of a number of sugar utilisation operons, including the *lac* operon. However, the influence of CRP reaches far beyond just carbon source utilisation and so we shall consider this transcription regulator in detail.

1.14 Transcription regulation by CRP

CRP: regulation by an allosteric effector

The cAMP responsive protein, CRP, also known as the catabolite activator protein, CAP, is a global gene regulator in *Escherichia coli*. CRP has three functional domains: the N-terminus cAMP binding domain, a short flexible hinge region, and a C-terminal DNA binding domain (Figure 1.5). In solution CRP exists as a homodimer with each monomer associating via a dimerisation interface formed by an α helix from each monomer known as the C-helix (Harman, 2001). DNA binding is mediated by the DNA recognition helices of the DNA binding domain which have a helix-turn-helix motif. Structures for CRP in different conformations have provided insight into the mechanism behind its activity.

In an absence of cAMP, apo-CRP has non-specific, weak, DNA binding activity (Katouzian-Safadi *et al.*, 1993). The C-helices of apo-CRP form two coiled coils that are fifteen residues in length, the DNA recognition helices are aligned in a linear

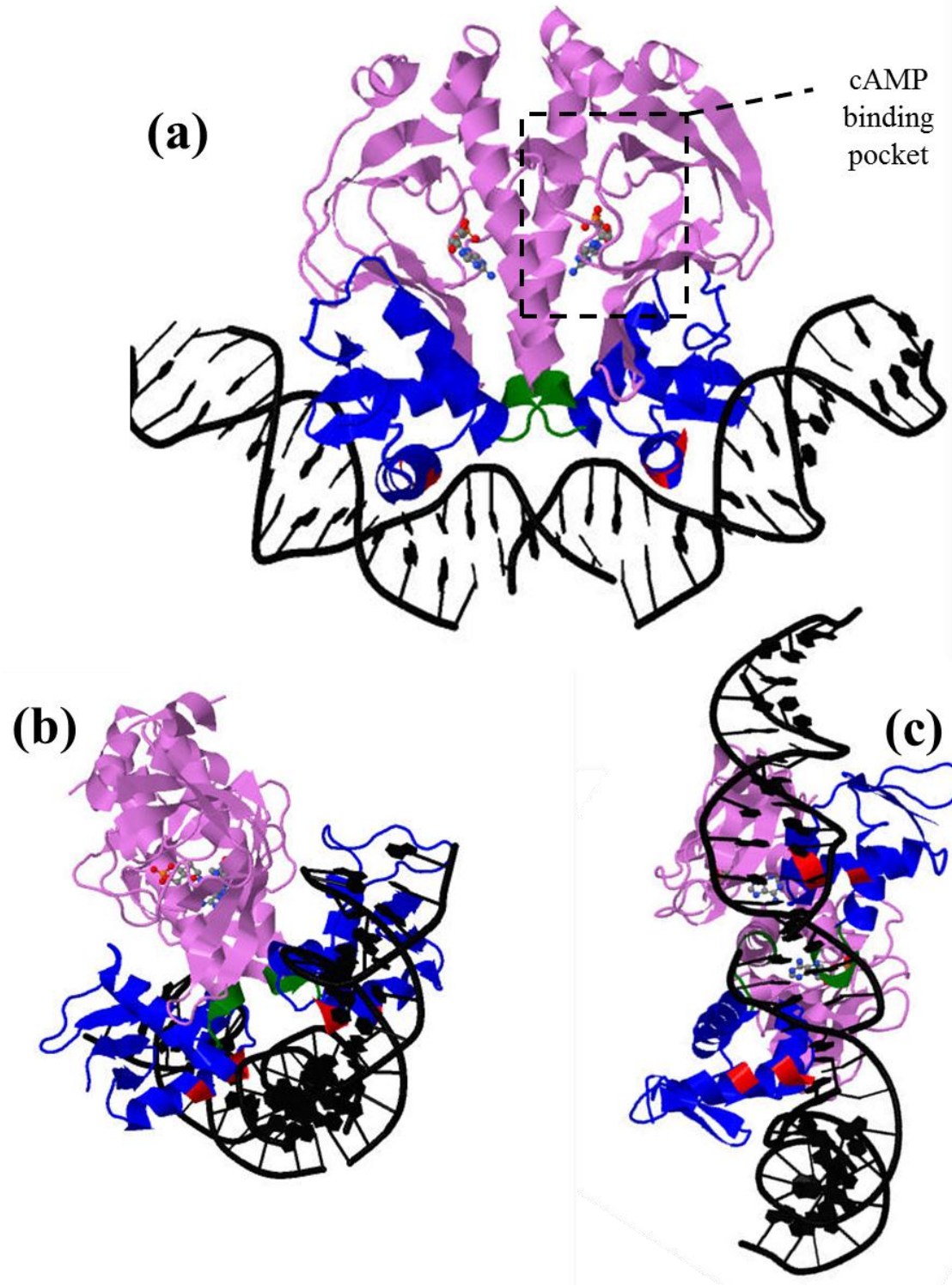

(a)
cAMP
binding
pocket
(b)
(c)

Figure 1.5: The crystal structure of the cAMP-CRP-DNA complex. (a) Complex structure viewed as a cartoon. Dimeric CRP binds to DNA and cAMP with each monomer binding a molecule of cAMP and associating with the DNA target via interactions between the DNA recognition helix and the major groove of the double helix. **(b)** Structure rotated 90 º horizontally. **(c)** Structure rotated 90 º vertically. Note the parallel arrangement of the DNA recognition helices. N-terminal cAMP binding domain is coloured violet, hinge region is coloured green, DNA binding domain is coloured blue, important DNA recognition residues 180, 181 and 185 are coloured red and DNA is shown in black (Parkinson *et al.*, 1996).

arrangement, and two residues of the cAMP binding pocket, a threonine and a serine, are pointing away from the cAMP binding site (Popovych *et al.*, 2009). The key reason for the poor DNA binding qualities of apo-CRP is the linear arrangement of the DNA binding helices that is not a suitable conformation for fitting into the major grooves of the DNA double helix. Indeed, the DNA recognition helices are tucked up against the protein and can be described as being buried and solvent inaccessible (Sharma *et al.*, 2009; Popovych *et al.*, 2009).

Upon binding cAMP an allosteric change takes place that is transmitted throughout the protein structure (an overview of this transition is depicted in Figure 1.6). The most notable changes are that cAMP binding causes the threonine and serine residues of the cAMP binding pocket, with which cAMP hydrogen bonds, to change orientation. This reorientation is believed to be the cause of structural isomerisation of residues adjacent to the C-helices, which result in the C-helices extending in length by three turns (Popovych *et al.*, 2009). This change causes further interactions between the cAMP binding domain and the DNA binding domain to be established. This extension of the C-helices result in re-orientation of the DNA recognition helices which move from a linear, solvent inaccessible arrangement, to become parallel and solvent accessible so that they may interact with the major grooves of the DNA double helix (Popovych *et al.*, 2009; Sharma *et al.*, 2009).

There is some dispute over the structure of apo-CRP as multiple conformations have been proposed. In one structure, apo-CRP is an asymmetric dimer with the DNA recognition helices of each monomer being mis-aligned (Sharma *et al.*, 2009). This asymmetry between recognition helices is believed to be critical for the dissociation of

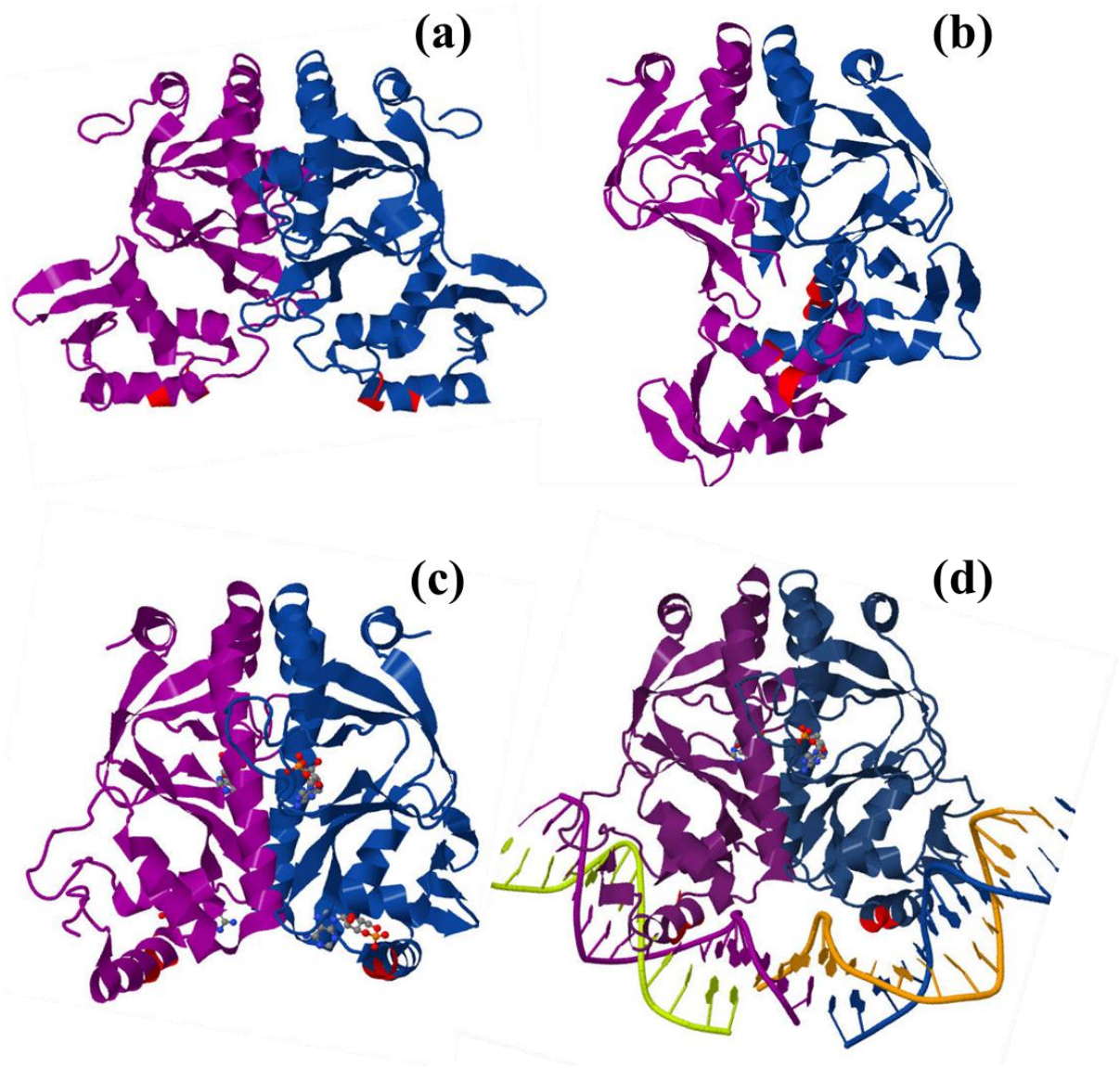


Figure 1.6: The binding of the allosteric effector cAMP to CRP causes a conformational change (a) apo-CRP structure with linear arrangement of DNA recognition helices, **(b)** alternative structure of apo-CRP with obvious asymmetry between the CRP monomers, **(c)** structure of cAMP-CRP complex, **(d)** structure of the cAMP-CRP-DNA complex. Note that specifc DNA binding is not possible in either structure (a) or (b), but that once cAMP is bound as in (c) and (d) the DNA recognition helices run parallel to each other and favour DNA binding. (Popovych *et al.*, 2009; Sharma *et al.*, 2009; Parkinson *et al.*, 1996).

CRP target DNA (Gallagher *et al.*, 2009). The variation between apo-CRP structures is probably due to some degree of disorder in the absence of effector.

The DNA targets of CRP

Following the conformational changes mediated by cAMP binding to CRP, holo-CRP binds to target DNA sites, usually within the regulatory region of a gene, and modulates transcription by repression or activation. The consensus sequence of DNA sites targeted by CRP is an inverted repeat sequence: TGTGA[N_6]TCACA (de Crombrugghe *et al.*, 1984). Each CRP monomer contacts one half of the inverted repeat sequence (Schultz *et al.*, 1991). The major contacts are hydrogen bonds between arginine, glutamic acid, and arginine residues at positions 1, 2 and 6 of each DNA recognition helix and DNA phosphate groups across the DNA target site (Parkinson *et al.*, 1996). DNA binding by CRP results in a bend of approximately 90° in the target DNA (Parkinson *et al.*, 1996). The affinity of CRP for a DNA target site is determined by its sequence. Deviations from the consensus sequence generally result in decreased affinity for that particular site.

Activation and repression of transcription by CRP

CRP is able to activate transcription by a variety of direct interactions with RNA polymerase (RNAP). Activation by CRP and CRP-activated promoters can be classified as class I, class II or class III depending upon the type of CRP-RNAP interaction and the distance between the RNAP and CRP binding sites (Figure 1.7). Activation at either class I or class II promoters is achieved by a single CRP dimer bound within the promoter regulatory region, whereas class III promoters require more than one CRP dimer or some other auxiliary factor (Busby & Ebright, 1999).

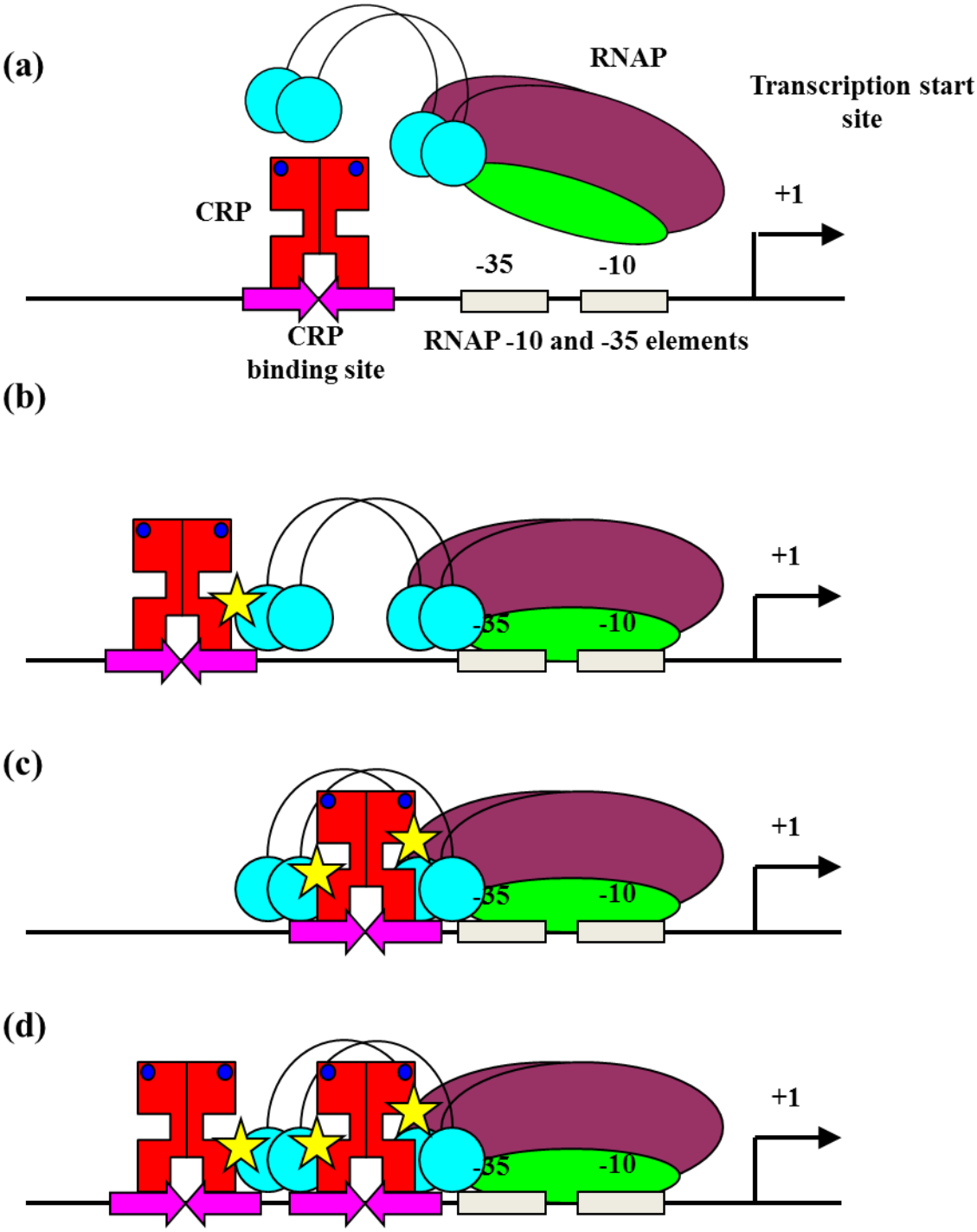


Figure 1.7: Overview of the regulation of transcription by CRP. (a) CRP repressing transcription by steric hinderance of RNAP, **(b)** class I activation by CRP, **(c)** class II activation by CRP and **(d)** class III activation by CRP (figure adapted from Browning & Busby, 2004). Refer to text for details.

At class I promoters CRP enhances binding of RNAP to DNA by interacting directly with the RNAP α subunit C-terminal domain (CTD). For CRP to act as a Class I activator it must bind promoter DNA upstream of RNAP. CRP interacts with RNAP αCTD via CRP residues 152-166, known as activating region 1 (AR1) (Zhou *et al.*, 1993). In class I activation only the downstream CRP monomer interacts with RNAP and this interaction has been characterised by structural analyses (Ebright, 1993; Hudson *et al.*, 2009; Benoff *et al.*, 2002).

At class II promoters CRP binds promoter DNA near to, and actually obscuring, the -35 site for RNAP. RNAP binds DNA downstream of CRP but the αCTD, which is joined to the α subunit N-terminal domain (αNTD) by a flexible linker**,** binds DNA upstream of CRP. The RNAP α subunit can be described as straddling CRP. The downstream-orientated CRP monomer interacts with αNTD via activating region 2 (AR2), which is comprised of CRP residues 19, 21, 96, and 101 (Niu *et al.*, 1996). Simultaneously, the AR1 of the upstream-orientated CRP monomer can interact with αCTD (Zhou *et al.*, 1994; Rhodius *et al.*, 1997). These two different interactions of CRP with RNAP reflect two different mechanisms of transcriptional activation at class II promoters, AR1-αCTD interactions or AR2-αNTD interactions resulting in activation by anti-inhibition or direct activation, respectively (Busby and Ebright, 1997).

Class III activation involves CRP to interact with RNAP via a class I or class II mechanism and the influence of an additional transcription factor. The *acs* gene, which encodes a protein involved in acetate utilisation, can be activated by a class III mechanism dependent upon the binding of CRP to two locations at the *acs* promoter (Beatty *et al.*, 2003). A CRP dimer bound to DNA at -69.5 makes class I interactions

with RNAP sufficient for activation but for maximal expression of *acs* a second CRP dimer must be bound at -122.5 where additional class I interactions can be mediated (Beatty *et al.*, 2003).

Repression of transcription by CRP may be by steric hindrance of RNAP binding. In this situation, CRP binding occludes the DNA elements to which RNAP binds. Repression may also be caused by CRP contributing to the bending of DNA into a looped or 'closed' structure, again restricting RNAP access to DNA. Repression may also be cooperative, being mediated by CRP and some additional transcription regulator (Browning & Busby, 2004). At some loci CRP interacts with the cytidine regulator, CytR, which is a transcription repressor. CytR, a homodimeric protein, is unable to exert an influence upon transcription directly and is dependent upon CRP (Søgaard-Andersen *et al.*, 1993). Promoters regulated by CytR typically have two sites for CRP binding where CRP may act as an activator. CytR, in an absence of cytidine, binds to both CRP dimers occluding promoter elements and surface areas of CRP necessary for activation of transcription. Cytidine, the allosteric effector of CytR, binds to CytR causing structural changes that abolish interactions with CRP. Thus, CRP and CytR work synergistically at some promoters (Valentin-Hansen *et al.*, 1996).

The *Escherichia coli* CRP regulon

As mentioned previously, CRP regulates the expression of genes involved in carbon metabolism. However, CRP is a global regulator of transcription in every sense. CRP is involved in the regulation of genes for osmoregulation, biofilm formation, virulence, nitrate reduction and antibiotics resistance in addition to genes involved in central metabolism (Balsalobre *et al.*, 2006; Jackson *et al.*, 2002; Nishino *et al.*, 2008; Stewart

et al., 2009; Khankal *et al.*, 2009). In addition, CRP is an autoregulator, repressing transcription of *crp*.

The number of targets for CRP in *E. coli* has been predicted to be as many as two hundred. A comparative transcriptome analysis in *E. coli* identified differential expression of 231 genes between *crp*+ and *crp*- strains (Khankal *et al.*, 2009). That study relied upon expression of mutant CRP protein with constitutive DNA binding activity. It is possible that false-positives were recorded. Sixty-eight targets were identified in an investigation using chromatin immunoprecipitation and microarray analysis (ChIP-chip) to measure CRP binding *in vivo* throughout the *E. coli* chromosome (Grainger *et al.*, 2005). This number is likely to be an under-representation of the true number of CRP binding sites as high levels of background CRP binding signal were recorded. This high background signal for CRP is believed to be the result of CRP binding to the thousands of low-strength CRP sites scattered throughout the CRP chromosome (Grainger *et al.*, 2005). Thus, due to technical limitations, it is unlikely that the true number of CRP binding sites can be identified.

Adaption to anaerobic growth by FNR

Another *E. coli* global gene regulator, the fumarate and nitrate reductase regulator protein (FNR), has structural resemblance to CRP. Like CRP, FNR is made up of distinct functional domains including an N-terminal ligand binding domain, a dimerisation domain and a C-terminal DNA binding domain (Bell *et al.*, 1989). However, despite these similarities, FNR and CRP are distinct from one another in the way that their particular signals are perceived. Whilst CRP receives its signal via the

binding of a secondary messenger molecule, FNR senses an effector molecule via its iron-containing prosthetic group.

The N-terminal region of FNR is cysteine rich with four of these residues being important for the coordination of iron-sulphur clusters. FNR binds a single [4Fe-4S] or [2Fe-2S] cluster per monomer (Khoroshilova *et al.*, 1997). The oligomerisation state of FNR is dependent upon the type of cluster it is bound to. Under anaerobic conditions FNR binds to [4Fe-4S] clusters and forms homodimers with specific DNA binding activity towards DNA sequences conforming to the consensus TTGAT[N_4]ATCAA (Bell *et al.*, 1989; Moore & Kiley, 2001). When bound to target DNA, FNR may regulate gene expression in a manner similar to CRP. Expression may be activated or repressed by FNR and activation may be divided into different classes according to the type of FNR-RNAP interactions and the distance between RNAP and FNR binding sites (Wing *et al.*, 1995).

Many of the genes regulated by FNR encode products that are involved in the switch between aerobic and anaerobic growth and the [4Fe-4S] cluster is critical in this switch (Grainger *et al.*, 2007). Oxygen sensing by FNR is mediated by its [4Fe-4S] clusters that are extremely sensitive to oxygen and reactive oxygen species. Under anaerobic conditions dimeric FNR containing [4Fe-4S] clusters influences transcription. Upon exposure to oxygen the [4Fe-4S] cluster undergoes a two stage conversion to a [2Fe-2S] cluster (Crack *et al.*, 2008). First, a [3Fe-4S] cluster is formed by oxidation with a single electron from oxygen. Iron is released as Fe^{2+} and molecular oxygen, on losing an electron, forms superoxide (O_2^-). Following this oxygen dependent step the [3Fe-4S] cluster spontaneously converts to a [2Fe-2S] cluster independently of oxygen. This

second step releases Fe^{3+} and two sulphide ions (S^{2-}) (Crack *et al.*, 2008). Once the conversion to a [2Fe-2S] cluster is complete the FNR dimer dissociates into monomers resulting in a decrease in specific DNA binding by the protein (Lazazzera *et al.*, 1996).

The regulon of FNR includes up to one hundred targets that are directly regulated with the number of indirectly regulated targets numbering up to a thousand (Constantinidou *et al.*, 2006; Grainger *et al.*, 2007). Major targets for FNR include nitrate reductase genes, nitrite reductase genes, nitrosative stress genes, and genes for superoxide dismutase. FNR works concurrently with CRP at the *ansB* and *napF* promoters (Jennings *et al.*, 1993; Stewart *et al.*, 2009). Like CRP, FNR homologues may be found in many bacteria. In fact CRP and FNR are the best known representatives of a superfamily of gene regulators; the CRP/FNR family of transcription regulators.

1.15 Transcription regulators implicated in nitrate-nitrite dependent growth of *E. coli.*

The expression of genes encoding nitrate/nitrite reductases and associated proteins in *E. coli* are under tight control by a host of transcription factors that includes FNR. An understanding of this regulatory network provides insight for the study of similar pathways and stress responses in other bacteria.

The NarXL and NarQP two-component regulatory systems respond directly to the presence of nitrate and nitrite. The sensor histidine kinases NarX and NarQ autophosphorylate in the presence of nitrate or nitrite and, in turn, phosphorylate the response regulators NarL and NarP. Phosphorylation of NarL and NarQ results in an increase in their DNA binding affinities. Once bound to their specific DNA targets NarL

and NarQ can modulate the expression of target genes by activation or repression (Rabin & Stewart, 1993; Stewart, 1993). The activity of NarX is stimulated to a greater extent by nitrate than by nitrite whereas NarQ exhibits no significant bias (Noriega *et al.*, 2010). Furthermore, cross-talk between the two systems occurs. NarX and NarQ are able to function as kinases and, under certain circumstances, phosphatases for either response regulator (Noriega *et al.*, 2010). Thus, the NarXL and NarQP systems are extremely versatile mediating a fine-tuned response to nitrate and nitrite.

The nitrite sensitive repressor, NsrR, binds a [2Fe-2S] cluster that is sensitive to nitric oxide (Tucker *et al.*, 2008). NsrR functions as a repressor binding to DNA targets upstream of a range of genes including *hcp*, *ytfE*, *nrf* and *hmp* (Filenko *et al.*, 2007). In the presence of nitric oxide this DNA binding affinity is relinquished allowing transcription of the associated genes (Tucker *et al.*, 2010). NsrR is from the Rrf2 family of transcription factors as is the iron-sulphur cluster assembly regulator, IscR. Like NsrR, IscR also binds a [2Fe-2S] cluster which can be lost from the protein on exposure to oxygen. Interestingly, there are two different DNA binding sites for IscR: those bound by IscR containing the cluster and those lacking the cluster. Thus the activity of IscR is not modulated by a loss of DNA binding activity but by a change in its activity when bound to DNA. IscR functions as a repressor of *nap* in *E. coli* (Giel *et al.*, 2006).

The oxidative stress response regulator, OxyR, responds to intracellular redox state. Redox state is sensed by OxyR via two cysteine residues that form a disulphide bond under oxidising conditions. These cysteines also function as sensors of nitric oxide as they are sensitive to S-nitrosylation (Seth *et al.*, 2012). Similar to IscR, OxyR retains its DNA binding activity in the presence or absence of its signal.

Unlike the iron-sulphur cluster binding proteins, NsrR and FNR, the nitric oxide responsive regulator NorR senses nitric oxide via a non-haem iron cofactor (D'Autreaux *et al.*, 2005). Nitric oxide functions as the allosteric effector of NorR, a protein which is composed of three domains: the cofactor-binding N-terminal GAF domain, a central ATPase AAA+ domain and a C-terminal H-T-H DNA binding domain (Bush *et al.*, 2011). NorR is able to activate transcription from the sigma-54 dependent *norVW* promoter (Gardner *et al.*, 2003). Transcription from sigma-54 promoters is reliant upon interactions between the RNAP-sigma-54 complex and DNA-binding activator proteins. Typically, these activator proteins bind to DNA sites 100-150 bp upstream of the RNAP-sigma-54 consensus DNA binding sites that are centred at -12 and -24 from the transcription start site (Lee *et al.*, 2012). Significant DNA bending, usually imparted by an additional transcription factor such as the integration host factor, IHF, is required for these activator proteins to make contact with sigma-54 from this relatively large distance. The activity of NorR at the *norVW* represents a fine example of sigma-54 dependent transcription.

NorR dimers bind to three sites upstream of the *norVW* promoter and are believed to form a homohexamer (Tucker *et al.*, 2004; Bush *et al.*, 2011). IHF binds to a single site between NorR and RNAP-sigma-54, introducing a bend in the DNA that brings the NorR multimer and RNAP-sigma-54 into close proximity with one another (Tucker *et al.*, 2004). In an absence of nitric oxide the ATPase activity of the NorR AAA+ domains is inhibited by the GAF domains which prevent ATP hydrolysis by intramolecular inhibition. The binding of nitric oxide to the NorR iron co-factor triggers a conformational change that relieves this inhibition leading to ATP hydrolysis which in turn drives interactions with- and conformational changes in- sigma-54 (D'Autreaux *et*

al., 2005). This conformation change of sigma-54 drives open complex formation by RNAP-sigma-54 and transcription of the *norVW* operon (Tucker *et al.*, 2010). Since the *norR* and *norVW* promoters are divergent from each other the NorR binding sites are positioned sufficiently for auto-repression of *norR* expression (Tucker *et al.*, 2006).

There is a multitude of transcription factors regulating the expression of nitrate reductases, nitrite reductases and auxiliary proteins related to these pathways in *E. coli.* Similar, complex regulatory networks would be expected to be underpinning these pathways in other bacteria also.

1.16 Aims and objectives

HcpR is predicted to regulate the transcription of genes responsible for sulphate reduction and nitrosative stress response in *Desulfovibrio* species. Furthermore, an HcpR protein or some other CRP-like transcription factor, is predicted to regulate the expression of *nap* in *D. desulfuricans*, a process central to sulphate-nitrate diauxie. The initial aim of this study was to identify transcription networks involved in regulating these processes in *D. desulfuricans. In silico* methodologies were be used to identify genes encoding putative CRP family proteins in *D. desulfuricans* and their cognate DNA target sites. Scanning the *D. desulfuricans* genome with these DNA sequences allowed the identification of putative regulons. In turn, this allowed the CRP homologues to be assessed for involvement in nitrosative stress and diauxie. Homologues of known nitrostive stress response genes are also identified.

Another aim of this study was to resolve the controversies regarding terminal electron acceptor utilisation by *D. desulfuricans.* Conflict in the literature was addressed in a series of physiological experiments and transcription measurements. Growth in the presence of combinations of terminal electron acceptors was observed and the expression of genes involved in their metabolism was quantified. These endeavours confirmed the nature of terminal electron acceptor selection by *D. desulfuricans*.

The final aim of this study was to characterise transcription factors believed to be responsible for the regulation of diauxie and nitrosative stress. A combination of *in vitro* and *in vivo* analyses provided insight into the properties and mode of action of these transcription factors. The results presented here are evaluated with consideration of the current literature and discussed within the context of bacterial survival strategies.

Chapter 2

Materials and methods

2.1 Growth of bacteria

Growth of *D. desulfuricans*

Liquid cultures of *D. desulfuricans* ATCC27774 were grown anaerobically in sterile Postgate media in sealed serum bottles at 30 ºC (Postgate, 1984). Glycerol stocks of *D. desulfuricans* ATCC27774 that had been stored at -80 ºC were revived by culturing into the sulphate-containing Postgate B (PgB) medium (KH_2PO_4, 0.5 g l^{-1}; NH_4Cl, 1 g l^{-1}; Na_2SO_4, 1 g l^{-1}; $CaCl_2.6H_2O$, 0.1 g l^{-1}; $MgSO_4.7H_2O$, 2 g l^{-1}; Sodium lactate, 3.5 g l^{-1}; Yeast extract, 1 g l^{-1}; Ascorbic acid, 0.1 g l^{-1}; $FeSO_4.7H_2O$, 0.5 g l^{-1}; Thioglycolic acid, 0.1 g l^{-1}; pH 7.0). Lactate functions as the electron donor and sulphate as the electron acceptor in this medium. PgB was not used for growth experiments as it contains ferrous salts that form a black precipitate with sulphide.

Postgate Zero (PgZ) medium (KH_2PO_4, 0.5 g l^{-1}; NH_4Cl, 1 g l^{-1}; $CaCl_2.6H_2O$, 0.1 g l^{-1}; $MgCl_2$, 2.5 g l^{-1}; Sodium lactate, 3.5 g l^{-1}; Yeast extract, 1 g l^{-1}; Ascorbic acid, 0.1 g l^{-1}; $FeCl_3$, 0.05 g l^{-1}; pH 7.0) was used for growing *D. desulfuricans* when it was necessary to measure cell densities or to culture *D. desulfuricans* with terminal electron acceptors other than sulphate. PgZ contains very low levels of ferrous salts and so does not form a black precipitate when sulphide is present. Since PgZ does not contain any sulphate it was possible to supplement this medium with different terminal electron acceptors at different concentrations as necessary and thus represented the base medium for all growth experiments.

Sealed serum bottles of media were flushed with N_2 gas prior to inoculation to provide an anaerobic environment. Generally, cultures of *D. desufuricans* that had grown for 48 hours or until stationary phase were used as inoculum. Cultures were

seeded with 5 % or 10 % inoculum as necessary and for some growth experiments it was necessary to adjust the amount of inoculum to provide consistent optical densities at the start of growth experiments. Often it was also necessary to flush the cultures with N_2 gas following inoculation. This was particularly necessary when sulphate or sulphite grown cultures, which contain sulphide, were used to inoculate nitrate-containing medium. Culture purity was assessed by Gram staining, inoculating solid Lennox Broth media with culture and then incubating at 30 ºC aerobically and also by sub-culturing into PgB and then checking the formation of a black precipitate.

Growth of *E. coli*

Escherichia coli strains were used for various applications and the strains used in this study are detailed in Table 2.1. *E. coli* strains were used as hosts for recombinant plasmids, overexpression of recombinant proteins and for β-galactosidase assays. Two types of media were used for culturing *E. coli*: Lennox Broth and M9 salts. Lennox Broth (tryptone, 10 g l^{-1}; yeast extract, 5 g l^{-1}; NaCl, 5 g l^{-1}) was used for general culture of *E. coli* for plasmid production, protein production, or for generating inocula for other experiments. M9 minimal salts medium was used for growing *E. coli* for β-galactosidase activity assays. One hundred ml of 1x M9 medium was prepared from a sterile 10x concentrated stock (60 g l^{-1} Na_2HPO_4; 30 g l^{-1} KH_2PO_4; 5 g l^{-1} NaCl; 10 g l^{-1} NH_4Cl; 10 mg l^{-1} Biotin; 10 mg l^{-1} thiamine; pH 7.4) supplemented with sterile additives (200 µl 1 M $MgSO_4$; 100 µl 0.1 M $CaCl_2$; 0.5 ml 20 % casamino acids; 20 % fructose). Agar plates of these different media were created by supplementing with agar (12 g l^{-1}). When necessary, media were supplemented with antibiotics or inducers such as carbenicillin (100 µg ml^{-1}), kanamycin (75 µg ml^{-1}), tetracycline (30 µg ml^{-1}),

Table 2.1: Strains used in this study

Strain	Genotype	Source
M182	Δ*(lac* I*POZY)* X74, *gal* K, *gal* U, *str* A	Casadaban & Cohen (1980)
M182 Δ*crp*	Δ*crp* derivative of M182	Busby *et al.* (1983)
JM109	*endA1, recA1, gyrA96, thi, hsdR17 (rk–, mk+), relA1, supE44, Δ(lac-proAB), [F′ traD36, proAB, laqIqZΔM15]*	Promega
BL21 star (DE3)	$F^{'}$ *ompT hsdS* $_B$ *(*r_B^- m_B^-*) gal dcm* λ(DE3 [*lacI lacUV5 -T7 gene 1 ind1 sam7 nin5*])	Studier & Moffatt (1986)
D. desulfuricans	Wild-type strain	Postgate (1984)

Table 2.2: Plasmids used in this study		
Plasmid	**Description**	**Source**
pET21(a)+	High copy number plasmid for protein overexpression. Contains a multiple cloning site for in-frame fusions of genes to sequences encoding a His-tag. $Carb^R$.	Novagen
pETHcpR	pET21a(+) derivative containing the *D. desulfuricans* Ddes_0528 ORF minus the stop codon. Used for overexpression of His-tagged HcpR protein and for heterologous expression of HcpR in *E. coli* strains harbouring pRW50 derivatives.	This work.
pETHcpR2	pET21a(+) derivative containing the *D. desulfuricans* Ddes_1827 ORF minus the stop codon. Used for overexpression of His-tagged HcpR2 protein.	This work.
pGEM T-easy	High copy number plasmid supplied linearised with T-overhangs flanking a multiple cloning site. Used for restriction-free cloning of PCR products. $Carb^R$.	Promega
pT*napWT*	pGEM T-easy derivative containing the ATG start codon of *napC* from *D. desulfuricans* and an additional 257 bp of upstream DNA sequences. The *nap* promoter sequences are flanked with HindIII and EcoRI restriction sites for generating DNA fragments for EMSAs and DNaseI footprinting assays.	Marietou (2009)
pT*sat*	pGEM T-easy derivative containing promoter sequences of *sat* from *D. desulfuricans.*	This work.
pT*hcpR*	pGEM T-easy derivative containing promoter sequences of *hcpR* from *D. desulfuricans.*	This work.
pT*apr*	pGEM T-easy derivative containing promoter sequences of *aprB* from *D. desulfuricans.*	This work.
pT1825	pGEM T-easy derivative containing promoter sequences of *Ddes_1825* from *D. desulfuricans.*	This work.
pT*hcpR2*	pGEM T-easy derivative containing intergenic DNA sequences between Ddes_1826 and *hcp* from *D. desulfuricans.*	This work.
pTAM01	pGEM T-easy derivative containing a truncated copy of the *nap* promoter sequence (fragment AM01).	Marietou (2009)
pTAM02	pGEM T-easy derivative containing a truncated copy of the *nap* promoter sequence (fragment AM02).	Marietou (2009)
pTAM03	pGEM T-easy derivative containing a truncated copy of the *nap* promoter sequence fragment AM03).	Marietou (2009)

Table 2.1: Plasmids used in this study (continued)		
Plasmid	**Description**	**Source**
pTAM04	pGEM T-easy derivative containing a truncated copy of the *nap* promoter sequence (fragment AM04).	Marietou (2009)
pRW50	Vector containing a multiple cloning site upstream of *lacZ* for creating promoer::*lacZ* fusions. Tet^R.	Lodge *et al.* (1992)
pRW*nap*	pRW50 derivative containing the *nap* promoter fused to *lacZ*.	Marietou (2009)
pRW*apr*	pRW50 derivative containing the *aprB* promoter fused to *lacZ*.	This work.
pRW*hcpR*	pRW50 derivative containing the *hcpR* promoter fused to *lacZ*.	This work.
pRW*sat*	pRW50 derivative containing the *sat* promoter fused to *lacZ*.	This work.

chloramphenicol (30 µg ml^{-1}), X-gal (40 µg ml^{-1}) and IPTG (100 µg ml^{-1}). Antibiotics and inducers were purchased from Sigma-Aldrich.

Plasmids

Plasmids used in this study are listed in Table 2.2.

Preparation of competent cells

The protocol used for preparing competent *E. coli* cells was adapted from that given in the Qiagen bench guide, a free laboratory guide available from the Qiagen website. One ml of an overnight culture of *E. coli* was used to inoculate 100 ml LB which was then incubated at 37°C to an OD_{650} of 0.4-0.6. The culture was chilled on ice for 10 minutes and then cells were harvested by centrifugation at 3,200 x g for 5 minutes at 4ºC. Cell pellets were resuspended in 50 ml of sterile ice-cold TFB1 (100 mM RbCl; 50 mM $MnCl_2$; 30 mM potassium acetate; 10 mM $CaCl_2$; 15 % glycerol; pH 5.8) by gentle pipetting. Resuspended cells were incubated on ice for ~90 minutes prior to another round of centrifugation. The pelleted cells were resuspended in 4 ml of ice-cold 0.1M $CaCl_2$ and 10% (v/v) glycerol and frozen as 200-400 µl aliquots in liquid nitrogen. Competent cells were then stored at -80ºC until required.

Transformation of *E. coli* with plasmid DNA

Aliquots of 50-100 µl of *E. coli* competent cells were mixed with 0.5-3 µl (1-10 ng) of plasmid DNA or 5-10 µl of ligation mixture in 2 ml eppendorf tubes and incubated on ice for 20-60 minutes. Transformation mixtures were heat-shocked at 42 ºC for 90 seconds, placed on ice for 1 minute and then immediately supplemented with 700 µl of SOC broth (tryptone, 20 g l^{-1}; yeast extract, 20 g l^{-1}; NaCl 0.5 g l^{-1}; 2.5 mM KCl;

10 mM $MgCl_2$; 20 mM glucose) pre-heated to 37ºC. The mixture was incubated in a dry orbital shaker at 37 ºC for 45-90 minutes. *E. coli* cells were harvested by centrifugation and then spread onto LB agar plates supplemented with appropriate antibiotics. Plates were incubated at 37ºC for 12-22 hours.

Preparation of nitric oxide saturated water

Nitric oxide saturated water for use in growth experiments and mPEG-mal assays was prepared as described in Vine (2012). Approximately 5 ml of water was sealed in a glass bijoux bottle and flushed with nitrogen gas for 30-40 minutes followed by flushing with nitric oxide gas for at least 30 minutes. Nitric oxide saturated water prepared in this way contains 2 mM nitric oxide (Vine, 2012). Nitric oxide saturated water was prepared when required and was introduced to cultures by syringes to prevent exposure to oxygen. Serial dilutions of nitric oxide saturated water for use in mPEG-mal assays were made in sealed bijoux bottles of nitrogen-flushed water.

2.2 Purification of DNA

Purification of gDNA

Genomic DNA was isolated from cultures of bacteria that had grown to late exponential phase. For this purpose, *D. desulfuricans* was grown in PgZ supplemented with nitrate (30 mM) and *E. coli* was grown in Lennox Broth. Cells were harvested by centrifugation and genomic DNA was purified using the GFX^{TM} Genomic Blood DNA Purification Kit (Amersham Biosciences) according to the kit instructions with modifications outlined in Marietou (2009).

Purification of plasmid DNA

In general, plasmid DNA was purified using the QIAprep Spin Miniprep Kit (QIAGEN) according to the kit protocol. Cultures of *E. coli* for this purpose were 2.5-5 ml of Lennox Broth supplemented with appropriate antibiotics and seeded from single colonies. Cultures were grown aerobically at 37 ºC with shaking for ~16 hours and then harvested by centrifugation. DNA was eluted from the QIAprep Spin columns with 30 µl of sterile distilled water. Large quantities of plasmid DNA were purified with the QIAprep Maxiprep Kit (Qiagen) using the kit instructions.

For purification of large plasmids (> 10 kbp), such as those derived from pRW50, a modified QIAprep Spin Miniprep Kit (Qiagen) protocol was used. In brief, 5 ml cultures of *E. coli* harbouring plasmid DNA were grown as described. Cells were harvested by centrifugation and then subject to the re-suspension, lysis, neutralisation and centrifugation steps of the QIAprep Spin Miniprep Kit protocol. Since the QIAprep spin columns have a limited capacity for binding large plasmids the kit protocol was modified from this stage. Rather than loading the centrifuged cell lysate onto the QIAprep spin column the supernatant was transferred to 15 ml Corning tubes (Corning Life Sciences) and used for phenol-chloroform extraction (see below) using 800 µl of phenol-chloroform (Sigma-Aldrich). If necessary, this stage was repeated with fresh phenol-chloroform until any ambiguity between the aqueous and organic phases at the aqueous-organic interface had been resolved. The aqueous phase was removed, supplemented with 10% (v/v) 3M sodium acetate (pH 5.3) and 2.5 volumes of 100 % ethanol (-20 ºC), and then incubated at -20 ºC for 1 hour. The sample was centrifuged (14,000 r.c.f., 4 ºC, 15 minutes) and the resulting pellet was washed with 1 ml of 70 % (v/v) ethanol (-20 ºC) prior to another centrifugation

step. The ethanol precipitated pellet was air dried under vacuum and then re-suspended in 40 µl TE buffer (10 mM Tris-HCl, pH 7.5; 1 mM EDTA).

Purification of PCR products and linear DNA fragments

Linear DNA fragments generated by PCR or restriction digest were purified using the QIAquick PCR Purification Kit (Qiagen) according to the kit protocol. When specific linear DNA fragments were likely to be contaminated by other DNA fragments the QIAquick Gel Extraction Kit (Qiagen) was used according to the manufacturer's protocol. When DNA fragments of very high quality were required these were prepared by polyacrylamide gel electrophoresis (PAGE) followed by electro-elution, phenol-chloroform extraction and ethanol precipitation (see section 2.6).

Phenol-chloroform extraction and ethanol precipitation of DNA

Phenol chloroform extraction and ethanol precipitation was used to remove protein contaminants and/or concentrate DNA samples. For phenol-chloroform extraction, DNA samples were supplemented with an equal volume of phenol chloroform, vortexed for 10 seconds and then centrifuged at 2,500x g for 3 minutes. The aqueous phase was removed from the organic phase by aspiration and transferred to sterile 1.5 ml eppendorf tubes. To increase DNA yields from the phenol-chloroform extraction process 50-100 µl of SDW was added to the organic phase and processed as described. The two aqueous phases were pooled and subject to ethanol precipitation.

DNA-containing samples were concentrated or transferred to alternative buffers by ethanol precipitation. Samples were supplemented with 0.3 M sodium acetate pH5.3, 1 µl 20 mg ml^{-1} glycogen and adjusted with ice-cold 100% ethanol to a final

concentration of ~75% ethanol. The sample was incubated at –80°C for 30 min and then centrifuged at 14,000x g for 15 minutes at 4°C. Supernatant was removed from the DNA pellet by aspiration, washed with 1 ml ice-cold 70% ethanol and the centrifuged for an additional 10 minutes. Supernatant was removed and the DNA pellet was dried in a vacuum concentrator for 10-20 minutes. The dried DNA pellet was resuspended in an appropriate volume of SDW unless otherwise stated.

2.3 Analysis and manipulation of DNA

Polymerase Chain Reaction (PCR)

Specific DNA fragments were amplified by PCR using a variety of different commercially available DNA polymerases depending upon the application. Custom oligonucleotide primers used in PCR reactions were synthesized by Alta Biosciences, University of Birmingham. The melting temperatures (Tm) of primers were calculated and the likelihood of primers forming heterodimers, homodimers or hairpins was assessed using the IDT Oligo Analyzer tool (Integrated DNA Technologies). In general, primers were designed to have 18-28 nucleotides complementary to target sequences and have a melting temperature of 50-60 ºC. When possible, the 3' end of primers would include multiple G or C bases to provide stability when annealing to the target DNA sequences. Additional sequences, such as those recognized by restriction enzymes, were included at the 5' end of some primers to facilitate downstream applications. Primers used for cloning and promoter fragment generation are detailed in Table 2.3. Primers designed for RNA analyses are discussed in section 2.4.

Typically, PCRs were set up in a total volume of 50 µl and contained 1 unit of polymerase, 1 mM dNTPs, 0.4 µM of each primer and 1 pg-10 ng of DNA when the template was

Table 2.3: Primers used in this study		
Primer name	**Sequence**	**Description**
0528OE-F2	TTAATCATATGACAAACCGACAATATGCCGCC	Primer pair used in conjunction to amplify the HcpR ORF. Introduces NdeI and NotI restriction sites to facilitate cloning of *hcpR* into pET21a(+).
0528OE-R	TTAATGCGGCCGCGCCTTGCGCCCGCAGTTTC	
1827OE-F2	TATATCATATGAATCAGGCCCTGAAAAGCTGCG	Primer pair used in conjunction to amplify the HcpR2 ORF. Introduces NdeI and NotI restriction sites to facilitate cloning of *hcpR2* into pET21a(+).
1827OE-R2	TATATGCGGCCGCCGGAACAGAATAATCGTAAAATTC	
p0454RW50-F	TTTTTGAATTCCGGCGATTGCGGCAAAACC	Primer pair used to amplify a 300 bp fragment of the *sat* promoter including ~250 bp of upstream sequence. Introduces HindIII and EcoRI restriction sites to facilitate cloning into pRW50. Resulting fragment also used in EMSAs.
p0454RW50-R	TTTTTAAGCTTCTTGCCTTCAAGCAGGCAAC	
p0528RW50-F	TTTTTGAATTCCCGGCAGGTGCAAAACAATGC	Primer pair used to amplify a 300 bp fragment of the *hcpR* promoter including ~250 bp of upstream sequence. Introduces HindIII and EcoRI restriction sites to facilitate cloning into pRW50.
p0528RW50-R	TTTTTAAGCTTGGCTTGCAGGCTTTCTTCGTTG	
p0528-F	TACTGCATCCAGGACATTTCACC	Primer pair used to amplify a ~250 bp fragment of the *hcpR* promoter for use in EMSAs. Also used in transcript mapping strategies.
p0528-R	CATAGTACAATCTCCCGGGCTTTCG	
p1827-F	TAACAGAAATTCCCTGGGGC	Primer pair used to amplify a ~250 bp fragment of the *hcpR2* promoter for use in EMSAs.
p1827-R	CATGCGTTCTTCCAGCGTC	
p1827cTERM-F	CAACGGAAAAAACATCTCCC	Primer pair used to amplify a ~200 bp fragment of the short intergenic region between *hcpR2* and Ddes_1828. DNA fragment for use in EMSAs. Also used in transcript mapping strategies.
p1827cTERM-R	GGGCAGCGCGGTGGCGTAATCC	
Ddes_1828-F	CTTGTTCAGAATGATGCCGTGG	Primer pair amplifies a 180 bp fragment internal to the Ddes_1828 coding region. Also individually used in conjunction with other primers for transcript mapping strategies.
Ddes_1828-R	GATGGACTCTCCGGCCTTGAG	
Ddes_0527-F	ATTACGACTGCCTGGCCGTG	Primer pair amplifies a 180 bp fragment internal to the Ddes_0527 coding region. Also individually used in conjunction with other primers for transcript mapping strategies.
Ddes_0527-R	CGGAGTCATCGGGTGGGTAC	
Ddes_0526-F2	TGAGGGGCACAAGCTGGACT	Primer pair amplifies a 180 bp fragment internal to the Ddes_0526 coding region. Also individually used in conjunction with other primers for transcript mapping strategies.
Ddes_0526-R	GCATAGCGGACGGCAATGG	

plasmid DNA or 50-250 ng of DNA when the template was gDNA. Cycling parameters were dictated by the particular DNA polymerase being used, as described by the manufacturer, with the exception that an initial 5-10 minute denaturation step of 95 ºC was always included when gDNA was used as template. PCR optimization was achieved by varying the times/temperatures of annealing/extension steps and by the addition of $MgCl_2$ or DMSO. Touchdown and gradient protocols were employed for particularly difficult PCR reactions (Don *et al.*, 1991). PCRs were performed with BioMix Red (BioLine), PCR SuperMix High Fidelity (Invitrogen) or Phusion High-Fidelity DNA Polymerase (NEB).

DNA restriction digests, modifications and ligations

Restriction enzymes and DNA modifying enzymes were used according to instructions provided by the manufacturer and were supplied by NEB unless otherwise stated. Restriction enzymes were used to cut DNA at specific sequences. Calf intestinal alkaline phosphatase (CIP) was utilised to remove phosphate groups from the 5' ends of DNA fragments. This treatment prevents re-circularisation of digested plasmid DNA and also facilitates end-labeling of DNA fragments. T_4 DNA ligase was used to ligate DNA fragments. DNA ligation reactions were typically 10-20 µl in volume and contained 50-100 ng of vector DNA. When ligations were made between vector DNA and a DNA fragment this additional fragment was included in the ligation mixture at a ratio of 3:1 fragment to vector with quantities normalised for the relative sizes of the fragments.

Agarose gel electrophoresis of DNA

Agarose gel electrophoresis was used to assess and to quantify DNA fragments, plasmids and genomic DNA. In general, gels were prepared with molten 1% (w/v)

agarose in 1xTBE (90 mM Tris borate; 2 mM EDTA) and run in a tank of 1xTBE buffer supplemented with 0.1 ug ml^{-1} ethidium bromide. DNA samples were supplemented with an appropriate volume of 5x DNA loading dye (0.25 % bromophenol blue; 0.25 % xylene cyanol; 40 % (w/v) glycerol) prior to loading into wells in the solid gel. Separation was achieved with a current of 80 – 120 V for 30-90 minutes depending upon the expected sizes of the DNA fragments. Gels were visualised under UV light using the Gel Doc XR+ System and images were analysed using QuantityOne software (BioRad).

Polyacrylamide gel electrophoresis of DNA

Polyacrylamide gel electrophoresis (PAGE) was used to assess DNA fragments of less than 200 bp in length and was employed as part of a purification strategy for DNA fragments to be used in EMSAs and DNaseI footprinting assays (see section 2.6). Polyacrylamide gels were prepared with stock solutions containing 6-8% (v/v) acrylamide, 4% (v/v) glycerol and 1x TBE. Polymerisation of acrylamide was achieved by supplementing the stock solution with 0.1% (w/v) ammonium persulphate and 0.1% (v/v) TEMED (N,N,N′,N′-tetramethylethylenediamine). DNA samples were supplemented with an appropriate volume of 5x DNA loading dye prior to loading into wells in the polyacrylamide gel. Electrophoresis was achieved in tanks containing 1x TBE with a current of 180 V for 60-240 minutes. Gels were then soaked in 1x TBE buffer supplemented with 0.1 µg ml^{-1} ethidium bromide for 10 minutes prior to being visualised as described previously.

Cloning of DNA fragments into vectors

DNA fragments were introduced to plasmids by various strategies. PCR products were cloned without the need for restriction digest into the vector pGEM T-easy (Promega) according to the kit instructions. Cloning of DNA fragments into pET21(a)+ (Novagen) and pRW50 was dependent upon restriction digest and followed a generalised protocol. Briefly, target DNA sequences were amplified from gDNA by PCR. The primers used in this strategy also introduced restriction sites and non-specific flanking sequences to each end of the generated PCR fragment (refer to Table 2.3 for further details). PCR products were purified as described in section 2.2. The PCR products and destination vectors were digested with appropriate restriction enzymes in parallel and then purified using the QIAprep PCR purification kit (Qiagen). Samples of purified DNA fragments were resolved by agarose gel electrophoresis and quantified by comparison with 100 bp and 1 kb DNA ladder standards (NEB). Ligation mixtures were prepared as described earlier in this section and transformed into *E. coli* as described in section 2.1.

DNA Sequencing

Plasmid DNA was sequenced by the Functional Genomics Laboratory at the University of Birmingham. Sequencing reactions included 3 pmol of sequencing primer and ~250 ng of plasmid DNA in a volume of 10 µl. Sequencing was by chain termination using Big Dye Terminator (Life Technologies) and the resulting chromatograms were assessed using Chromas software (Technelysium).

2.4 RNA techniques

Purification of RNA

Cultures of *D. desulfuricans* were grown as described and 5-15 ml samples were harvested by centrifugation at 4 ºC. Cell pellets were re-suspended in 3 ml RNAlater (Ambion). Cell suspensions in RNAlater were snap-frozen in liquid nitrogen and stored at -80 ºC for up to two weeks until required.

Total RNA was purified from cells with the QIAGEN RNeasy mini kit according to the manufacturer's instructions with the inclusion of the optional on-column DNaseI digest step to eliminate contaminating DNA. RNA was eluted from the RNeasy spin columns with 30 µl RNase-free water and stored at -80 ºC for up to one month. RNA integrity was assessed with a NanoDrop ND1000 Spectrophotometer. Samples with an A_{260}/A_{280} of less than 1.8 and/or an A_{260}/A_{230} outside the range 2.0-2.2 were rejected as were samples with an RNA concentration of less than 200 ng/µl.

Reverse transcription reactions (RT-PCR)

RNA was reverse transcribed to cDNA with random hexamer primers using the Tetro cDNA Synthesis kit (BIOLINE) according to the manufacturer's instructions. Each RT-PCR reaction included 2 µg of total RNA. Multiple RT-PCR reactions were prepared from each RNA sample to provide a cDNA pool for each RNA sample.

Quantitative PCR (qPCR)

qPCR was performed on an Stratagene Mxp3005 machine set to detect SYBR green fluorescence. qPCR reactions were made using the Brilliant III Ultra-Fast SYBR® Green QPCR Mastermix kit (Agilent) in 96-well plates capped with optical strip tops. Gene specific primers were included in in reactions to a final concentration of 400 nM. cDNA template was included at a concentration of 5-50 ng. Cycling parameters were as recommended by the manufacturer except denaturation steps were for 20 seconds and

annealing steps were for 20 seconds at 56 ºC. The dissociation curve for each qPCR reaction was calculated using the pre-programmed Mxp3005 protocol and allowed assessment of PCR efficiency for each reaction. qPCRs that provided a dissociation curve with multiple peaks or a peak with an incorrect profile were rejected. Primer specificity was also assessed by agarose gel electrophoresis. Transcript levels were quantified by the ΔΔCt method using the levels of *polA* as a standard (Livak & Schnittgen, 2001). For each growth condition tested in qRT-PCR analyses RNA was prepared from at least three biological replicates and each qPCR was reaction was run in triplicate. Thus each qRT-PCR measurement was the result of at least nine individual reactions.

Primers for qPCR

qPCR primers were designed according to a strict set of criteria using the software Primer3 (Rozen & Skaletsky, 1998) and IDT Oligo Analyzer (Integrated DNA Technologies). qPCR primers were designed 18-24 nt long with a Tm of 55-60 ºC and a 3' terminal sequence containing all four different nucleotides wherever possible. qPCR reaction products were between 45-55 % GC and 175-185 bp in length from a region central to the target ORF. Sequences and description for qPCR primers are given in Table 2.4.

2.5 Protein techniques

SDS-PAGE of protein samples

Electrophoretic separation of proteins was achieved using SDS-PAGE gels. Gels were composed of 15 % (w/v) acrylamide, 0.375 M Tris-HCl pH 8.8 and 0.1% (w/v) SDS.

Table 2.4: qRT-PCR Primers used in this study

Primer name	Sequence	Description
q*polA* -F	CATCTGGACGAAATGTTCACC	Primer pair designed to amplify a 180 bp fragment internal to the *polA* transcript for use in qRT-PCR analyses.
q*polA* -R	CTGCATGCGTTCAAGAGAAG	
q0528-F	AACCATCACGAAAGGGATGT	Primer pair designed to amplify a 180 bp fragment internal to the *hcpR* transcript for use in qRT-PCR analyses. Also used in transcript mapping strategies.
q0528-R	GGAATGCACGAGGTGGAGTA	
q1827-F	CGTGATGGCCCGTATTGA	Primer pair designed to amplify a 180 bp fragment internal to the *hcpR2* transcript for use in qRT-PCR analyses. Also used in transcript mapping strategies.
q1827-R	TGTTGCGTATGATCTGTGCAT	
q1829-F	CCAGGAAACCGTGGGTAAC	Primer pair designed to amplify a 180 bp fragment internal to the *hcp* transcript for use in qRT-PCR analyses. Also used in transcript mapping strategies.
q1829-R	AACCAGGCGGTCTATCCTGT	
q0454-F	TTCATGAACAAGGCCGACTG	Primer pair designed to amplify a 180 bp fragment internal to the *aprB* transcript for use in qRT-PCR analyses.
q0454-R	TTTCTTCGACCTTCATGGTG	
q2130-F	ACGACCTCATGATCCTCGAT	Primer pair designed to amplify a 180 bp fragment internal to the *dsrB* transcript for use in qRT-PCR analyses.
q2130-R	CCGTCCACATAATGGAGTCTG	
q0614-F	TTATCGGCAGCGTCATTCT	Primer pair designed to amplify a 180 bp fragment internal to the *napC* transcript for use in qRT-PCR analyses.
q0614-R	GGAATGTGGCATTGAGAACA	
q2150-F	GGCCTATGACGGTTACTGGT	Primer pair designed to amplify a 180 bp fragment internal to the *ssC* transcript for use in qRT-PCR analyses.
q2150-R	TAAAGAGCGCCACAGATGGT	
q2038-F	GACAACTGCGAGACCTGTCA	Primer pair designed to amplify a 180 bp fragment internal to the *nhcC* transcript for use in qRT-PCR analyses.
q2038-R	TCTTTGGTTTGCTGTTCGTG	
q1951-F	CAATCTGGCAGACGGTTATG	Primer pair designed to amplify a 180 bp fragment internal to the *fld* transcript for use in qRT-PCR analyses.
q1951-R	CGCCGCAGTAATGCTCATATT	
q2013-F	GACAAGCCTGTCGAAGTCA	Primer pair designed to amplify a 180 bp fragment internal to the *tpIc3* transcript for use in qRT-PCR analyses.
q2013-R	GACGTAGTACAGGCTCTTTTCG	
q2126-F	AAACGCTGCACGGAAGAAT	Primer pair designed to amplify a 180 bp fragment internal to the *qmoB* transcript for use in qRT-PCR analyses.
q2126-R	ACCTGCACTTCACGGATCAT	
q0451-F	CAACTTCGGTTCCTTCACCT	Primer pair designed to amplify a 180 bp fragment internal to the *dsrM* transcript for use in qRT-PCR analyses.
q0451-R	CGGGGATTTCCATATTAGCC	

Polymerisation of the acrylamide was achieved with the addition of 0.08% (w/v) APS and 0.05% (v/v) *N*,*N*,*N′*,*N′*-Tetramethylethylenediamine. This 15 % (w/v) acrylamide gel was over-laid with 6.8 % (w/v) acrylamide, 0.125 M Tris-HCl pH 8.2, 0.1 % (w/v) SDS gel into which wells for sample loading were introduced. Proteins were separated at 120 V for 20-30 minutes and then 160 V for 60-90 minutes in tanks filled with SDS-PAGE buffer (25 mM Tris; 200 mM glycine; 0.1 % SDS (w/v)). Protein samples from purification procedures were mixed with an equal volume of 4 x protein sample buffer (50 mM Tris-HCl, pH 7.0; 0.1 % SDS (w/v); 40 % glycerol (w/v); 4 % β-mercaptoethanol (v/v); 50 mM EDTA; 0.1 % bromophenol blue (w/v)). Cell pellets of *E. coli* or *D. desulfuricans* were resuspended in a volume of protein sample buffer determined by the equation:

Volume of protein sample buffer (µl) = (culture OD_{650}/0.015) x volume of sample (ml).

Protein samples were heated to 95 ºC for 10 minutes prior to 1-20 µl being loaded onto SDS-PAGE gels. The Broad Range Prestained Protein Marker, 7-175 kDa (New England Biolabs) was used as a standard for calibration of MW. For non-denaturing PAGE the techniques were the same except reagents were not supplemented β-mercaptoethanol or SDS and the heating stage was omitted.

Following electrophoresis, SDS-PAGE gels were washed in water for 1 minute and then transferred to a container containing Coomassie Solution (10 % acetic acid (v/v); 50 % methanol (v/v); 0.1 % Coomassie blue (w/v)). The container was sealed and stored at room temperature for 2-3 hours with gentle agitation. The Coomassie Solution was poured off the stained gel which was then agitated at room temperature for 30 minutes with Destain Solution (20 % methanol (v/v); 10 % acetic acid (v/v)). Sequential washes

with Destain solution were made until protein bands on the gel could be clearly visualized. Gel images were captured on a GS800 Image Acquisition Scanner and QuantityOne Software (BIO-RAD).

Protein purification

His-tagged HcpR and HcpR2 was overexpressed in *E. coli* strain BL21 Star harbouring either plasmid pETHcpR or pETHcpR2. Ten ml of an over-night culture was used to inoculate 500 ml LB supplemented with 2 % glucose and appropriate antibiotics. These cultures were incubated at 30ºC with shaking until an OD_{650} of ~0.5 and then supplemented with 0.1M IPTG to a final concentration of 50 µM for HcpR or 500 µM for HcpR2. Cultures were harvested by centrifugation at 8,000 x g for 5 minutes at either 5 or 24 hours after the addition of IPTG. Cell pellets were frozen in liquid nitrogen and stored at -80ºC until required.

For the preparation of protein lysates, the frozen cell pellets were supplemented with ice-cold Buffer A (50 mM Tris-HCl, pH 8.0; 10 mM imidazole; 250 mM NaCl; 5 % glycerol (w/v)) to a final volume of 35 ml. Lysozyme was added to a final concentration of 1 mg/ml and the cell pellet was resuspended by homogenization. After 45 minutes incubation at 4ºC the cell mixture was sonicated for 3 x 45 seconds. The lysate was clarified by centrifugation at 35,000 x g for 30 minutes and then 55,000 x g for 1 hour.

Purifications were conducted with an *Äkta* Prime HPLC system (GE Healthcare). Clarified lysate was loaded onto a 1 ml Nickel-agarose column (GE Healthcare) that had been pre-equilibrated with Buffer A. The column was then washed with 20-40 column volumes of Buffer A and then 20 column volumes of Buffer A + 10% Buffer B (as Buffer A but

including 500 mM imidazole). Proteins bound to the nickel-agarose matrix were eluted in a linear gradient of 10-100% Buffer B over 20 column volumes. Fractions collected during the purification process were supplemented with 1 mM EDTA pH 7.0.

In the case of HcpR2 an additional ion-exchange purification step was necessary to yield pure protein. Fractions containing target protein were pooled and dialysed against Buffer C (50 mM Tris-HCl, pH 8.0; 50 mM NaCl; 5 % glycerol (w/v)). The dialysed sample was then loaded onto a 5 ml SP-FF column (GE Healthcare) that had been pre-equilibrated with Buffer C. Proteins were eluted in a linear gradient of 0-100 % Buffer D (as buffer C but containing 1 M NaCl).

Fractions containing purified protein were pooled and concentrated on Vivaspin 5 kDa spin columns by centrifugation at 3,200 x g for 1-4 hours at 4ºC. Protein concentrations were quantified using the Bradford assay reagent (BioRad) according to the enclosed instructions.

Polyclonal anti-HcpR antibody production

Purified HcpR protein and transferred into 50 mM Tris-HCl pH 7.5, 10% (v/v) glycerol by buffer exchange in a Vivaspin 10 kDa MW cut-off column and concentrated to 5 mg/ml. Polyclonal antibodies were raised in a single rabbit by CovalAb UK. The protocol consisted of one injection of 50 µg antigen in 0.5 ml mixed with 0.5 ml complete Freund's adjuvant at day 0 of the immunization protocol. A further two injections were made at 14 and 28 days after the initial injection. Bleeds were taken at day 0 and at 39 and 53 days after the initial immunization. Blood cells were removed and the sera were stored at -20 ºC until required.

Measuring HcpR levels using western blot analysis

HcpR protein levels in *D. desulfuricans* were measured by western blot using anti-HcpR antibodies. Cultures were grown with different terminal electron acceptors and in some cases treated with nitric oxide dissolved in water. Cell pellets were harvested by centrifugation and separated by SDS-PAGE as described. Gels were soaked in Blotting Buffer (25 mM Tris-HCl; 200 mM glycine; 20 % methanol (v/v)) for 5 minutes and then placed on top of a nitrocellulose membrane that had been prewashed with Blotting Buffer and then soaked in 100 % methanol for 2 minutes. The gel and nitrocellulose membrane were then sandwiched between blotting paper saturated with Blotting Buffer and then placed into a BioRad Semi-dry Transfer System with the nitrocellulose membrane being between the gel and the anode. Transfer of proteins from the SDS-PAGE gel onto the nitrocellulose membrane was achieved with 0.25 mA for 60 minutes. Following transfer, the membrane was washed with 50 ml of 1 x TBS (50 mM Tris-HCl, pH 8.0; 200 mM NaCl) for 15 minutes and then sealed in a bag containing 5 % (w/v) Blocking powder (BioRad) in 1 x TBS. The bag was incubated at 4 ºC with gentle agitation for 14 – 18 hours. The membrane was removed from the Blocking powder solution and washed in 30 ml 1 x TBS for 3 x 5 minutes. The membrane was then transferred to a bag containing 30 ml of 2.5 % (w/v) Blocking powder in 1 x TBS supplemented with 4.5 µl of anti-HcpR serum. The bag was incubated at room temperature for 2 hours with gentle agitation. The membrane was then washed in TBS as described previously, transferred to a new bag of 30 ml 2.5 % (w/v) Blocking powder in 1 x TBS supplemented with 3 µl of horseradish peroxidise-conjugated anti-rabbit secondary antibody (GE Healthcare) and then incubated at room temperature for 1 hour with gentle agitation. The membrane was washed with TBS as described previously and then treated with Amersham ECL Plus Western blotting detection reagents (GE

Healthcare) according to the manufacturer's intructions. Western blots were visualised by exposure to Amersham Hyperfilm ECL (GE Healthcare) in a dark room and developed with an Xograph.

TPTZ assay

Total iron concentration of protein samples were determined using the 2,4,6-tripyridyl-*s*-triazine (TPTZ) method (Fisher & Price, 1964). Protein samples of known concentrations were diluted to 1 ml and supplemented with 0.5 ml of 2 N HCl. Samples were vortexed and incubated for 10 minutes at room temperature. After incubation, 0.5 ml of 20 % (w/v) trichloroacetic acid was added to the samples which were then vortexed and incubated for a further 5 minutes. Precipitate was removed from the samples by centrifugation at 3,000 x g for 15 minutes. The clarified supernatant was decanted and then 1 ml added to a cuvette containing 0.5 ml of buffered chromagen (50% (w/v) ammonium acetate, 10% (w/v) hydroxylammonium chloride, 0.004 M TPTZ) and incubated at room temperature for 10 minutes. Absorbance was measured at 593 nm against blanks prepared with appropriate buffer in place of protein sample. Standard curves were prepared with serial dilutions of known concentrations of $FeCl_2$.

mPEG-mal labelling of proteins

The alkylating reagent mPEG-maleimide 5000 kDa (mPEG-mal; Sigma-Aldrich) was used to determine the oxidation state of the cysteine residues of HcpR protein. Protein samples were supplemented with oxidizing or reducing agents and incubated at 4 ºC overnight. H_2O_2 or dithiothreitol were used at concentrations of 0.075, 0.75 or 7.5 mM to oxidise and reduce proteins. Samples were then supplemented with 10 mM mPEG-mal, mixed and incubated at room temperature for 45 minutes. Treated proteins were

then precipitated by the addition of ice-cold 10 % (w/v) trichloroacteic acid, vortexing and then incubation on ice for 60 minutes. Precipitated protein was harvested by centrifugation at 14,000 x g for 20 minutes at 4 ºC. The protein pellet was washed with 1 ml of ice cold acetone and centrifuged again. The supernatant was discarded and the pellet air dried at room temperature for 10 minutes before resuspension in 50 µl of Protein loading buffer –β-mercaptoethanol. mPEG-mal-treated proteins were separated by non-reducing SDS-PAGE.

2.6 DNA binding assays

Electroelution of DNA

DNA fragments were resolved by PAGE, stained and visualized as described. Sections of gel containing the desired DNA fragments were excised and transferred to dialysis tubing (10 kDa MWCO; Visking) containing 0.1 x TBE buffer. The dialysis tubing was sealed and then exposed to a 25 mA electrical current for 25 mins to elute DNA from the gel into the buffer. The buffer was then removed from the dialysis tubing and used in phenol-chloroform extraction and ethanol precipitation as described.

Electromobility shift assays (EMSAs)

DNA fragments containing promoter proximal DNA sequences were amplified from gDNA by PCR and cloned in pGEM T-easy vector. T-easy-derived plasmids containing promoter fragments were purified from *E. coli*, digested with appropriate restriction enzymes, typically EcoRI and HindIII, and then treated with CIP. The excised promoter fragments were purified by electroelution, phenol-chloroform extraction and ethanol precipitation.

Purified DNA fragments were end-labelled with using T4 polynucleotide kinase (NEB). The end-labelling reaction consisted of 2 µl PNK buffer, 1 µl γ ^{32}P-ATP (111TBq/mmol; Perkin Elmer), 10-16 µl of DNA fragment, 1µl T4 polynucleotide kinase and SDW to a total volume of 20 µl. Labelling reactions were incubated at 37 ºC for 1 hour and then excess γ ^{32}P-ATP was removed by passing the reaction mixture through two 200 µl bed volumes of Sephadex G-50 which had be pre-equilibrated with 1 x TE buffer pH 8.0.

EMSA incubation mixtures were prepared to a final volume of 10 µl and included: 0.2-1 µl of radiolabelled DNA fragment, 1 µl of 10 x Binding buffer (20 mM Tris-HCl, pH 8.0; 100 mM KCl; 2 mM $MgCl_2$; 10 % glycerol (w/v)), 0.5 µl 4 mM spermidine, 0.5 µl 400 ng/µl herring sperm DNA, 0.5 µl 1mg/ml bovine serum albumin and 1 µl of HcpR or HcpR2 at an appropriate concentration. Incubation mixtures were also supplemented with additional additives where noted. EMSAs were also performed with non-labelled DNA fragments and in the absence of competitor DNA. Non-labelled fragments were visualised by staining with ethidium bromide and exposure to UV light. The CRP and *D. vulgaris* HcpR proteins used in some of these experiments were kindly provided by Dr. David Lee and Dr. Angeliki Marietou, University of Birmingham. EMSA mixtures were incubated at 25 ºC for 30 minutes and then loaded onto 6 % acrylamide gels prepared with 0.25 x TBE and 0.2 % (v/v) glycerol. Electrophoresis was in 0.25 x TBE at 160 V for 90-180 minutes.

Following electrophoresis, gels were fixed in 10% (v/v) acetic acid and 10% (v/v) methanol for 10 minutes. Fixed gels were transferred to 3 mm Whatman filter paper and dried under vacuum. Dried gels were stored in cassettes with a Fuji Imaging Phosphor

screen overnight which were then visualised with the Bio-Rad Molecular FX Imager System and QuantityOne software (BioRad).

DNaseI footprinting assays

Fragments for DNaseI footprinting were liberated from the plasmid pT*nap*WT by restriction digest. Plasmid DNA was digested with HindIII and then treated with CIP. The digest mixture was purified by phenol-chloroform and ethanol precipitation and then digested with EcoRI. The resulting fragment was purified by electroelution, phenol-chloroform extraction and ethanol precipitation prior to labeling with γ-^{32}P-ATP as described previously.

Maxam-Gilbert G+A sequencing reactions were prepared as standards for DNaseI footprinting assays. End-labeled DNA fragments were treated with formic acid for 90 seconds at room temperature and the reaction was stopped by ethanol precipitation. The purified DNA was re-suspended in 1 M piperidine and incubated at 90 ºC for 30 minutes. DNA was purified by ethanol precipitation and the DNA pellet re-suspended in loading buffer. G+A reactions were stored at -20 ºC until required.

End-labeled DNA fragments were used in *in vitro* DNaseI footprinting assays to map HcpR binding. Incubation mixtures were prepared as described for EMSAs using end-labeled DNA fragments in volumes of 20 µl. After 30 minutes at 25 ºC the incubation mixtures were supplemented with a dilution series of DNaseI (Roche Applied Science) ranging from 0-0.003 U and then incubated for an additional 40 seconds prior to inactivation of DNaseI with 200 µl of 500 mM EDTA. Digest mixtures were purified by phenol-chloroform extraction and ethanol precipitation. Purified DNA pellets were resuspended in denaturing gel loading buffer and stored at -20 ºC until required.

DNaseI footprinting reactions and G+A sequencing reactions were resolved by electrophoresis on 6% acrylamide denaturing urea gels prepared using the SequaGel UreaGel system (National Diagnostics) according to the manufacturer's instructions. Samples were heated to 90 ºC prior to loading onto gels. Electrophoresis was achieved in 1xTBE buffer at 60W for ~2 hours. Gels were fixed, dried and visualised as described for EMSAs.

2.7 β-Galactosidase assays

Gene expression from promoters fused to *lacZ* in pRW50-derived plasmids was measured by β-galactosidase assay (Miller, 1972). In general, *E. coli* strains harbouring appropriate plasmids were grown in LB overnight at 37 ºC and used to inoculate flasks containing M9 medium supplemented with appropriate terminal electron acceptors, carbon sources and antibiotics. For aerobic assays, 5 ml of M9 medium was used and for anaerobic assays 25 ml of M9 medium was used. Cultures were incubated at 37 ºC with shaking for aerobic assays or without shaking for anaerobic assays until an OD_{650} of 0.25-0.45 was reached. Cultures were then killed and lysed by the addition of 2-10 drops of toluene and 1 % sodium deoxycholate depending upon the culture size. Lysates were incubated at 37 °C with shaking for 30 minutes. The β-galactosidase activities of each culture were determined by adding 100 µl of lysate to 2.5 ml of Z Buffer (60 mM Na_2HPO_4; 40 mM NaH_2PO_4; 10 mM KCl; 1 mM $MgSO_4$; 50 mM β-mercaptoethanol) supplemented with 13 mM 2-nitrophenyl-β-D-galactopyranoside (ONPG). Immediately after this addition, the assay mixtures were vortexed and incubated at 37 °C until the mixtures had developed a yellow colouration. Assay reactions were then stopped by the addition of 1 ml 1 M sodium

carbonate and vortexing. The assay was timed and absorbance at 420 nm was measured. β-galactosidase activity was determined with the formula:

Activity (nmol ONPG hydrolysed/min/mg) = $[(2.5 \times 3.6 \times OD_{420})/(OD_{650} \times t \times v)]/0.0045$

2.5: coefficient for conversion of OD_{650} to mg dry cell weight

3.6: total assay volume (ml)

0.0045: molar extinction coefficient of o-nitrophenyl (1 nmol/ml/cm ONP = OD_{420} of 0.0045)

t: assay incubation time (minutes)

v: volume of lysate used in assay(ml)

β-Galactosidase activities for each strain and plasmid combination were determined by assaying three biological replicates and results were representative of at least two independent experiments.

2.8 Measurements of terminal electron acceptor concentrations

Quantification of terminal electron acceptors in growth medium

Terminal electron acceptor concentrations were quantified by a range of different techniques. In general, 1 ml of the culture was collected and clarified by centrifugation at 14,000 x g for 10 minutes prior to use in terminal electron acceptor quantification assays.

Nitrate concentrations were determined with a nitrate ion-specific electrode (Cole-Parmer) fitted to a Jenway Ion Meter 3345. The nitrate electrode apparatus was

calibrated with stock solutions of 2 mM, 1 mM and 0.5 mM nitrate prepared in 50 mM phosphate buffer pH 7.4. Culture supernatant samples were diluted in phosphate buffer pH 7.4 to provide appropriate readings on the Ion Meter.

Sulphate concentrations were determined by a turbidometric method using $BaCl_2$. Clarified culture supernatant (10-100 µl) was added to S reagent (0.1 % glycerol (w/v); 0.05 % conc HCl (v/v); 25 mM NaCl; 0.2 % ethanol (v/v)) to a final volume of 1 ml. Samples were then supplemented with 0.1 ml of 1M $BaCl_2$, mixed and incubated at room temperature for 45 minutes. Concentrations were determined by generating standard curve of known sulphate concentrations and measuring A_{420}.

Sulphite concentrations were determined using Sulfite LR tablets (Panwell-Tech). The exact formulation of these tablets are not disclosed but relies upon the reaction of sulphite with 5,5'-dithio-*bis*-(2-nitrobenzoic acid) (DTNB) to yield 2-nitro-5-thiobenzoic acid (TNB). TNB is yellow in colour and can be measured spectrophotometrically at A_{430}. Sulfite LR tablets were dissolved in half the recommended concentration in water. This 200 % stock was then dispensed into 500 µl aliquots and diluted to 100 % strength with clarified culture supernatant and water. A_{430} was measured after incubating at room temperature for 10 minutes and concentrations were determined from standard curves generated with known concentrations of sulphite. It was noted that nitrite must prevent the formation of or interfere with the absorbance of TNB. The presence of nitrite in reaction mixtures completely masked the assay sensitivity.

Nitrite concentrations were determined spectrophotometrically. Culture supernatant, 10-50 µl, was added to 3 ml of 1 % (w/v) sulphanilamide in 1N HCl in a test tube. The

mixture was vortexed, supplemented with 300 µl N-napthylethylene diamine dihydrochloride and then vortexed again. Standards of known nitrite concentrations were prepared by the same method. Samples were incubated at room temperature for 30 minutes and then absorbance at 540 nm was measured against a blank prepared with water in the place of culture supernatant. Sulphite was noted to decrease the sensitivity of the assay.

Nitrite reductase activity assay.

Nitrite reductase assays were performed with the assistance of Matthew Faulkner. Cells from 200 ml of *D. desulfuricans* culture were harvested by centrifugation, washed with ice-cold PBS, and then resuspended in ~1 ml ice-cold PBS to provide an OD_{600} of ~75. Test-tubes containing 4.85 ml potassium phosphate buffer supplemented with 30 mM lactate were pre-warmed to 30 ºC in a water bath and then 150 µl of cell suspension added. Tubes were mixed and then incubated for 5 minutes. Reactions were then supplemented with 50 µl of 0.1 M sodium nitrite and mixed. Samples of the reaction mixture were taken at 3 minute intervals and added to tubes containing 3 ml sulphanilamide in 1N HCl and then used for nitrite quantification as described previously. Standards were prepared using 60 µl of 1 mM sodium nitrite. Nitrite reduction rates (nmol nitrite reduced min^{-1} (mg dry cell mass)$^{-1}$) were calculated with the equation:

Rate of nitrite reduction = $(\Delta A_{540} min^{-1} \times 30 \times 20 \times 5)/(A_{540}(St) \times 0.1 \times (A_{650}) \times 0.4)$

30 = nmol of nitrite in the standard

20 = conversion factor (50 µl of a 5 mL reaction used in the assay)

5 = represents the total assay volume (ml)

$A_{540}(St) = A_{540}$ of the standard

0.1 = volume of bacterial suspension in the assay (ml)

0.4 = coefficient to convert A_{650} into mg dry cell mass.

2.9 Computational techniques

P values

Statistical significance of data was assessed using the paired samples t-test in Microsoft Excel. The p values indicated data significantly different where $p \leq 0.050$. For RT-qPCR assays the p values were determined from the ΔCt values.

Bioinformatics

DNA and protein sequences were analysed with a range of on-line tools. Putative RNAP -10 and -35 sequences were identified using the Softberry BPROM tool (Softberry Inc., Mount Kisco, NY, USA). CRP binding sites were identified in promoters and whole genome sequences using Virtual Footprint and PRODORIC (Münch *et al.,* 2005). Genome sequences were scanned for custom sequences using the EMBOSS program fuzznuc (Rice *et al.*, 2000). Groups of DNA or protein sequences were scanned for conserved motifs using the MEME tool (Bailey *et al.*, 2009). Multiple alignments of DNA sequences and proteins were made using ClustalW (Larkin *et al.*, 2007). Protein structure homology searches were made using the PHYRE2 tool (Kelly & Sternberg, 2009).

Chapter 3

Results

An *in silico* analysis of nitrate metabolism and the CRP family proteins of *Desulfovibrio desulfuricans*

3.1 Introduction

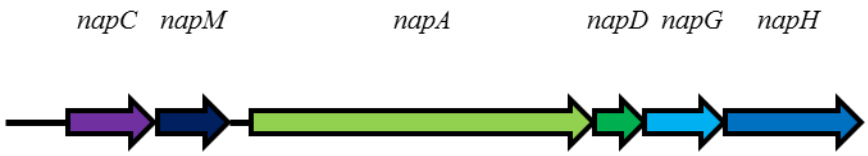
There are CRP-like DNA inverted repeat sequences upstream of the *D. desulfuricans nap* gene cluster and it has been speculated that these could be targets for a CRP/FNR family protein (Marietou *et al.*, 2009). A putative CRP/FNR family protein, HcpR, has been identified by *in silico* methods in the genomes of other *Desulfovibrio* species, specifically *D. vulgaris* and *Desulfovibrio* G20 (Rodionov *et al.*, 2004; Rodionov *et al.*, 2005). In these bacteria HcpR is believed to bind to DNA inverted repeat sequences that are almost identical to those bound by CRP from *E. coli*. The HcpR regulon includes genes involved in sulphate reduction and nitrosative stress. Therefore it seems likely that if the *D. desulfuricans* genome includes a gene for HcpR then this protein could potentially be the regulator responsible for controlling expression of the *nap* gene cluster of *D. desulfuricans*.

This chapter will provide a detailed analysis of CRP/FNR homologues in the genome of *D. desulfuricans* in an attempt to identify potential regulatory factors influencing the expression of *nap* in this bacterium. Homologues will be identified, their DNA target sites and regulons predicted and ultimately a putative function for each regulator identified where possible. Since the genomic analyses that first identified the HcpR group of transcription regulators, a large number of additional sequence data from the SRB group has become available (Rodionov *et al.*, 2004; Rodionov *et al.*, 2005). The *hcpR* loci of *D. vulgaris* and *Desulfovibrio* G20 are very similar with clear synteny. Thus, comparisons between the *hcpR* locus of *D. desulfuricans* will be made with those of *D. vulgaris, Desulfovibrio* G20 and other bacteria to assess how conserved the *hcpR* genomic regions are in *Desulfovibrio* species. Also, the sequences of HcpR proteins will

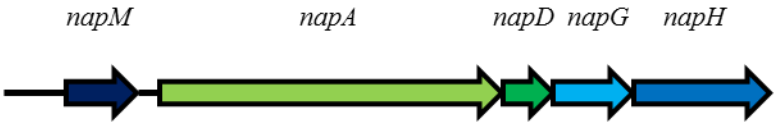
be analysed to identify residues that could potentially be involved in ligand binding or sensing of small molecules. In addition to an *in silico* analysis of the CRP family proteins of *D. desulfuricans*, attempts will be made to identify regulatory motifs upstream of genes encoding nitrite reductase and other genes related to growth upon nitrate and nitrite. Finally, a model of the transcription regulation behind the nitrate-sulphate diauxie described by Marietou *et al.* (2009) will be constructed. The first part of this chapter, however, will detail the *nap* gene clusters of some other SRB and assess whether these too have CRP-like inverted repeat sequences in their upstream DNA sequences.

3.2 Conserved *nap* gene clusters and their regulatory motifs in *Desulfovibrio* species

Since Marietou *et al.* (2006) identified and sequenced the *nap* gene cluster of *D. desulfuricans*, a great number of SRB genomes have been sequenced. The sequence of the *D. desulfuricans* NapM subunit was used in blast searches to identify *nap* gene clusters with a high level of similarity to that of *D. desulfuricans* with particular emphasis upon those belonging to SRB and similar bacteria (Figure 3.1). These searches identified three additional distinct *Desulfovibrio* species with *napCMADGH* clusters: *Desulfovibrio* sp. 6_1_46AFAA, *Desulfovibrio* sp. 3_1_syn3 and *Desulfovibrio* sp. A2. The genomes of these species vary in size from 2.87-4.15 Mb with GC contents of 58.1-67.2 %. In terms of sequence similarity of Nap proteins these three bacteria are the most similar to *D. desulfuricans.* This type of *nap* gene cluster was also noted in the sulphite reducing bacteria *Bilophila* sp. 4_1_30 and *Bilophila wadsworthia* 3_1_6. A number of other bacteria with *nap* gene clusters were



Species: *Desulfovibrio desulfuricans, Desulfovibrio* sp. *6_1_46AFAA, Desulfovibrio sp. 3_1_syn3, Desulfovibrio* sp. A2, *Bilophila* sp. 4_1_30 and *Bilophila wadsworthia.*



Species: *Denitrovibrio acetiphilus* DSM 12809, *Desulfurispirillum indicum* S5, *Thermovibrio ammonificans* HB-1, *Deferribacter desulfuricans* SSM1, *Thermodesulfatator indicus* DSM 15286 and *Desulfobulbus propionicus* DSM 2032.

Figure 3.1 Nap gene clusters of *Desulfovibrio* and related bacteria. Gene clusters were identified by blast searches. Two different *nap* clusters were identified.

identified using the NapM sequence. Intriguingly, most of these species have *napMADGH* gene clusters lacking a gene for NapC. It seems that the NapM subunit, novel when identified in *D. desulfuricans*, is conserved in nitrate-reducing SRB and similar bacteria.

The DNA sequences upstream of a selection of these *nap* gene clusters were scanned for the presence of CRP-like inverted repeats similar to those upstream of the *nap* gene cluster in *D. desulfuricans.* These DNA sequences represent DNA regions where one would expect to find motifs that regulatory proteins would bind to in order to regulate the expression of the downstream genes. Of the ten sequences scanned, seven contained CRP-like inverted repeats with an 8/10 match to the consensus TGTGA[N_6]TCACA. The positions of these sites relative to the first codon of the *nap* gene cluster is variable with some of the sites overlapping the first codon of the first gene of the *nap* cluster and some being further upstream (Figure 3.2). This is suggestive that some of these other *nap* gene clusters could also potentially be regulated by a CRP family member. However, the mode of regulation by the CRP family member might not be the same for all these bacteria due to the varied positioning of these CRP-like sites. For example, in *D. desulfuricans*, *Desulfovibrio* sp. 6_1_46AFAA and *Desulfovibrio* sp. 3_1_syn3 there are multiple CRP-like sites some distance upstream of the first *nap* translation start codon whereas in *Deferribacter desulfuricans* the CRP-like site overlaps the start codon of *napM*. The position of the CRP site is critical in determining the activity of CRP at a given promoter. The positioning of the sites in the *Desulfovibrio* species suggests class III activation whereas in *Deferribacter* the site is suitably positioned for repression. Should these bacteria with these conserved motifs also possess a conserved CRP homologue it seems likely that the activity of this regulator should be different, with

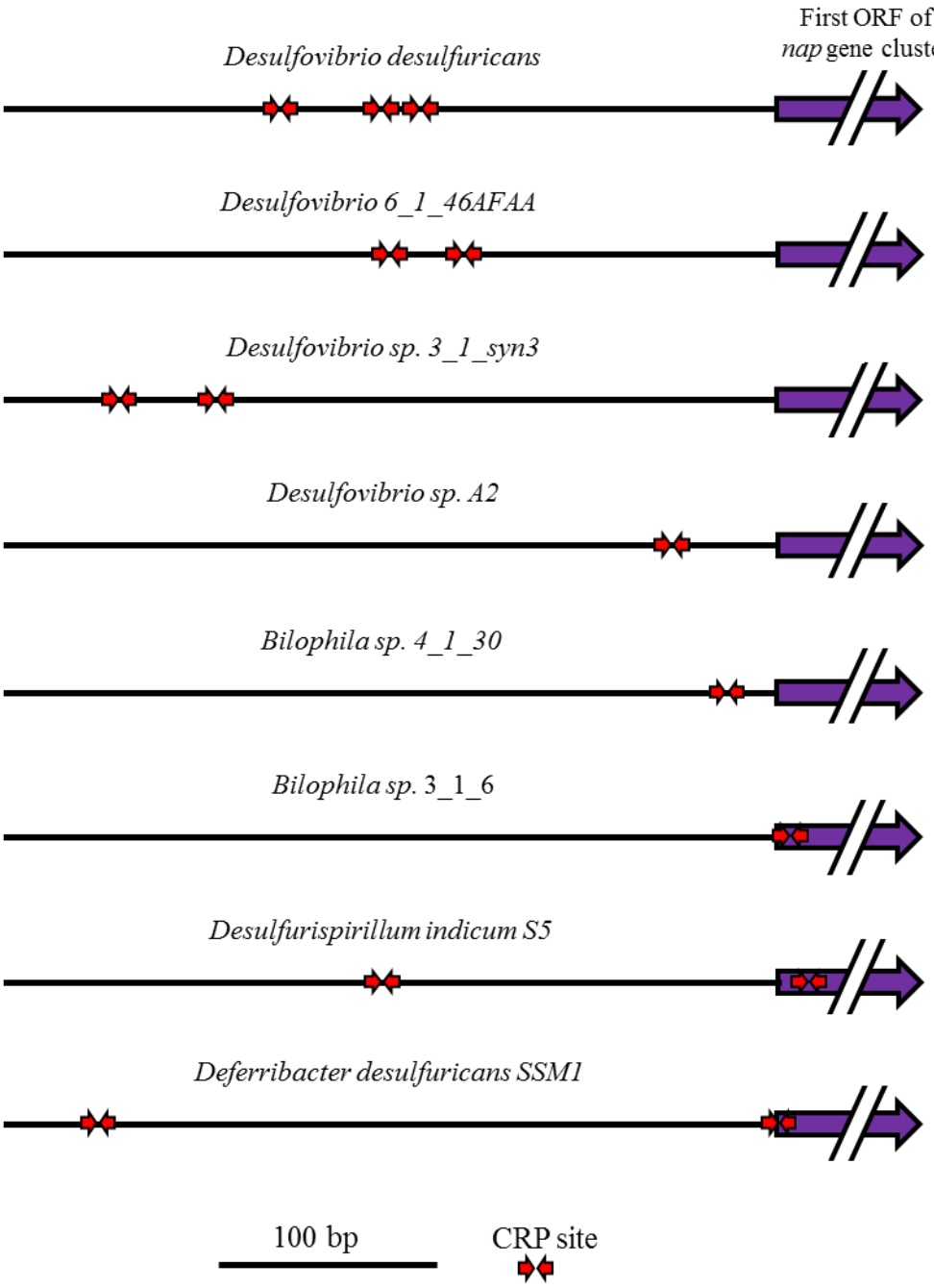


Figure 3.2 CRP-like sites upstream of the *nap* gene clusters of *Desulfovibrio* and related bacteria. CRP-like inverted repeats were identified using PRODORIC**.**

respect to *nap* regulation, in these different bacteria. Whilst searching for CRP sites in these sequences an additional conserved inverted repeat was detected upstream of the *nap* gene clusters of *D. desulfuricans*, *Desulfovibrio* sp. 6_1_46AFAA, *Desulfovibrio* sp. 3_1_syn3, *Desulfovibrio* sp. A2 and the *Bilophila* species. This motif has the sequence GTCATK[N_6]MTGAC (where K = A or G and M = T or C) and indicates that *nap* expression in *Desulfovibrio* is likely to be subject to complex regulation. These additional sites will be discussed in further detail later in this chapter. Since CRP-like motifs have been detected upstream of a number of *nap* gene clusters an assessment of the CRP family proteins of *D. desulfuricans* was undertaken.

3.3 Identification of CRP/FNR family proteins of *D. desulfuricans*

It has previously been reported that *Desulfovibrio* G20 and *D. vulgaris* each have four genes encoding putative CRP homologues (Marietou *et al.*, 2009). Both of these bacteria have genes encoding HcpR, CooA and two unidentified regulators. The sequences for these proteins, in addition to the sequences for *E. coli* CRP and FNR, were used for blast searches against the *D. desulfuricans* genome. Five putative CRP/FNR homologues were identified in *D. desulfuricans*. Identity scores between CRP, FNR and the CRP/FNR homologues of the three *Desulfovibrio* species were generated to assess whether the CRP/FNR family proteins of *D. vulgaris* and *Desulfovibrio* G20 have counterparts in *D. desulfuricans* (Table 3.1). Three of the four CRP/FNR proteins from *D. vulgaris* and *Desulfovibrio* G20 have high sequence identity to each other in excess of 35 % identity. This suggests that these proteins could be three distinct regulators that are equivalent in these two species. For example, the HcpR proteins of these two species share 64 % identity, the CooA proteins share 39 %

Table 3.1 Identities of CRP/FNR homologues from selected *Desulfovibrio* species generated by ClustalW.

Bacterium		*E. coli* K-12		*D. vulgaris* Hildenborough				*D. desulfuricans* G20				*D. desulfuricans* ATCC27774				
	Protein identifier	CRP	FNR	DVU0379	DVU2097	DVU2547	DVU3111	Dde_0463	Dde_1200	Dde_2644	Dde_3027	Ddes_0383	Ddes_0528	Ddes_1411	Ddes_1827	Ddes_2092
E. coli K-12	CRP	X	18	17	15	20	15	20	13	19	15	18	20	16	17	20
	FNR	18	X	20	16	22	15	18	11	21	21	17	13	10	16	13
D. vulgaris Hildenborough	DVU0379	17	20	X	5	18	20	38	20	18	4	9	16	19	17	30
	DVU2097	15	16	5	X	23	15	12	14	21	39	37	11	12	15	4
	DVU2547	20	22	18	23	X	18	18	16	64	20	19	25	16	25	15
	DVU3111	15	15	20	15	18	X	25	18	20	13	16	13	15	15	18
D. desulfuricans G20	Dde_0463	20	18	38	12	18	25	X	23	17	14	14	17	22	19	33
	Dde_1200	13	11	20	14	16	18	23	X	19	14	15	19	18	15	22
	Dde_2644	19	21	18	21	64	20	17	19	X	22	20	24	14	24	18
	Dde_3027	15	21	4	39	20	13	14	14	22	X	42	19	12	12	11
D. desulfuricans ATCC27774	Ddes_0383	18	17	9	37	19	16	14	15	20	42	X	14	9	5	13
	Ddes_0528	20	13	16	11	25	13	17	19	24	19	14	X	13	20	13
	Ddes_1411	16	10	19	12	16	15	22	18	14	12	9	13	X	16	35
	Ddes_1827	17	16	17	15	25	15	19	15	24	12	5	20	16	X	18
	Ddes_2092	20	13	30	4	15	18	33	22	18	11	13	13	35	18	X

identity, and the unidentified CRP/FNR regulators DVU0379 and Dde0463 share 38 % identity to each other. Whether the remaining CRP/FNR family proteins of these two bacteria, DVU3111 and Dde_1200, are equivalents of one another cannot be predicted as they share a lower level of identity than the other homologues. As such these proteins might be distinct from each other. Identities shared between putative counterparts are shaded in Table 3.1.

The five CRP/FNR homologues of *D. desulfuricans* were compared with those of *D. vulgaris* and *Desulfovibrio* G20. The sequence identities shared between the *D. desulfuricans* CRP/FNR homologues and those of *D. vulgaris* and *Desulfovibrio* G20 are lower than those shared between the latter pair of bacteria. However, a candidate CooA protein, Ddes_0383, with significant identities to those of *D. vulgaris* (37 %) and *Desulfovibrio* G20 (42 %) was identified from *D. desulfuricans*. Interestingly, there are two potential HcpR regulators, Ddes_0528 and Ddes_1827, in the genome of *D. desulfuricans*. These two regulators both share 25 % and 24 % identity with the HcpRs of *D. vulgaris* and *Desulfovibrio* G20, respectively. The proteins Ddes_0528 and Ddes_1827 will hereafter be referred to as HcpR and HcpR2 from *D. desulfuricans.* Ddes_2092 shares 30 % and 33 % identity with the CRP/FNR homologues DVU0379 and Dde_0463 and so these regulators could be equivalents in these three species. Ddes_1411 did not have any obvious counterpart in either *D. vulgaris* or *Desulfovibrio* G20 but shares 35 % identity with Ddes_2092.

A generalised work schedule was used for further *in silico* characterisation of the CRP/FNR homologues of *D. desulfuricans* (Figure 3.3). This work scheme is based upon simple tools, available free of charge on-line, the details of which are covered in

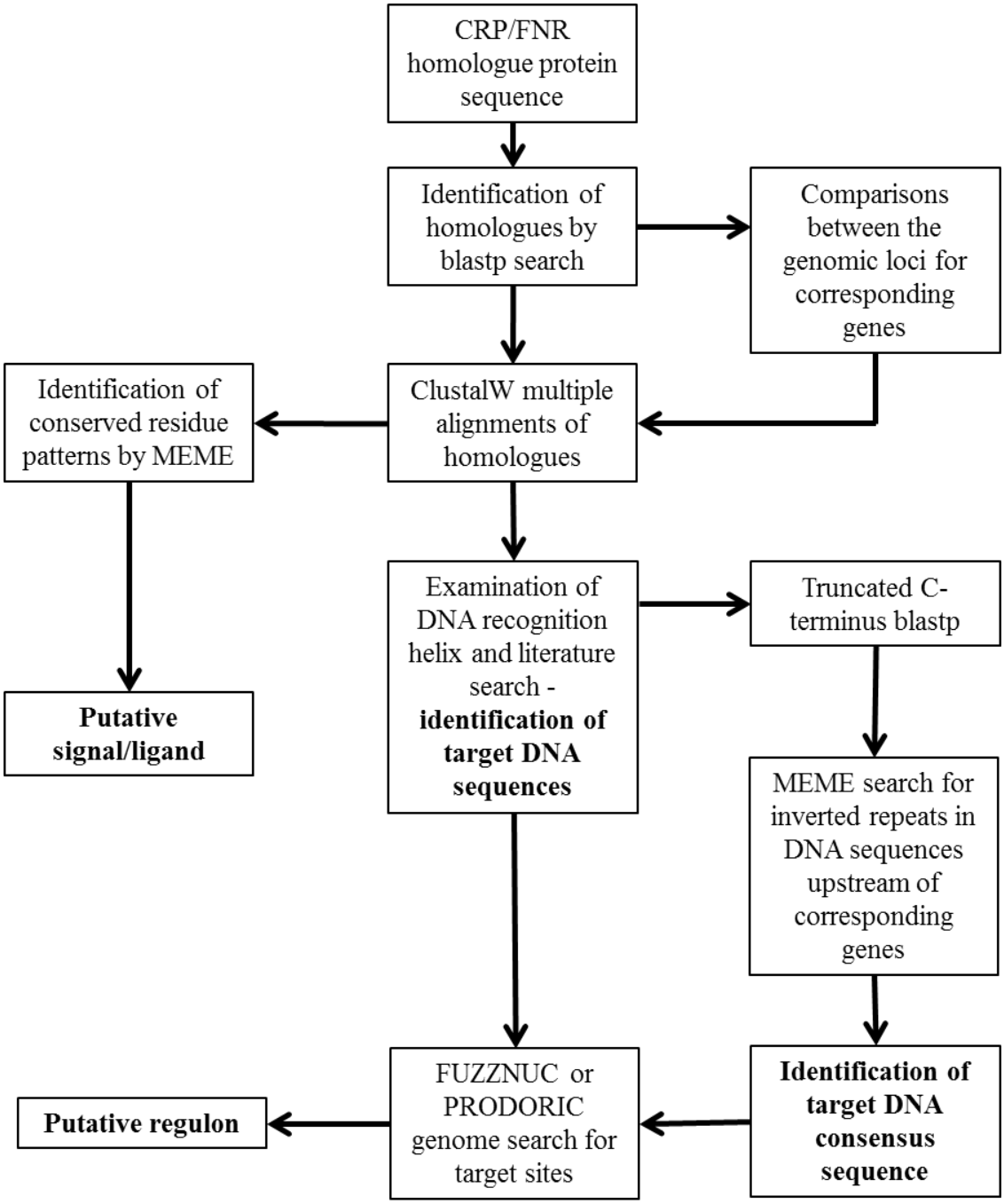


Figure 3.3: Generalised work scheme for *in silico* analysis of CRP/FNR homolgues.

Arrows indicate the sequence of analyses and key objectives and outcomes are in bold.

Chapter 2 of this thesis. The scheme provides the means to identify three key points for each CRP/FNR homologue: the consensus target DNA binding sequence, the putative regulon and the conserved protein residues of each CRP/FNR homologue. Using these three key points it is possible to speculate what the function of each regulator is and to what signal it might respond. Parts of the work scheme can be changed to suit the CRP/FNR homologue being studied.

3.4 CooA proteins in *Desulfovibrio*

A candidate CooA protein was identified in *D. desulfuricans* using sequence identity. To confirm this assignment a multiple alignment of the *Desulfovibrio* CooA proteins and the CooA from *Rhodospirillum rubrum* was generated (Figure 3.4a). CooA from *R. rubrum* has been extensively studied and as such provides a useful tool for comparison. Residues R, Q and S at positions 1, 2 and 5 of the DNA recognition helix of *R. rubrum* are responsible for DNA sequence recognition by CooA, which binds specifically to DNA targets with the consensus sequence TGTCA[N_6]TGACA (Aono *et al.,* 1999). From the multiple alignments between these proteins it is apparent that these proteins share a high level of conservation between their recognition helices with the pattern of residues RQTxST present at positions 1-6 of the DNA binding helices of the aligned proteins (Figure 3.4a). Conservation of these residues is strongly suggestive that they share sequence-specific DNA recognition qualities.

Since CooA proteins are involved in the regulation of genes encoding carbon monoxide dehydrogenases the genomic contexts of the predicted CooA proteins from *Desulfovibrio* species were compared (Figure 3.4b). All three species share a high level of synteny with regard to their putative *cooA* and *cooSC* loci, with identical

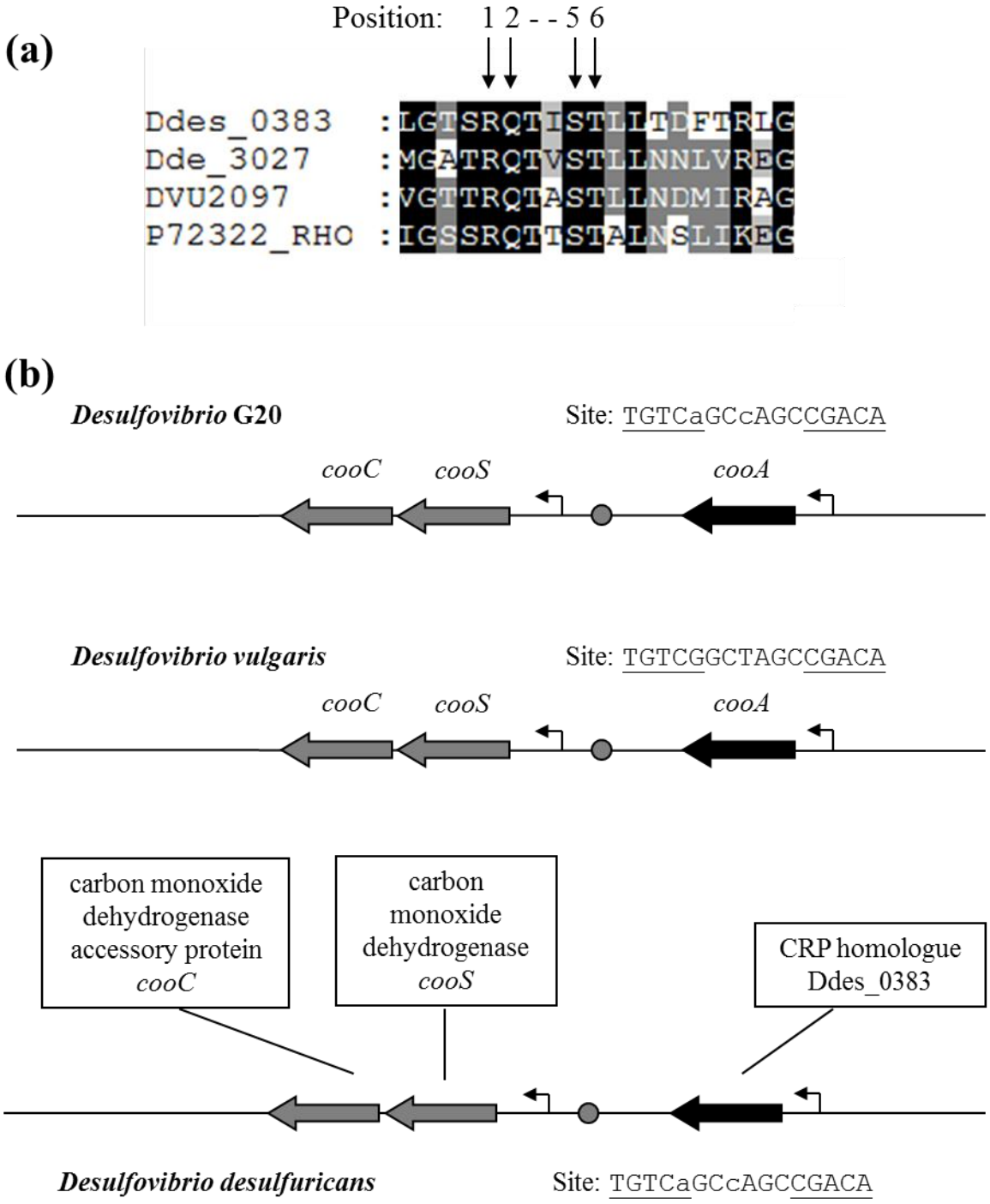

(a)
Position: 1 2 - - 5 6
Ddes_0383 :LGTSRQTISTLLTDFTRLG
Dde_3027 :MGATRQTVSTLLNNLVREG
DVU2097 :VGTTRQTASTLLNDMIRAG
P72322_RHO :IGSSRQTTSTALNSLIKEG
(b)
Desulfovibrio G20
Site: TGTCaGCcAGCCGACA
cooC
cooS
cooA
Desulfovibrio vulgaris
Site: TGTCGGCTAGCCGACA
cooC
cooS
cooA
carbon monoxide dehydrogenase accessory protein cooC
carbon monoxide dehydrogenase cooS
CRP homologue Ddes_0383
Desulfovibrio desulfuricans
Site: TGTCaGCcAGCCGACA
: putative CooA binding sites

Figure 3.4: The DNA recognition helices of *Desulfovibrio* CooA proteins and *Rhodospirillum rubrum* CooA, and the genomic context of *Desulfovibrio* CooA proteins. (a) Multiple alignment of *Rhodospirillum rubrum* CooA [RrCooA], *D. desulfuricans* G20 CooA [Dde_3027], *D. vulgaris* Hildenborough CooA [DVU2097] and *D. desulfuricans* ATCC27774 protein Ddes_0383. Positions are relative to the DNA recognition helix of CRP. * denotes absolute conservation at this position in all proteins, : denotes functionally conserved residues at this position in all proteins, and . denotes incomplete functional conservation at this position. **(b)** Gene maps of *Desulfovibrio cooA* genes and putative CooA DNA binding sites.

arrangements present at all three loci. Candidate CooA binding sites in *Desulfovibrio* G20 and *D. vulgaris* conform to the same consensus as *R. rubrum,* TGTCA[N_6]TGACA (Rodionov *et al.,* 2005). A candidate CooA site was located downstream of *D. desulfuricans* CooA that is identical to that of the *cooSC* operon of *Desulfovibrio* G20. In *D. vulgaris* CooA also regulates the *cooMKLXUHF* operon. However, *D. desulfuricans* lacks this operon. Scanning the *D. desulfuricans* genome for more CooA target sites indicates that the site upstream of the *cooSC* operon is likely to be the only target for *cooA* in this bacterium.

The *Desulfovibrio* CooA proteins share a high level of conservation with respect to DNA recognition helices, putative DNA binding sites and genomic synteny. Next, the potential for cofactor binding by these proteins was assessed. In CooA from *R. rubrum* residues C_{75} and H_{77} are involved in binding of a CO-sensing heme ligand with H_{77} being important in transmitting the protein conformation change resulting from CO binding (Shelver *et al.,* 1999). This CxH motif is absent from the *Desulfovibrio* proteins. However, a histidine residue was identified at an equivalent position in these proteins. It seems likely that CooA proteins sense CO by a heme ligand but it seems unlikely that co-ordination of this prosthetic group could be mediated by a single histidine residue. To identify conserved residues that may coordinate the heme group of the *Desulfovibrio* CooA proteins a multiple alignment of ten putative CooA sequences was generated. The genomic contexts of the genes for these CooA homologues were examined and in every case *cooSC* were observed to be in close proximity. The multiple alignment highlights the conservation of the aforementioned histidine residue in all ten CooA proteins (Figure 3.5). Adjacent to the conserved histidine residue in all the aligned homologues are between one and three serine or threonine residues.

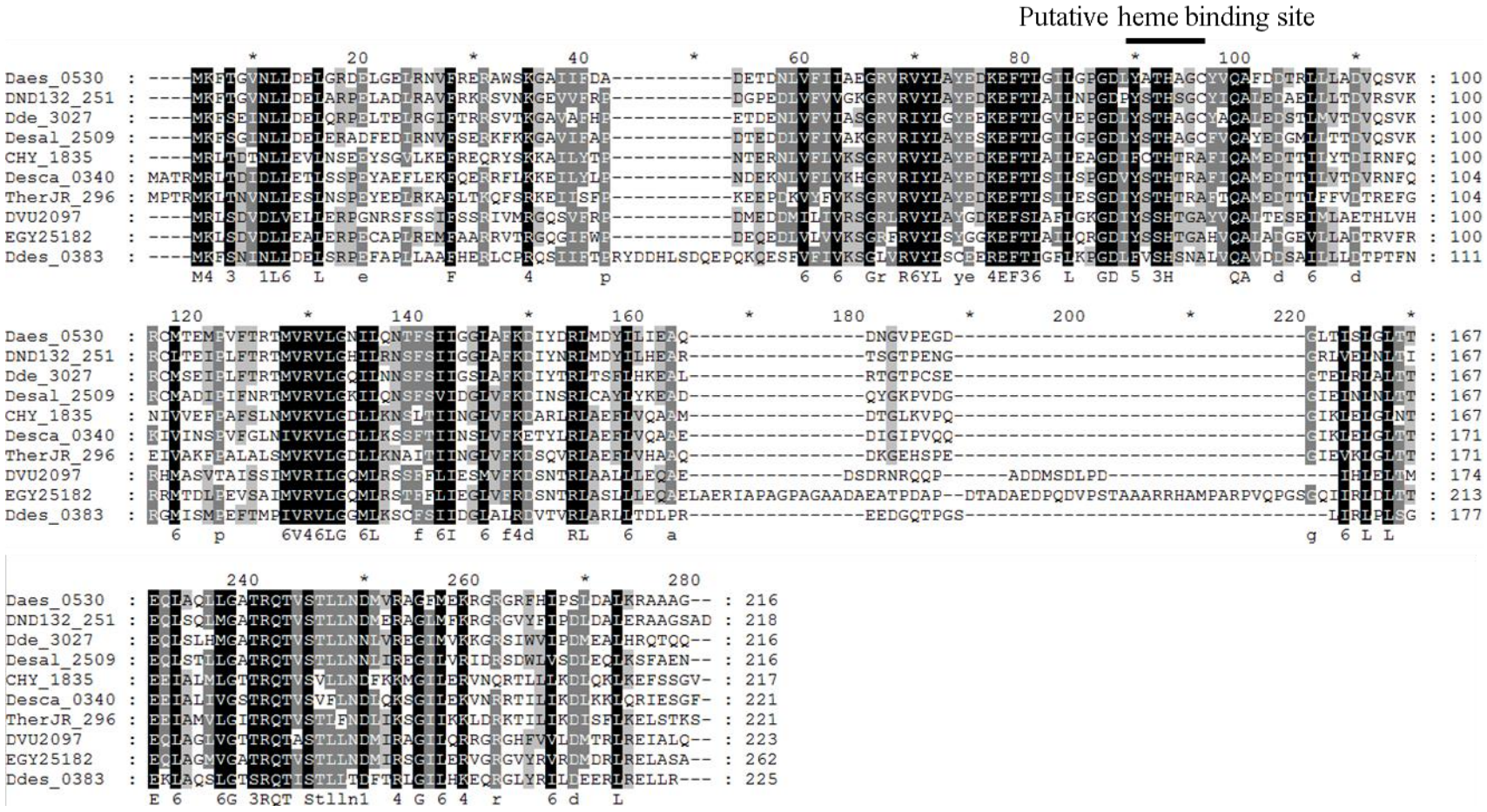

Putative heme binding site

Figure 3.5: Multiple alignment of CooA proteins. Alignment generated with ClustalW. The region containing the conserved histidine residue and the associated serine, threonine and cysteine residues is marked 'Putative heme binding site'. Proteins included in the alignment are from the following organisms: *Desulfovibrio desulfuricans* (Ddes_0383); *Desulfovibrio vulgaris* Hildenborough (DVU2097); *Desulfovibrio desulfuricans* G20 (Dde_3027), *Desulfovibrio salexigens* (Desap_2509); *Thermincola potens* JR (TherJR_2968); *Desulfovibrio aespoeensis* Aspo-2 (Daes_0530); *Desulfovibrio desulfuricans* ND132 (DND132_251); *Desulfovibrio* sp. A2 (EGY25182); *Carboxydothermus hydrogenoformans* Z-2901 (CHY_1835); *Desulfotomaculum carboxydivorans* CO-1-SRB (Desca_0340).

Some of the CooA sequences have a cysteine residue in close proximity to the histidine residues. In all of these CooA proteins the histidine residue is in close proximity to a minimum of two of these serine, threonine or cysteine residues. The mentioned residues are all recognised as having metal cofactor binding affinities and so it seems likely that these CooA proteins bind heme and these residues are involved in heme coordination, compensating for the missing cysteine residue, in these proteins.

3.5 Two unidentified CRP/FNR homologues from *D. desulfuricans*

Ddes_1411, Ddes_2092 and their homologues

Following the identification of CooA in *D. desulfuricans* the two unknown CRP/FNR homologues, Ddes_1411 and Ddes_2092, were assessed. As mentioned earlier, based on sequence similarities Ddes_2092 seems to be an equivalent of another CRP/FNR homologue in *Desulfovibrio* G20 and *D. vulgaris* whereas Ddes_1411 does not have any clear counterpart in these bacteria. Homologues of Ddes_2092 were identified by blastp searches. The best matches to Ddes_2092 included homologues from *Desulfovibrio* sp. 6_1_46AFAA (64 % identity), *Desulfovibrio* sp. 3_1_syn3 (64% identity) and Ddes_1411 (38% identity). Other strong matches included three homologues from *Bilophila* sp. 4_1_30 and another three from *Bilophila wadsworthia* 3_1_6. No experimentally characterised homologues were identified by the blastp search and the majority of the output proteins were simply annotated as ‘cAMP-binding protein’ or ‘Crp family protein’. However, a few of these sequence homologues were annotated in the NCBI database as TrmB or CarD family proteins. CarD, from *Mycobacterium tuberculosis* is a global transcription regulator that influences transcription of over 300 genes including those for rRNAs. It is also important in

infection and persistence by this bacterium and expression of *carD* is upregulated in response to chromosome breakage, oxidative stress and starvation (Stallings *et al.*, 2009). The other protein, TrmB, is a sugar sensitive transcription repressor in *Thermococcus litoralis, Halobacterium salinarum* and *Pyrococcus furiosus*. In *P. furiosus* it is responsible for regulating expression of the trehalose-maltose and maltodextrin ABC transporter genes (Lee *et al.*, 2005). Interestingly TrmB regulates expression of these two separate gene clusters by having differential responses to different sugars. Repression of each gene cluster is specifically alleviated by the presence of the corresponding sugar (Lee *et al.*, 2005). Similarly, in *H. salinarum* TrmB is believed to be a global regulator of gene expression in response to certain carbon sources (Schmid *et al.*, 2009). Comparisons between the sequences of representative TrmB and CarD proteins with those of Ddes_2092 and Ddes_1411 revealed no significant similarity between these proteins. However, since the NCBI blast program detected conserved TrmB domains Ddes_2092 could potentially have sugar binding properties.

The genes adjacent to the coding regions for Ddes_2092 and Ddes_1411 were compared with those adjacent to the genes for the best twenty Ddes_2092 homologues identified in the blastp search. Any synteny between loci was interpreted as a possible indication of conserved function between the regulators. Divergent from the coding region for Ddes_2092 is an operon of three genes encoding an arylsulphate transferase, a sodium sulphate symporter, and a porin. Sulphate transferases, also known as sulpho-transferases, catalyse the reversible transfer of a sulphate group from one molecule, usually PAPS, to another (Malojčić & Glockshuber, 2010). The arylsulphate transferases of bacteria transfer sulphate groups from one phenolic compound to another and the

activities of these enzymes have been linked to diverse processes including pathogenicity, a mechanism for the detoxification of phenols and oxidative response in bacteria (Malojčić & Glockshuber, 2010). The hydroxyl groups of tyrosine residues in proteins can also be the targets of sulphate transfer (Han *et al.*, 2012). Sodium sulphate symporters contain transmembrane regions and are involved in the uptake of sodium concomitantly with the uptake of other molecules, typically sulphate**.** Similarly, bacterial porins are generally outermembrane proteins that facilitate the import or export of various molecules or compounds. This divergent operon seems to have a role in the transport of molecules into or out of the cell; potentially these molecules could be sulphate anions.

In comparing the Ddes_2092 locus with those of the Ddes_2092 homologues identified in the earlier blast search, there were some that had noticeable synteny. These homologues syntenous with Ddes_2092 were CRP/FNR family proteins from *Desulfovibrio* sp. 6_1_46AFAA, *Desulfovibrio* sp. 3_1_syn3, *Bilophila* sp. 4_1_30 and *Bilophila wadsworthia* 3_1_6. An overview of these loci, and that of Ddes_1411, is summarised in Figure 3.6. The loci of the genes encoding the Ddes_2092 homologues in *Desulfovibrio* sp. 6_1_46AFAA and *Desulfovibrio* sp. 3_1_syn3 have the same arrangement with divergent operons. However, in addition to the three aforementioned genes, the operons of these bacteria are extended with an extra five genes. These genes are annotated as: an MFS general substrate transporter, another arylsulphate transferase distinct from the first in amino acid sequence, an NrdH-like thioredoxin, an LpdA-like lipoamide dehydrogenase and a GvcH-like glycine cleavage protein. It was noticed that these extra genes from *Desulfovibrio* sp. 6_1_46AFAA and *Desulfovibrio* sp. 3_1_syn3 are also present in *D. desulfuricans* but rather than being co-localised with Ddes_2092

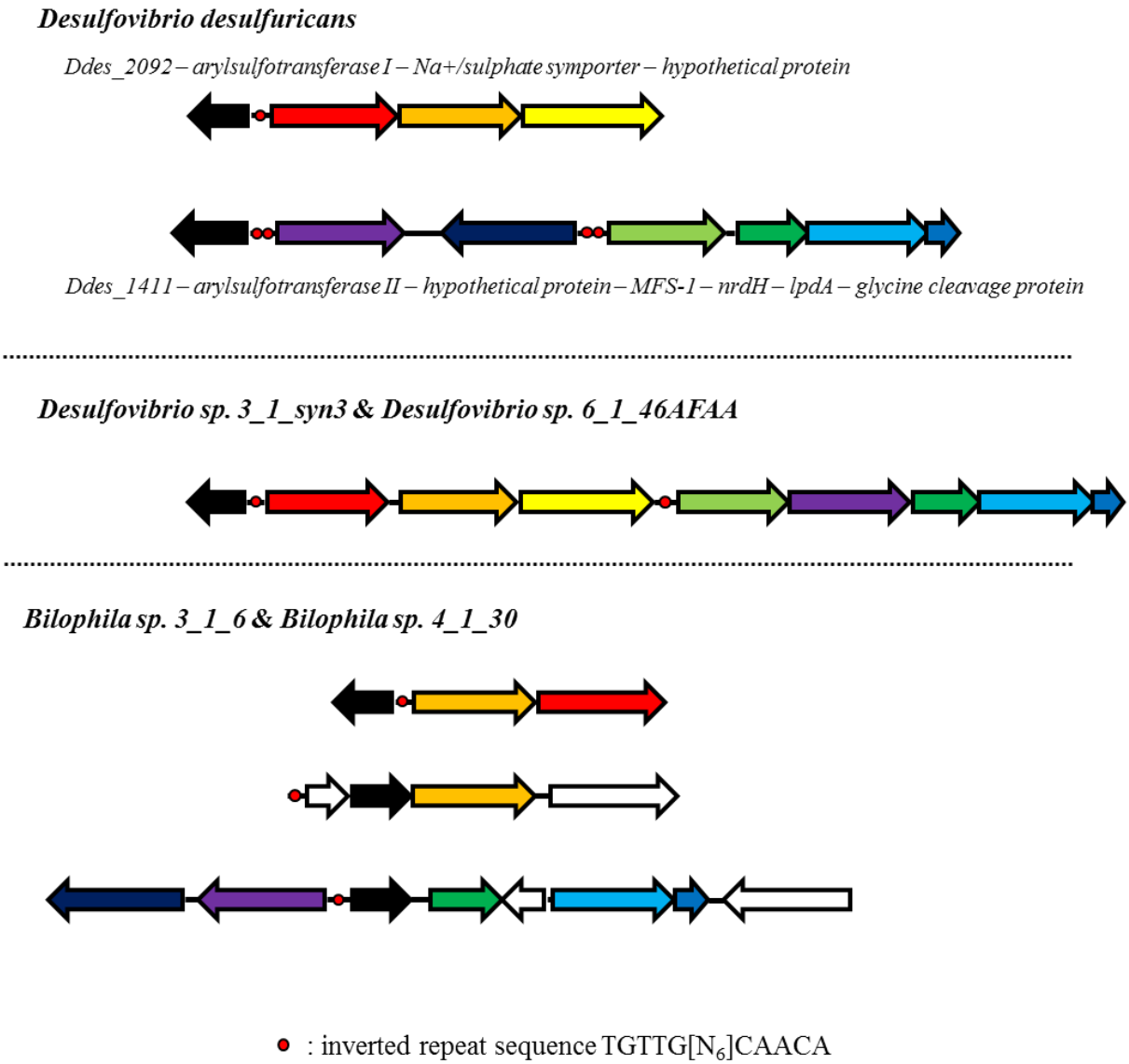


Figure 3.6: The genomic contexts of the genes encoding Ddes_2092, Ddes_1411 and homologues. Colours indicate genes with conserved protein products. White arrows represent genes not conserved at the illustrated loci in other species.

they are adjacent to the Ddes_2092 homologue, Ddes_1411, and with an alternative arrangement. The Ddes_1411 locus also has an additional gene encoding another distinct transmembrane transport protein. It seems that these operons of *Desulfovibrio* sp. 6_1_46AFAA and *Desulfovibrio* sp. 3_1_syn3 have been divided between two different loci in *D. desulfuricans*. These two loci also have individual genes for a CRP-family protein. Interestingly, almost all of these genes are also present in the *Bilophila* species but are divided between three different genomic locations. Each of these loci also has a gene for a CRP-family protein. These loci in the *Bilophila* species have some additional genes not present in the equivalent loci of the other bacteria. From examining these loci it seems that these Ddes_2092 homologues could share similar functions: they are similar in sequence and are also in close proximity to similar genes. However, the division of these genes between multiple loci in some of these bacteria and the presence of Ddes_2092 homologues at each of these loci suggests that these different bacteria could regulate these genes in different levels of complexity.

Many of the other Ddes_2092 homologues, those not syntenous with Ddes_2092 and not depicted in Figure 3.6, share synteny with each other. Typically the gene for the Ddes_2092 homologue is proximal to genes encoding sulphatases, NhaC-like transporters and various membrane proteins. These genes seem to have a similar function to those found in proximity to Ddes_2092 or Ddes_1411 in *D. desulfuricans*. However, the sequences of the gene products and the genomic organisation of these loci differ sufficiently from those of *D. desulfuricans, Desulfovibrio* sp. 6_1_46AFAA, *Desulfovibrio* sp. 3_1_syn3 and the *Bilophila* species to suggest that they may be regarded as distinct. Thus, the Ddes_2092 homologues may be sub-divided into two groups based on synteny: those similar to *D. desulfuricans* and those dissimilar to *D.*

desulfuricans. An in-depth description of the exact details of these dissimilar loci is beyond the scope of this study but for reference the species falling into this group include: *Desulfovibrio* G20, *Desulfovibrio salexigens*, *Pelosinus fermentans* A11, *Desulfovibrio vulgaris* Hildenborough, *Desulfitobacterium hafniense* Y51, *Desulfitobacterium hafniense* DCB-2, *Desulfitobacterium hafniense* DP7 and *Desulfotomaculum reducens*.

Potential DNA targets for Ddes_1411 and Ddes_2092-like regulators

Multiple alignments of the Ddes_2092 homologues were created. Unfortunately this did not provide any clues to help identify the ligands for these proteins. However, by examining the C-terminal DNA recognition helices of the aligned homologues it was clear that the majority of them had the residues R and either I, V or H at the critical positions for sequence-specific DNA recognition. Also, all of these homologues had an H residue immediately before the DNA recognition helix. Identifying putative DNA binding sites for these homologues would in turn allow identification of putative regulons for Ddes_2092 and Ddes_1411. Since many transcription regulators influence transcription from their own promoters, DNA sequences upstream of the genes encoding homologues of Ddes_2092 were scanned for palindromic sequences similar to that of CRP from *E. coli*. Surprisingly, a conserved palindromic sequence was found in the majority of scanned DNA sequences within 300 bp of the start codon of the Ddes_2092 homologues. These DNA sequences are summarised in Figure 3.7. The consensus sequence derived from these sequences is TGTTGC[N_6]GCAACA and represents a potential binding site for these regulators. Since these proteins have different amino acid residues at some of the positions of their DNA recognition helices it would be

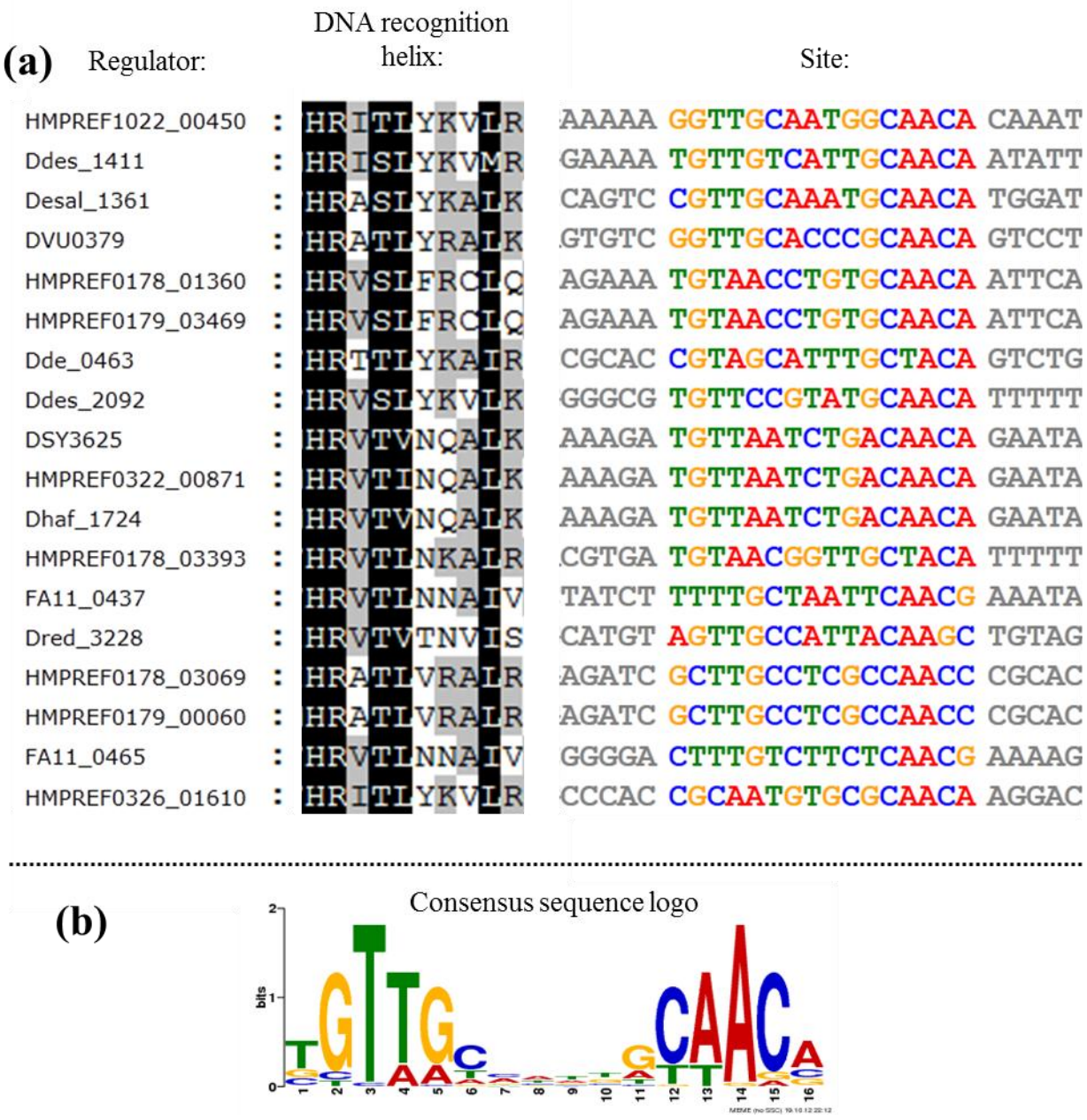

(a)
Regulator:
DNA recognition helix:
Site:
HMPREF1022_00450 : HRITLYKVLR AAAAA GGTTGCAATGGCAACA CAAAT
Ddes_1411 : HRISLYKVMR GAAAA TGTTGTCATTGCAACA ATATT
Desal_1361 : HRASLYKALK CAGTC CGTTGCAAATGCAACA TGGAT
DVU0379 : HRATLYRALK GTGTC GGTTGCACCCGCAACA GTCCT
HMPREF0178_01360 : HRVSLFRCLQ AGAAA TGTAACCTGTGCAACA ATTCA
HMPREF0179_03469 : HRVSLFRCLQ AGAAA TGTAACCTGTGCAACA ATTCA
Dde_0463 : HRITLYKALR CGCAC CGTAGCATTTGCTACA GTCTG
Ddes_2092 : HRVSLYKVLK GGGCG TGTTCCGTATGCAACA TTTTT
DSY3625 : HRVTVNQALK AAAGA TGTTAATCTGACAACA GAATA
HMPREF0322_00871 : HRVTINQALK AAAGA TGTTAATCTGACAACA GAATA
Dhaf_1724 : HRVTVNQALK AAAGA TGTTAATCTGACAACA GAATA
HMPREF0178_03393 : HRVTLNKALR CGTGA TGTAACGGTTGCTACA TTTTT
FA11_0437 : HRVTLNNAIV TATCT TTTTGCTAATTCAACG AAATA
Dred_3228 : HRVTVTNVIS CATGT AGTTGCCATTACAAGC TGTAG
HMPREF0178_03069 : HRATLVRAIR AGATC GCTTGCCTCGCCAACC CGCAC
HMPREF0179_00060 : HRATLVRAIR AGATC GCTTGCCTCGCCAACC CGCAC
FA11_0465 : HRVTLNNAIV GGGGA CTTTGTCTTCTCAACG AAAAG
HMPREF0326_01610 : HRITLYKVLR CCCAC CGCAATGTGCGCAACA AGGAC
(b)
Consensus sequence logo
bits
2
1
0
1 2 3 4 5 6 7 8 9 10 11 12 13 14 15 16

Figure 3.7: The DNA recognition helices and putative DNA binding sites of Ddes_2092, Ddes_1411 and their homologues. (a) The amino acid residues of the DNA recognition helices of the Ddes_2092/Ddes_1411 homologues were aligned with ClustalW and inverted repeat sequences were detected in upstream DNA using MEME. **(b)** The consensus sequence of the DNA target sites. Sequences used in the analysis came from the following bacteria: *Desulfovibrio desulfuricans* (Ddes_1411, Ddes_2092); *Desulfovibrio* sp. 3_1_syn3(HMPREF0178_03069; *Desulfovibrio* sp. 6_4_46AFAA (HMPREF0179_00060); *Desulfovibrio vulgaris* Hildenborough (DVU0379); *Desulfovibrio desulfuricans* G20 (Dde_0463); *Desulfovibrio salexigens* (Desal_1361); *Desulfitobacterium hafniense* Y51 (DSY3625); *Desulfitobacterium hafniense* DCB-2 (Dhaf_1742); *Desulfotomaculum reducens* (Dred_3228); *Pelosinus fermentans* A11 (FA11_0465); *Bilophila* sp. 3_1 (HMPREF0326_01610) and *Bilophila* sp. 4_1 (0322_00871).

reasonable to assume that the sequences of their DNA targets would also be different. However, the DNA target sequences for each regulator conformed to the derived consensus irrespective of whether that regulator had an I, V or A residues at position 2 of its DNA recognition helix. This would suggest that CRP homologues with residues R(I/V/A) at positions 1 and 2 of their recognition helices and preceded by an H residue all bind to the similar DNA sequences. Thus, these results suggest that Ddes_2092 and Ddes_1411 both bind to DNA sites conforming to the same consensus sequence.

The positions of the palindromic DNA sequences found in *D. desulfuricans, D. desulfuricans, Desulfovibrio* sp. 6_1_46AFAA, *Desulfovibrio* sp. 3_1_syn3 and the *Bilophila* species were positioned within 250 bp of the genes for the Ddes_2092 and also within this distance of the start codon of the first gene of the operons divergent from the Ddes_2092 homologue (shown in cartoon in Figure 3.6). Therefore, it is likely that should a regulator bind these sites then it could influence transcription in both directions. The consensus DNA target sequence for Ddes_2092 and Ddes_1411, TGTTGC[N_6]GCAACA, was used for scanning the *D. desulfuricans* genome. Many sites conforming to this consensus sequence were identified proximal to the coding regions for genes and so a putative regulon was assembled (Table 3.2). This putative regulon includes genes and operons with varied functions. Genes in this regulon are annotated as encoding proteins involved in amino acid, purine and thiazole biosynthesis and a putative Fe-Mo cofactor biosynthesis protein in addition to the aforementioned sulphotransferases. These putative gene functions hint that Ddes_1411 and Ddes_2092 could be involved in the regulation of protein production and/or post-translational modifications. The presence of genes annotated as encoding transporter complexes, an EamA-like transporter, a TetR encoding gene and various flagellar components suggest

Table 3.2: A putative regulon for regulators Ddes_2092 and Ddes_1411

Gene & protein identifiers	Operon	Site	Position
Ddes_0315	phosphoribosylaminoimidazolesuccinocarboxamide synthase	TCTTGCGACTGCAACA	-301
Ddes_0338 -0334	predicted phospho-2-dehydro-3-deoxyheptonate aldolase 3-dehydroquinate synthase chorismate mutase 3-phosphoshikimate 1-carboxyvinyltransferase prephenate dehydrogenase	TGTTGTTTCTGCAAAA	-275
Ddes_0391-0394	protein of unknown function DUF1078 domain protein FlgEFG-like flagellar basal-body rod protein FlgG flagella basal body P-ring formation protein FlgA flagellar L-ring protein FlgH	TGTTGCAACAGAAACA	-277
Ddes_0604	hypothetical protein Ddes_0604	TGCTGCTGGCGCAACA	-299
Ddes_0698 -0696	flagellar export protein FliJ hypothetical protein Ddes_0697/ flagellar protein FlbB tRNA pseudouridine synthase A TruA	TGTTGTATTGACAAGA	-73
Ddes_0873	protein of unknown function DUF6 transmembrane	TGTCGAAGGCGCAACA	-41
Ddes_1411	cyclic nucleotide-binding protein	TGTTGCAATGACAACA	-173
Ddes_1412	aryl sulphotransferase	TGTTGCAATGACAACA	-127
Ddes_1414-1417	major facilitator superfamily MFS_1 hypothetical protein Ddes_1415 FAD-dependent pyridine nucleotide-disulphide oxidoreductase glycine cleavage system H protein	TGTTGCCCATGCAACA TGTTGCACCAACAACA	-250 -124
Ddes_1413	hypothetical protein Ddes_1413	TGTTGCACCAACAACA	-211
Ddes_1472-1474	hypothetical protein Ddes_1472 cobalt ABC transporter, inner membrane subunit CbiQ ABC transporter related	TTTTGCCCGTGCAACA	-69
Ddes_1543	FAD-dependent pyridine nucleotide-disulphide oxidoreductase	TGTTGTACGCGCAACA	-335
Ddes_1863 -1862	protein of unknown function DUF134 transcriptional regulator, TetR family	TGTTGTGCCGGGAACA	-217
Ddes_1893	oligopeptide/dipeptide ABC transporter, ATPase subunit	TGTGGCAAAAACAACA	-105
Ddes_2092	cyclic nucleotide-binding protein	TGTTGCATACGGAACA	-81
Ddes_2093 -2095	hypothetical protein Ddes_2093 sodium/sulphate symporter hypothetical protein Ddes_2095	TGTTGCATACGGAACA	-128
Ddes_2166 -2168	thiazole biosynthesis family protein thiG thiazole biosynthesis protein ThiH UBA/THIF-type NAD/FAD binding protein thiG	TGCTGCGCATACAACA	-208
Ddes_2261	diguanylate cyclase	TGCTGCGCCCGCAACA	-208

potential roles in metabolite transport, antibiotic resistance and motility. Interestingly, a gene annotated as a diguanylate cyclase is also present in the putative regulon. Cyclic-di-GMP is an important messenger molecule for bacteria and functions in signalling pathways with diverse purposes. Particularly, cyclic-di-GMP is recognised as being crucial in the regulation of biofilm formation and dispersal, the switch between sessile and motile lifestyles, and also cell-cell interactions in some bacteria (Römling *et al.*, 2013). Cyclic-di-GMP has also been demonstrated to function in signalling pathways responsive to nitric oxide (Plate & Marletta, 2012). It is worth noting that putative diguanylate cyclase genes were found in close proximity to the majority of the genes for the other Ddes_2092-like regulators. It seems possible that c-di-GMP or GTP could be the allosteric effector molecule for Ddes_2092 and/or Ddes_1411. Indeed, Clp, a CRP family protein from *Xanthomonas campestris* has been demonstrated to bind cyclic-di-GMP as an allosteric effector molecule and that binding seems to be dependent upon specific D and R residues (Chin *et al.*, 2010). A comparison between the sequences of Ddes_1411, Ddes_2092 and Clp indicate that the Ddes_2092 lacks the majority of the residues known to be involved in the binding of cyclic-di-GMP by Clp and Ddes_1411 contains only half of the necessary residues.

3.6 HcpR from *D. desulfuricans*

DNA recognition by HcpR

Two putative HcpR proteins were identified from *D. desulfuricans* using the sequences of HcpR from *D. vulgaris* and *Desulfovibrio* G20. Both of these *D. desulfuricans* HcpR homologues are 24-25 % identical to those of *D. vulgaris* and *Desulfovibrio* G20 whereas the HcpRs from the latter species share 64 % identity. Thus it seems that the

HcpR proteins from *D. desulfuricans* are distinct from those of *D vulgaris* and *Desulfovibrio* G20 and could represent a separate branch of the HcpR family tree. Before discussing these two putative HcpR proteins further it is prudent to consider the defining characteristics of HcpR proteins according to Rodionov *et al*. in the initial articles describing these proteins (Rodionov *et al.*, 2004; Rodionov *et al.*, 2005). First, HcpR is named as the *hcp* regulator and so *hcp* should be part of the HcpR regulon. In *Desulfovibrio* species, HcpR is co-localised with the *hcp* gene which is part of a transcriptional unit with the ferredoxin encoding *frdX*. Regulation of these two genes is a defining characteristic of HcpR. Second, the *Desulfovibrio* HcpR regulon also includes *sat, apsAB, adhE* and a host of genes encoding uncharacterised or unidentified proteins. These unidentified proteins include a pair of nitrite-sulphite reductase-like proteins, a polyferredoxin, a conserved Archaeal protein and putative PhcAB proteins for thiosulphate reductase. Finally, the candidate binding site for HcpR in the *Desulfovibrio* species is TTGTGA[N_6]TCACAA. This is identical to the consensus binding site for *E. coli* CRP. This is due to the presence of the residues R, E and R at positions 1, 2 and 6 of the DNA recognition helices of these proteins (Parkinson *et al.*, 1996).

The DNA recognition helices of the *D. desulfuricans* HcpR proteins were compared with those of the other *Desulfovibrio* HcpRs and *E. coli* CRP. Ddes_0528 fulfilled the requirements for binding to DNA sites with the consensus TGTGA[N_6]TCACA by having the appropriate residues for DNA recognition (Figure 3.8). It is interesting to note that *E. coli* FNR binds to sites with the consensus TTGAT[N_4]ATCAA because of the presence of an S residue at position 5 of the DNA recognition helix (Spiro *et al.*, 1990). *D. desulfuricans* HcpR also has an S residue at this position. This nucleophilic S residue in HcpR could make additional contacts with the target DNA. Thus,

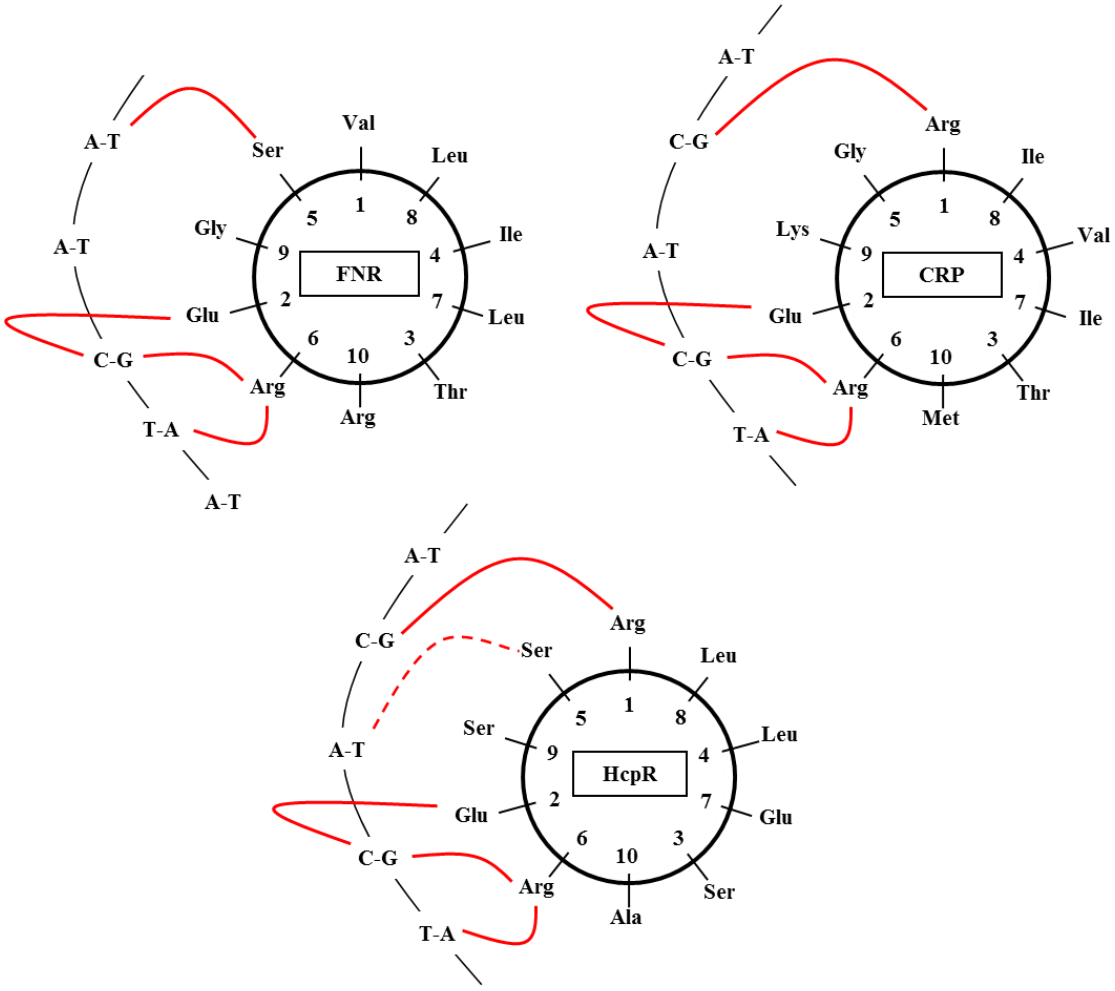


Figure 3.8: The DNA recognition helices of *D. desulfuricans* HcpR, *E. coli* CRP and FNR. Helical wheel representation of CRP, FNR and HcpR DNA recognition helices. Numbers are with respect to position within DNA recognition helices. Red lines indicate amino acid – DNA interactions. Broken red line indicates potential FNR-like contact between *D. desulfuricans* HcpR and DNA. The HcpR proteins of *D. vulgaris* and *Desulfovibrio* G20 also contain the residues necessary for contacting DNA in a CRP-like manner. Figure adapted from Green *et al.* (2001).

D. desulfuricans HcpR fulfils the requirements for binding to both CRP- and FNR-type DNA binding sites and could therefore have more stringent DNA recognition than CRP. The other HcpR family protein of *D. desulfuricans*, Ddes_1827 or HcpR2, lacks CRP or FNR-like DNA recognition residues and will be discussed later.

The *D. desulfuricans* HcpR locus

The genomic context of the gene for the putative HcpR protein of *D. desulfuricans* was checked and compared to that of *D. vulgaris* and *Desulfovibrio* G20 to assess any synteny between these loci. In comparing these loci it is apparent that *D. desulfuricans* HcpR is distinct from the other two *Desulfovibrio* HcpRs (Figure 3.9). HcpR from *D. desulfuricans*, rather than being in close proximity to an operon containing *hcp*, *frdX* or *ushA*, is upstream from genes encoding three unrelated proteins. One of these uncharacterised genes was initially thought to be an *frdX* homologue as it is annotated as encoding a ferredoxin-type protein. However, in comparing sequences it became apparent that this gene encodes a protein that is more similar to the *D. vulgaris* HcpR regulon member DVU1081, which is annotated as being a polyferredoxin nitrite-sulphite reductase. The *hcpR2* gene from *D. desulfuricans* is in close proximity to *hcp* and will be disucussed in greater detail later. It seems that the genomic location of the candidate *hcpR* from *D. desulfuricans* is not syntenous with those of *hcpR* from *D. vulgaris* and *Desulfovibrio* G20. In *D. vulgaris* and *Desulfovibrio* G20 there are HcpR DNA target sites upstream of the neighbouring gene clusters (Figure 3.9). The *D. desulfuricans hcpR* locus was scanned for the presence of HcpR DNA target sites using the *E. coli* CRP PWM since the consensus sequences for these two proteins are almost identical. A perfect inverted repeat target site upstream of the candidate *hcpR* was detected

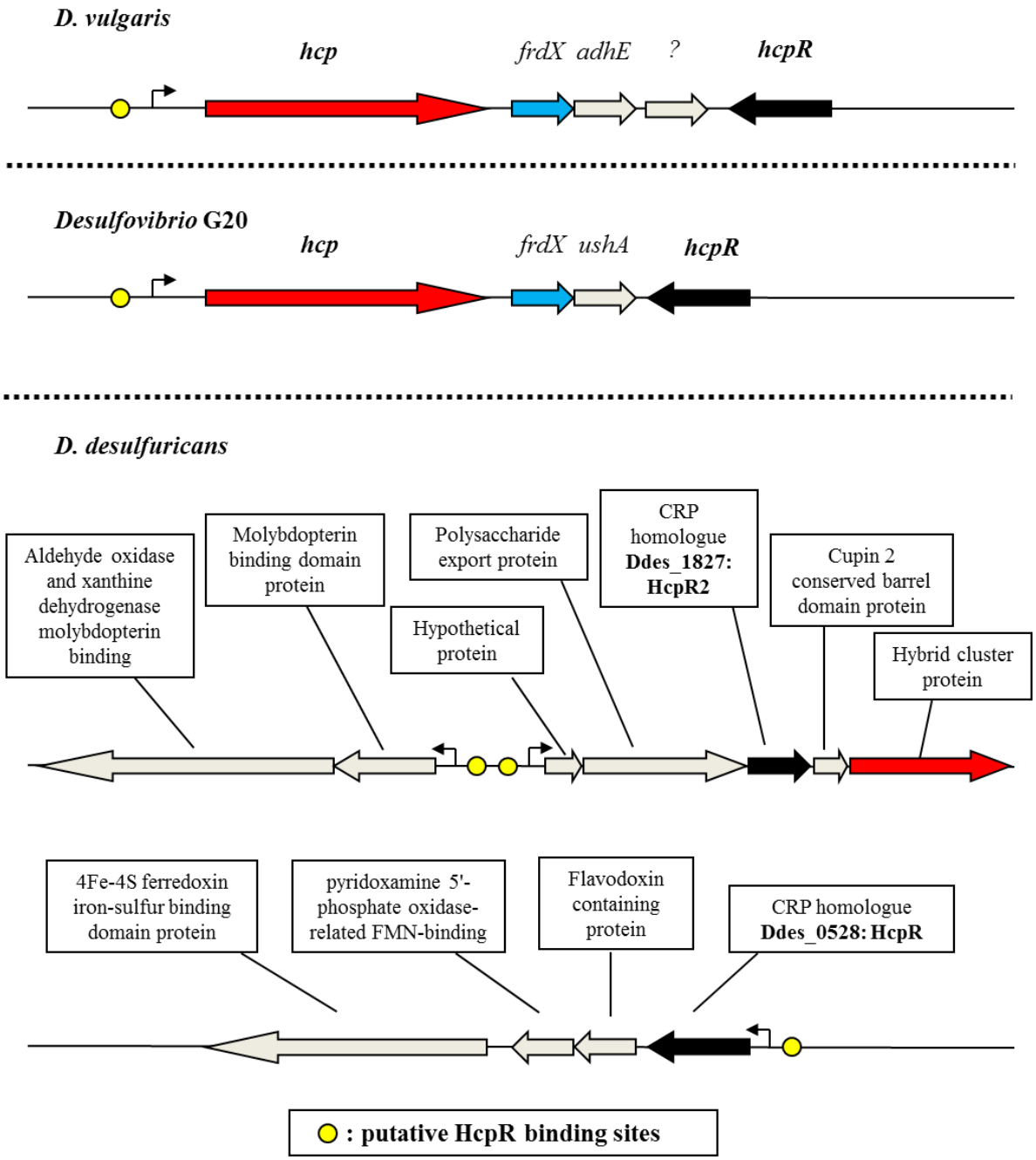


Figure 3.9: Comparison of the *hcpR* loci of *D. vulgaris*, *Desulfovibrio* G20 and *D. desulfuricans*. Gene annotation for *D. vulgaris* and *Desulfovibrio* G20 are the same as those given in Rodionov *et al.* (2005) whereas those for *D. desulfuricans* are derived from the NCBI Gene database. Genes not conserved between loci are coloured grey.

suggesting that HcpR from *D. desulfuricans* could potentially be subject to auto-regulation and also, should the downstream polyferredoxin be part of the same operon, regulate expression of a conserved HcpR regulon member.

The HcpR regulon

The *Desulfovibrio* regulon members reported by Rodionov *et al.* (2005) were used in blast searches to identify homologues in *D. desulfuricans.* The majority of the *Desulfovibrio* HcpR regulon members have homologues in *D. desulfuricans* with the exception of conserved *Archae* protein DVU0186, the *cooMLXUHXF* operon, DVU2546, arylsulfatase, and DVU1080. No obvious homologues of these proteins could be identified in *D. desulfuricans*. The corresponding promoter DNA sequences for each of the *Desulfovibrio* HcpR regulon homologues were scanned for the presence of HcpR target sites to confirm whether these genes are also part of the HcpR regulon in *D. desulfuricans.* Putative sites and their target genes were listed according to their scores with respect to *E. coli* CRP PWM (Table 3.3). Candidate HcpR sites were found upstream of most of the core regulon members with varying scores with respect to *E. coli* CRP PWM. The sites found upstream of the genes and operons encoding *sat, hcp, cckA-drrA, frdX, phcAB* and *adhE* were amongst the highest scoring, suggesting conserved regulation of these genes by HcpR in *Desulfovibrio* species. Some of the HcpR regulon members identified appear to be in transcriptional units with novel regulon members, most notably *hcpR, hcpR2,* and a large gene cluster encoding a Nuo-like oxidoreductase. Additionally, some of the HcpR regulon members form different transcription units compared with the other *Desulfovibrio* species. For example, *hcp* and

Table 3.3: Candidate binding sites for HcpR upstream of *Desulfovibrio desulfuricans* core HcpR regulon members.

Gene & protein identifiers	Operon	Site	Score	Position
Ddes_0528-0525	*hcpR-wrbA-nimA-?*	TGTGActgtagTCACA	8.85	-152.5
Ddes_1568-1567	*cckA-drrA*	TGaGAattatgTCACA	7.55	-258.5
		cGgcAgatttgTCAaA	6.86	-318.5
Ddes_1825-1829	*?-wza-hcpR2-ylbA-hcp*	TGTGcttagcgTaACA	6.94	-257.5
		TGTGgtcatgaTaACt	6.6	-199.5
Ddes_0454	*sat*	TGTGAataatcTaACA	6.92	-98.5
Ddes_1667-1654	*phcA-phcB*-large gene cluster encoding NADH-quinone oxidoreductases Nuo family	gtTGAaaatacTCACt	6.89	-98.5
		gGTaAgctctaTCAaA	6.44	-187.5
Ddes_1080-1079	*frdX-?*	gcTGAaacaatgCAtA	6.88	195.5
Ddes_1943	*adhE*	TGTGtaaaaagTaACA	6.68	-178.5
		gGTGAacaatcaaACA	6.57	-232.5
		aGTGgtacatgTCgCg	6.46	-40.5
Ddes_1146	*flrA*	gGcGAccatctTtACA	6.81	-274.5
Ddes_1355-1368	gene cluster encoding carboxysome shell proteins and aldehyde dehydrogenases	gaTGAcaggttcCACA	6.73	-264.5
		gGTGgcttgcggCACA	6.72	-31.5
Ddes_2093-2095	*?*-sodium/sulphate symporter-*?*	TGTGAaaaatgTtgCA	6.73	-129.5
Ddes_2154	*gatA* 6-aminohexanoate-cyclic-dimer hydrolase	TtTcAaagccgTCAgA	6.51	-191.5
Ddes_0873	permease	TGTaAaaaaaaaCAgA	6.50	-327.5
Ddes_1199-1202	thioredoxin-thioredoxin reductase-*?-?*	TGTcAgaaacaTgAgA	6.46	-145.5
Ddes_2130-2128	*apsA-apsB*	TagaActtttttCACA	6.40	-245.5
Ddes_0770	*?*	TaTGAcaagttTtAtA	6.38	-186.5
Ddes_0761	*uspA*	gGTaAtctttgTgAaA	6.15	-104.5

frdX along with either *uspA* or *adhE* are in the same gene clusters in *D. vulgaris* and *Desulfovibrio* G20, whereas in *D. desulfuricans* these genes are in separate transcription units. It is likely that the selection of core HcpR regulon members presented here is an over representation of the HcpR regulon due to the use of the CRP PWM which provides a score for target sites based not only upon the TGTGA[N_6]TCACA motif but also upon the flanking sequences.

In addition to the search for conserved HcpR regulon members, the *E. coli* CRP PWM was used to scan the *D. desulfuricans* genome for novel HcpR regulon members. The results are summarised in Table 3.4. The HcpR regulon of *D. desulfuricans* seems to be extended by comparison to those of the other *Desulfovibrio* species and comprises a large number of transcription units that are putatively involved in electron transport and central metabolism. The *nap* operon and *sat* are part of the regulon and so potentially HcpR could regulate terminal electron acceptor selection by *D. desulfuricans*. Additionally, the *ech* operon for *E. coli*-like hydrogenases, *hmc-hybAB* operon for 9 heme cytochrome *c* and hydrogenases, *atp* operon for ATP synthase and the flavodoxin encoding *fldA* units are all part of the HcpR regulon. The *ssc* gene, which encodes the split-soret cytochrome, is also part of the *D. desulfuricans* operon. This cytochrome is suspected to play a role in nitrate reduction by *D. desulfuricans* (da Silva *et al.*, 2012). There are also several other transcription regulators that seem to be under the influence of HcpR including two-component systems, an IscR-NsrR-like regulator and the CRP homologue, Ddes_1411. Should expression of these regulators be controlled by HcpR then the secondary effects of regulation by HcpR would be likely to be wide reaching. It seems that the HcpR regulon of *D. desulfuricans* contains a large number of genes

Table 3.4: Novel HcpR regulon members in *D. desulfuricans*

Gene & protein identifiers	Gene names & putative functions	Site	Score	Distance
Ddes_0397	[glycosyltransferase]	TtTGAtgtccaTCACa	8.54	-45.5
Ddes_0614-0619	*napCMADGH* [periplasmic nitrate reductase operon]	TaTGAaactggTCAtA	8.04	-230.5
		TGTGAtgttttTCtCA	8.14	-187.5
		aGTGAgtaataTCACA	8.84	-168.5
Ddes_0704	*?*	aGTGAcgaatttTtACt	7.85	-39.5
Ddes_0834	[hydrogenase maturation protease]	gtTGAaatgttTtACA	7.70	-115.5
Ddes_0984	*?*	TtTGAcaatctTCAtC	7.81	-307.5
Ddes_1164-1165	[cupin 2 barrel domain protein]-*?*	TGTGcgtatacTCACA	7.91	-90.5
Ddes_1204-1206	*efp-ftsK-lolA* [elongation factor P – cell division protein – outer membrane protein]	cGTGAtttcctTCAaA	7.91	-105.5
Ddes_1203	[GTP binding protein]	cGTGAtttcctTCAtA		-83.5
Ddes_1228	*?*	TaTGAttaatcTCACc	8.12	6.5
Ddes_1237-1245	[cytochrome *c* and Rnf-like electron transport components]	TGTGAaaaataTCACc	8.03	-204.5
Ddes_1252-1261	[operon encoding: biosynthesis of secondary metabolites, fatty acid metabolism, anti-sigma factor antagonist, glycosyl transferase] – *fliK- flgD- flgE* [flagellar components]	TGTGAcgtgctTCACc	8.21	-65.5
Ddes_1526	*?*	TGTtAtatgtttTtAtA	7.87	-136.5
Ddes_1527-1532	[anion transporter-succinate dehydrogenase/fumarate reductase operon]	TGTGAttttttTtACA	8.10	-230.5
Ddes_1538	[extracellular solute binding protein]	TaTGAaaaaaaTaAat	7.78	-6.5
Ddes_1539	[non-specific serine/threonine protein kinase]	TaTGAaaaaaaTaAat	7.78	-125.5
Ddes_1673-1668	*echABCDEF* [*E. coli*-like hydrogenase operon]	gGTGAagttttTCACA	7.95	-34.5

Table 3.4: Novel HcpR regulon members in *D. desulfuricans* (continued)

Gene & protein identifiers	Gene names & putative functions	Site	Score	Distance
Ddes_1951	*fldA* [flavodoxin]	TGTGAgcgcgaTCACA	8.35	-249.5
Ddes_2228-2229	[transposase-integrase]	TGTtAtattcaTaACA	7.94	-125.5
Ddes_2286-2287	*panC-metK* [amino acid metabolism]	caTaAactataTCACA	7.74	-18.5
Ddes_2124	*?*	cGTaAttttatTCAat	6.92	-29.5
Ddes_2183-2189	*atpF$_1$F$_2$HAGDC* [ATP synthase]	TGcGAaatttgTCACc	6.60	-103.5
Ddes_2038-2041	*hmc-hybA-hybB-*? [9 heme cytochrome *c* and hydrogenases]	aaTGAaatattTCtCA	6.50	-194.5
Ddes_2252-2253	*?*	gcTGagataatTtACA	6.70	-101.5
Ddes_1136-1134	[putative sodium ion transport operon]	caTGAtgctccTCAaA	7.00	-151.5
Ddes_1956-1957	[nucleotide metabolism]	TGTGcaaaaaagcACA	6.71	-41.5
Ddes_1078-1075	*metA-?-nifU-nifS* [suphur metabolism operon and Rrf2-family transcription regulator]	TGcGAcagcgtTaACA	6.36	-52.5
Ddes_0339-0340	[cysteine and methionine metabolism]	TGCGAtcgcgtTCGCC	6.56	-92.5
Ddes_1568-1565	[operon encoding putative pyruvate metabolism genes and two-component regulator system]	TGaGAattatgTCACA	7.55	-257.5
		cGgcAgatttgTCAaA	6.87	-318.5
Ddes_2292	[AMMECR1 domain protein]	TtTGcactataTCgCA	6.41	-32.5
Ddes_0843-0844	[Rrf2-like TF and response regulator]	TGcGAaagactTCACA	6.88	-173.5
		TtTcAaagccgTCAgA	6.57	-191.5
Ddes_1411	[CRP homologue]	TGcaAcaatatTCACA	6.72	-171.5
Ddes_1437-1438	[amidohydrolase operon]	TGaGAaaagtgTCACA	7.09	-122.5
Ddes_2150	*ssc* [split soret cytochrome *c*]	aGTGAttttttaACtA	6.90	-49.5
		TGTGtctgccgTgACA	6.65	-27.5

involved in central metabolic processes and electron transport and seems to be a global regulator

It is apparent that the HcpR from *D. desulfuricans* is distinct from those of *D. vulgaris* and *Desulfovibrio* G20 in sequence, synteny and, to a certain extent, its regulatory targets. Blast searches indicate that the closest homologues of *D. desulfuricans* HcpR are found in *Desulfovibrio* sp. 6_1_46AFAA, *Desulfovibrio* sp. 3_1_syn3, *Desulfovibrio piger* and *Bilophila* species. The genomic contexts of the corresponding genes of these homologues were examined and compared with that of HcpR from *D. desulfuricans* (Figure 3.10). Intriguingly the HcpR locus of *D. desulfuricans* shares a high level of synteny with those of *Desulfovibrio* sp. 6_1_46AFAA and *Desulfovibrio* sp. 3_1_syn3 except that in the latter two species *hcp* is located at the upstream end of the *hcpR* operon. The similarity between these loci is high and as such it seems that these bacteria could be closely related with the translocation of *hcp* occurring in one of these species. A critical point is that the HcpR TGTGA[N_6]TCACA motif was located upstream of *hcp* in these *Desulfovibrio* species. In *D. piger hcpR* is preceded by *hcp* and also in an operon with *wrbA* and *nimA* (not illustrated). However, downstream of these genes and also in the *hcpR* operon is *uspA*, *hisC* and a putative cytidylate kinase. As already mentioned, *uspA* is found in the HcpR locus of *D. vulgaris* and is a core HcpR regulon member. Thus, the *hcpR* locus of *D. piger* seems to be an intermediate between those of *D. desulfuricans* and those of *D. vulgaris* and *Desulfovibrio* G20. The genes *hisC* and putative cytidylate kinase are not conserved HcpR regulon members. In the *Bilophila* species *hcpR* is co-localised with *hcp* but the other genes at this locus in *Bilophila* encode uncharacterised proteins. The close association of *hcp* and *hcpR* seems to be a defining feature of the *hcpR* gene in most cases, with *D. desulfuricans* an exception.

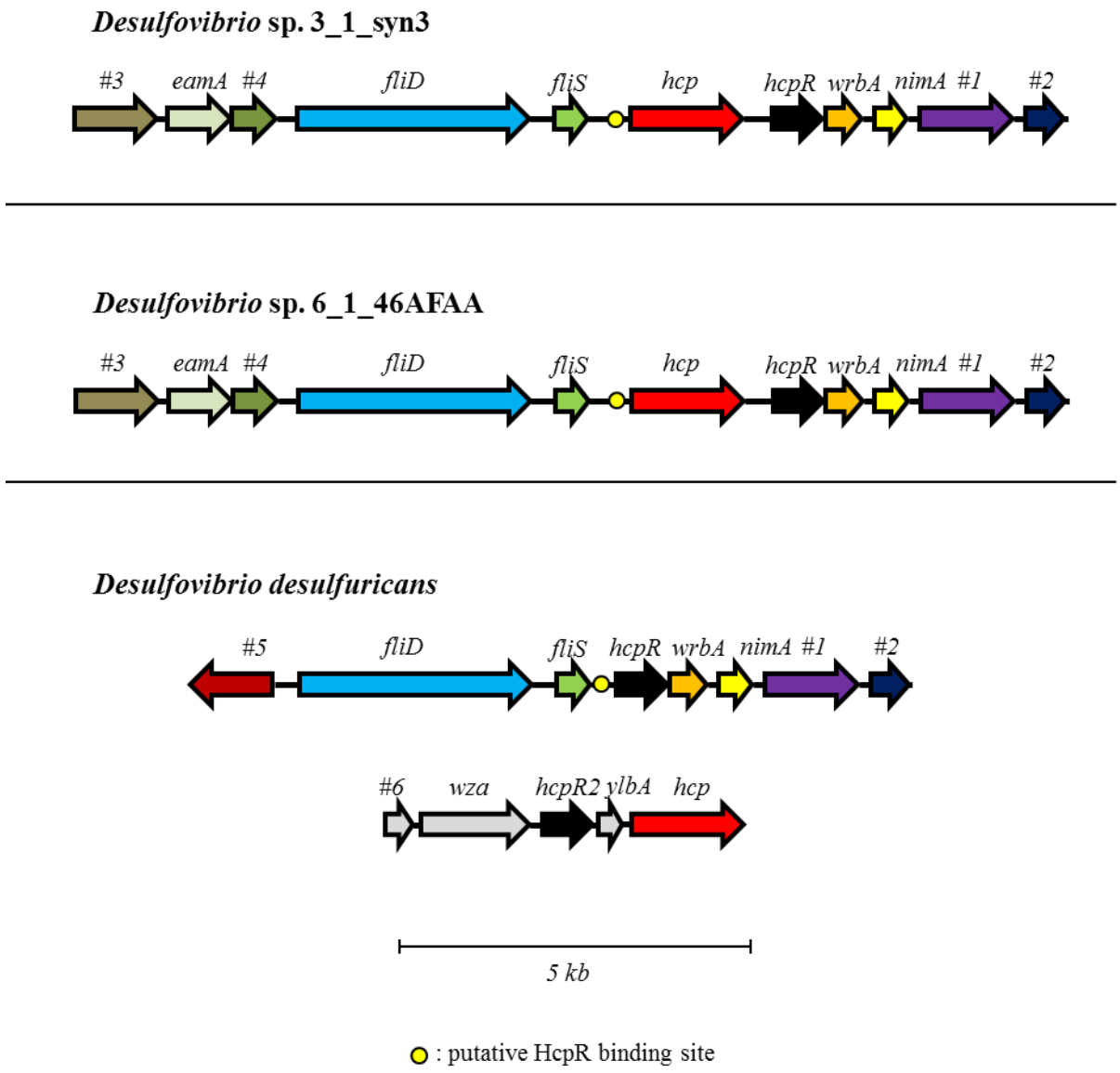
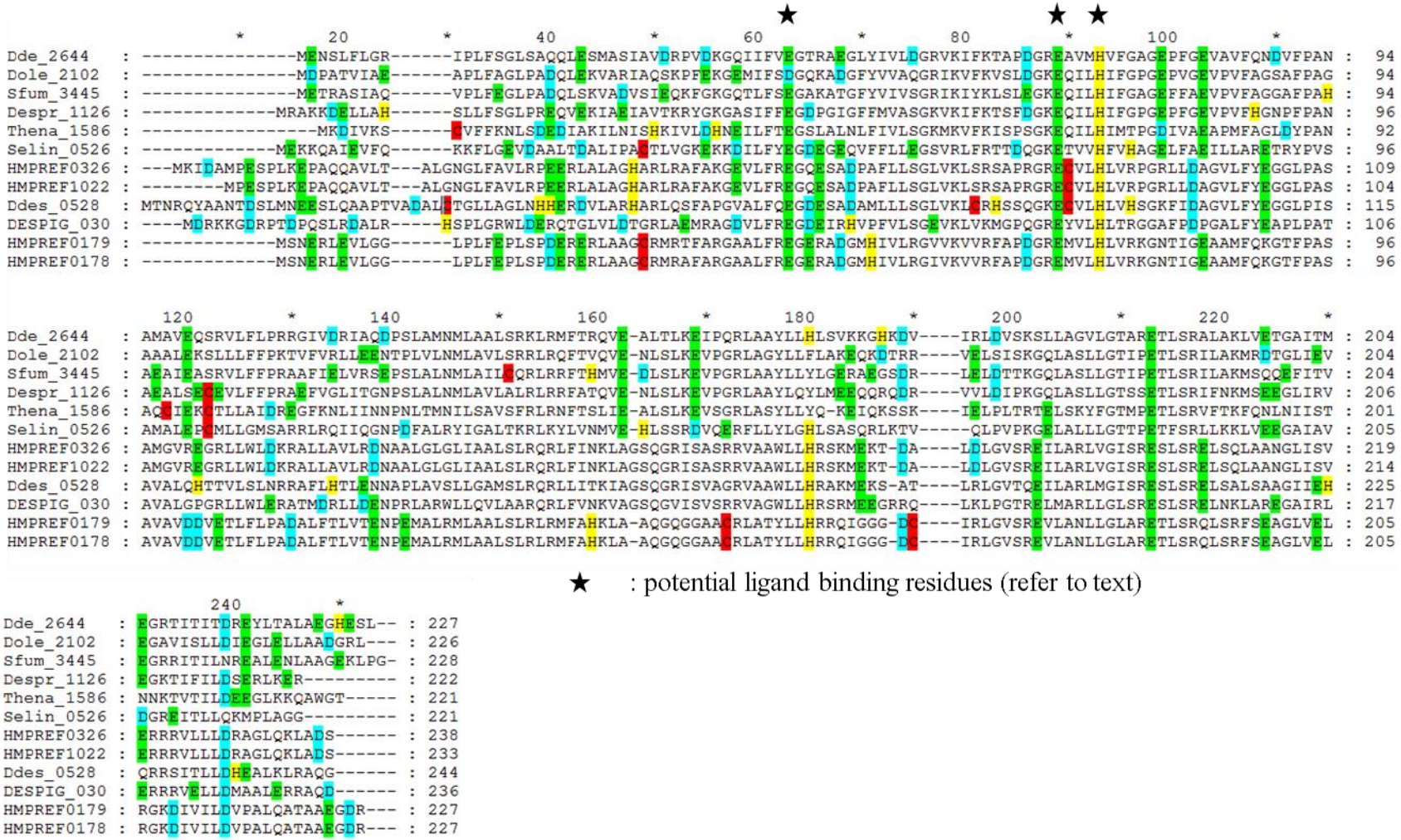


Figure 3.10: Genomic context of *hcpR* and *hcp* in the sulphate reducing bacteria *Desulfovibrio* sp. 3_1_syn3, *Desulfovibrio* sp. 6_1_46AFAA and *Desulfovibrio desulfuricans.* Putative gene names are given where possible whereas those encoding products with unknown functions are identified with a number.

Modulation of HcpR activity

Since HcpR is predicted to regulate *nap*, *sat* and *aps* it seems plausible that the effector for modulating HcpR activity could be nitrate, sulphate or a product of their metabolism. Alternatively, since the HcpR regulon includes putative redox proteins, it is possible that HcpR is redox sensitive. Another hypothesis is that since HcpR normally regulates expression of *hcp*, which is up-regulated by nitric oxide, it could contain a nitric oxide sensitive heme, iron or iron-sulphur cluster prosthetic group. A multiple alignment of *D. desulfuricans* HcpR and close homologues was generated and checked for conserved motifs that could be involved in any of these activities (Figure 3.11). Homologues of *D. desulfuricans* HcpR were included in the alignment if their corresponding genes were in close proximity to core HcpR regulon members. From scanning the sequences it was difficult to identify any conserved motif there are a number of conserved D, E and H residues that could potentially function in the co-ordination of a metal cofactor in the N-terminal portion of HcpR proteins. It seems probable that HcpR proteins might bind a metal co-factor and function through the sensing of redox state, or nitric oxide, or both. Examining the alignment closely it seems that there are separate clusters of HcpR proteins. HcpR from *D. desulfuricans*, *Desulfovibrio* sp. 3_1_syn3 and *Desulfovibrio* sp. 6_1_46AFAA have a conserved C residue that forms a CxxH motif with a conserved H residue. Additionally, just upstream from this motif in *D. desulfuricans* is a CxH motif. Both of these motifs are known to be involved in metal-binding (Schmidt *et al.*, 2010).

To test this proposal a hypothetical structure of HcpR from *D. desulfuricans* was generated using the PHYRE2 tool (Kelly & Sternberg, 2009). The structure used for the model was that of CRP from *Thermus thermophilus* and 86 % of the HcpR sequence



★ : potential ligand binding residues (refer to text)

Figure 3.11: Multiple alignment of selected HcpR proteins. Multiple alignment was generated with ClustalW. The amino acids most frequently involved in the co-ordination of metal cofactors are highlighted: C– Red; H – Yellow; E – Green; and D – Blue.

was modelled on this structure with 100 % confidence (Hudson *et al.*, 2012). The hypothetical structure of the HcpR monomer resembles that of a typical CRP-family member (Figure 3.12a). Close examination of a region in the C-terminus highlights two key features, first the presence of two C residues in close proximity to one another (Figure 3.12b) and second the presence of H and E residues in close proximity to these residues. The close proximity of the two C residues is suggestive of disulphide bonding whereas the C, H and E residues together form a potential metal chelating motif. Thus, it can be predicted that HcpR from *D. desulfuricans* either contains a metal cofactor or is responsive to redox state via disulphide bond isomerisation.

3.7 Regulation of nitrosative stress response in *D. desulfuricans* by HcpR2

HcpR2 is distinct from the HcpR proteins of other *Desulfovibrio* species

The HcpR of *D. desulfuricans* was identified by sequence identity, DNA recognition helix residues, regulon members and synteny with the genes for HcpR from *Desulfovibrio* sp. 6_1_46AFAA and *Desulfovibrio* sp. 3_1_syn3. However, *hcpR* from *D. desulfuricans* in not co-localised with *hcp*. Instead the *hcp* gene is co-localised with an additional *hcpR* gene, *hcpR2*. As illustrated in Figures 3.9 and 3.10**,** *hcp* from *D. desulfuricans* seems part of an operon with a number of other genes including *hcpR2* and genes lacking annotation. This arrangement at the *hcp* locus seems to be in contrast with the *hcp* loci of other *Desulfovibrio* species. Homologues of the protein products of *hcpR2* and its neighbouring genes were identified by blast searches. Intriguingly, the closest matches to HcpR2 were mainly CRP family proteins from *Clostridium, Eubactericeae, Lachnospiraceae* and *Selenomonas* species with no *Desulfovibrio,*

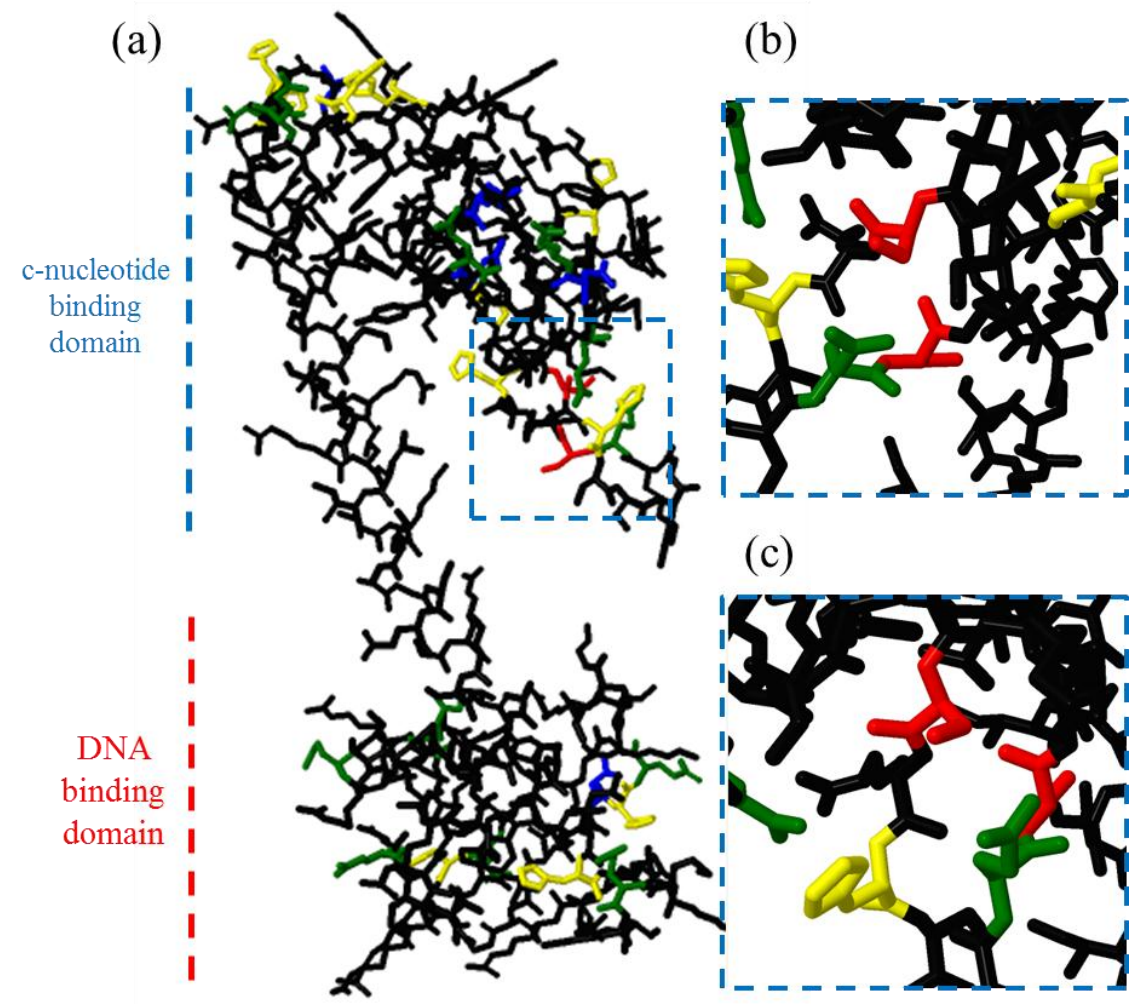


Figure 3.12: Hypothetical three-dimensional structure of HcpR from *Desulfovibrio desulfuricans*. (a) overall structure of HcpR monomer, (b) and (c) close up view of putative regulatory region. Structure generated by PHYRE2 and based upon the structure of the catabolite repressor protein from *Thermus thermophilus*. Specific residues have been coloured: C (red), H (yellow), E (green) and D (blue).

Bilophila or *Geobacter* homologues in the top 100 blastp search results. The co-localisation of *hcpR2* and *hcp* was noted for many of the HcpR2 homologues identified including those of *Johnsonella ignava* ATCC 51276, *Eubacterium saburreum* DSM 3986, *Lachnospiraceae bacterium* ICM7, *Peptoniphilus indolicus* ATCC 29427, *Treponema denticola* ATCC 35405, *Pelotomaculum thermopropionicum* SI, *Finegoldia magna* ATCC 29328, *Clostridium ljungdahlii* DSM 13528, *Veillonella parvula* DSM 2008 and *Clostridium kluyveri* DSM 555.

Some of the genes encoding HcpR2 homologues were co-localised with a gene encoding a 4Fe-4S ferredoxin similar to *frdX*, rather than *hcp*. This arrangement was noted for *Heliobacterium modesticaldum* Ice1, *Clostridium cellulolyticum* H10, *Clostridium* sp. BNL1100 and *Desulfosporosinus orientis* DSM 765. Thus, the HcpR2 homologues identified fulfil the criteria for being HcpR family proteins in terms of synteny and co-localisation with *hcp* or *frdX*. Other variations upon these arrangements were noted. The gene for HcpR2 in *Treponema brennaborense* DSM 12168 is co-localised with both *hcp* and *frdX*. This arrangement was also noted in *Tepidanaerobacter* sp. Re1 but here HcpR2 is also co-localised with a homologue of Ddes_1828. HcpR2, *hcp* and a gene encoding a Ddes_1828 homologue are also co-localised in *Clostridium* sp. MTSE9 in a putative operon divergent from an operon encoding a NorV-like protein.

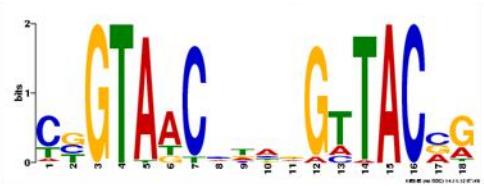
The co-localisation of HcpR2 and Ddes_1828 seems to be uncommon. To explore this further, Ddes_1828 homologues were identified and then their genomic contexts checked. Genes encoding Ddes_1828 homologues were found co-localised with *hcp* in a variety of bacteria including some *Ruminococcus*, *Sphaerochaeta*, *Acetobacterium* and *Alkaliphilus* species in addition to those mentioned above. It seems that the co-

localisation of *hcp* with Ddes_1828 in *D. desulfuricans* is conserved but this linkage is under-represented in the databases. As such it can be speculated that Ddes_1828 has some relevance to *hcp* activities and is therefore likely to be involved in some nitrosative stress response. A similar analysis of the genes preceding HcpR2 in *D. desulfuricans* was used to assess whether these genes are found co-localised with *hcpR2* or *hcp* in other bacteria. Ddes_1825 is under-represented in the sequence databases with fewer than 10 full length homologues identified in the blastp search. However, Ddes_1825 and Ddes_1826 do not seem to be co-localised with *hcp* or *hcpR2* in any other bacteria.

DNA recognition by HcpR2

HcpR2 of *D. desulfuricans* seems to be more similar to CRP-family proteins of bacteria other than *Desulfovibrio*, particularly *Clostridium* species. Positions 1 and 2 of the DNA-recognition helix of HcpR2 are occupied by residues R and P, respectively. A thorough literature search suggests that there is no experimentally verified consensus DNA target site for CRP-family proteins with these residues in their DNA recognition helix. A collection of HcpR2 homologues was assembled in an attempt to identify a consensus binding site for HcpR2. Homologues were included in the collection if they included the critical R and P residues and were co-localised with *hcp* and/or *frdX*. A total of 18 homologues fulfilling these criteria were used in a multiple alignment. DNA sequences upstream the relevant *hcpR2*, *frdX* and *hcp* genes were then scanned for inverted repeat sequences similar to that of CRP. A conserved inverted repeat sequence with the consensus GTAAC[N_4]GTTAC was identified at all of the *hcpR2* loci used in the study (Figure 3.13). The arrangement of the *hcpR2, hcp* and/or *frdX* genes for these 18 homologues was variable with the gene for *hcpR2* being divergent from, continuous

HcpR2 identifier:	DNA recognition helix residues:	Putative target site:	
CLOSCI_032	LNVARPSLSRELMRM	AAT CCGTAACAAATGTTACGG ATT	
HMPREF1141	MNTARPSLSRELMKM	AAT CCGTAACGCCGGTTACGG ATT	
Ddes_1827	LGVTRPSLSRELAAM	GTT CCGTAACAATTGTTACGG ACG	
CKL_0934	LNVSRPSMSREMCRM	ATT CGGTAACTTAGGATACGA AAA	★
PTH_0781	LNVSRPSLSRELGRM	AAT TGGTAACCGCGGTTACCA AAA	★
HMPREF1152	LGVTRPSISRELMKM	GAA TTGTAACATAGGTTACAG ATT	
Desor_3650	LNVSRPSMSREMGKM	AGT CGGTAGCTGAGGATACAG AAT	★
HM1_0005	LNVSRPSMSREMARM	AAT CGGTAGCCATGGCTACCG AAA	★
CLJU_c0772	LNVSRPSLSREMCHM	AAT CGGTATCCTCTGTTACCA AAT	★
TDE0478	LAVPRPSLSRELMSM	TCC ACGTAACATCCGTTACCG ACT	
HMPREF9129	LGVPRPSVSRELMNM	TTG ACGTAACATATGTTACAG ATG	
FMG_0410	LATTRPSLSRELLSM	CAA ATGTAACTTATGTTACAG AAA	
HMPREF0381	LNAARPSLSRELMKM	GCT CGGTAATGTAAGTTACAG TTT	
HMPREF9970	LNAARPSLSRELMKM	AAA CTGTAACTTACATTACCG AGC	
TepRe1_258	LNVSRPSMSREMSRM	TTT CGGTAGCTGTGGCTACAA AAA	★
Ccel_1360	LNISRPSMSREMGVM	AAT CGGTATCTCTGGATACCA AAA	★
Clo1100_10	LNISRPSMSREMGIM	GTT CGGTATCTGGAGATACAA AAG	★
HMPREF9333	TARPSLSRELMRMQK	ATA GCGTAACCCAAGTAACGG AAT	



★ : binding site identified upstream of HcpR2

Figure 3.13: Identification of a putative consensus DNA binding site for HcpR2-type CRP regulators. A multiple alignment of homologues of HcpR2 with residues R and P at position 1 and 2 of their DNA recognition helices was generated with ClustalW. DNA sequences upstream of the genes encoding these homologues or upstream of *hcp* were scanned for inverted repeat sequences using MEME. A conserved inverted repeat sequence was identified. Protein and DNA sequences used for the analysis came from the following bacteria: *Desulfovibrio desulfuricans* (Ddes_1827); *Clostridium scindens* ATCC 35704 (CLOSCI_03220); *Clostridium* sp. MSTE9 (HMPREF1141_2562); *Mogibacterium* sp. CM50 (HMPREF1152_1386); *Johnsonella ignava* ATCC 51276 (HMPREF9333_00217); *Dorea longicatena* DSM 13814 (DORLON_00955); *Eubacterium saburreum* F0468 (HMPREF9970_2685); *Eubacterium saburreum* DSM 3986 (HMPREF0381_2284); *Peptoniphilus indolicus* ATCC 29427 (HMPREF9129_1156); *Treponema denticola* ATCC 35405 (TDE0478); *Heliobacterium modesticaldum* Ice1 (HM1_0005); *Pelotomaculum thermopropionicum* SI (PTH_0781); *Finegoldia magna* ATCC 29328 (FMG_0410); *Clostridium cellulolyticum* H10 (Ccel_1360); *Clostridium* sp. BNL1100 (Clo1100_1045); *Desulfosporosinus orientis* DSM 765 (Desor_3650); *Clostridium ljungdahlii* DSM 13528 (CLJU_c07720); *Tepidanaerobacter* sp. Re1 (TepRe1_2581) and *Clostridium kluyveri* DSM 555 (CKL_0934).

with, or in a putative operon with the genes for *hcp* and/or *frdX*. The identified repeat sequences are positioned so that HcpR2 could control expression of *hcp* and/or *frdX*. Additionally, eight of these inverted repeat sequences were also located upstream of the *hcpR2* gene suggesting auto-regulation of HcpR2 in some cases (Figure 3.13, marked with a star). The majority of these putative HcpR2 binding sites were located within close proximity, less than 100 bp, to the start codon of the downstream genes. The presence of this conserved inverted repeat sequence in close proximity to the *hcpR2*, *hcp* and *frdX* genes in these various bacteria suggests that this sequence could be the DNA target of HcpR2 and that once bound to this site HcpR2 could exert some influence over the transcription of these genes.

A multiple alignment of the HcpR2 homologues was examined for conserved residues (data not shown). The HcpR2 protein sequences are variable and it was not possible to identify a conserved motif for the binding of co-factors or ligands. Some of the HcpR2 proteins, including that of *D. desulfuricans*, contained multiple C residues. *D. desulfuricans* has seven C residues suggesting that HcpR2 in this bacterium might be redox responsive or bind to a metal cofactor.

The HcpR2 regulon

The putative HcpR2 target sequence was used for a genome wide scan in *D. desulfuricans* to identify a putative HcpR2 regulon. Five sites were discovered within promoter-proximal DNA sequences (Figure 3.14). One of these sites is adjacent to the *hcp* locus and has already been described. Another site is upsteam from an operon encoding Dfx, desulfoferredoxin, a rubredoxin-type protein, Rd1, and a beta-lactamase domain containing protein. Desulfoferredoxin is a flavo-diiron protein with superoxide

Genes/Functions:	Position:	Site:	
Cupin 2 barrel protein – *hcp* / nitrosative stress	-62.5	CGTAACAATTGTTACG	Ddes_1828-Ddes_1829
dfx – *rd1* – beta-lactamase flavodoxin protein / superoxide reductase and electron transport	-109.5	GGTATCCGGGGCTACA	Ddes_2010-Ddes_2011-Ddes_2012
Two component system OmpR family	-37.5	TGTACCCGAGGGTACG	Ddes_2272-Ddes_2271
Hypothetical protein – hypothetical protein – single stranded DNA binding protein	-158.5	TGTGCCCCCGGGTACG	Ddes_0457-Ddes_0456-Ddes_0455
Lipopolysaccharide biosynthesis protein – hypothetical protein – lipopolysaccharide biosynthesis protein	-139.5	GGTACTCAAGGGTACT	Ddes_2211-Ddes_2210-Ddes_2209

0 :putative Ddes_1827 binding site 0 :putative HcpR binding site

Consensus:

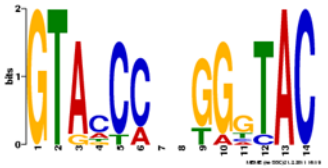


Figure 3.14: The putative regulon of HcpR2 from *D. desulfuricans*. Positions of HcpR binding sites are listed relative to translation start codons.

and nitric oxide reductase activity (Riebe *et al.*, 2007; Silaghi-Dumitrescu *et al.*, 2005). The rubredoxin protein is relatively short being only 45 amino acids long. Blast searches with this sequence against *E. coli* genomes indicated that the amino acid sequence of this protein is similar to a region of the nitric oxide reductase, NorV. Furthermore, blast searches with the sequence of the beta-lactamase protein from *D. desulfuricans* against *E. coli* genomes indicated that this protein is very similar to the nitric oxide reductase NorV in terms of sequence. Another locus where HcpR2 sites were discovered is immediately upsteam of an operon encoding an OmpR-type two-component regulatory system. OmpR-like proteins, such as CosR, have been shown to be involved in regulating oxidative stress response (Hwang *et al.*, 2011). These three loci seem to share a very clear function regulating the response to nitrosative and oxidative stresses. Thus, it can be predicted that HcpR2 is a regulator of one or both of these responses and that it is highly likely that the abundance of C residues contribute to the sensing of nitric oxide or superoxide.

3.8 Genes potentially related to nitrate-nitrite reduction and nitrosative stress in *D. desulfuricans*

The genome of *D. desulfuricans* was searched for the presence of genes known to be implicated in nitrate or nitrite reduction and nitrosative stress. Scanning the upstream DNA sequences of any identified genes could in turn identify conserved regulatory motifs. Much has already been written of the *nap* gene cluster of *D. desulfuricans*, with these analyses pre-dating the sequencing of the *D. desulfuricans* genome (Marietou *et al.*, 2005; Marietou *et al.*, 2009; Marietou, 2009). Using the sequences of other representative nitrate reductases it seems that the *D. desulfuricans* genome does not

encode any other nitrate reductase complexes in addition to Nap. Similarly, *D. desulfuricans* has been reported to encode genes for the nitrite reductase NrfHA (Almeida *et al.*, 2003; Liu & Peck, 1981). No other nitrite reductases could be identified using the protein sequences of other representative nitrite reductases. Thus it seems that the reported ability of *D. desulfuricans* to use nitrate and nitrite as terminal electron acceptors for growth is provided by just two enzyme complexes and is in stark contrast with the multiple enzyme complexes employed by bacteria such as *E. coli.*

As explained in Chapter 1, one of the consequences of nitrate or nitrite metabolism is the production of nitric oxide. *Escherichia coli* has a host of genes which are or believed to be responsible for dealing with this toxic molecule and these have been summarised in Vine (2012). Considering *D. desulfuricans* seems to be minimally equipped for metabolising nitrate and nitrite it would be interesting to see if this is reflected in the genes encoding nitrosative stress response proteins in this bacterium. The protein sequences for a range of nitrosative stress response proteins of *E. coli* were used to identify homologues in *D. desulfuricans*. As already mentioned, *D. desulfuricans* has an *hcp* gene and regulation of this gene is predicted to be influenced by one or two of the CRP family regulators. In *E. coli* this gene is co-transcribed with a gene that encodes the Hcp reductase, Hcr (van den Berg *et al.*, 2000; Filenko *et al.*, 2005). No Hcr homologue could be identified by the blast search. Presumably Hcp from *D. desulfuricans* is reduced by some other reductase, maybe the product of the unidentified gene preceding *hcp*. Also mentioned earlier was the presence of a NorV homologue in an operon with *dfx* and *rd1* under the control of HcpR2. No obvious homologues of YjbA, YeaR, YoaG, YibI or YibH, genes believed to be involved in nitrosative stress in *E. coli*, could be

identified. Apparent homologues of Hmp and Ogt were identified but the genes encoding these proteins are not members of the CRP-like regulons identified earlier.

Escherichia coli also has multiple transcription regulators that control nitrate or nitrite reduction and nitrosative stress response and so the sequences of these proteins were also used to identify homologues in *D. desulfuricans*. Homologues of FNR in *D. desulfuricans* have already been identified in this study. Searching with the two-component regulators NarQP and NarXL identified a number of similar regulatory systems in *D. desulfuricans* that could potentially be counterparts of NarXL-NarQP.

Multiple homologues of NsrR and NorR were identified in *D. desulfuricans.* Both of the NsrR-like proteins of *D. desulfuricans* contain conserved cysteine residues at the correct positions for co-ordination of the nitric oxide sensing [2Fe-2S] cofactor and both are predicted to be regulated by HcpR. One of the genes encoding one of these NsrR-like proteins is in an operon with iron-sulphur cluster assembly genes and is likely to be an IscR counterpart in this bacterium. The other NsrR homologue is encoded by a gene that is divergent from a gene encoding another Rrf2 family transcription regulator. Also, downstream from the gene encoding this NsrR homologue is an operon containing a gene annotated as a nitrate reductase gamma subunit. Searching with this protein sequence gave no results from either *E. coli* or *D. vulgaris* and a general search gave results that were also annotated as nitrate reductase gamma subunits. Other genes in this operon encode a putative iron-sulphur cluster binding protein and a short hypothetical protein. Potentially this operon could be involved in nitrate or nitrite utilisation or nitric oxide stress response. It is worth noting that *D. desulfuricans* possesses an *rpoN* gene

encoding a sigma-54 unit and that numerous NorR-like homologues were identified suggesting that a NorR-NorVW system could exist in this bacterium.

The DNA sequences upstream of the *nrfHA* locus were examined to identify regulatory motifs. The *nrfHA* operon of *D. desulfuricans* is divergent from an operon encoding a two component regulatory system. This is a common arrangement seen for the *nrf* genes in SRB. A study of two-component regulators in *D. vulgaris* detailed the binding of the equivalent regulator in *D. vulgaris* to a short DNA sequence between these two operons (Rajeev *et al.*, 2011). The specific sequences that the regulator bound to were not identified in that study. However, from browsing the sequence of the DNA fragment used in that study a direct repeat sequence can be seen with the sequence: GTCATCTTTTTCATGtcacctGTCATCTTTTTCATG. A similar sequence was noted upstream of the *D. desulfuricans nrf* operon. Also, this repeat sequence was seen upstream of the *nrf* operons of *Desulfovibrio* sp. 6_1_46AFAA, *Desulfovibrio* sp. 3_1_syn3 and other *D. vulgaris* species (data not shown). A similar sequence was also detected upstream of the *nrf* operon of some *Bilophila* species but these were singular sequences rather than tandem repeats. Conservation of this sequence in these bacteria suggests that it could be a conserved regulatory element to which a transcription factor binds. To identify any other potential regulatory sequences between these divergent operons the intergenic DNA sequence was scanned for inverted repeats. A perfect inverted repeat was identified with the sequence GGGTGAAGAgcggTCTTCACCC. However, this sequence in not conserved in any other species checked and seems unique to the *nrf* intergenic region of *D. desulfuricans*. Scanning the *D. desulfuricans* genome for this motif identified similar inverted repeats upstream of a number of genes but none of these seemed to encode genes related to nitrite utilisation. From this evidence it can

be predicted that *nrf* in *D. desulfuricans* is regulated by a divergent two-component regulator. This two-component regulator could respond to the presence of nitrite, resulting in phosphorylation of the transcription regulator by the histidine kinase. This regulator could then bind to one of the identified DNA sequences and up-regulate expression of *nrf.* However, there is some controversy over whether *nrf* is regulated in *D. desulfuricans*. This will be investigated in greater detail in the next chapter.

3.9 Discussion

This chapter has provided a detailed *in silico* examination of the five CRP-family proteins of *D. desulfuricans*. The gene for CooA, its target operon *cooSC* and the CooA binding site upstream of this operon in *D. desulfuricans* are arranged identically to those of *Desulfovibrio* G20 and *D. vulgaris*. Furthermore, these CooA proteins are predicted to bind a heme cofactor via residues different to CooA from *Rhodospirillum rubrum.* CooA from *D. desulfuricans*, with its single DNA target site and conserved residues, represents the simplest of the CRP-family proteins. It is likely that the sole purpose of CooA in *D. desulfuricans* is to sense CO via the heme cofactor and then activate transcription of the *cooSC* operon in response to this stress.

In contrast with the simplicity of CooA, the two unidentified regulators Ddes_1411 and Ddes_2092 represent significant regulatory complexity. These two proteins are conserved in a variety of other SRB in terms of their DNA recognition helices, putative DNA targets and the genomic neighbourhood of their corresponding genes. The regulon for these two proteins is much larger than that of CooA and contains genes encoding machinery for molecular export and import, flagellar components, sulpho-transferase and genes involved in thiazole biosynthesis. The fact that this regulon is shared between

two regulators suggests that control of these genes may be responsive to a range of different signals. For example, Ddes_2092, when used as a query for a blast search on the NCBI website, is annotated as being TrmB-like. The possibility that Ddes_2092 might respond to different sugars seems plausible: the various transporter complexes in the regulon could be responsible for the uptake of certain carbohydrates. Ddes_1411 is co-localised with a diguanylate cyclase, suggesting that the effector for this regulator could be cyclic-GMP or cyclic-diGMP. Cyclic-diGMP is a messenger molecule that influences a range of biological processes in bacteria including the switch between motile and sessile lifestyles (Simm *et al.*, 2004). This also seems plausible due to the flagellar proteins in the regulon. Ddes_1411, Ddes_2092 and their putative targets are very interesting but do not seem to be obviously involved in the nitrate-sulphate diauxie of *D. desulfuricans* or in regulating genes for nitrosative stress response unlike the remaining two CRP-family proteins of *D. desulfuricans*: HcpR and HcpR2.

HcpR of *D. desulfuricans* seems to have the largest regulon of the *D. desulfuricans* CRP-family proteins. It is an anomaly in its status as an HcpR protein since its gene it is not co-localised with *hcp* like the other HcpRs of *Desulfovibrio* species. However, comparing the genomic context of *hcpR* in *D. desulfuricans* with those of *Desulfovibrio* sp. 3_1_syn3 and *Desulfovibrio* sp. 6_1_46AFAA indicates an identical arrangement at these loci in these bacteria except the latter two species do possess *hcp* adjacent to *hcpR*. These *Desulfovibrio* species appear to be subject to various gene translocations as this sort of observation was made numerous times whilst compiling this article. Furthermore, much of the core HcpR regulon is conserved in *D. desulfuricans* supporting the classification of HcpR in *D. desulfuricans*. The HcpR regulon of *D. desulfuricans* includes a range of genes with different functions but there are numerous genes

encoding proteins involved in electron transport or redox processes. This observation is supported by the prediction that HcpR is a redox sensitive protein that potentially utilises a metal based co-factor. It is suggested that the HcpR regulon contains *nap*, *sat*, *aps* and various cytochromes, and that it is highly likely that this regulator is involved in controlling the nitrate-sulphate diauxie of *D. desulfuricans.*

The putative regulon of HcpR2 is relatively small and the regulon components seem to have a conserved function. The predicted function of HcpR2 is to regulate the response to oxidative and nitrosative stress. Surprisingly, HcpR2 is more similar to the HcpR proteins found in *Clostridium* species. This observation further highlights the earlier statement that *Desulfovibrio* may be subject to numerous gene translocations, these translocations might also be horizontal between other species. HcpR2 in *D. desulfuricans* regulates the expression of *hcp* and is likely to respond to nitric oxide or reactive oxygen species via a metal cofactor or disulphide bonds.

In *D. vulgaris* and *Desulfovibrio* G20 it is predicted that HcpR represses expression of *sat* and *aps* by binding to DNA overlapping the -10 and -35 promoter elements (Rodionov *et al.*, 2004). Binding sites for HcpR are present upstream of both *aps* and *sat* in *D. desulfuricans* (Figure 3.15). At the *sat* promoter the binding site for HcpR appears to overlap the putative -10 and -35 elements and so it can be assumed that HcpR could act as a repressor of *sat* in this bacterium (Figure 3.15a). However, it was not possible to identify any -10 or -35 elements in the *aps* promoter and so the activity of HcpR at this loci cannot be predicted (Figure 3.15b).

The *nap* and *nrf* gene clusters are predicted to be regulated by HcpR and another transcription factor (Figure 3.16) The three HcpR sites of the *nap* promoter are centred

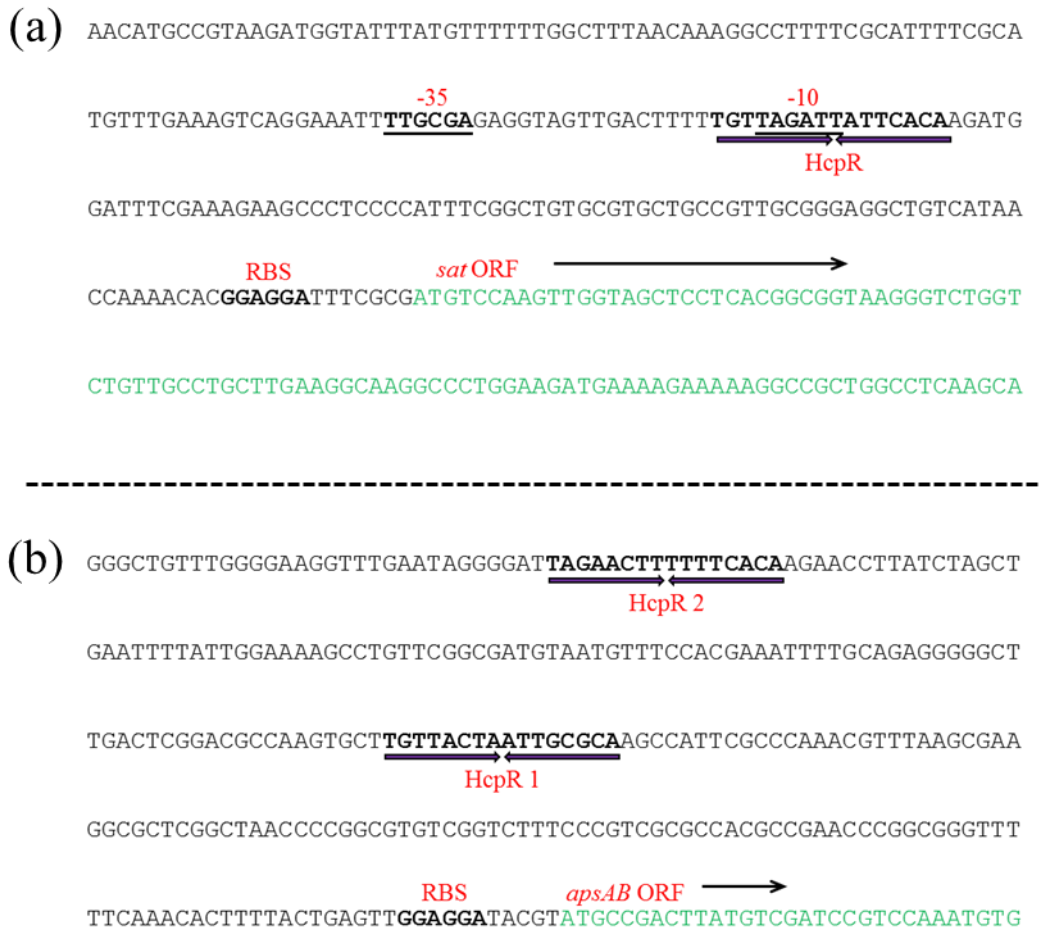


Figure 3.15: The promoter proximal DNA sequences of *sat* and *aps* of *D. desulfuricans.* (a) the *sat* promoter and (b) the *aps* promoter regions. Coding regions of genes are coloured blue or green whereas intergenic sequences are coloured black. The -10 and -35 elements of the *sat* promoter are those identified with the online tool Softberry. No -10 and -35 elements could be identified in the *aps* promoter with the BPROM tool (Softberry, Mount Kisco, NY, USA).

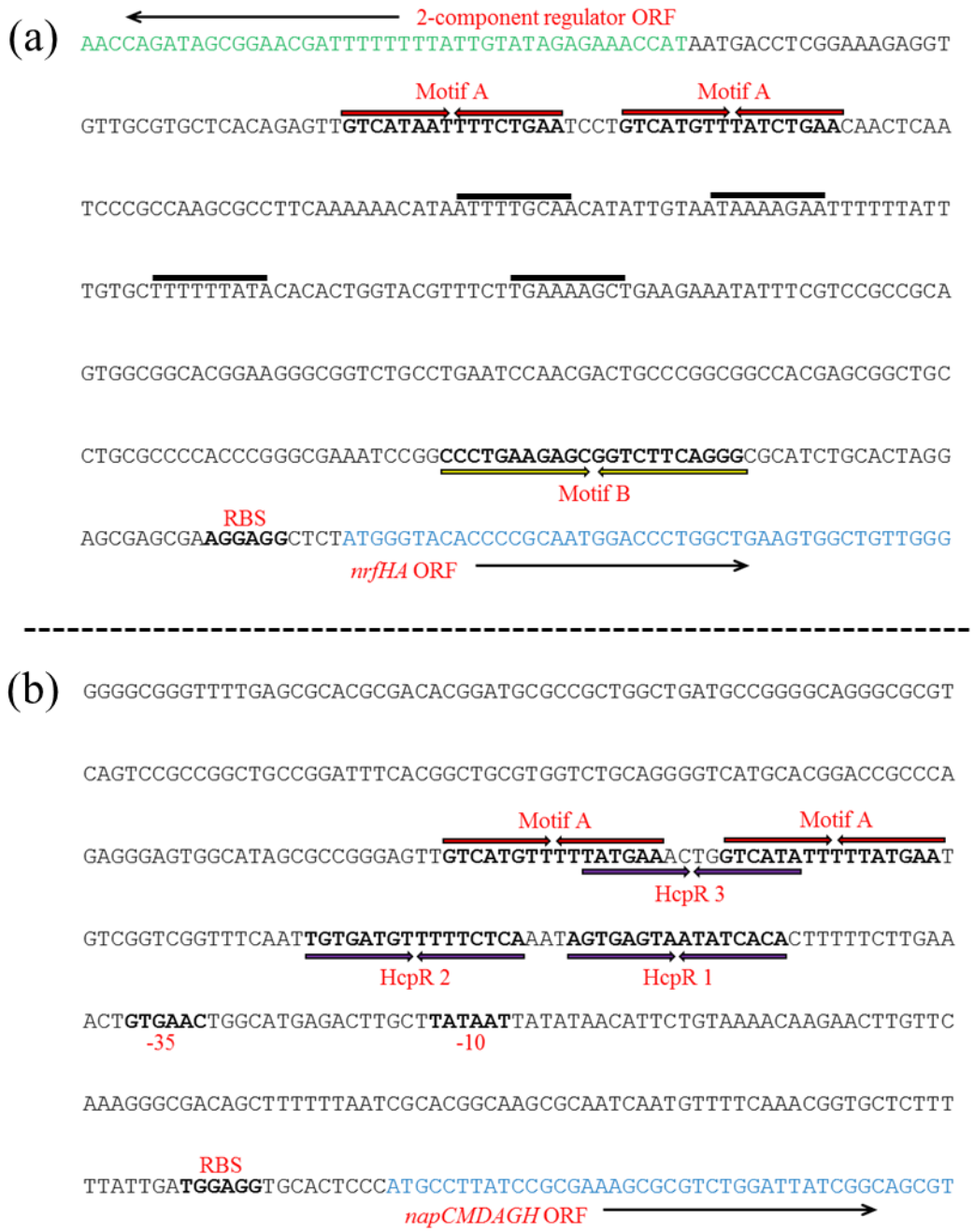


Figure 3.16: The promoter proximal DNA sequences of *nrf* and *nap* of *D. desulfuricans.* (a) the *nrf* promoter and (b) the *nap* promoter regions. Coding regions of genes are coloured blue or green whereas intergenic sequences are coloured black. The -10 and -35 elements of the *nap* promoter are those reported in Marietou *et al.* (2009). No -10 and -35 elements could be identified in the *nrfHA* promoter with the the BPROM tool (Softberry, Mount Kisco, NY, USA).

at positions -56.5, -75.5 and -128.5 relative to the transcription start site experimentally determined by Marietou *et al.* (2009) (Figure 3.16b). Although these positions are not typical for activation by CRP there are examples of CRP-family proteins activating from -56.5 and -76.5. The CRP-family protein CcpA from *Bacillus subtilis* is able to bind to a site at position -56.5 upstream of the *ackA* promoter and this site is essential for transcription activation of this gene (Turinsky *et al.*, 1998). Likewise, maximal expression of the *yihU-yshA* operon in *Salmonella enterica* is provided by CRP binding to a site at -76.5 relative to the transcription start site (Villarreal *et al.*, 2011). There is also an example of DNA bending by *E. coli* CRP at position -55.5 resulting in transcription activation from a sigma-54 promoter (Huo *et al.*, 2006). Thus, it is plausible that HcpR could be an activator of the *nap* operon. Since the sequences of the HcpR sites vary it is likely that there would be preferential binding to certain sites and that the occupation of the different sites would provide different rates of transcription.

The nature of *nrf* expression in *D. desulfuricans* is subject to controversy with reports stating that *nrf* is expressed constitutively and opposing reports stating that *nrf* in *Desulfovibrio* is regulated (Marietou *et al.*, 2009; Dalsgaard & Bak, 1994; Haveman *et al.*, 2004; He *et al.*, 2006). In observing the *nrf* promoter of *D. desulfuricans* two distinct inverted repeat sequences were detected (Figure 3.16a). The positioning of one of these inverted repeats, motif B, is such that should a regulator bind here it could repress expression of *nrf*. This is due to the site being in close proximity to the translation start codon of *nrfH*. Similarly, the other inverted repeat sequence, motif A, is positioned such that it could repress expression of the divergent operon encoding a two component regulatory system. Indeed, a homologue of this regulator from *D. vulgaris* has been demonstrated to bind to a DNA fragment containing a similar sequence (Rajeev *et al.*,

2011). Thus, *nrf* could be subject to regulation by two different transcription factors in *D. desulfuricans*. A product of the operon divergent from *nrf* might repress expression from its own promoter by competing with RNAP for binding and in turn resulting in enhanced recruitment of RNAP to the *nrf* promoter. Further evidence that motif A is a target for a transcription factor is supported by the fact that two of these sites, almost identical to those of the *nrf* promoter and with the same 4 bp spacer between the two sites, were identified upstream of the *nap* promoter (Figure 3.16b). The presence of these sites upstream of *nrf* and *nap* in *D. desulfuricans* seem unlikely to be coincidence due to the related function of the downstream gene functions and the size of the tandem motifs. Perhaps the regulator that binds to these sites is nitrate responsive and provides activation or enhancement of transcription of these two operons in the presence of nitrate.

Finally, the *hcp* locus was checked (Figure 3.17). Two sites for HcpR upstream of the putative *hcp* operon suggests that expression of *hcp* may be partly regulated by HcpR. However, the presence of a site for HcpR2 immediately upstream of Ddes_1828 suggests that stricter control of *hcp* is imparted by HcpR2. No -10 or -35 promoter elements could be identified in the HcpR2-Ddes_1828 intergenic region and so it is difficult to predict what the action of HcpR2 could be. Since *hcp* in other bacteria is up-regulated in response to nitrosative stress it could be speculated that HcpR2 enhances recruitment of RNAP upstream of Ddes_1828 and *hcp* in response to nitrosative stress. It seems less likely that HcpR2 would be repressing at this position as if this were the case it would seem that up-regulation of *hcp* would also require a corresponding increase in the expression of the preceding genes. This strategy of *hcp* regulation would

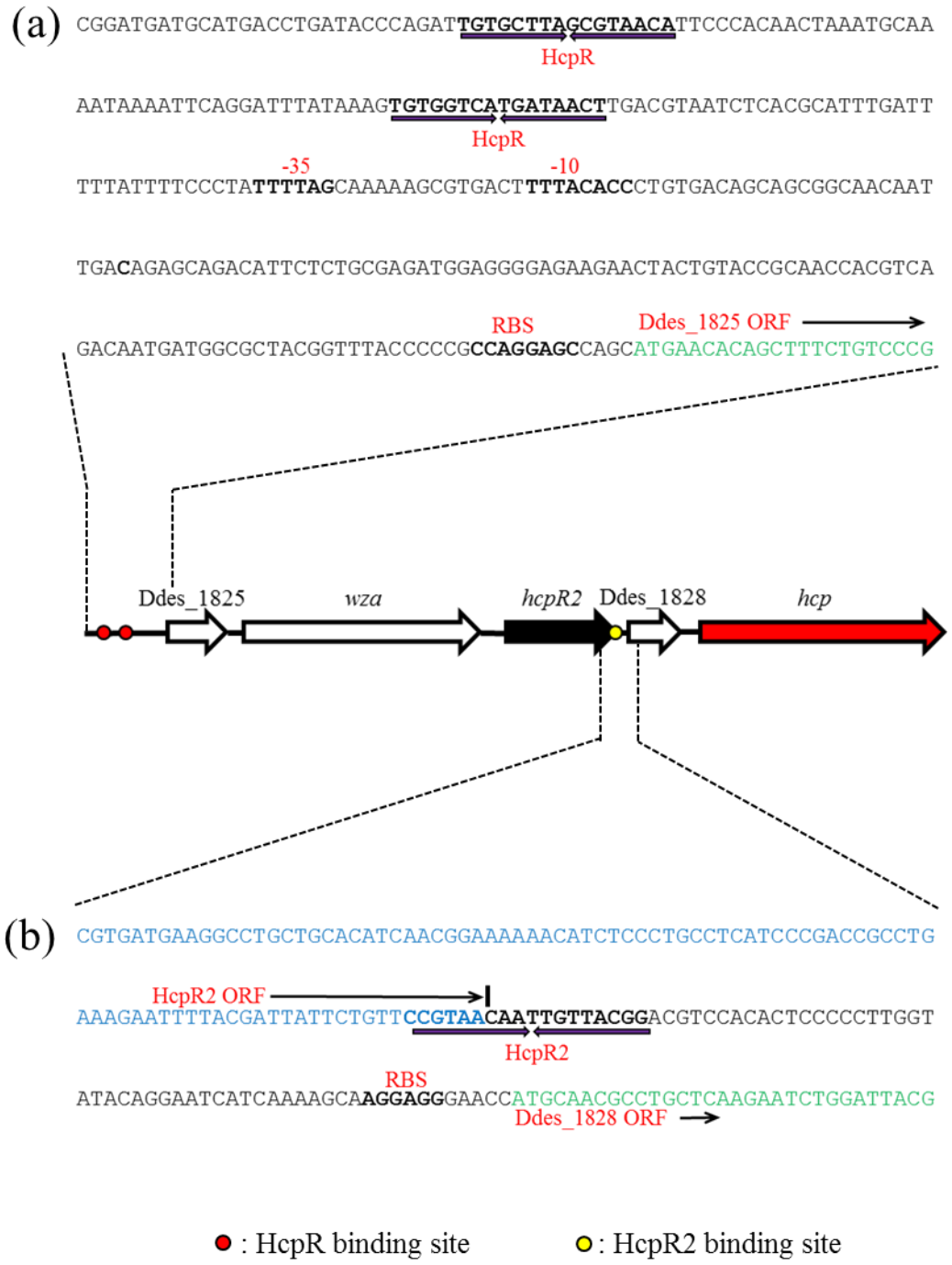


Figure 3.17: The promoter proximal DNA sequences of Ddes_1825 and Ddes_1828 of *D. desulfuricans*. (a) the Ddes_1825 promoter and (b) the Ddes_1828 promoter regions. Coding regions of genes are coloured blue or green whereas intergenic sequences are coloured black. The -10 and -35 elements of the Ddes_1825 promoter are those identified with BPROM (Softberry, Mount Kisco, NY, USA).

not be economical with cellular resources. Thus, it is predicted that HcpR has a minor role in regulating the expression of the *hcp* operon whereas HcpR2 is responsible for full induction of *hcp* in response to nitrosative stress.

This chapter has provided clues that HcpR and HcpR2 are critical for *D. desulfuricans* to switch between utilising sulphate or nitrate as the terminal electron acceptor for growth and also for coping with the stresses associated with nitrate dependant growth. To further explore these hypotheses the next chapter will move from *in silico* to direct physiological and transcription analyses.

Chapter 4

Results

Growth and gene expression profiles of *D. desulfuricans* in response to different terminal electron acceptors

4.1 Introduction

The *in silico* analysis in Chapter 3 yielded a simple model for the regulation of genes involved in terminal electron acceptor selection and nitrosative stress. HcpR family proteins were predicted to be central in this model. This chapter will present the results of physiological experiments and gene expression data to test predictions resulting from the *in silico* analysis.

The ability of *D. desulfuricans* to utilise nitrate as a terminal electron acceptor for growth has been recognised since the 1950s. Baumann & Denk (1950) reported that sulphate inhibits nitrate reduction. Recently, Marietou *et al.* (2009) reported a thorough investigation of the nitrate-sulphate diauxie in which sulphate is utilised preferentially to nitrate. This diauxie is in part due to repression and induction of the *nap* operon with sulphide being inhibitory to nitrate reduction. Evidence was given suggesting that sulphate reduction and nitrite reduction are constitutive since levels of the *nrfA* and *dsrA* transcripts remained constant irrespective of the terminal electron acceptors available (Marietou *et al.*, 2009). This proposal is supported by the earlier observations of Dalsgaard & Bak (1994) who reported that nitrite reduction by sulphate-grown *D. desulfuricans* strain C4S occurred without a period of induction. Contrary to these findings, up-regulation of *nrfHA* in response to nitrite has been recorded in *D. vulgaris* Hildenborough**,** suggesting that nitrite reduction in *Desulfovibrio* is subject to regulation (Haveman *et al.*, 2004; He *et al.*, 2006). It is also possible that *nrf* is expressed differentially in these two lineages of *Desulfovibrio*.

Since there are controversies regarding which terminal electron acceptors are used preferentially, this chapter will begin with experiments in which *D. desulfuricans* was

grown in the presence of nitrate, sulphate, nitrite, sulphite and combinations of these terminal electron acceptors. The concentrations of each of these terminal electron acceptors were measured during growth. Particular attention will be given to nitrite reduction by *D. desulfuricans*. Any changes in the expression profiles of genes encoding relevant reductases will indicate whether terminal electron acceptor selection might be regulated at the transcription level. Some of these genes are predicted to be components of the HcpR regulon. Gene expression profiles of other putative HcpR and HcpR2 regulon members will also be determined. Together these results will provide crucial information regarding terminal electron acceptor utilisation and also any regulatory processes underpinning these selections. These findings can then be related back to the predictions made in Chapter 3.

4.2 Growth of *D. desulfuricans* in the presence of individual terminal electron acceptors

Growth in the presence of different terminal electron acceptors was measured to determine whether their reduction is subject to a period of induction. Sulphate-grown *D. desulfuricans* was used as the inoculum for medium that was supplemented with either 7.5 mM nitrate, sulphate or sulphite and, because it is toxic, with a lower concentration of 2.5 mM nitrite. Culture optical densities and the concentrations of terminal electron acceptors were measured at intervals (Figure 4.1). All four terminal electron acceptors supported growth (Figure 4.1a). Similar growth occurred in the presence of nitrate or sulphate during the first 22 hours. However, between 22 and 44 hours, there was increased growth in cultures supplemented with nitrate resulting in a higher final yield compared with cultures supplemented with sulphate. Growth in the presence of sulphite

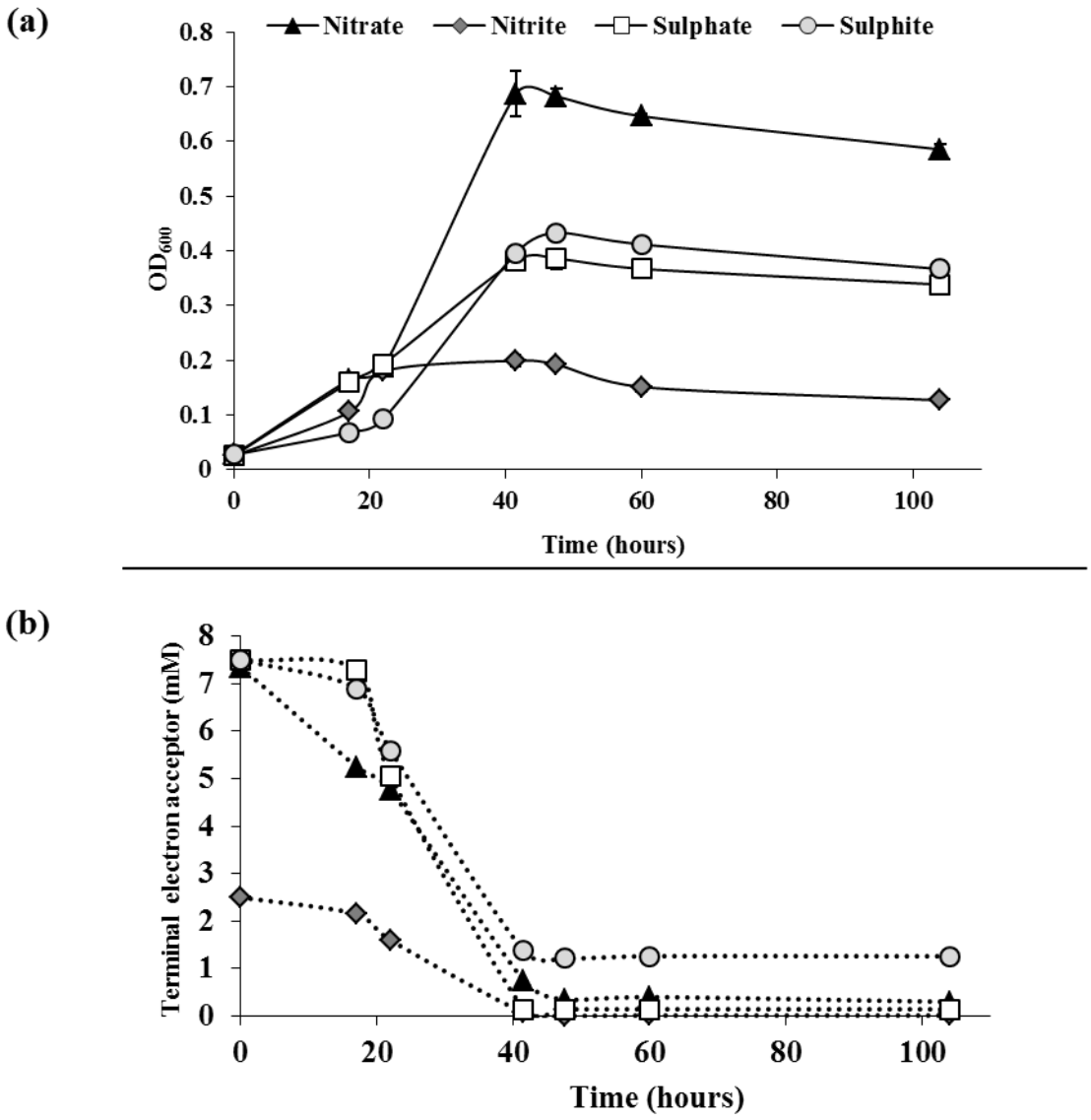


Figure 4.1: The effects of different terminal electron acceptors upon growth of *D. desulfuricans.* Sulphate-grown cells were used to inoculate PgZ medium supplemented with 7.5 mM nitrate, sulphate, sulphite or 2.5 mM nitrite. **(a)** Optical densities of cultures were measured **(solid lines).** Values are the average of three biological replicates and error bars represent standard deviations. **(b)** Samples of the culture supernatants were used to measure the concentrations of terminal electron acceptors **(broken lines).** Terminal electron acceptor concentrations are single measurements and are representative of those given by three biological replicates.

or nitrite was preceded by an initial lag phase compared with sulphate or nitrate. These lag phases were followed by more rapid growth, especially in the presence of nitrite. After 44 hours all cultures, except those with sulphite as the terminal electron acceptor, had reached their maximum recorded optical density and had entered stationary phase. Cultures supplemented with sulphite were subject to the longest period of induction and reached stationary phase at a later time, after 48 hours. In all cultures, growth was accompanied by a decrease in the concentrations of the terminal electron acceptor (Figure 4.1b). All of the terminal electron acceptor in each culture had apparently been depleted by 44 hours. Because nitrite is toxic the experiment was repeated with sequential additions of 1.5 mM nitrite to a total concentration of 7.5 mM (data not shown). Thus, the growth yields provided by equimolar concentrations of each terminal electron acceptor were compared. Increasing the concentration of nitrite resulted in a higher cell density (OD650 ~0.3). Yields in the presence of nitrate were significantly higher than those obtained in the presence of the same concentrations of sulphate or sulphite whereas yields in the presence of nitrite were significantly lower.

The results agree with the observations of Marietou *et al.* (2009) who reported that the growth yield in the presence of nitrate is higher than with sulphate or nitrite. The lag phase in the presence of nitrate alone was consistent with the report that nitrate reduction is regulated and subject to induction. Sulphite seems to be equivalent to sulphate in terms of yields. This is perhaps surprising since sulphate reduction requires activation by Sat and represents a drain of ATP. An equimolar concentration of sulphite, which does not require activation, could be expected to provide the higher yield. This assumption was not supported by the growth experiment results. Nitrite is the least favourable terminal electron acceptor tested probably due to its toxicity. However,

despite this toxicity, nitrite can support growth of *D. desulfuricans.* In monitoring *D. desulfuricans* growth over time it seemed that different terminal electron acceptors were utilised in different ways. It is claimed that the sulphate utilisation pathway of *Desulfovibrio desulfuricans* is expressed constitutively (Marietou *et al.*, 2009). Indeed, in support of this claim, no discernible lag phase was observed when the medium was supplemented with sulphate. However, the initial lag phase in cultures supplemented with sulphite is suggestive that the molecular components necessary for sulphite metabolism are subject to a period of induction. Since the sulphite reduction pathway is part of the sulphate reduction pathway these observations seem contradictory. Similar observations were made for *D. desulfuricans* grown in the presence of nitrite. Nitrite dependent growth was preceded by a comparatively long lag phase. These observations seem to be in agreement with those made with *D. vulgaris* Hildenborough and disagree with the observations made for *D. desulfuricans* and for *D. desulfuricans* C4S (Haveman *et al.*, 2004; He *et al.*, 2006; Marietou *et al.*,2009; Daalsgard & Bak, 1994).

Terminal electron acceptor utilisation and selection by *D. desulfuricans* seems to be complex and there are disagreements in the literature regarding these topics. Additional growth experiments were designed in an endeavour to resolve these disagreements.

4.3 Terminal electron acceptor selection by *D. desulfuricans*

The effects of sulphate and sulphite upon nitrate and nitrite reduction

To confirm the sulphate-nitrate diauxie, sulphate-adapted *D. desulfuricans* was grown in medium supplemented with nitrate. Some cultures were given an additional supplement of sulphate or sulphite. Optical densities and nitrate concentrations were determined at

intervals (Figure 4.2a and 4.2b). In the presence of both nitrate and sulphate, growth and yields were almost identical to those in the presence of sulphate alone (Figure 4.2a). A similar observation was made for cultures supplemented with both nitrate and sulphite. The concentrations of nitrate in these two conditions remained constant throughout the experiment (Figure 4.2b). Nitrate reduction was only detected in cultures supplemented with nitrate alone. These results are in agreement with the proposed diauxie that sulphate is preferred to nitrate despite nitrate being more favourable in terms of yields (Marietou *et al.,* 2009). The presence of sulphate completely prevented nitrate reduction. Crucially, the presence of sulphite also repressed nitrate reduction. Thus, sulphite is also reduced preferentially to nitrate. These results indicate that nitrate reduction is inhibited and/or repressed by sulphite and/or by a product of sulphite reduction.

To determine whether nitrite reduction is also prevented during growth in the presence of sulphate or sulphite, *D. desulfuricans* was grown in the presence of nitrite alone, nitrite with sulphate and nitrite with sulphite (Figure 4.2c and 4.2d). Yields in the presence of nitrite alone were significantly lower than those of cultures also supplemented with sulphate or sulphite (Figure 4.2c). Growth in the presence of both nitrite and sulphate was biphasic, being comparable to growth in the presence of nitrite alone during the early phase of the experiment and then diverging. Cultures supplemented with both nitrite and sulphite were subject to a lag phase before more rapid growth. Nitrite was completely reduced within 42 hours in the three culture conditions (Figure 4.2d). The presence of sulphite in the nitrite quantification assay resulted in a masking effect on the nitrite assay (refer to Chapter 2 for details). Thus, it is possible that nitrite was still present in cultures containing sulphite

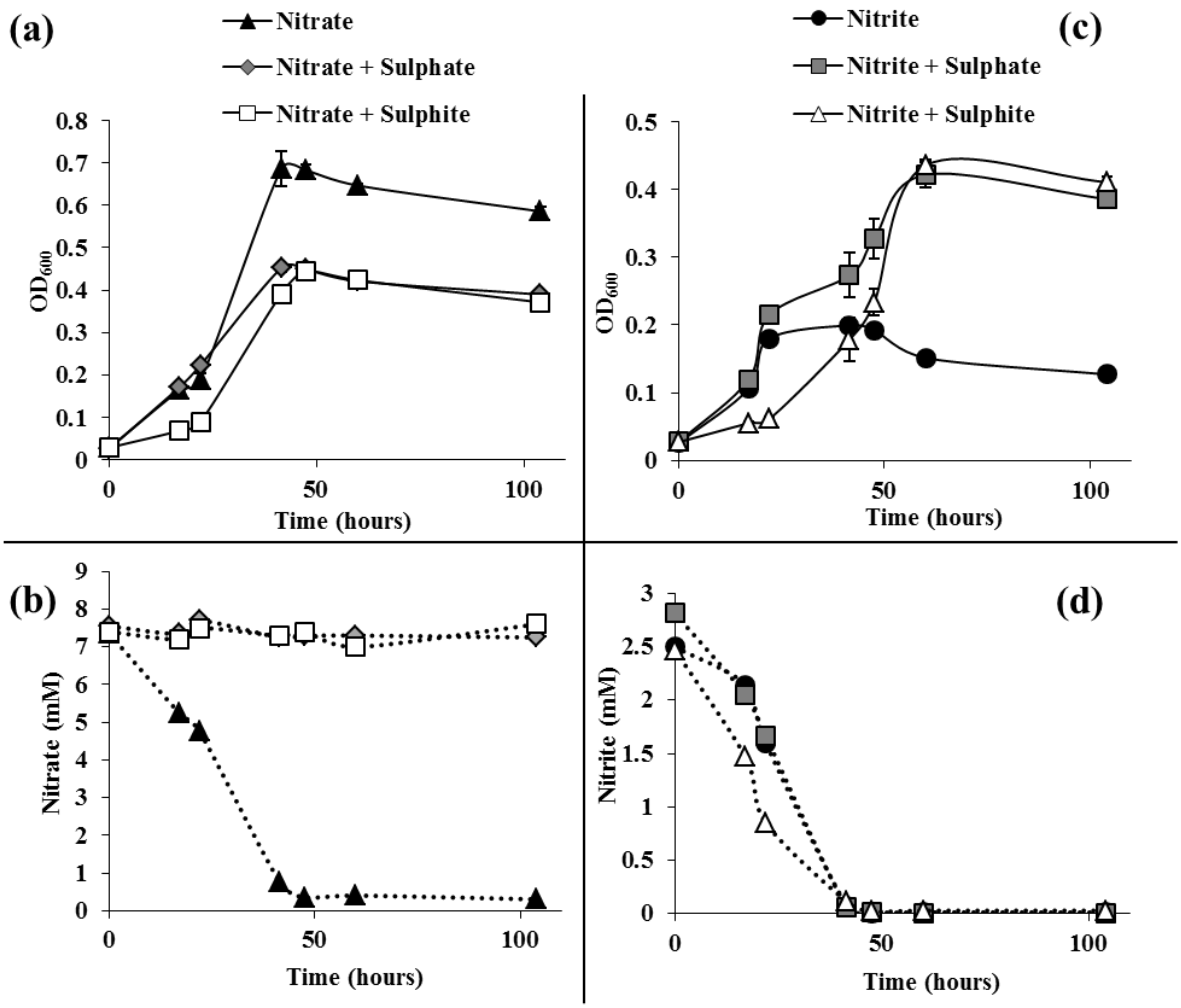


Figure 4.2: The effects of sulphate and sulphite on growth and nitrate and nitrite reduction by *D. desulfuricans*. Sulphate-grown cells were used as the inoculum for PgZ cultures supplemented with different terminal electron acceptors. Nitrate, sulphate and sulphite were used at a final concentration of 7.5 mM whereas nitrite was used at 2.5 mM. Growth was assessed by measuring culture optical densities at intervals (solid lines, **(a)** and **(c)**). Values are the average given by three biological replicates and error bars indicate standard errors. Samples of the culture supernatant were used to determine nitrate or nitrite concentrations in cultures **(**broken lines, **(b)** and **(d)**). Concentrations are single measurements representative of those given by three biological replicates.

after 42 hours. However, the apparent concentrations of nitrite in the presence of nitrite and sulphite decreased throughout the experiment indicating that nitrite was eliminated from the medium prior to all of the sulphite being reduced. If sulphite was reduced prior to nitrite reduction then the apparent concentration of nitrite would have increased due to an increase in the sensitivity of the nitrite assay. Therefore, the results indicate that nitrite reduction by *D. desulfuricans* occurs preferentially to or simultaneously with sulphate and sulphite reduction.

The effects of nitrite and nitrate upon the reduction of sulphate and sulphite

Growth in the presence of sulphate, sulphate with nitrate and sulphate with nitrite was compared and samples of culture supernatant were used to determine the concentrations of sulphate and sulphite (Figure 4.3a and 4.3b). Yields in the presence of sulphate with nitrate or sulphate with nitrite were slightly higher than with sulphate alone (Figure 4.3a). In the presence of nitrite and sulphate this increased yield was likely to be due to nitrite dependent growth. Since nitrate reduction is prevented in the presence of sulphate the increased yield in the presence of both nitrate and sulphate is presumably due to a low basal level of nitrate reduction that could not be detected in this study**.** Sulphate reduction in all three culture conditions was accompanied by the liberation of sulphite into the medium (Figure 4.3b). Sulphate reduction was impeded in the presence of nitrite and, accordingly, sulphite release into the medium occurred later in this condition compared with the other cultures. Thus, sulphate reduction was inhibited or repressed by the presence of nitrite.

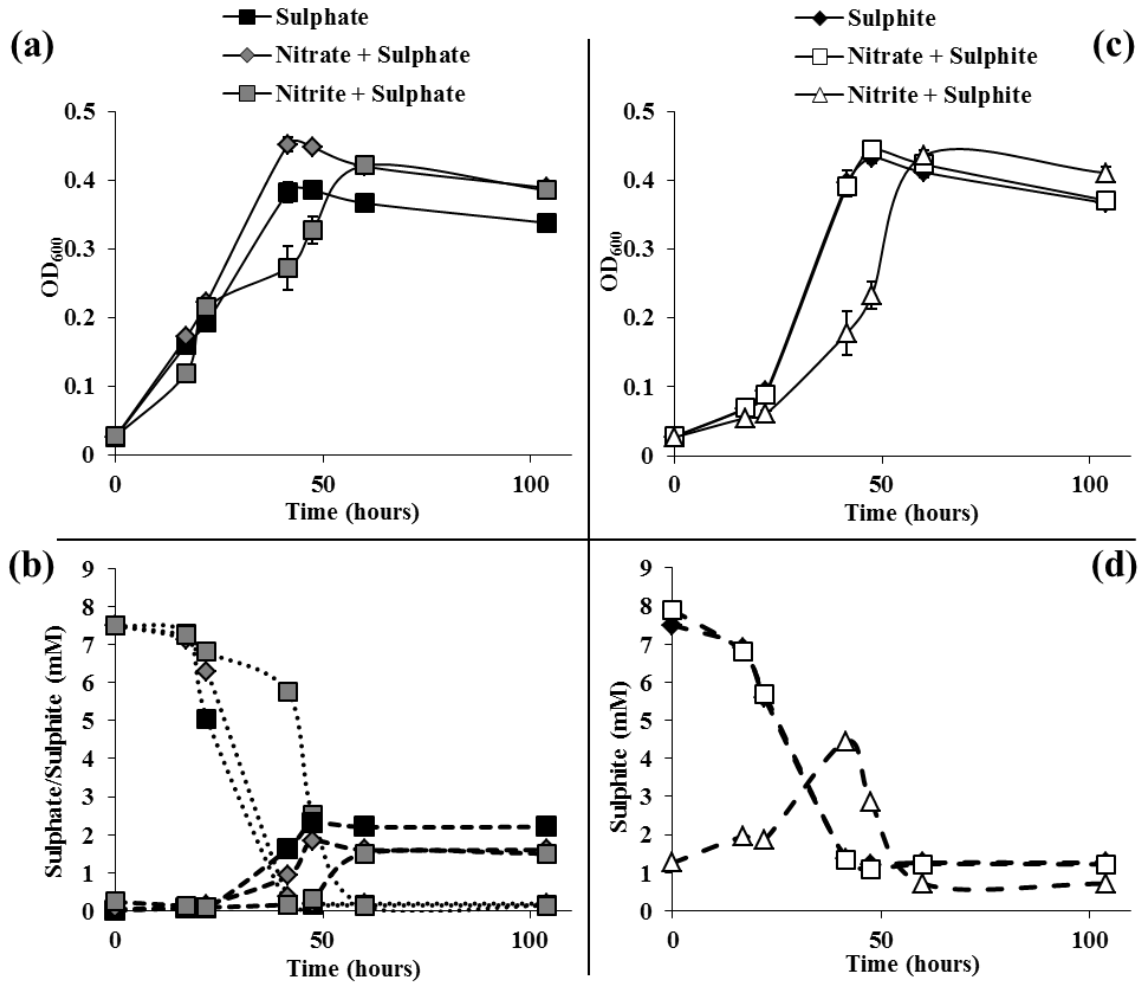


Figure 4.3: The effects of nitrate and nitrite on growth and sulphate and sulphite reduction by *D. desulfuricans*. Sulphate-grown cells were used as the inoculum for PgZ cultures supplemented with different terminal electron acceptors. Nitrate, sulphate and sulphite were used at a final concentration of 7.5 mM whereas nitrite was used at 2.5 mM. Growth was assessed by measuring culture optical densities at intervals (**solid lines**, **(a)** and **(c))**. Values are the average given by three biological replicates and error bars indicate standard errors. Samples of the culture supernatant were used to determine sulphate concentrations (**thin broken lines**, **(b))** and/or sulphite concentrations (**thick broken lines**, (**b)** and (**d))** in cultures. Concentrations are single measurements representative of those given by three biological replicates.

The effects of nitrate or nitrite on growth in the presence of sulphite were also determined (Figure 4.3c and 4.3d). Yields obtained with these three conditions were similar but growth in the presence of nitrite and sulphite was slower compared with the other conditions (Figure 4.3c). Sulphite reduction was seemingly unaffected by the presence of nitrate (Figure 4.3d). As mentioned earlier, sulphite interferes with the nitrite assay: similarly, nitrite lowers the sensitivity of the sulphite assay by having a masking effect (see Chapter 2). Thus, at the beginning of this experiment, when nitrite and sulphite were both present in the medium, the apparent concentration of sulphite determined by the assay was ~1 mM despite the actual concentration being 7.5 mM sulphite. The apparent increase and subsequent decrease in sulphite concentrations in the presence of nitrite can be explained by nitrite reduction. Once nitrite had been eliminated from the medium the sensitivity of the sulphite assay was restored and the apparent sulphite levels increased. Thus, the presence of nitrite resulted in impaired growth and repression or inhibition of sulphite reduction. Nitrite reduction occurred simultaneously with or preferentially to sulphite reduction.

4.4 Induction of nitrite reduction and resistance to nitrosative stress

The observation that nitrite reduction by *D. desulfuricans* proceeds without delay and is generally unaffected by other terminal electron acceptors is indicative that nitrite reductase is synthesized constitutively. However, in routine culturing of *D. desulfuricans* it was noted that cells grown on certain terminal electron acceptors had a higher tolerance to nitrite, raising the question whether nitrite reduction and tolerance to nitrite is regulated. Nitrate or sulphate grown cultures were used to inoculate medium supplemented with either 1 or 3.5 mM nitrite (Figure 4.4). Cultures

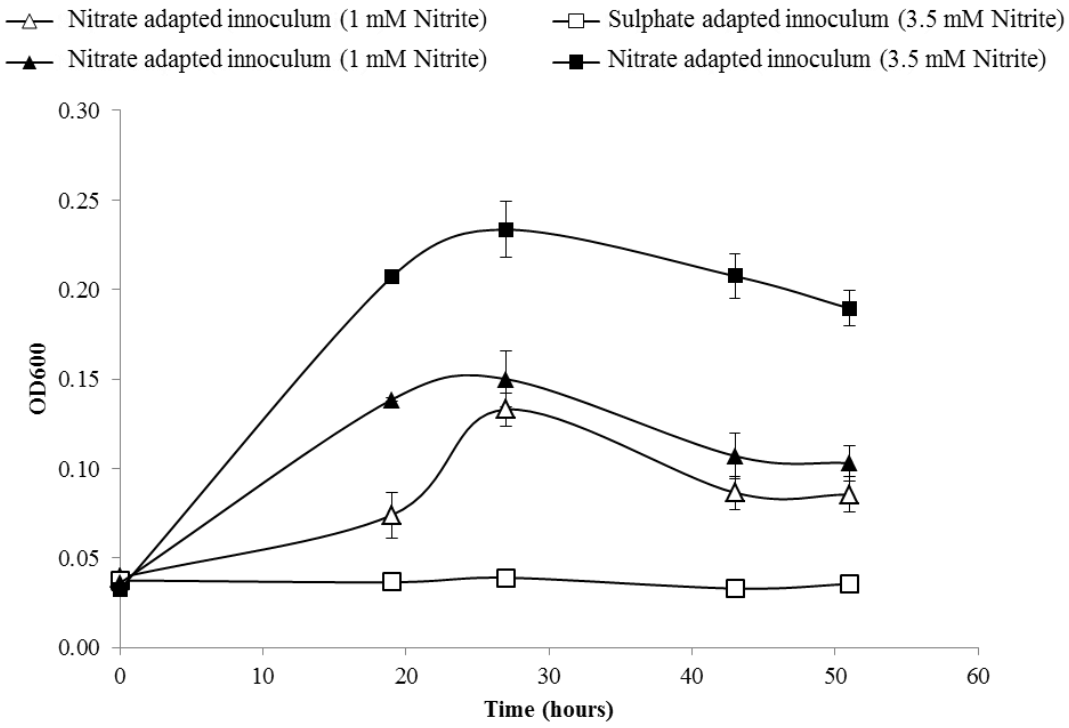


Figure 4.4: The effects of culture pre-treatment upon nitrite-dependent growth. PgZ medium was supplemented with 1 mM or 3.5 mM nitrite and inoculated with *D. desulfuricans* grown in the presence of nitrate (**filled symbols**) or sulphate (**open symbols**). The amount of each inoculum was adjusted to provide near identical starting optical densities. The values given are the average optical densities given for three biological isolates and error bars indicate standard deviations.

inoculated with nitrate-adapted cells grew to a higher optical density in the presence of nitrite than those inoculated with sulphate-adapted cells. An increased concentration of nitrite resulted in a higher growth yield in nitrate-adapted cultures whereas this increase in nitrite concentrations was toxic to sulphate-adapted cells. Indeed, 3.5 mM nitrite was sufficient to kill or completely suppress growth of the sulphate-grown inoculum. Thus, it is possible to increase tolerance to nitrite stress by pre-treatment. Since the nitrate-grown inoculum had already been exposed to nitrite these cultures seem to have been pre-induced to cope with nitrite toxicity.

The nitrite reduction rates of nitrate-adapted and sulphate-adapted cultures were measured (Figure 4.5). Both sulphate and nitrate-grown cells were able to reduce nitrite and provide measurable nitrite reduction rates. However, nitrate-grown cells were able to reduce nitrite at a rate ~85 % higher than sulphate-grown cells. The nitrite reductase activity of *D. desulfuricans* can be induced by pre-exposure to nitrate and therefore to nitrite. The results also suggest that nitrite reductase is expressed at a lower basal level sufficient for nitrite reduction without pre-induction but can be further induced.

4.5 Transcription of the nitrate-nitrite and sulphate-sulphite pathways

The initial physiological experiments revealed that nitrate reduction is inhibited and/or repressed by sulphite in a way similar to sulphate. In contrast, nitrite is reduced preferentially to or simultaneously with sulphate and sulphite. The presence of nitrite inhibits and/or represses sulphate and sulphite reduction. Also, due to a lag phase, sulphite reduction might be subject to regulation. In an attempt to determine the mechanisms behind these observations, RNA was isolated from cultures of *D. desulfuricans* during growth in the presence of various terminal electron acceptors and

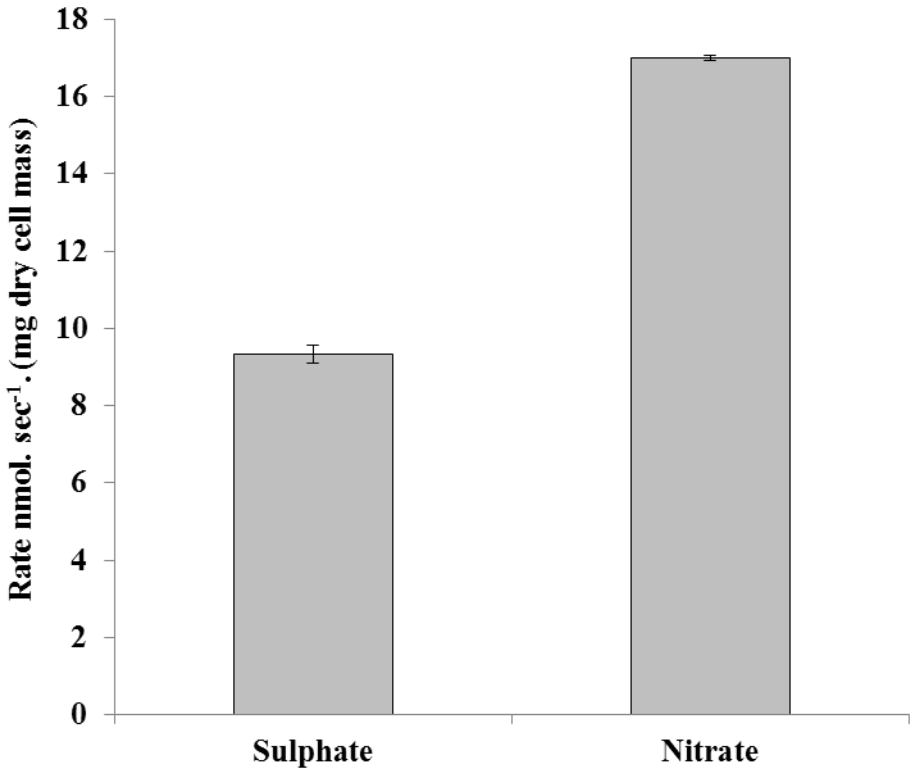


Figure 4.5: Nitrite reduction rates of nitrate or sulphate adapted *D. desulfuricans.* *D. desulfuricans* was grown in PgZ media in the presence of nitrate or sulphate and then harvested during exponential growth (OD_{600}~0.3). Rates of lactate-dependent nitrite reduction by washed bacteria suspensions were determined. Rate values are derived from three experimental replicates and are representative of two independent experiments. Error bars represent standard deviations.

used in gene expression analysis. Isolated RNA was reverse-transcribed with random hexamer primers and the resulting cDNA was used for quantitative PCR using gene-specific primers. Primers were designed against genes for terminal electron acceptor utilisation, central metabolism and HcpR regulon members. All of the qPCR data presented here are normalised to levels of the *polA* transcript.

Expression of *napC* and *nrfA* in response to different terminal electron acceptors

Consistent with previous reports, nitrate reductase was strongly up-regulated in the presence of nitrate with relative expression of *napC* being ~80 fold higher in nitrate-grown cultures compared with sulphate-grown cultures (Figure 4.6a). This level of *napC* induction is substantially higher than the ~10 fold increase reported by Marietou *et al.* (2009). This difference in relative expression is probably due to the use of different *napC* specific primers in this study and the previous study. Different qPCR primers are likely to work with different efficiencies, particularly when used in combination with cDNA generated with random hexamers. Furthermore, and in contrast to the previous report in which nitrite did not induce expression of *napC*, nitrite-grown cultures gave a ~20 fold up-regulation of *napC* compared with sulphate-grown cultures. In the presence of sulphate or sulphite the levels of *napC* were similar and significantly lower than in the presence of nitrite or nitrate.

Previous reports claim that nitrite reduction in *D. desulfuricans* is constitutive and expression of *nrfA* does not change greatly in the presence of nitrate, nitrite or sulphate (Marietou *et al.*, 2009; Dalsgaard & Bak, 1994). The levels of *nrfA* transcript induced in the presence of nitrate, nitrite, sulphate and sulphite were determined (Figure 4.6b). Contrary to those other reports, the levels of *nrfA* were significantly higher in the

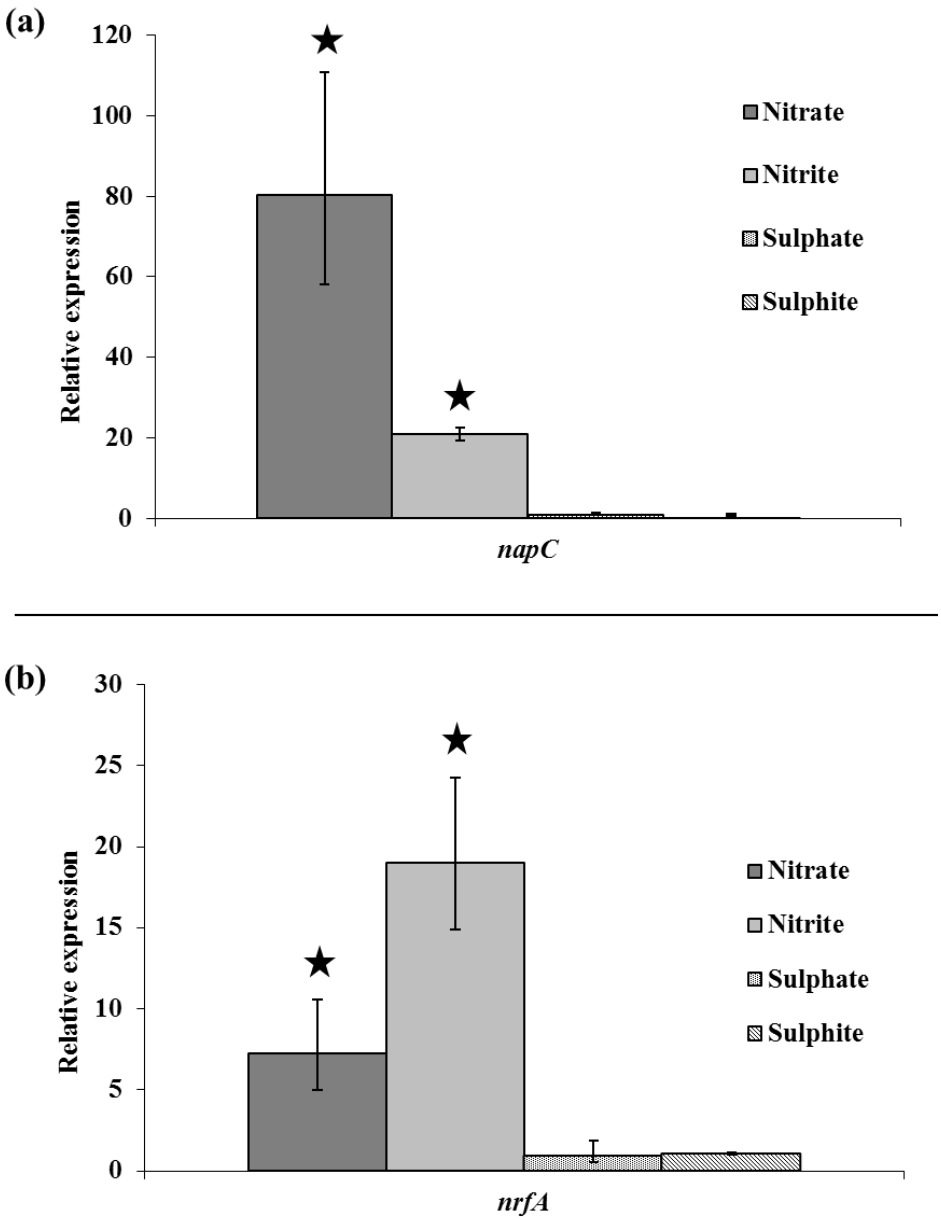


Figure 4.6: RT-qPCR of genes involved in nitrate and nitrite reduction in *D. desulfuricans.* RNA was purified from cells grown on PgZ medium containing nitrate, nitrite, sulphate or sulphite as the sole terminal electron acceptor and used in RT-qPCR analysis. Transcript levels were normalised against *polA* levels. Expression levels are derived from three biological replicates and triplicate qPCR reactions. Values are normalised to those given by sulphate-grown cells. Stars indicate data derived from ΔCt values statistically significantly different to that for sulphate-grown cultures ($P<0.05$).

presence of nitrite and nitrate compared with sulphate- and sulphite-grown *D. desulfuricans*. Nitrite and nitrate induced a ~15 and ~5 fold up-regulation of *nrfA*, respectively.

Expression of *sat, apsB, dsrA, qmoB* and *dsrJ* in response to different terminal electron acceptors

To determine whether the sulphate-sulphite reduction pathway is also regulated, the levels of the *sat, apsB* and *dsrA* transcripts in the presence of nitrate, nitrite, sulphate and sulphite were measured (Figure 4.7a). Slightly elevated levels of *sat, apsB* and *dsrA* were recorded in the presence of nitrate. None of the differences between the levels of these transcripts were statistically significant relative to sulphate grown *D. desulfuricans*. Thus, it seems that the genes directly involved in the sulphate and sulphite reduction pathway are expressed constitutively or regulated only within a narrow range**.** Results presented earlier in this study suggested that nitrite might repress or inhibit sulphate and sulphite reduction. Expression of *sat, apsB* and *dsrA* in the presence of nitrite was similar in the presence of sulphate and sulphite and so nitrite does not seem to significantly affect transcription of genes encoding sulphate and sulphite reductases. However, it is possible that nitrite might inhibit sulphate and sulphite reduction by repressing expression of some other genes necessary for passing electrons to either *apsB* or *dsrA*. Thus, the levels of *qmoB* and *dsrJ* were measured in response to the four terminal electron acceptors (Figure 4.7b). The transcript levels of *qmoB* and *dsrJ* did not vary greatly, though some statistically significant differences were observed. In particular, *dsrJ* levels were increased in the presence of nitrate whereas the levels of both *dsrJ* and *qmoB* were down-regulated in the presence of

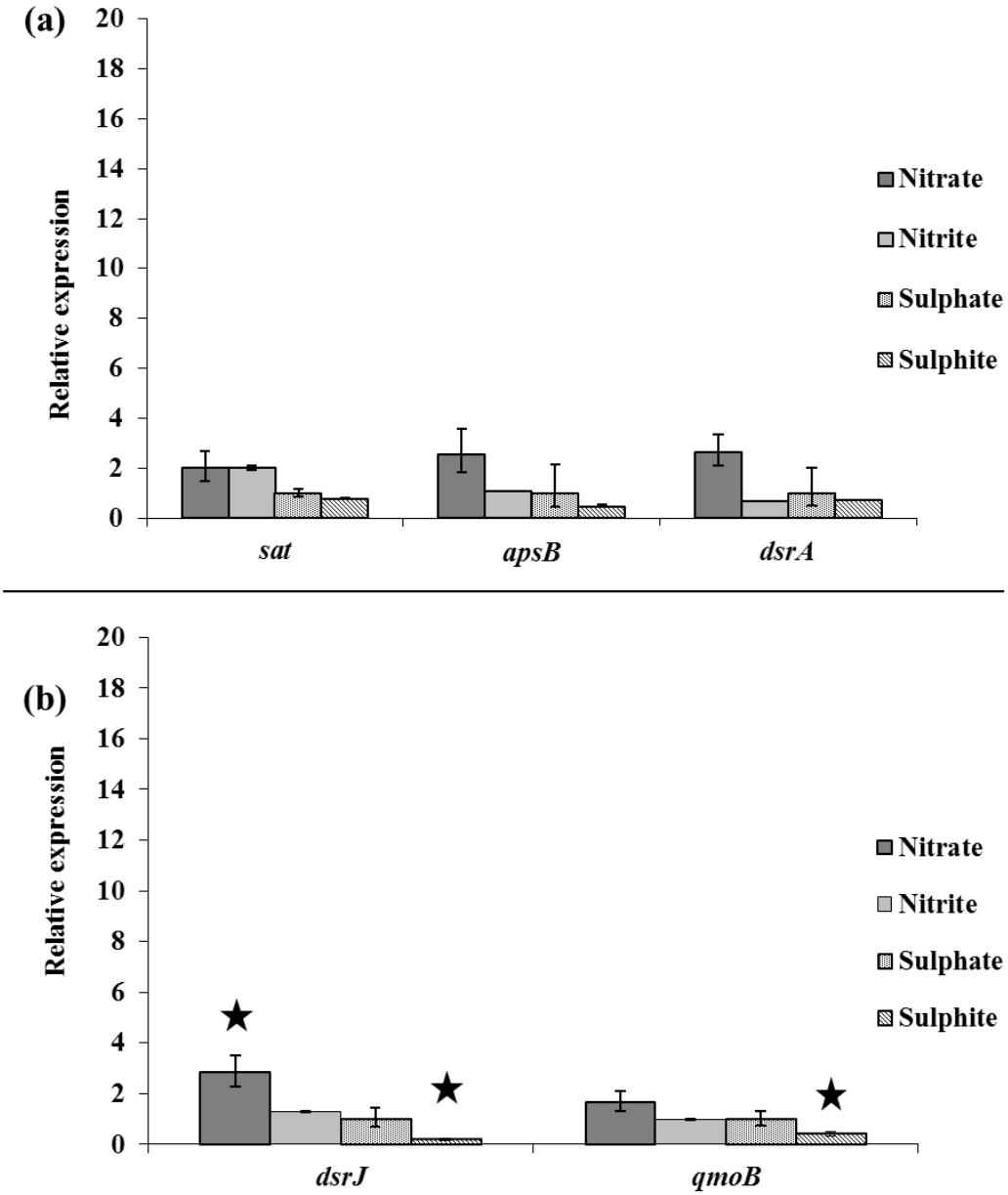


Figure 4.7: RT-qPCR of genes involved in the sulphate reduction pathway in *D. desulfuricans.* RNA was purified from cells grown on PgZ medium containing nitrate, nitrite, sulphate or sulphite as the sole terminal electron acceptor and used for RT-qPCR analysis. Transcript levels were normalised against *polA* levels. Expression levels are derived from three biological replicates and triplicate qPCR reactions. Expression levels are normalised to those of sulphate grown cells. Stars indicate data derived from ΔCt values statistically significantly different to that for sulphate-grown cultures ($P<0.05$).

sulphite. It would be logical to assume that *qmoB* and *dsrJ* would be up-regulated in the presence of sulphate and sulphite, respectively, to allow increased electron flow to the appropriate reductases. This assumption was not reflected in the results. Up-regulation of *dsrJ* in the presence of nitrate could indicate involvement of this complex in relaying electrons to Nap. However, this seems unlikely. The relatively narrow range of expression levels for *dsrJ* and *qmoB* in combination with the other transcript measurements suggest that the sulphate-sulphite reduction pathway and necessary respiratory complexes are expressed constitutively or are regulated within a narrow range.

4.6 Transcript abundances of *hcpR, hcpR2* and key regulon members

Differential expression of *hcpR* and *hcpR2*

In Chapter 3, two genes encoding putative HcpR proteins were identified and a putative regulon for each of these proteins was identified. These regulons included genes involved in nitrate and sulphate reduction. The transcript levels of *hcpR*, *hcpR2* and some key regulon members were therefore measured. The levels of the *hcpR* transcript varied greatly depending upon the terminal electron acceptor present (Figure 4.8a). When cultures were supplemented with nitrate or nitrite the levels of the *hcpR* transcript were elevated ~50 and ~140 fold, respectively, compared to sulphate. In the presence of sulphate or sulphite the levels of the *hcpR* transcript were similar and low with no statistically significant difference between *hcpR* levels in these two conditions. In contrast, the levels of *hcpR2* did not vary between the different growth conditions and were all within a narrow range (Figure 4.8b). The two *hcpR* genes of *D. desulfuricans*

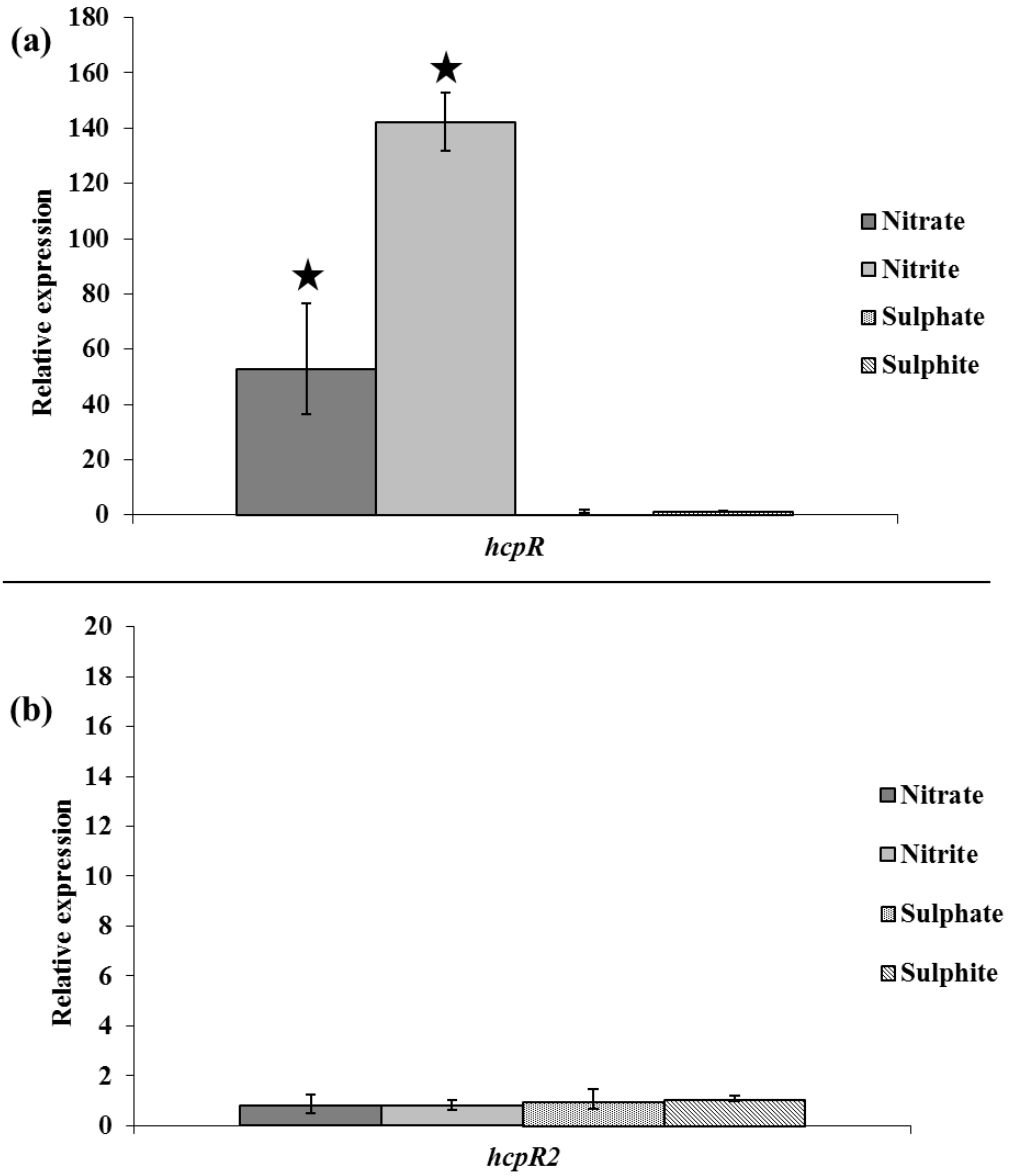


Figure 4.8: RT-qPCR of genes encoding HcpR proteins in *D. desulfuricans.* RNA was purified from cells grown on PgZ medium containing nitrate, nitrite, sulphate or sulphite as the sole terminal electron acceptor and used in RT-qPCR analysis. Transcript levels were normalised against *polA* levels. Expression levels are derived from three biological replicates and triplicate qPCR reactions. Expression levels are normalised to those given by sulphate grown cells. Stars indicate data derived from ΔCt values statistically significantly different to that for sulphate-grown cultures ($P<0.05$).

seem to be expressed differentially in response to the terminal electron acceptors used in this study.

The expression of cytochromes and *hcp* in response to different terminal electron acceptors

The *hcpR* regulon members *ssc*, *tpIc*$_3$ and *nhc*, which encode putative cytochromes, were analysed by qRT-PCR (Figure 4.9). The availability of different terminal electron acceptors seemed to have little effect upon the levels of the *tpIc*$_3$ and *nhc* transcripts. Contrastingly, the levels of the *ssc* were greatly elevated in the presence of nitrate and nitrite with the greatest level of induction being produced in the presence of nitrate. Up-regulation of *ssc* in response to nitrate but not sulphate was previously reported by Abreu *et al.* (2002). Furthermore, this observation is in agreement with the proposal made by da Silva *et al.* (2012) that the Split-soret cytochrome could be involved in the relay of electrons to the Nap complex.

Finally, the expression levels of a putative HcpR2 regulon member, *hcp*, were recorded in the presence of the different terminal electron acceptors (Figure 4.10). In the presence of nitrite a ~30 fold increase in expression of *hcp* was recorded. A more modest increase in expression, ~7 fold, was recorded in the presence of nitrate whereas expression of *hcp* was similar and low for sulphate and sulphite. These observations were expected since the *E. coli hcp* gene has been reported to be being highly expressed in the presence of nitrate and nitrite (van den Berg *et al.*, 2000). In Chapter 3 *hcp* was predicted to be in an operon with *hcpR2*. Since these two genes are expressed differentially in response to different terminal electron acceptors it seems they are transcribed from two distinct promoters.

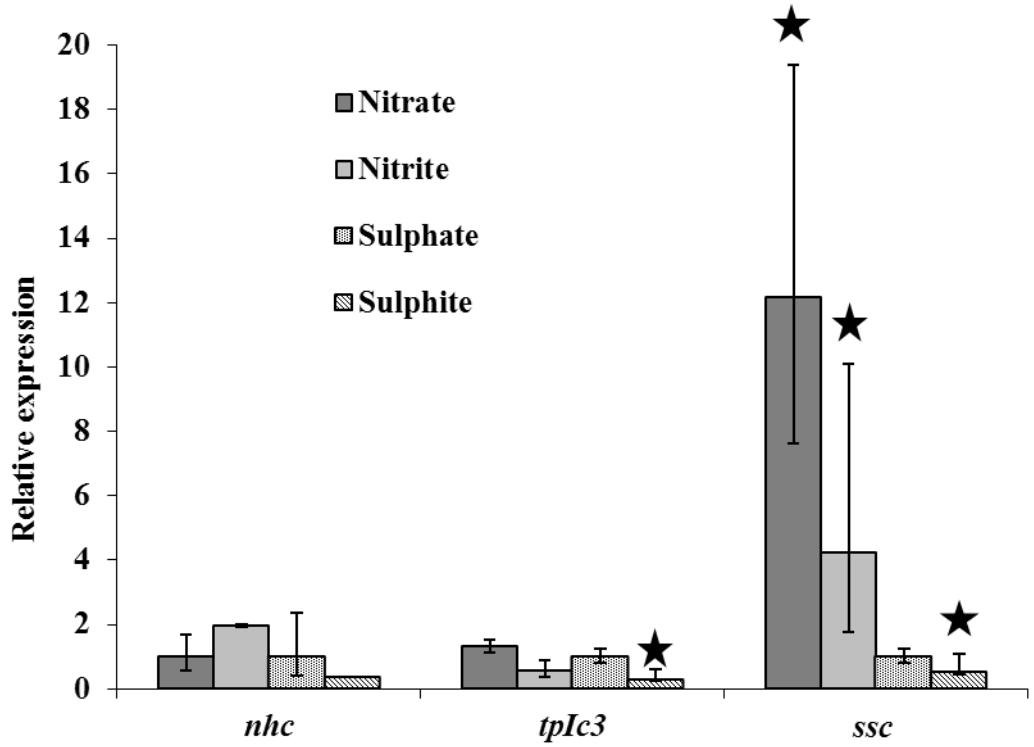


Figure 4.9: RT-qPCR of genes encoding periplasmic cyctochromes in *D. desulfuricans.* RNA was purified from cells grown on PgZ medium containing nitrate, nitrite, sulphate or sulphite as the sole terminal electron acceptor and used for RT-qPCR analysis. Transcript levels were normalised against *polA* levels. Expression levels are derived from three biological replicates and triplicate qPCR reactions. Levels are normalised to those given by sulphate grown cells. Stars indicate data derived from ΔCt values statistically significantly different to that for sulphate-grown cultures ($P<0.05$).

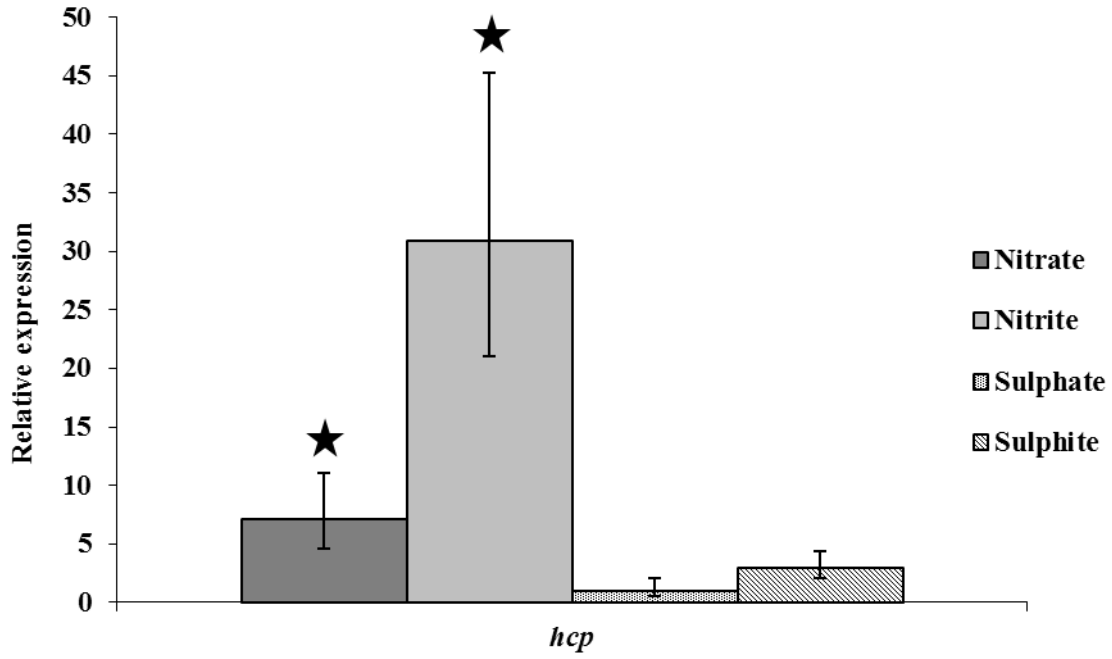


Figure 4.10: RT-qPCR of *hcp* in *D. desulfuricans.* RNA was purified from cells grown on PgZ medium containing nitrate, nitrite, sulphate or sulphite as the sole terminal electron acceptor. RNA was reverse-transcribed with random hexamers and used for qPCR analysis. Transcript levels were normalised against *polA* levels. Expression levels are derived from three biological replicates and triplicate qPCR reactions. Expression levels are normalised to those given by sulphate grown cells. Stars indicate data derived from ΔCt values statistically significantly different to that for sulphate-grown cultures ($P<0.05$).

4.7 Discussion

Sulphate and sulphite reduction by *D. desulfuricans*

In this chapter, growth and gene expression of *D. desulfuricans* in the presence of sulphate, sulphite, nitrate and nitrite was examined. Sulphate dependent growth and sulphate reduction were unaffected by the presence of nitrate. However, biphasic growth was observed in cultures supplemented with sulphate and nitrite, growth was slowed and sulphate reduction was delayed compared to cultures supplemented with sulphate alone. These observations suggest that nitrite is reduced preferentially when both sulphate and nitrite are present in the medium. qRT-PCR analysis of the *sat* and *apsB* genes suggest that the sulphate reduction pathway is not strongly regulated at the transcription level and that expression of *sat*, *apsB* and *qmoB* can be regarded as constitutive in *D. desulfuricans*. In *D. vulgaris* the genes encoding the components of the sulphate reduction pathway are regulated in response to different growth conditions and stresses. These regulatory responses include down-regulation of *apsBA* in the absence of sulphate and variations in the levels of *dsrAB* in response to growth phase and nitrite stress (Haveman *et al.*, 2004; He *et al.*, 2006; Zane *et al.*, 2010; Keller & Wall, 2011). However, these changes in expression are relatively small and since these genes are also reported as being amongst the top 1% most highly expressed genes in *D. vulgaris*, it seems unlikely that these changes in expression would impact greatly upon sulphate-sulphite utilisation.

Growth of *D. desulfuricans* in the presence of sulphite was preceded by a prolonged lag phase compared with growth in the presence of sulphate. Since the inoculum for these experiments had been grown in the presence of sulphate, this period of adaptation was

unexpected. Pre-exposure of *D. desulfuricans* to sulphate equates to pre-exposure to sulphite and so the necessary components for sulphite reduction should have already been induced. Additionally, qRT-PCR analysis of *dsrA* and *dsrJ* indicated that these critical components of the sulphite reduction pathway are expressed within a comparatively narrow range irrespective of terminal electron acceptor availability. This constitutive expression of *dsrA* was also reported by Marietou *et al.* (2009).

Potentially, the period of induction observed for sulphite reduction could be due to regulation of sulphite uptake genes rather than sulphite reductases. Alternatively, expression of *dsrA* in *D. desulfuricans* could be regulated by growth phase in a manner similar to the SRB *Desulfobacterium autotrophicum* (Neretin *et al.*, 2003). Since the inoculum used in the present study was entering stationary phase this could explain the extended lag phase prior to sulphite-dependent growth and sulphite reduction. Additionally, RNA used for the qRT-PCR analysis in this study was isolated from exponentially growing cells**.** Thus, if the levels of *dsrA* in *D. desulfuricans* vary with growth phase then these fluctuations would not have been captured in this study. It seems that sulphite reduction by *D. desulfuricans* is subject to a period of induction but whether this induction period is due to changes in the levels of the *dsrA* transcript remain unknown. Similar to sulphate, the presence of nitrate had no effect upon sulphite reduction or sulphite dependent growth. Also, similar to sulphate, cultures supplemented with nitrite and sulphite grew slowly and gave a lower rate of sulphite reduction compared with cultures supplemented with sulphite only.

Growth yields in the presence of sulphate and sulphite were similar. As sulphate dependent growth represents a drain of ATP to the cell this result seems surprising.

Theoretically, sulphite, which does not require an activation step, would be an energetically more favourable terminal electron acceptor. Indeed, previous reports indicate that SRB can reach higher growth yields on sulphite or thiosulphite compared to sulphate (Cypionka & Pfennig, 1986). The results presented here indicate that sulphate and sulphite were both completely reduced in these cultures. Increasing concentrations of sulphide inhibit growth and affects cell size in *Desulfovibrio* (Caffrey & Voordouw, 2010; Okabe *et al.*, 1992). Perhaps final yields were limited by the presence of sulphide in these cultures, which were grown in sealed flasks. Removal of sulphide from SRB cultures can increase yields (Cypionka, 1986).

Nitrite reduction by *D. desulfuricans*

Growth yields in the presence of nitrite were lower than with any of the other terminal electron acceptors. Thus, nitrite is the least favourable terminal electron acceptor of those tested. Despite this observation, nitrite is readily reduced by *D. desulfuricans* and was eliminated from the medium first when present in combination with sulphate or sulphite. Thus, nitrite is reduced preferentially to or simultaneously with sulphate or sulphite. Distinguishing whether nitrite reduction is simultaneous or preferential is difficult because of limitations with the assays for sulphate and sulphite. The turbidometric sulphate assay used in this study is extremely error prone even in attempts to create a standard curve for sulphate dissolved in water. The Postgate medium is also likely to contain chemicals that interfere with the assay. Thus, it is difficult to achieve accurate measurements of sulphate concentrations. Despite these problems, the sulphate assays suggest that a low rate of sulphate reduction does occur simultaneously with nitrite reduction. Since nitrite has a masking effect upon the sulphite assay it is not

possible to determine from the experimentally determined sulphite concentrations whether sulphite reduction occurs simultaneously with nitrite reduction. The distinctive aroma of hydrogen sulphide detected when sampling cultures supplemented with nitrite and sulphate or sulphite suggested that nitrite reduction occurs simultaneously with sulphate and sulphite reduction and can therefore be regarded as constitutive.

The effects of nitrite upon sulphate or sulphite reduction and growth can be rationalised by considering the structural similarity between nitrite and sulphite reductases (Crane & Getzoff, 1996). Indeed, Nrf from *D. desulfuricans* has been demonstrated to have sulphite reductase activity and Dsr from *D. vulgaris* has been demonstrated to have nitrite reductase activity (Pereira *et al.*, 1996; Wolfe *et al.*, 1994). Thus, in *D. desulfuricans*, sulphite can occupy the active site of Nrf and nitrite is likely to be able to occupy the active site of Dsr. The ability of nitrite to function as a competitive inhibitor of sulphite reduction would decrease the rate of sulphite reduction and slow sulphite dependent growth. Sulphite could have a similar effect upon nitrite reductase and nitrite dependent growth. Furthermore, a lowered nitrite reductase effect would prolong exposure of the cells to toxic nitrite and so exacerbate the lowered growth rates. Hence, the extended lag phase witnessed for *D. desulfuricans* in the presence of nitrite and sulphite**.**

A similar effect would occur with cultures supplemented with both nitrite and sulphate. Initially, sulphate activation and APS reduction would be unaffected by nitrite. However, sulphite would accumulate due to inhibited sulphite reductase activity by nitrite. Growth would stall and concentrations of sulphite would increase. In turn, increased concentrations of sulphite could affect the net rate of APS reduction since this

reaction, catalysed by Apr, is reversible (Schiffer *et al.*, 2006). Thus, sulphate-dependent growth would be inhibited until all nitrite had been reduced. This inhibitory effect provides an explanation for the biphasic growth observed for nitrite and sulphate. This biphasic growth is not diauxie but transient inhibition by nitrite. Nitrite reduction seems to be unaffected by the presence of sulphite despite its potential to act as a competitive inhibitor of nitrite reduction.

The apparently constitutive reduction of nitrite by *D. desulfuricans* seems to contradict the qRT-PCR analysis that indicated that *nrfA* is regulated at the transcription level in response to nitrite and nitrate reduction. Therefore expression of *nrfA* is regulated at the transcription level in *D. desulfuricans*. Indeed, the rate of nitrite reduction by *D. desulfuricans* can be increased by culture pre-treatment with nitrate. However, nitrite was reduced at a lower rate by cells that had not been pre-treated with nitrate so Nrf is present at appreciable levels without pre-treatment. Thus, nitrite reduction by *D. desulfuricans* can be regarded as both constitutive and regulated as the basal levels of Nrf are sufficient for nitrite reduction but are also up-regulated when necessary. The observation that sulphate- and nitrate-adapted *D. desulfuricans* exhibited different growth rates in the presence of 1.5 mM nitrite provides additional support for this proposal. The observation that *nrfA* is regulated at the transcriptional level contradicts the qRT-PCR results presented by Marietou *et al.* (2009).

Nitrate reduction by *D. desulfuricans*

Nitrate reduction by *D. desulfuricans* is also subject to regulation. Expression of *napC* is completely repressed in the presence of sulphate or sulphite, even when nitrate is present. Previous studies reported that sulphide is responsible for repressing nitrate

reduction (Marietou *et al.*, 2009). When culturing *D. desulfuricans* in sealed flasks it was necessary to flush these flasks with an anaerobic gas mixture to provide a strictly anaerobic environment. When nitrate supplemented medium was inoculated with sulphate or sulphite grown *D. desulfuricans*, growth was only observed if those flasks were flushed after inoculation (Marietou, 2009). Flushing of the culture flasks with anaerobic gas not only removes oxygen but also any small quantities of hydrogen sulphide introduced to the culture with the inoculum. Presumably there is a sulphide-responsive transcription factor that represses *nap* expression in *D. desulfuricans*. Sulphide functions as a signalling molecule in a range of systems and so this presumption seems plausible (Lloyd, 2006).

Expression of *napC* was greatly up-regulated in the presence of nitrate but there was also a lower level of up-regulation in the presence of nitrite. Marietou *et al.* (2009) reported that nitrite did not induce expression of *napC* and that *napC* is responsive exclusively to nitrate. Up-regulation of *napC* in the presence of nitrite could be due to low levels of nitrate reductase catalysing the reverse reaction of nitrite to nitrate. The nitrite oxidases of *Nitrobacter*, which are similar to dissimilatory nitrate reductases, are able to catalyse both nitrite oxidation and nitrate reduction (Kirstein & Bock, 1993). This would then lead to induction of nitrate dependent *napC* expression. Alternatively, nitrite or a product of nitrite reduction could be an inducer of *napC* expression. In this instance maximal expression of *napC* would require an additional regulatory factor.

Nitrate and nitrite responsive genes *ssc* and *hcp*

Growth of *D. desulfuricans* in the presence of nitrate and nitrite induced other transcription responses in addition to the up-regulation of *napC* and *nrfA*. The levels of

the *hcp*, *ssc* and *hcpR* transcripts were all significantly increased in *D. desulfuricans* cultures reducing nitrate or nitrite. Since Hcp is implicated in coping with the consequences of nitrate and nitrite reduction it is unsurprising that the *hcp* gene is up-regulated in response to nitrate and nitrate reduction (Vine, 2012). Pre-treatment of *D. desulfuricans* with nitrate lead to increased tolerance to nitrite stress and perhaps this observation was in part due to induction of *hcp*.

The up-regulation of *ssc*, which encodes a periplasmic cytochrome, in response to nitrate suggests that this gene is implicated in nitrate reduction. Maximal expression of *ssc* was recorded in the presence of nitrate with a lower level of induction in the presence of nitrite. The expression levels of two other transcripts encoding periplasmic cytochromes, *tpIc*$_3$ and *nhc*, did not change when cultures were supplemented with alternative terminal electron acceptors. Thus, up-regulation of *ssc* in response to nitrate is a specific response rather than a general up-regulation of cytochromes. The proteins responsible for relaying electrons to the Nap complex of *D. desulfuricans* have not been identified but it has been suggested that the *ssc* cytochrome could be responsible for this activity (da Silva *et al.*, 2012). The up-regulation of *ssc* in response to nitrate supports this proposal. Furthermore, the stacked haem arrangement of Ssc is very similar to that of NapB (Brigé *et al.*, 2002). Potentially, Ssc could be a functional replacement for NapB in *D. desulfuricans*. Expression of the *nap* and *ssc* genes could be influenced by one or more common regulatory factors that are nitrate-responsive. In the previous chapter HcpR was predicted to be a transcription regulator of *nap* and *ssc* in *D. desulfuricans*. Consistent with this prediction, *hcpR* was also up-regulated in the presence of nitrate, implicating this gene in nitrate metabolism. However, maximal expression of *hcpR* was recorded in the presence of nitrite. The expression patterns of

nap and *ssc* do not correlate perfectly with that of *hcpR*. If *nap* and *ssc* expression is dependent upon HcpR then it seems likely that these genes also require an additional transcription factor.

Regulation of *hcpR* and *hcpR2*

Some of the genes responsible for the utilisation of nitrogen-based terminal electron acceptors and defence against their associated toxicity by *D. desulfuricans* are regulated at the transcription level. In the previous chapter two transcription regulators of the CRP family, HcpR and HcpR2, were predicted to be responsible for controlling the nitrate-sulphate diauxie and nitrosative stress response of *D. desulfuricans*. Evidence suggests that HcpR is a nitrate-nitrite responsive regulator and the predicted HcpR regulon members, *nap* and *ssc*, also respond to this stimulus. The *sat* and *aprB* genes were predicted to be repressed by HcpR. However, expression of these genes did not seem to change significantly with terminal electron acceptor availability or *hcpR* levels and so these predictions seem to be incorrect. Expression of the putative HcpR regulon member, *nhc*, also did not change. The levels of the *nrfA* transcript correlated with *hcpR* expression but *nrf* is not predicted to be influenced by HcpR. These observations challenge the proposed model in which HcpR regulates the nitrate-sulphate diauxie of *D. desulfuricans* by concurrent activation of *nap* and repression of *sat* and *apr* genes.

In contrast with the expression profile of *hcpR*, expression of *hcpR2* does not change in response to different terminal electron acceptors. It seems that *hcpR2* is expressed constitutively. However, expression of *hcp*, a putative HcpR2 regulon member, is greatly elevated in the presence of nitrate and nitrite. If HcpR2 does regulate expression of *hcp* then this would support the predicted role of HcpR2 in coping with nitrosative

stress. It was predicted that HcpR2 regulates expression of *hcp* from an inverted repeat DNA sequence at the 3' end of the coding region for HcpR2. If HcpR2 were to bind to this site and regulate expression of downstream genes then a different expression pattern for *hcpR2* and *hcp* would be observed. Since differential expression of *hcpr2* and *hcp* was witnessed the proposed model of HcpR2 regulation of *hcp* is supported by these results. In the next chapter the physiological and transcriptional observations presented here will be complemented by characterisation of HcpR and HcpR2 in an endeavour to assign functions to these regulators and provide further critical assessment for the predictions made in Chapter 3.

Chapter 5

Results

Characterisation of HcpR and HcpR2

5.1 Introduction

The *nap* gene cluster of *D. desulfuricans* is subject to complex regulatory control. HcpR is predicted to be critical in this regulation due to the high density of putative binding sites proximal to the *nap* promoter. In *E. coli*, expression of *nap* and *nrf* is, in part, controlled by another CRP-family regulator, FNR. Indeed, other members of this diverse family are involved in nitrate metabolism including NnrR and DNR (Tosques *et al.*, 1996; Mesa *et al.*, 2003; Rinaldo *et al.*, 2006). Thus, the involvement of CRP-family proteins in the processing of nitrogen oxides is well documented. The HcpR protein of *D. desulfuricans* is predicted to be involved in regulating terminal electron acceptor utilisation and nitrosative stress response. In support of this prediction, transcription measurements reported in Chapter 4 highlight that expression of *hcpR* is nitrite responsive. It was suggested that HcpR binds to CRP-like DNA sites and modulates transcription of target genes. Expression of *hcp*, a key component of the *E. coli* nitrosative stress response, is also regulated by FNR (Filenko *et al.*, 2005). Additional regulators of *E. coli hcp* include the nitric oxide and redox sensitive regulators OxyR and NsrR (Filenko *et al.*, 2007; Seth *et al.*, 2012). In *D. desulfuricans hcp* expression is predicted to be regulated by a second HcpR protein, HcpR2.

This chapter will present a detailed direct analysis of the exact roles of these two HcpR proteins. By overexpressing, purifying and then using in a series of *in vitro* experiments, the DNA binding activities of these regulators could be assessed. Heterologous expression of HcpR in *E. coli* provides clues to what the *in vivo* activity of HcpR could be. Additionally, by using protein-specific antibodies targeting HcpR, the temporal expression profile of HcpR in response to terminal electron acceptors and stress could

be determined. Finally, identification of the *hcpR* transcription units will provide insight into why these proteins are expressed differentially. Thus, a detailed account of HcpR proteins can be made by relating these final results back to the *in silico*, physiological and transcription analyses of Chapters 3 and 4.

5.2 Overexpression and purification of HcpR

In order to ascertain whether HcpR binds to DNA it was necessary to overexpress and purify the recombinant protein. The purified protein could then be used in *in vitro* assays and for the generation of HcpR-specific antibodies. The *hcpR* open reading frame, minus the *hcpR* stop codon, was cloned into the vector pET21a (Novagen). The resulting plasmid, pETHcpR, encodes HcpR protein with and additional His_6-tag at the C-terminus under the control of an IPTG inducible T7 promoter. Thus, the resulting plasmid, pETHcpR, could be used to produce C-terminal His_6-tagged HcpR with an approximate MW of 27 kDa in the host strain *E. coli* BL21*.

To determine optimum conditions for expression of recombinant HcpR, small-scale cultures of *E. coli* strain BL21* harbouring pETHcpR were grown in LB to an OD_{650} of ~0.5 and induced with 10, 50 or 500 μM IPTG. Culture samples were taken at 0, 2, 5 and 24 hours following induction. Total proteins for each culture, normalised to the culture OD_{650}, were analysed by SDS-PAGE (Figure 5.1). The addition of IPTG induced HcpR expression from two hours post-induction. Maximal levels of expression were recorded at 24 hours after induction with 10 μM IPTG. However, an additional smaller protein, probably a degradation product of HcpR, was also noticeable on the SDS-PAGE gel. Partially degraded HcpR was likely to have similar biochemical qualities to full-length HcpR and could potentially interfere or compete with intact

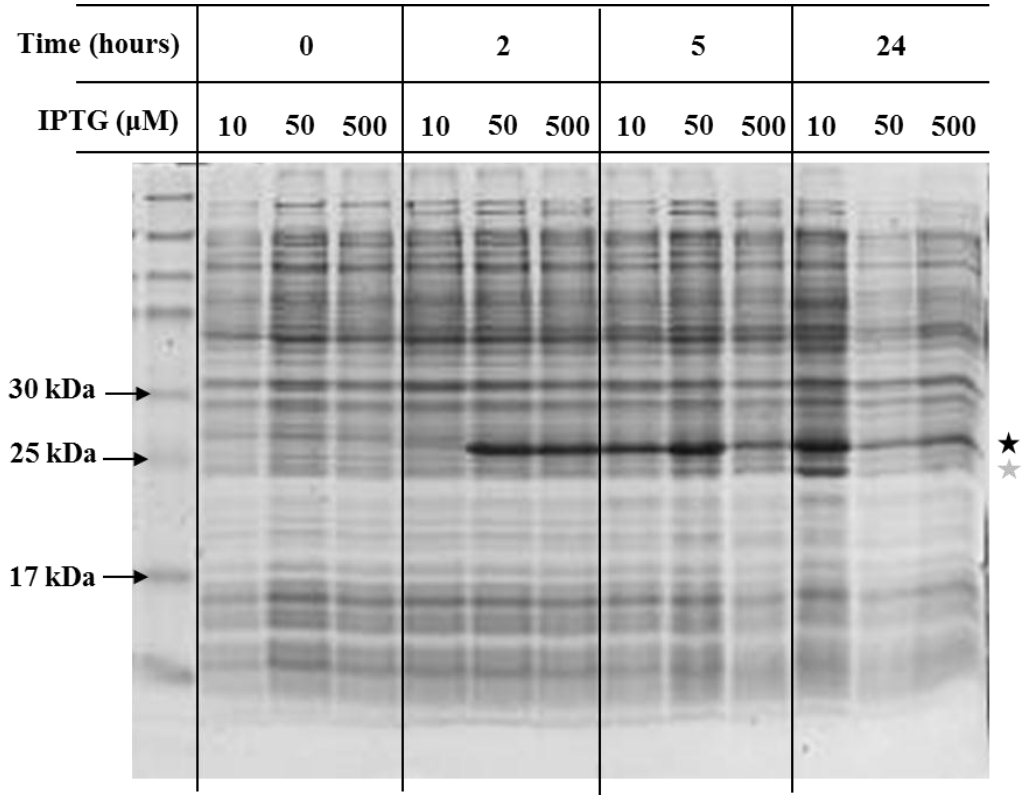


Figure 5.1: Overexpression of recombinant HcpR in *E. coli*. Cultures of strain BL21* harbouring plasmid pHcpR were induced with 10, 50 or 500 μM IPTG and cells were harvested at 0, 2, 5 and 24 post-induction. Total cell proteins were separated by SDS-PAGE. The theoretical MW of His-tagged recombinant HcpR protein is 27.6 kDa and is present on the gel between the 25 and 30 kDa marker proteins (marked by a **black star**). Partially degraded HcpR is present as a band smaller than 25 kDa in some of the lanes (marked by a **grey star**).

protein during later protein purification procedures and downstream processes. Thus, the cultures grown for 5 hours in the presence of 50 µM IPTG were deemed most suitable for providing cell extracts for HcpR purification. At this time point HcpR expression was high with negligible levels of degraded HcpR.

Following the identification of optimal production conditions, recombinant HcpR was expressed in large-scale 500 ml cultures for the purpose of protein purification. Cells were harvested by centrifugation, re-suspended in lysis buffer and disrupted by sonication. The lysate was clarified by centrifugation and recombinant HcpR was purified affinity chromatography using a nickel-agarose column (GE Healthcare) as described in Chapter 2. HcpR was eluted from the column in a linear gradient of imidazole and fractions containing purified protein were supplemented with 2 mM EDTA. Trial purifications indicated that this supplement decreased protein aggregation. Fractions from the purification were analysed by SDS-PAGE (Figure 5.2a). Typically, His-tagged proteins elute from nickel-agarose in a relatively small volume in a single peak. HcpR eluted over a large range of imidazole concentrations (from fractions 25 – 70, imidazole concentrations 100 – 400 mM). This elution profile could be the result of HcpR being in several different structural conformations in the lysate. The fractions analysed by SDS-PAGE were also assessed for protein content by the Bradford assay and those judged to contain HcpR of high purity were retained. These fractions were pooled, concentrated on a 10 kDa Vivaspin protein concentrator column (GE Healthcare) and then analysed by SDS-PAGE (Figure 5.2b). The pooled and concentrated fractions were judged to contain HcpR of high purity.

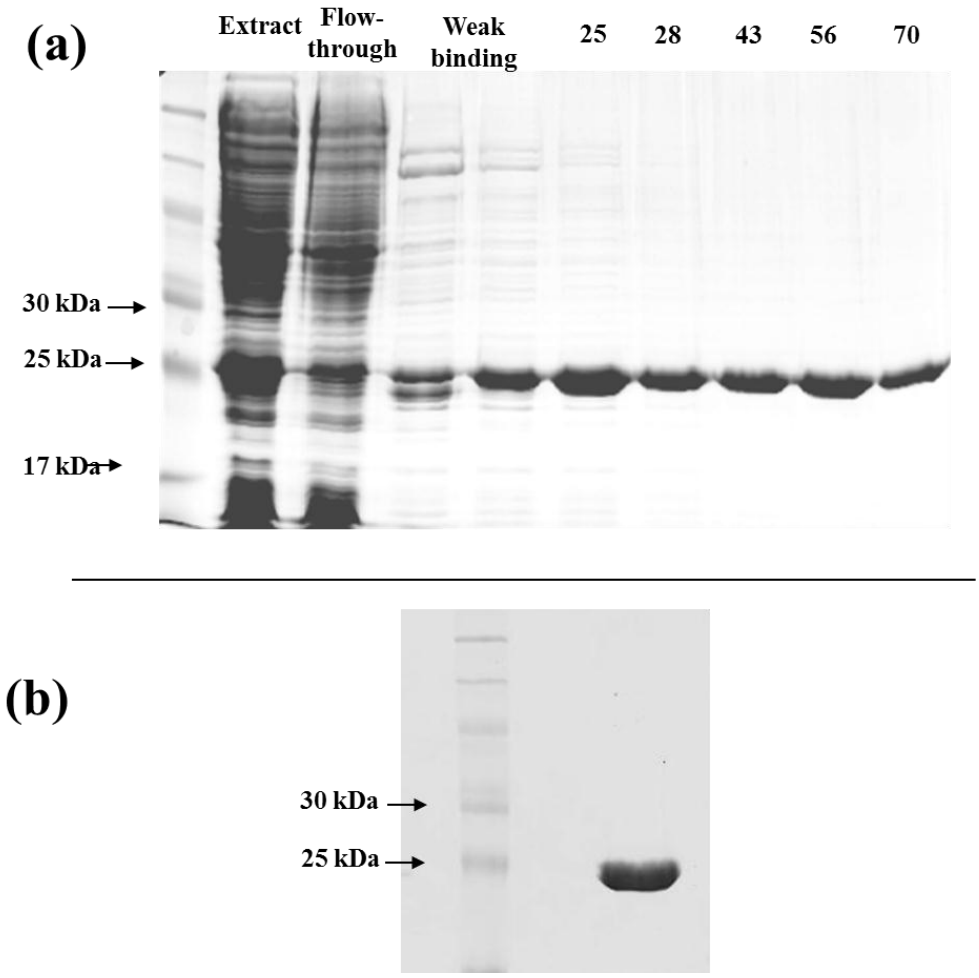


Figure 5.2: Purification of recombinant HcpR overexpressed in *E. coli*. 500 ml of culture was harvested by centrifugation and the cell pellet lysed with lysozyme and sonication. The resulting lysate was clarified by centrifugation and then subjected to affinity chromatography using a 1 ml nickel agarose column fitted to an *Äkta* Prime HPLC system (GE Healthcare). (**a)** Adsorbed proteins were eluted from nickel-agarose in a linear gradient of imidazole from 50 – 400 mM and 2 ml fractions were collected. Fractions were resolved by SDS-PAGE and assessed for HcpR content and purity. HcpR protein is present in fractions 25-70 on the gel at approximately 25 kDa. HcpR eluted in a series of small peaks. **(b)** Concentrated purified HcpR protein.

5.3 DNA binding of HcpR at the *nap* promoter

The *in vitro* DNA binding activity of HcpR was assessed using the purified protein in EMSAs. The DNA fragment used in these initial assays, p*nap*, contains promoter proximal DNA including the ATG start codon of *napC* and all three of the CRP-like inverted repeats upstream of the *nap* operon that were first reported by Marietou *et al.* (2009). This DNA fragment was radiolabelled, mixed with non-specific competitor DNA and incubated with various concentrations of HcpR protein prior to non-reducing, non-denaturing PAGE (Figure 5.3). As a control, the binding of *E. coli* CRP to the p*nap* fragment was also assayed. The use of CRP as a control necessitated the inclusion of cAMP at a concentration of 200 μM in the protein-DNA incubations and in the electrophoresis gel. Robust CRP-DNA complexes will not form in an absence of cAMP. The presence of discrete bands on the EMSA gel, in addition to that given by the p*nap* DNA fragment alone, indicated that both HcpR and CRP bound specifically to the p*nap* fragment. Since a band of higher molecular weight appeared with HcpR concentrations in excess of 25 nM it is apparent that HcpR bound specifically to one site on the p*nap* fragment with high affinity. A second specific site became bound by HcpR at concentrations of 200 nM and higher. Potentially a third site was occupied but with low affinity, this was suggested by the blurring of the DNA bands at 400 nM of HcpR. CRP was also able to bind to the p*nap* fragment at two sites with high specificity.

The binding patterns produced by CRP and HcpR in the EMSA allow comparisons between these two proteins. CRP had a higher affinity for the p*nap* fragment than HcpR. Also, CRP and HcpR shifted the DNA fragment to different positions on the gel with CRP retarding migration of the fragment more than HcpR. This was surprising since CRP and HcpR are both of similar molecular weights, each being approximately

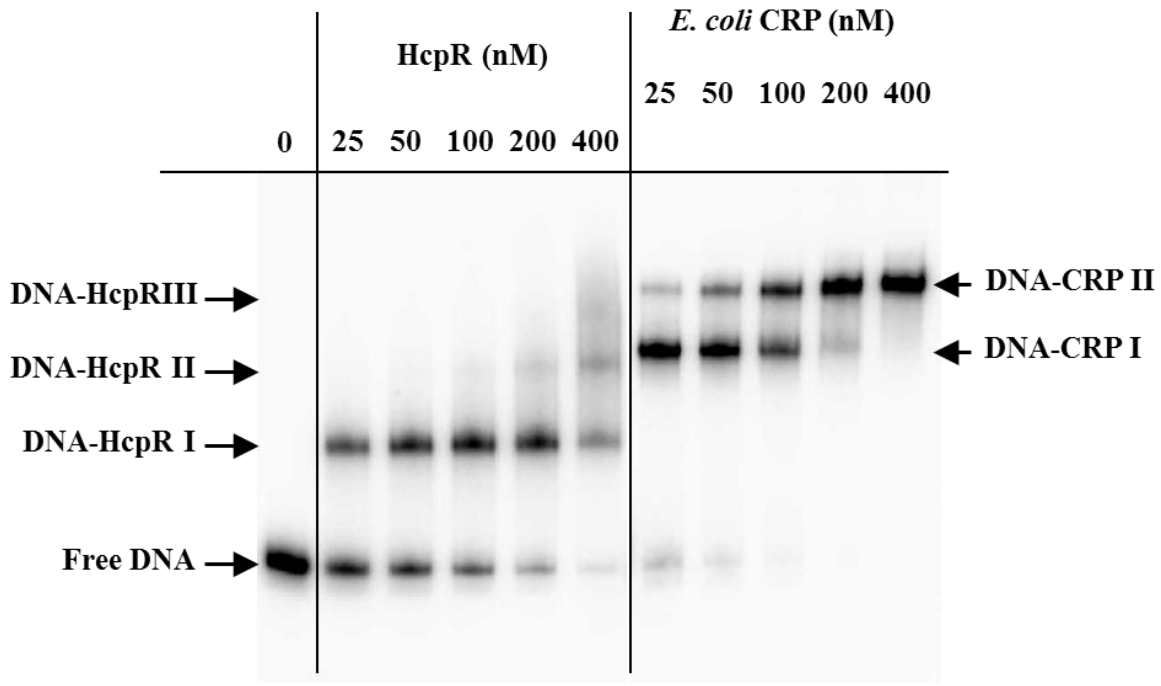


Figure 5.3: Comparison between the DNA binding affinities of HcpR and CRP for the *nap* promoter fragment in the presence of cAMP. DNA binding affinities were assessed by EMSA. ^{32}P-labelled *nap* promoter DNA fragment was incubated with increasing concentrations of HcpR or CRP protein in the presence of 200 μM cAMP and then resolved by non-denaturing PAGE. Herring sperm DNA was also included in the incubation mixtures to act as non-specific competitor DNA. Free DNA, DNA-HcpR and DNA-CRP complexes are marked with arrows.

25 kDa. Perhaps this difference in the shift pattern was caused by HcpR binding to p*nap* as a monomer. Since CRP binds as a dimer a single shift by CRP on the EMSA gel was caused by an addition of ~50 kDa to the molecular weight of the p*nap* fragment. HcpR binding as a monomer would provide an additional ~25 kDa and thus the two proteins would provide different migration patterns.

Alternatively, the DNA bending by the two proteins could be different. CRP bends its DNA target by 90º (Parkinson *et al.*, 1996). If HcpR bends its DNA target by significantly more or less than 80º then the result would be a more or less compact protein-DNA complex compared with that for CRP. These different complexes would be expected to migrate within the EMSA gel differently. An additional explanation for the two proteins shifting the p*nap* fragment to different positions could be that the proteins have different pIs (HcpR pI = 9.40; CRP pI = 8.38). The pI of a protein is a measure of its charge and is characteristic utilised in ion-exchange chromatography and isoelectric focussing. The pI of a protein influences its migration in the presence of an electric current, a characteristic exploited in techniques such as isoelectric focussing. Proteins with different pIs could provide a different shift pattern on the EMSA gel. Since cAMP was included in this EMSA at a constant concentration it was not possible to assess whether cAMP has any effect upon the DNA binding affinity of HcpR.

5.4 DNA binding by HcpR in the presence of effector molecules

EMSAs were used to determine whether the DNA binding activity of HcpR is affected by selected small molecules. The ability of HcpR to shift the p*nap* fragment in the presence or absence of cAMP was assayed (Figure 5.4). The concentration of cAMP had no effect upon DNA binding by HcpR.

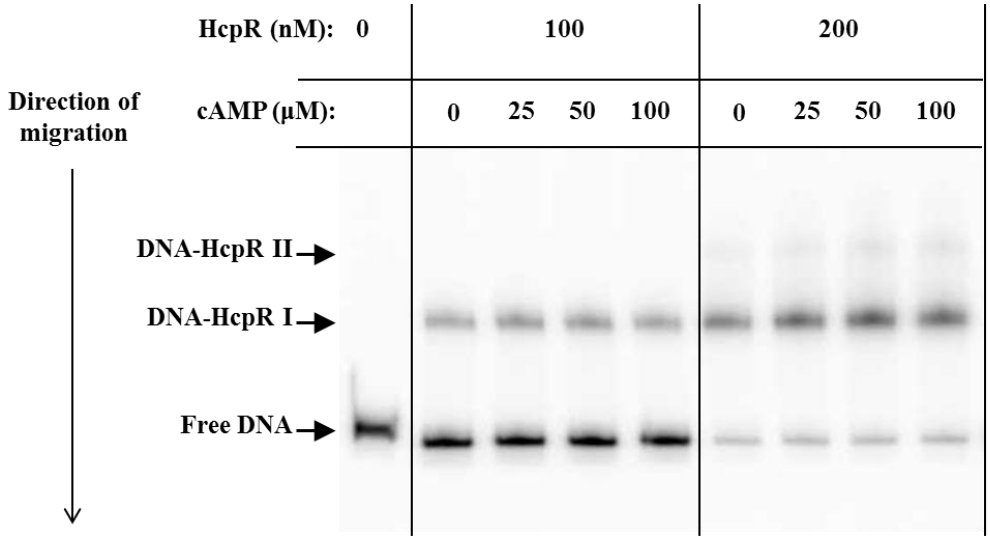


Figure 5.4: The effects of differing cAMP concentrations upon DNA binding by HcpR. DNA binding activities were measured by EMSA. ^{32}P-labelled *nap* promoter DNA fragment was incubated with either 100 or 200 nM HcpR and increasing concentrations of cAMP. Herring sperm DNA was also included in the incubation mixtures to act as non-specific competitor DNA. Incubation mixtures were then resolved by non-denaturing electrophoresis.

In an attempt to identify an effector molecule that modulates HcpR binding, protein-free cell lysates were prepared from *D. desulfuricans* grown in the presence of nitrate or sulphate. Cells were harvested from mid-exponential phase cultures and lysed by sonication. The lysate was heated to 90°C and loaded onto a 5 kDa Vivaspin size exclusion column to remove proteins that could potentially interfere with the EMSA. Flow-through from the columns were collected and used as protein-free extracts. To assess whether the protein-free cell lysates contained effector molecules sufficient to influence protein activities the lysates were used in an EMSA with the p*nap* fragment and CRP in an absence of cAMP (Figure 5.5a). The presence of cAMP in the lysate would result in an increase in DNA binding by CRP. There was a slight increase in the amount of DNA shifted by incubations containing protein-free lysates and CRP compared with those containing CRP but lacking lysate. This observation suggests that trace quantities of cAMP and presumably similar small molecules were present in the lysates. However, the inclusion of these lysates in an EMSA of HcpR with p*nap* did not cause any difference in the HcpR-DNA shift pattern (Figure 5.5b). Either the lysates lacked the appropriate small molecules or contained the small molecule but not in sufficient quantities to influence protein activity. It was possible that the appropriate effector had been lost or subject to chemical modification during the preparation.

Further EMSAs using HcpR supplemented with Postgate media, terminal electron acceptors and cGMP were also used (data not shown). However, none of these additives yielded any change in the shift pattern for HcpR with the p*nap* fragment. Thus, the DNA binding by HcpR *in vitro* is seemingly unaffected by small effector molecules. Perhaps HcpR, rather than binding to an effector molecule, responds to its signal via a bound cofactor or chemical modification.

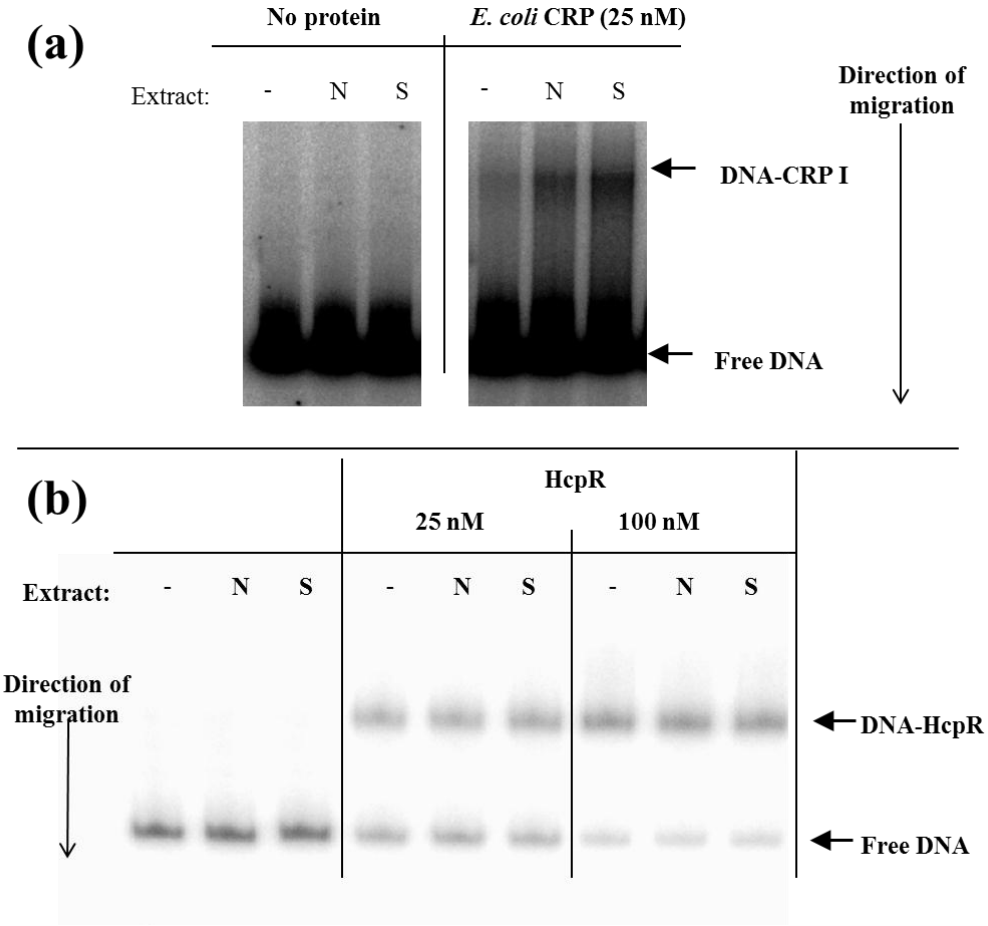


Figure 5.5: The effect of *D. desulfuricans* protein-free extracts upon DNA binding by CRP and HcpR. (a) EMSA of the *nap* promoter with CRP and protein-free extracts. ^{32}P-labelled *nap* promoter DNA fragment was incubated with CRP and protein-free cell extracts prepared from *D. desulfuricans* cells grown upon nitrate or sulphate. **(b**) EMSA of the *nap* promoter fragment with HcpR and protein-free cell extracts. ^{32}P-labelled *nap* promoter DNA fragment was incubated with HcpR and extracts prepared from *D. desulfuricans cells* grown upon nitrate or sulphate. **(-)** no extract included in protein-extract incubation, **(N)** incubation included extract prepared from nitrate grown cells, **(S)** incubation included extract prepared from sulphate grown cells. Herring sperm DNA was also included in the incubation mixtures to act as non-specific competitor DNA.

5.5 Identification of HcpR DNA target sites

The *in vitro* binding of HcpR to specific sites on the p*nap* fragment had been confirmed by EMSAs. However, the exact locations and sequences of these target sites could not be determined by EMSAs with full-length copies of the p*nap* fragment. Thus, truncated copies of the p*nap* fragment were generated with a series of primers and then used in EMSAs (Figure 5.6). The truncated p*nap* fragments, named AM1, AM2, AM3 and AM4, contain different combinations of the three CRP-like sites (Figure 5.6a). The three CRP-like sites of the *nap* promoter proximal region are hereafter referred to as IR1, IR2 and IR3, with IR1 being proximal to the *nap* coding region. Fragments AM4 and AM3 gave single shifts with low concentrations of HcpR protein (Figure 5.6b). The similarity between the migration patterns of AM4 and AM3 suggest that a common factor could have been responsible for the high affinity of HcpR for these fragments. Potentially, this common factor could be IR1. Indeed, the shift patterns generated with fragments AM2 and AM1 indicated that HcpR had a lower affinity for these fragments compared to AM4 or AM3. Both AM2 and AM1 lack IR1. The major difference between AM1 and AM2 is that AM1 lacks IR2. Since the shift patterns observed for these two fragments were similar it seems that IR3, which is common to both, could be a low affinity target of HcpR. These observations are supported by the earlier EMSA using the full-length p*nap* fragment. HcpR binds to two sites on the p*nap* fragment: one with high affinity and another with low affinity.

To clarify the locations of the HcpR binding sites on the p*nap* fragment more precisely a DNaseI footprinting assay was employed using increasing concentrations of HcpR protein (Figure 5.7a). The DNaseI footprinting assay relies upon controlled digestion of

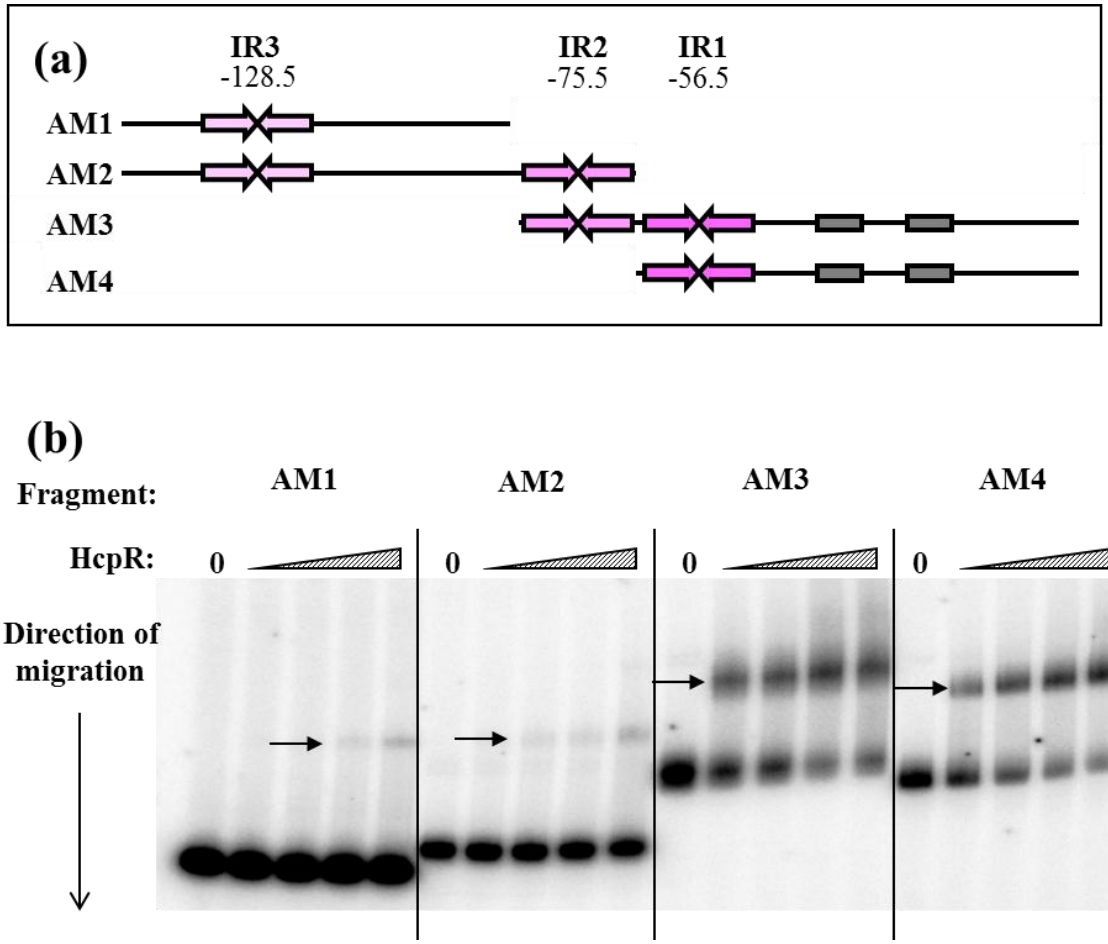


Figure 5.6: EMSA of truncated copies of the *nap* promoter with HcpR. (a) The *pnap* fragment was used as the template to generate four different DNA fragments containing different combinations of the three IRs (pink arrows) as described in Marieou (2009)**.** Fragments are named AM1, AM2, AM3 and AM4. Some fragments also included the putative -10 and -35 promoter elements (grey boxes). **(b)** ^{32}P-labelled truncated AM1, AM2, AM3 and AM4 DNA fragments were incubated with increasing concentrations of HcpR and then resolved by non-denaturing electrophoresis. Black arrows indicate HcpR-DNA complexes. Herring sperm DNA was also included in the incubation mixtures to act as non-specific competitor DNA. The concentrations of HcpR used in each set of incubations were: 0, 25, 50,100 and 200 nM.

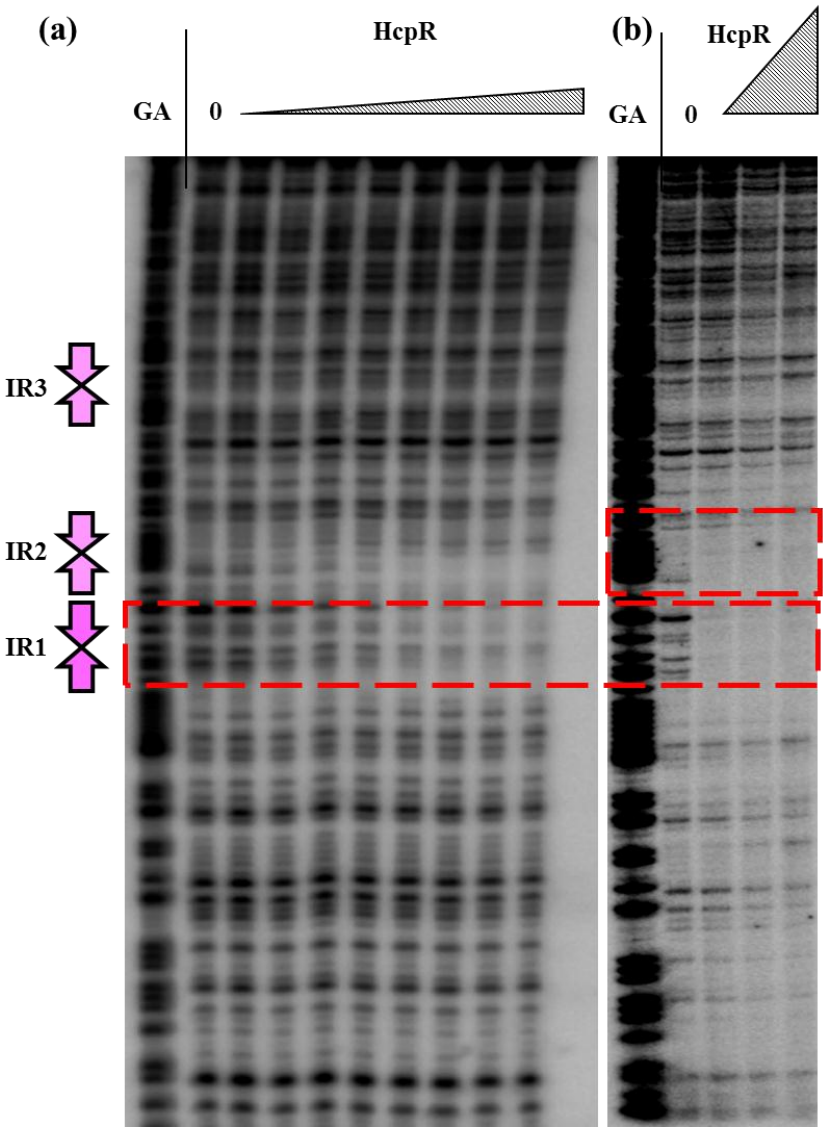


Figure 5.7: Measuring HcpR binding to the p*nap* DNA fragment by DNaseI footprinting assays. ^{32}P-end-labelled *nap* promoter DNA fragment was incubated with increasing concentrations of HcpR protein and digested with DNaseI. Digest mixtures were then resolved by denaturing electrophoresis on urea acrylamide gels. Sequences were identified by including Maxam-Gilbert sequencing reactions (GA) on gels. Protected regions are marked by boxes and the positions of the three IR sequences are marked with pink arrows. (**a)** DNaseI footprinting assay with 0, 5, 10, 20, 40, 80, 160, 360 and 720 nM HcpR. (**b**) DNaseI footprinting assay with 0, 0.8, 1.6 and 3.2 µM HcpR

a radioactively end-labelled DNA fragment using the nuclease DNaseI followed by electrophoresis. Regions of the DNA fragment that are bound by a protein will be protected from digestion and can be identified using a standard Maxam-Gilbert sequencing reaction (Maxam & Gilbert, 1977). As HcpR was titrated into the DNaseI reaction mixtures, an area of the p*nap* fragment coinciding exactly with IR1 became protected. HcpR bound preferentially to IR1. An additional DNaseI footprinting assay using higher concentrations of HcpR indicated that IR2 is the next site to become occupied by HcpR (Figure 5.7b). Thus, HcpR binds to sites similar to the target sites of CRP. Furthermore, since both halves of these inverted repeats were protected simultaneously we can reject the earlier suggestion that HcpR might bind as a monomer and conclude that HcpR binds to DNA as a dimer.

The observation that HcpR binds to CRP-like DNA sites indicates that some of the predictions made in Chapter 3 are correct. To identify other HcpR targets a collection of DNA fragments containing putative HcpR target sites were used in a series of EMSAs (Figure 5.8). HcpR shifted the p*hcpR*, p*1825* and p*sat* fragments suggesting that these fragments contain HcpR target sequences. HcpR had high affinity for the p*hcpR* fragment with all of the fragment shifting at the highest protein concentrations. The p*sat* and p*1825* fragments were bound by HcpR but with a lower affinity than the p*hcpR* fragment. No shift was observed for the p*apr* fragment.

5.6 The influence of HcpR on transcription in *E. coli*

To validate the observations of HcpR binding to DNA *in vitro* it was desirable to assay the *in vivo* binding of HcpR and any corresponding influence upon transcription. However, as yet there are no plasmids known to be supported in *D. desulfuricans* and

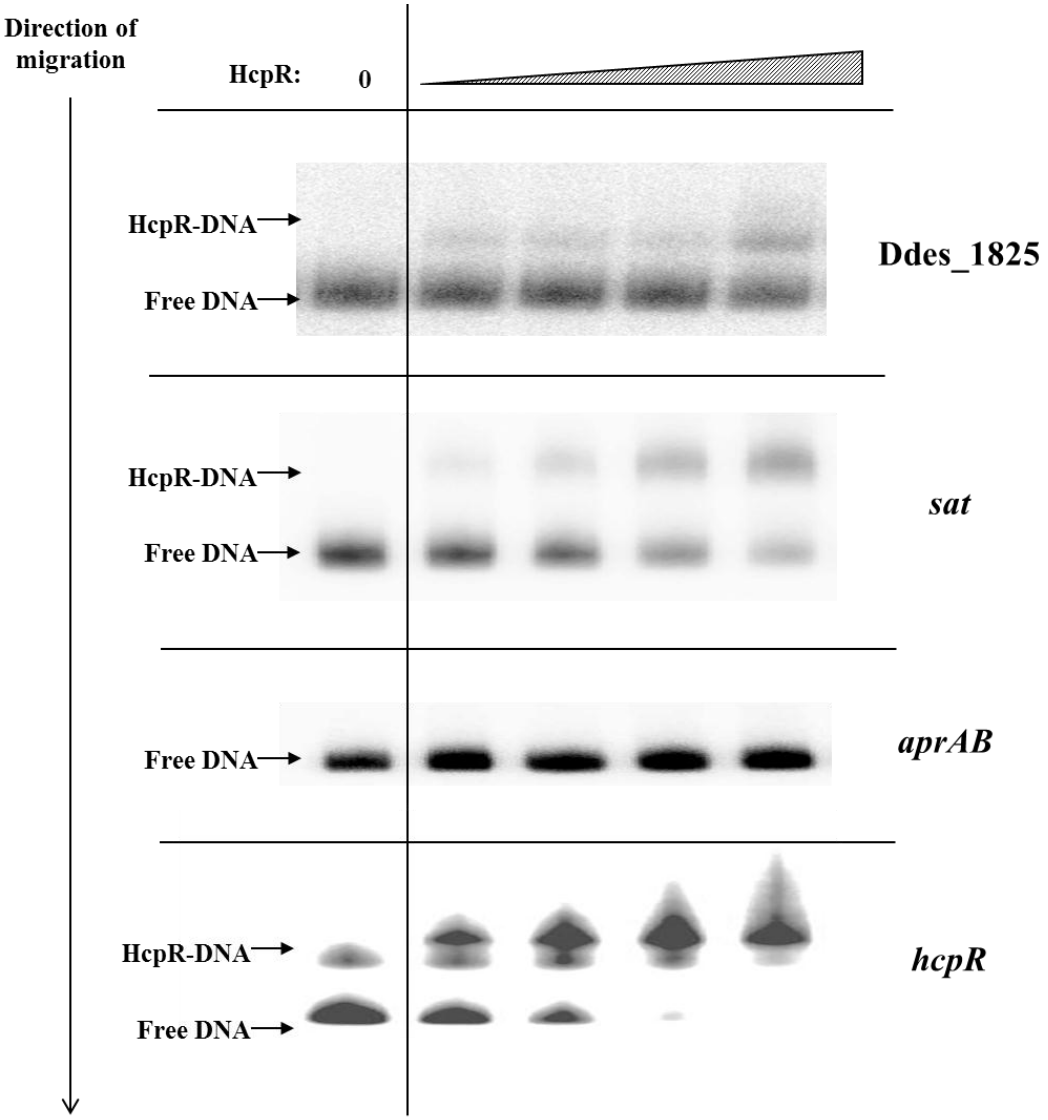


Figure 5.8: Binding of HcpR to the *D. desulfuricans* Ddes_1825, *sat, aprAB* and *hcpR* promoter fragments. DNA binding activities were measured by EMSA. ^{32}P-labelled promoter DNA fragments were incubated with increasing concentrations of HcpR protein and then resolved by non-denaturing electrophoresis. Free DNA and HcpR-DNA complexes are labelled with arrows. Herring sperm DNA was included as a non-specific competitor. HcpR was included in the incubations at 0, 25, 50, 100 and 200 nM.

attempts to introduce exogenous DNA into the *D. desulfuricans* chromosome have so far been unsuccessful (Marietou, 2009). Indeed, attempts made in this study were also unsuccessful (data not shown). This lack of genetic systems in *D. desulfuricans* made devising reporter assays for monitoring *in vivo* DNA binding by HcpR difficult. However, since HcpR and CRP bind to similar DNA sequences, the effect of HcpR binding to CRP sites in an *E. coli* system could be tested. This approach has been successfully used to characterise the DNA binding characteristics of *Mycobacterium* CRP (Spreadbury *et al.*, 2005).

E. coli strains M182 and M182Δ*crp* were transformed with plasmids pET21a or pETHcpR and additional plasmids carrying promoter::*lacZ* fusions in the vector pRW50. This resulted in a range of promoter and transcription factor combinations that could be assayed for β-galactosidase activity. Empty pRW50 vector was included as a control. The promoter p*CC-41.5* is a semi-synthetic class II CRP-dependent promoter with a consensus site for CRP binding centred at -41.5 with respect to the transcription start site (Gaston *et al.*, 1990). Expression from p*CC-41.5* is activated in the presence of CRP with very low activity in an absence of CRP. The promoter p*galP1* is also a class II promoter with a CRP site centred at -41.5 (Attey *et al.*, 1994). This CRP site is sub-optimal with the sequence TTTAT[N_6]TCACA. Significant expression is also achieved from p*galP1*, which is an extended -10 promoter, in the absence of CRP. Another promoter used in this experiment, p*galP1Δ4*, is derived from p*galP1* but four base pairs have been deleted from between the CRP site and the RNAP -35 consensus sequence (Bell *et al.*, 1990). Binding of CRP to a site centred at -37.5 occludes the RNAP -35 determinant sequences. Thus, expression from p*galP1Δ4* is repressed in the presence of CRP.

Aerobically grown cultures supplemented with fructose were assayed for β-galactosidase activity. As expected, *lacZ* expression from empty pRW50 was negligible irrespective of CRP or HcpR due to the lack of a promoter fragment fused to *lacZ* in this reporter plasmid (Figure 5.9). Expression of *lacZ* from p*CC-41.5*, p*galP1* and p*galP1Δ4* in strain M182 (*crp*+) was unaffected by the presence or absence of HcpR (Figure 5.9a). The expression levels from the different promoters varied in strain M182 with expression from p*CC-41.5* being moderate (~1500 β-galactosidase units), p*galP1* being high (~8,500 β-galactosidase units) and from p*galP1Δ4* being negligible. However, in strain M182Δ*crp* the presence of pETHcpR affected promoter activity (Figure 5.9b). M182Δ*crp* cells containing empty pET21a vector gave a significant level of *lacZ* expression from p*galP1Δ4* since repression by CRP in this strain is alleviated. The presence of pETHcpR partially restored this repression with expression from p*galP1Δ4* being reduced by ~80%. Intriguingly, HcpR also represses CRP independent expression from the *galP1* promoter to a similar magnitude. No activity was recorded from *CC-41.5* in the absence of CRP.

The heterologous expression of HcpR in the *E. coli* system provided some insight into the activities of HcpR. First, HcpR is able to bind to DNA *in vivo* in *E. coli* and can repress transcription from a CRP repressed promoter in an absence of CRP. Furthermore, HcpR can repress transcription from a class II CRP activated promoter in an absence of CRP. HcpR is unable to activate transcription from positions -41.5 or -37.5 in *E. coli*. Indeed, it is possible that transcription activation in *E. coli* by HcpR, should HcpR be able to act as a transcription activator, would require expression of additional *D. desulfuricans* proteins such as an appropriate sigma factor. CRP and HcpR are not able to form heterodimers. Heterodimerisation between HcpR and CRP would

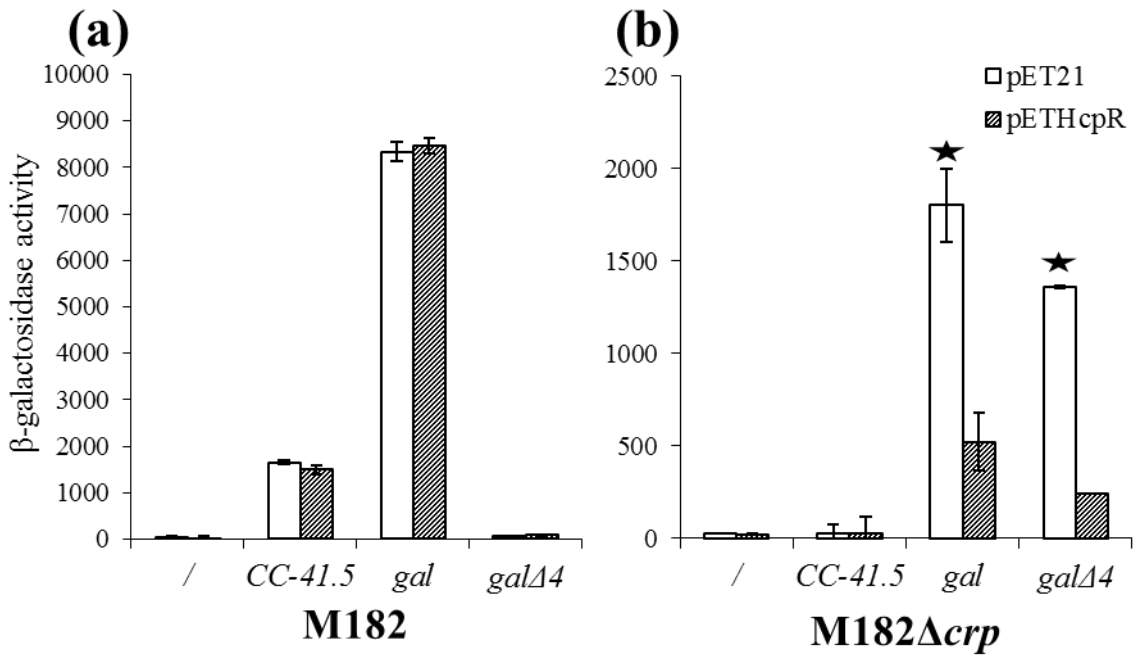


Figure 5.9: The effects of HcpR expression upon transcription from CRP regulated promoters in *E. coli* in the presence and absence of CRP. The activities of CRP influenced promoters in the presence of CRP and/or HcpR were assayed by by β-galactosidase assay. *E. coli* strains M182 (*crp+)* or M182*Δcrp* (*crp*-) were transformed with either empty pET21a(+) vector or pETHcpR. This resulted in four different strain/plasmid combinations: *crp+/hcpR-, crp+/hcpR-, crp-/hcpR+* and *crp-/hcpR-*. These were further transformed with pRW50 derived plasmids containing a promoter*::lacZ* fusion. The pRW50 derived plasmids used were pRW50 (empty vector), p*CC-41.5*, p*gal* and p*galΔ4*. The p*CC-41.5* and p*gal* plasmids both contain class II CRP activated promoters fused to *lacZ* whereas the p*galΔ4* plasmid contains a CRP repressed promoter fused to *lacZ.* Cultures were grown aerobically to an OD_{650} of ~0.3 and then assayed for β-galactosidase activity. (**a)** β-galactosidase activities of strain M182. (**b)** β-galactosidase activities of strain M182Δ*crp*. Activities that are significantly different between corresponding pET21a(+) or pETHcpR pairs are indicated by stars. Results were calculated from three biological replicates and error bars indicate the standard deviation. Results are representative of two independent experiments.

have resulted in a decrease in activity from CRP activated promoters in cells expressing both proteins. The affinity of HcpR for DNA is lower than that of CRP and when the two proteins are present CRP out-competes HcpR in terms of DNA binding. These statements are supported by the observation that CRP positive cells showed no reduction in β-galactosidase activity when HcpR was being expressed. This difference in the DNA binding affinities of these two proteins is in agreement with the EMSA results. Additionally, HcpR is active with respect to DNA binding in *E. coli* in the conditions tested. Since DNA binding by HcpR can be measured using the p*galP1* or p*galP1Δ4* promoters in a Δ*crp* background this system represents a potential screen for identifying conditions in which HcpR is inactive with respect to DNA binding.

Strain M182Δ*crp* carrying plasmids p*galΔ4*-pRW50 and either pET21a or pETHcpR was used to determine whether oxygen availability or nitrate reduction effects DNA binding by HcpR. Cultures were grown anaerobically with either nitrate, nitrite or DMSO as terminal electron acceptors and β-galactosidase activity was assayed (Figure 5.10). Despite slight differences in activity from the p*galΔ4* promoter in the different conditions tested, there was no significant alleviation of repression by HcpR. This suggests that the DNA binding affinity of HcpR is unaffected by DMSO, nitrate, nitrite or intermediates and end-products of the reduction of these terminal electron acceptors. The extent of HcpR repression from p*galΔ4*-pRW50 in anaerobic cultures was also comparable to those observed in the aerobic β-galactosidase assays suggesting that DNA binding by HcpR is unaffected by oxygen availability.

Since EMSAs indicated that HcpR is able to bind to the *nap*, *sat* and *hcpR* promoters, these promoter fragments were cloned into the plasmid pRW50 to provide *D. desulfuricans* derived promoter::*lacZ* fusions. These promoters were deemed likely

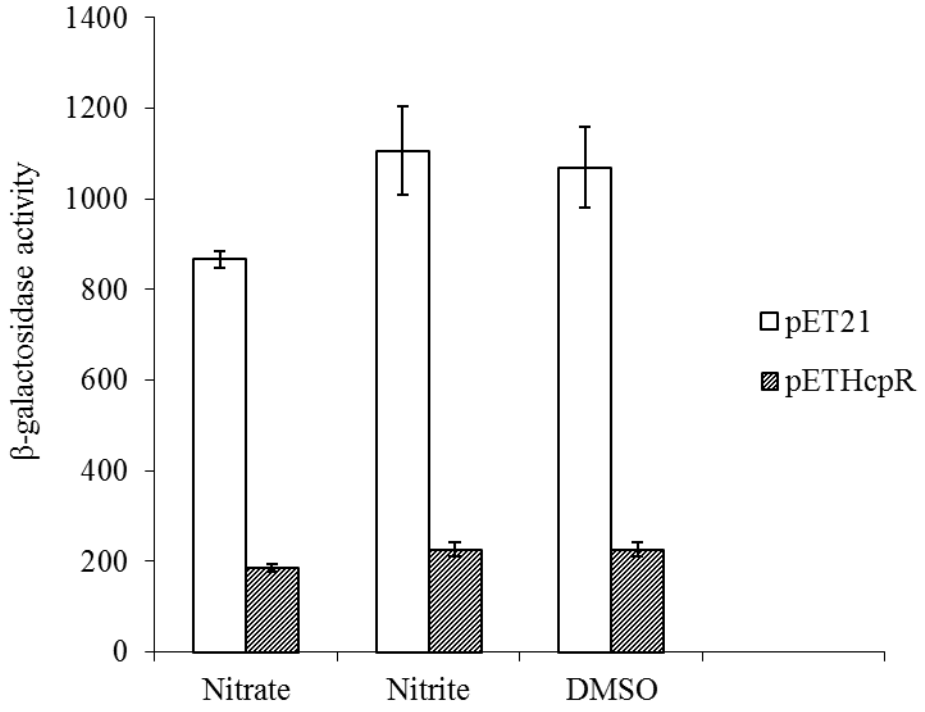


Figure 5.10: The effects of anaerobic growth upon HcpR-dependent repression of the p*galΔ4* promoter. *E. coli* strain M182Δ*crp* carrying plasmids pET21a(+) or pETHcpR were grown anaerobically in the presence of either nitrate (7.5 mM), nitrite (2 mM) or DMSO (7.5 mM) to an OD_{650} ~0.3 and then assayed for β-galactosidase activity. Activities were calculated from three biological replicates and error bars indicate the standard deviation. Results are representative of two independent experiments.

candidates for HcpR to modulate transcription and provide a measurable change in β-galactosidase activity in *E. coli.* Expression from each of these promoters was assayed by β-galactosidase activity in *E. coli* strains M182 and M182Δ*crp* carrying plasmids pET21a or pETHcpR (Figure 5.11). High levels of activity were measured from the *sat* promoter but this activity seemed to be unaffected by the presence or absence of HcpR (Figure 5.11a). The *nap* promoter gave negligible β-galactosidase activities, also irrespective of whether CRP or HcpR were present or absent (Figure 5.11b). Finally, moderate levels of expression were measured from the *hcpR* promoter (Figure 5.11c). Interestingly, expression was-CRP dependent with negligible β-galactosidase activity recorded in strain M182Δ*crp*. This expression was unaffected by HcpR. The fact that CRP can activate expression from the *hcpR* promoter suggests that the transcription start site for *hcpR* may be approximately -41.5 or -61.5 bp downstream from the centre of the HcpR/CRP binding site. Indeed, upon close examination of the *hcpR* promoter region putative -10 and -35 RNAP consensus binding sites were identified (Figure 5.11c). The positioning of these sites is such that the HcpR binding site is centred at -62.5 with respect to the transcription start site. Thus, CRP activation at the *hcpR* promoter is likely to be class I activation. Also, there is also a putative site for Ddes_1411/Ddes_2092 that overlaps the -35 element suggesting that one of these putative regulators might repress expression from this predicted promoter. HcpR did not have any significant effect upon transcription from the *D. desulfuricans* derived promoters assayed in *E. coli* and so the *in vivo* activity of HcpR at these promoters remains unknown.

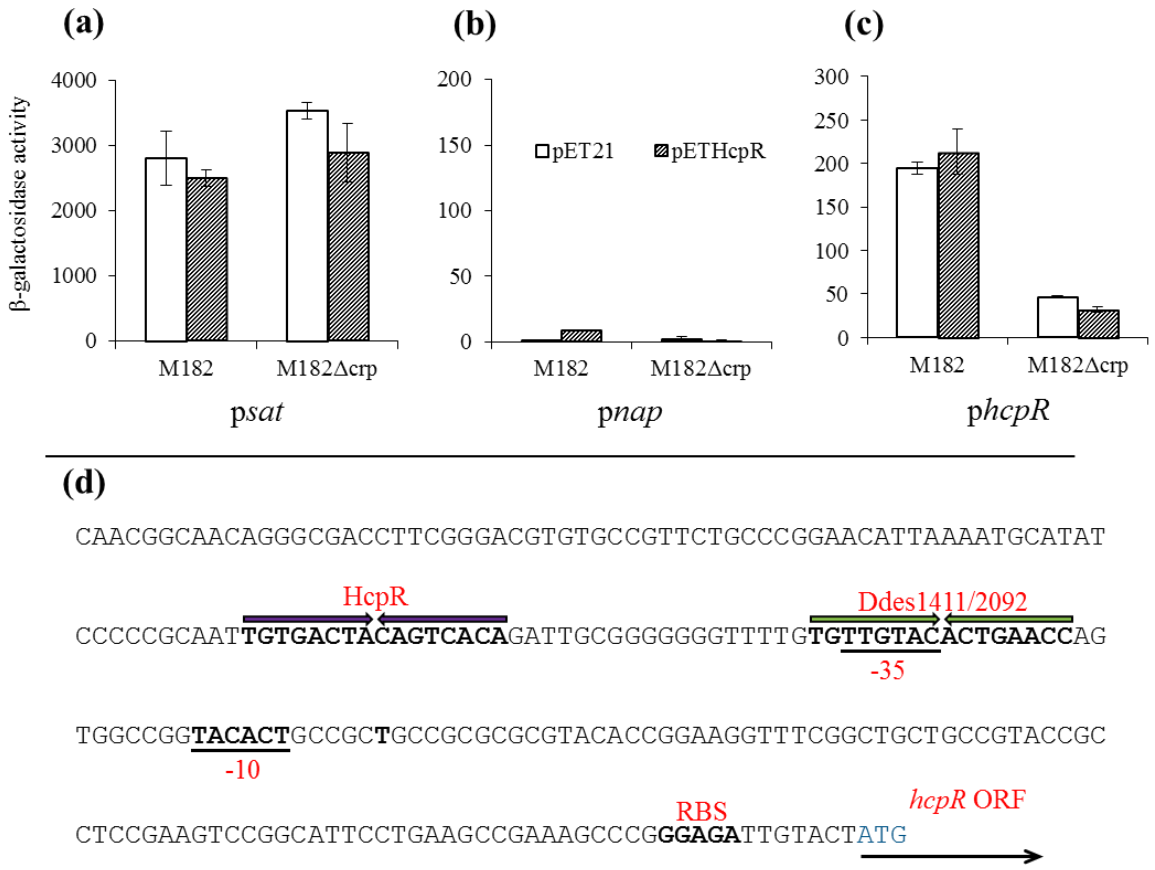


Figure 5.11: The effects of CRP and HcpR upon transcription from *D. desulfuricans* promoters. *E. coli* strains M182 and M182*Δcrp* were transformed with plasmids pET21a(+) or pETHcpR. The resulting strain-plasmid combinations were further transformed with pRW50 derived plasmids containing *D. desulfuricans* promoters fused to *lacZ*. Cells were grown aerobically and assayed for β-galactosidase activity from the p*sat* **(a),** p*nap* **(b)** and p*hcpR* **(c)** promoters. Sequences of p*nap* and p*sat* are given in Chapter 3. Promoter activities for each culture were determined from three biological replicates and error bars indicate the standard deviation. Results are representative of two independent experiments. **(d)** DNA sequence of the *hcpR* promoter proximal region. Putative protein binding sites are marked by arrows. The putative *hcpR* ORF, RBS and -10 and -35 promoter elements are labelled. The putative HcpR and Ddes1411/Ddes_2092 binding sites are marked with arrows and bold font. Coding regions shown in blue.

5.7 HcpR expression in response to terminal electron acceptors

Antibodies were raised in rabbits against recombinant HcpR protein by CovaLab UK. Serum was collected prior to immunisation, 39 days after immunisation and 56 days after immunisation. To test whether antibodies specific for HcpR were produced after immunisation the sera were used in western blots of SDS-PAGE gels of purified HcpR protein (Figure 5.12). HcpR protein was resolved by SDS-PAGE, transferred to a nitrocellulose membrane and then probed with the three different sera. Pre-immunisation serum did not detect HcpR. However, sera isolated 39- and 56- days after immunisation detected the purified protein indicating that an HcpR-specific immune response had been induced. A western blot using anti-HcpR antibodies was employed using total protein from *D. vulgaris* to assess the specificity of the anti-HcpR antibodies for *D. desulfuricans* HcpR. The antibodies did not bind to immobilised *D. vulgaris* proteins in the western blot. *D. vulgaris* has four CRP homologues with between 10 and 25% identity to *D. desulfuricans* HcpR. This range of identities is similar to those shared by the five *D. desulfuricans* CRP homologues. Thus, the observation that anti-HcpR antibodies failed to detect any *D. vulgaris* proteins in the western blot suggests that the anti-HcpR antibodies are specific for *D. desulfuricans* HcpR and not all CRP homologues. This procedure validated the anti-HcpR antibodies as a tool for qualitative and semi-quantitative detection of HcpR.

Anti-HcpR antibodies were used to monitor the levels of HcpR protein produced in response to growth in the presence of different terminal electron acceptors. Sulphate-adapted *D. desulfuricans* was grown in the presence 20 mM nitrate, sulphate, sulphite, thiosulphate, and combinations of these terminal electron acceptors to determine whether these compounds effect HcpR. Cell samples were taken at 20 and 156 hours

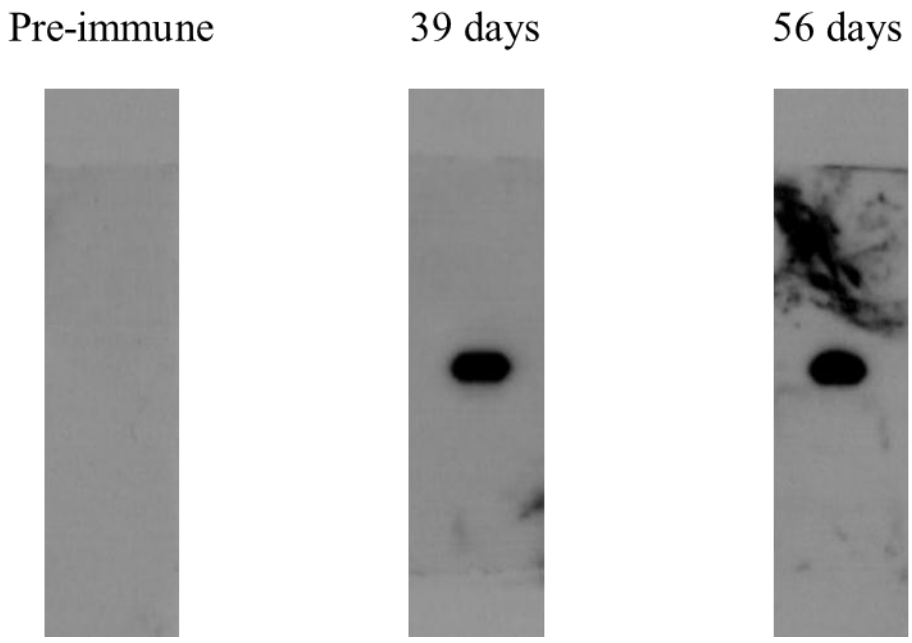


Figure 5.12: Detection of HcpR by western blot using anti-HcpR antibodies. Purified recombinant HcpR was used as the antigen in an immunisation protocol with a rabbit. Serum was sampled prior to immunisation (pre-immune), at 39 days and at 56 days post-immunisation. Standardised quantities of HcpR protein were resolved by SDS-PAGE, transferred to a nitrocellulose membrane and then probed by western blot using anti-HcpR antibodies. The presence of HcpR is shown as a black band on the blot.

corresponding to exponential growth and 75 hours into stationary phase. Total proteins were separated by SDS-PAGE and used for western blotting with anti-HcpR antibodies (Figure 5.13). A prominent band of HcpR was detected in cultures supplemented with nitrate alone and this high level of protein persisted into stationary phase. In the presence of sulphate, sulphite or thiosulphate the levels of HcpR were so low that they were barely perceptible by western blot analysis. Similarly, expression was negligible during exponential phase in cultures supplemented with nitrate and sulphate, sulphite or thiosulphate. An increase in HcpR levels was observed in these cultures in stationary phase. These expression profiles suggest that HcpR expression is induced in the presence of nitrate but repressed by sulphur-based terminal electron acceptors. Furthermore, if nitrate is also present in the growth medium then HcpR is up-regulated once growth has ceased. It seemed likely that sulphide, a common end product of the sulphate-sulphite-thiosulphate reduction pathways, is responsible for repressing HcpR synthesis whilst nitrate stimulates expression of HcpR.

Since nitrate is required for HcpR expression it was necessary to determine whether nitrite also induced expression. Sulphate-grown cells were used to inoculate medium supplemented with 7.5 mM of nitrate, sulphate, sulphite, 2.5 mM nitrite, or combinations of these terminal electron acceptors (Figure 5.14a). Cells were harvested for western blot analysis at two different time points corresponding to the exponential and stationary growth phases. The presence of nitrite in the growth medium induced expression of HcpR. Indeed, significant levels of HcpR were detected in the presence of nitrite and sulphate or sulphite for the duration of the growth experiment. Thus, nitrite can induce expression of HcpR similarly to nitrate but unlike nitrate this induction occurs irrespective of the presence of sulphate or sulphite. Since nitrite is reduced

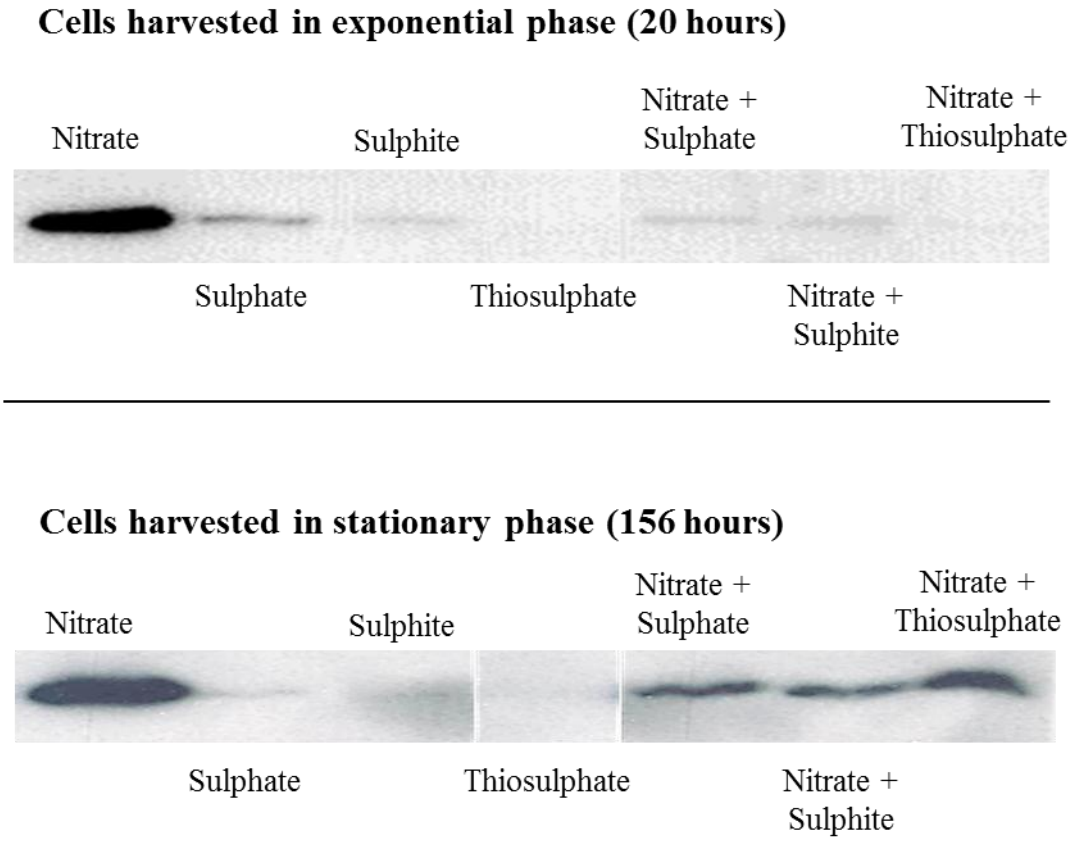


Figure 5.13: HcpR expression in the presence of nitrate, sulphate, sulphite and thiosulphate. Sulphate adapted cells were used as the inoculum for cultures supplemented with different terminal electron acceptors. Nitrate, sulphate, sulphite and thiosulphate were added to give a total concentration of 40 mM in each culture. Cells were harvested during exponential growth (20 hours) and in stationary phase (156 hours). Total protein samples were prepared from cells, standardised quantities of these proteins were then resolved by SDS-PAGE and subjected to western blot using anti-HcpR antibodies.

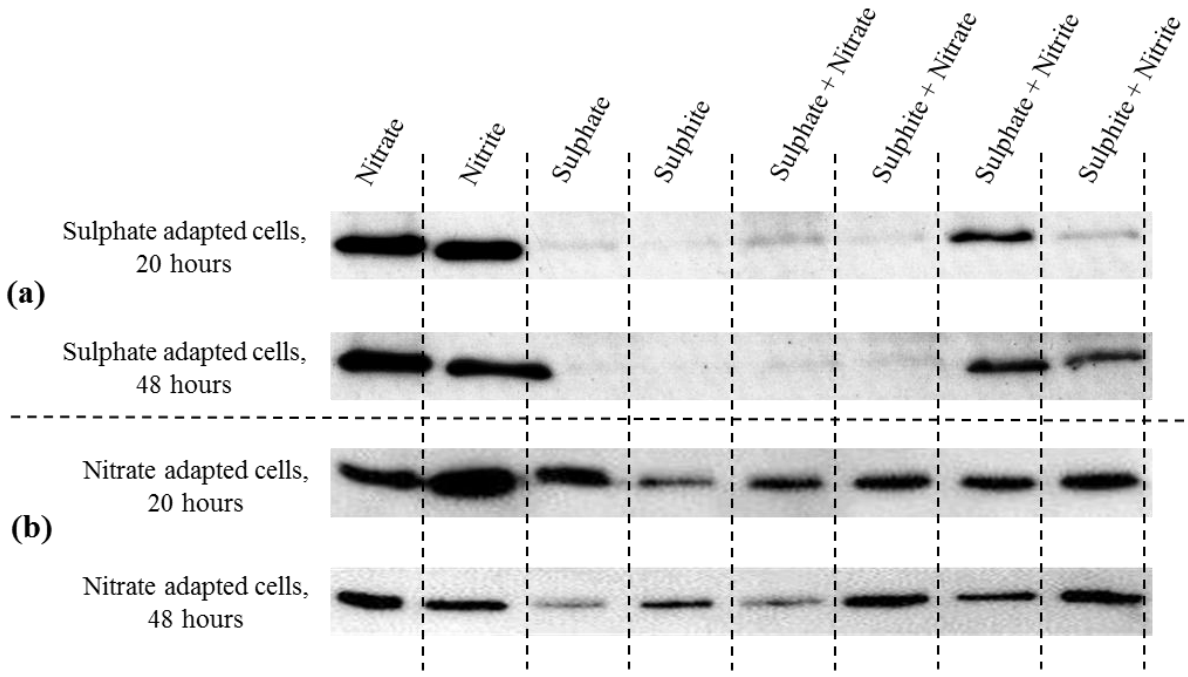


Figure 5.14: The effects of nitrite and HcpR pre-induction on HcpR synthesis. (a) Sulphate grown *D. desulfuricans* was used as the inoculum for cultures supplemented with 7.5 mM nitrate, sulphate, sulphite, 2.5 mM nitrite or combinations of these terminal electron acceptors. Cells were harvested during exponential (20 hours) and stationary (48 hours) growth phases. Standardised protein samples were prepared from cells, resolved by SDS-PAGE and used for Western blot analysis using anti-HcpR antibodies. **(b)** The experiment was repeated with nitrate grown *D. desulfuricans* as the inoculum.

simultaneously with sulphate or sulphite it seems that HcpR expression, rather than being repressed by sulphate or sulphite reduction, is induced by the presence of nitrite. Nitrate was unable to induce HcpR expression when sulphate or sulphite were present, presumably due to efficient repression of *nap* expression in these conditions.

As already demonstrated, culture pre-treatment can affect the ability of *D. desulfuricans* to utilise nitrite and tolerate nitrosative stress (Chapter 4). Thus, the growth and western blot analysis was repeated using nitrate-adapted cells as the inoculum and the results compared with those gained from sulphate-adapted cells (Figure 5.14b). Cultures prepared with nitrate-adapted inoculum had higher levels of HcpR protein compared with cultures seeded with sulphate-adapted inoculum. Indeed, appreciable levels of HcpR were present detected in all growth conditions, including cultures supplemented with sulphate or sulphite alone, when nitrate-adapted cells were the inoculum. This is consistent with the previous observations that HcpR persists long into stationary phase (Figure 5.13). However, the cells used in this western blot would have undergone multiple divisions in an absence of the putative effector, nitrite, and therefore the levels of HcpR detected in cultures supplemented with sulphate or sulphite seemed surprisingly high. A dilution effect would be expected unless HcpR was being actively synthesised in the sulphate and sulphite cultures. Expression of HcpR can evidently be pre-induced and cells have a long 'memory' of HcpR expression. Perhaps HcpR perpetuates its own production by auto-induction.

5.8 The effect of exogenous nitric oxide upon HcpR expression

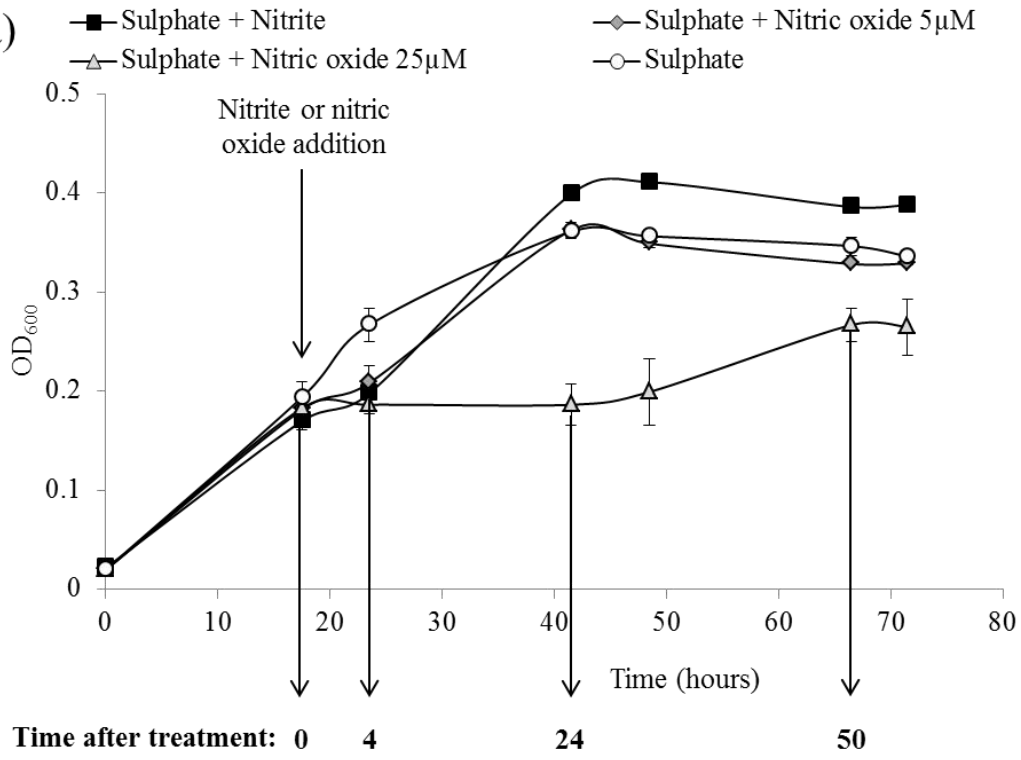
Expression of HcpR seems to be reliant upon the presence of nitrite. However, the presence of nitrite also results in the production of nitric oxide. Nitric oxide is recognised as an effector molecule for a number of transcription factors including NsrR,

FNR, OxyR, SoxR and NorR. Thus, to test the effects of nitric oxide upon *D. desulfuricans* and HcpR expression levels, cultures were treated with nitric oxide.

Sulphate-adapted cells were grown in the presence of sulphate to provide a background of no HcpR expression. Once these cultures had reached an optical density of ~0.2 they were then treated with different concentrations of nitric oxide. Some cultures were untreated to function as negative controls and some were treated with 1.5 mM nitrite to function as positive controls. Optical densities were measured and cells were harvested for SDS-PAGE and western blotting with anti-HcpR antibodies at various time points (Figure 5.15). Untreated cultures grew unchecked throughout the experiment whereas the addition of nitrite caused a slight interruption to growth (Figure 5.15a). A low dose of nitric oxide resulted in a similar pause but without the increase in final growth yield provided by nitrite. The high dose of nitric oxide totally inhibited growth for in excess of 24 hours. The cultures eventually recovered but the final yield was compromised by the treatment, giving a final optical density ~20 % lower than that achieved by cultures grown without treatment. Clearly, *D. desulfuricans* is sensitive to exogenous sources of nitric oxide and this stress compromises growth.

The western blots taken throughout this experiment support the earlier observation of HcpR being absent in the presence of sulphate alone but expressed in the presence of nitrite (Figure 5.15b). HcpR expression was induced within 4 hours of the addition of nitrite and continued for the duration of the experiment. A similar induction of HcpR was obtained with the low dose of nitric oxide. The high dose of nitric oxide also resulted in HcpR expression but HcpR was not detected in these cultures until 24 hours after treatment. This longer time required for HcpR induction could be explained by the high dose of nitric oxide being so detrimental that protein synthesis in these cultures

(a)


Sulphate + Nitrite
Sulphate + Nitric oxide 25µM
Sulphate + Nitric oxide 5µM
Sulphate
Nitrite or nitric oxide addition
OD600
0.5
0.4
0.3
0.2
0.1
0
0
10
20
30
40
50
60
70
80
Time (hours)
Time after treatment: 0 4 24 50

(b)

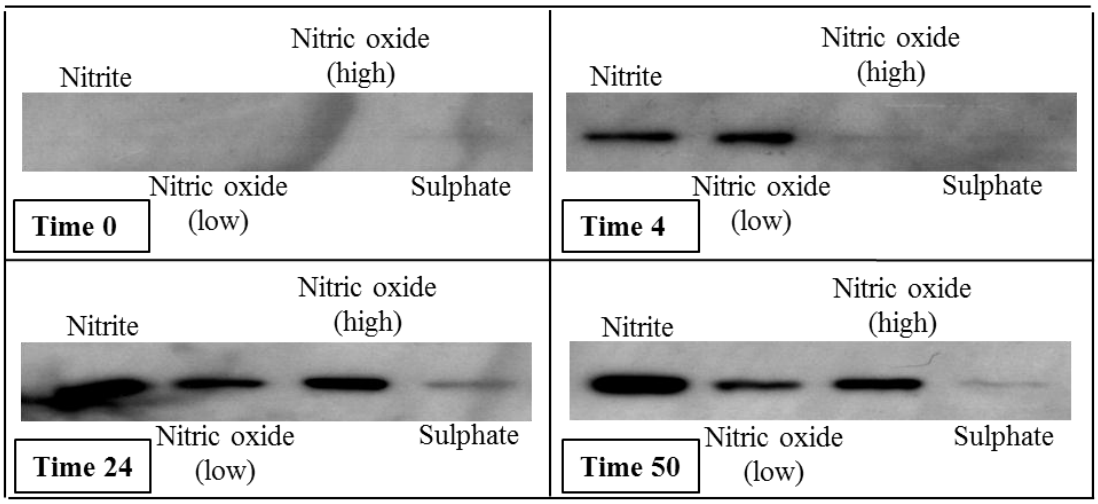

Nitrite
Nitric oxide (high)
Nitric oxide (low)
Sulphate
Time 0
Time 4
Time 24
Time 50

Figure 5.15: Growth of *D. desulfuricans* and HcpR synthesis in the presence of exogenous nitric oxide. (a) Sulphate grown cells were used to inoculate cultures supplemented with 7.5 mM sulphate. After 18 hours the cultures were treated with 2.5 mM nitrite, a low 5 μM dose of nitric oxide, a high 25 μM dose of nitric oxide or no treatment. Cell densities were measured over time. Results are the average of three separate biological replicates and error bars indicate standard deviations. **(b)** Cells were harvested at 0, 4, 24 or 50 hours post treatment and then used for SDS-PAGE of total proteins and western blot analysis using anti-HcpR antibodies

ceased temporarily. This suggestion is supported by the plateau in growth. Once the cultures had recovered from the initial shock from the high nitric oxide dose then protein synthesis could resume and hence HcpR was detected at the later time points. Potentially, recovery from nitric oxide stress requires HcpR expression. These observations indicate that nitric oxide stimulated a cascade of HcpR expression and was likely to be the trigger of HcpR expression in the other culture conditions tested.

To confirm these results, the levels of the *hcpR* transcript induced in response to nitric oxide treatment were measured by qRT-PCR (Figure 5.16). Expression of *hcpR* was elevated in the nitric oxide treated culture. Expression of *napC*, *nrfA* and *ssc* were also measured. In previous experiments the levels of these transcripts increased when levels of *hcpR* were elevated. However, expression of these genes was not induced by nitric oxide. This supports the earlier suggestion that *nap* requires an additional regulatory factor for maximal expression and that *nrf* is regulated independently of HcpR. It also seems that *nrf* is regulated independently of nitric oxide. Lack of induction of *ssc* in the presence of nitric oxide suggests that this cytochrome is implicated in nitrate and nitrite reduction, as stated in Chapter 4, but not nitrosative stress. The qRT-PCR analysis supports the western blot results and proves that HcpR is up-regulated in response to nitric oxide stress.

5.9 The cysteines of HcpR: potential nitric oxide sensors

The HcpR protein purified from *E. coli* for these analyses seems to be unresponsive to cAMP, cGMP and a cocktail of small molecules prepared from *D. desulfuricans* cultures grown in different conditions. Perhaps, rather than direct binding of an allosteric effector molecule, HcpR senses nitric oxide or redox state via a co-factor

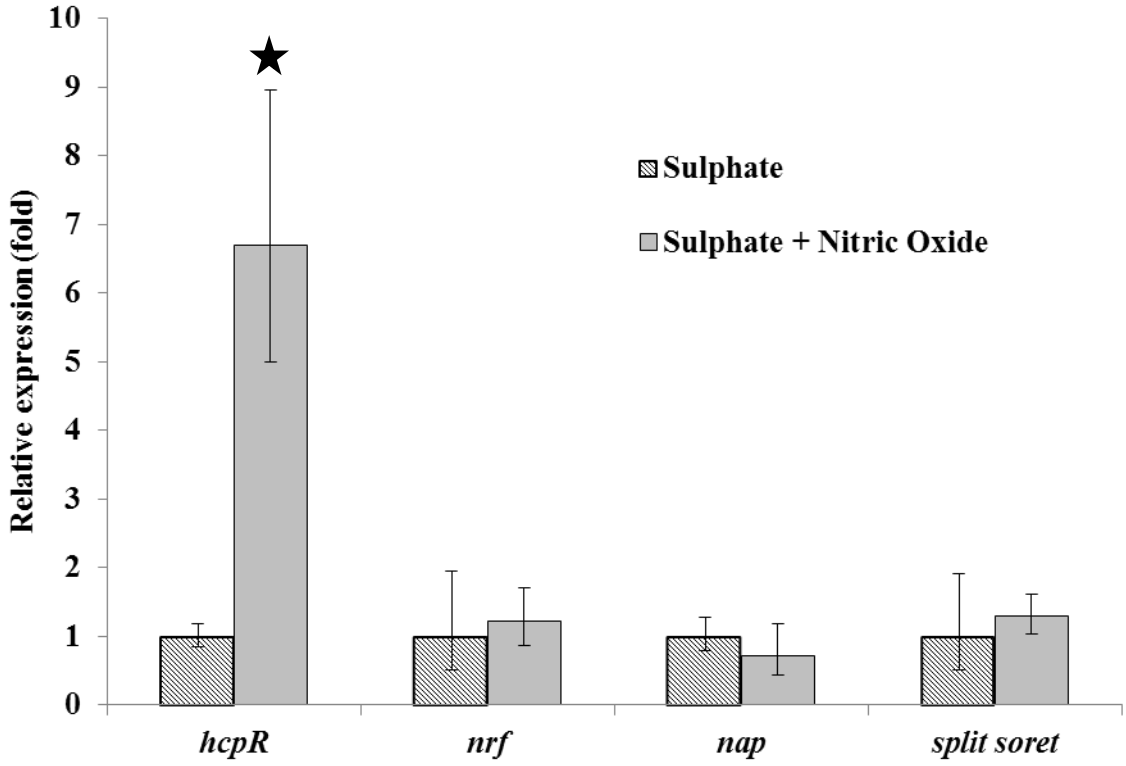


Figure 5.16: qRT-PCR analysis of *hcpR*, *nrf*, *nap* and *split soret* expression in response to nitric oxide treatment. Sulphate grown *D. desulfuricans* was used to inoculate cultures supplemented with 15 mM sulphate. Once cultures had reached an OD_{600} ~0.3 they were treated with 7.5 µM nitric oxide or no treatment. Cells were harvested after 20 hours and then used for RNA purification, RT with random hexamers and then qPCR. Expression levels are normalised to *polA* and then to the sulphate only values for individual genes. Error bars indicate standard deviation of the relative expression values. Stars represent nitric oxide treated ΔCt values that are significantly different from the corresponding no treatment ΔCt values ($P<0.05$).

bound to the protein. This proposal seems unlikely since common co-factors such as flavin and haem groups impart noticeable colour to proteins containing these co-factors and all preparations of HcpR were colourless. To explore this further, oxidised and reduced spectra for HcpR were measured. No significant peaks were observed in the difference spectra suggesting that the protein lacks an iron-based cofactor, a common feature of nitric oxide sensing transcription regulators. Furthermore, HcpR fractions were tested for the presence of iron using the TPTZ assay and this confirmed that this protein lacks an iron cofactor. Attempts to reconstitute HcpR with hemin failed.

As suggested in Chapter 3, HcpR from *D. desulfuricans* contains cysteine residues that could potentially sense nitric oxide or redox state. To explore this, purified HcpR was treated with a reducing agent, DTT, or oxidising agents, H_2O_2 or NO, overnight at 4 ºC. A sample of the treated protein was then used in an EMSA with the p*hcpR* fragment whilst the remainder was treated with the thiol-modifying agent mPEG-mal and then separated by non-reducing SDS-PAGE (Figure 5.17). mPEG-mal reacts with free thiols resulting in PEGylation of the protein. Each free thiol that mPEG-mal reacts with causes an increase of 5 kDa in the protein weight and gives a corresponding change in the position that the protein migrates to on an SDS-PAGE gel. Thus, if a protein contains cysteines that are involved in disulphide bonds then they will not be bound by mPEG-mal and the protein will migrate on a gel similarly to untreated protein. However, if the disulphide bonds in that same protein are reduced prior to treatment with mPEG-mal then the free thiols will become PEGylated and the protein will migrate as a larger protein on the gel. mPEG-mal reacts with SDS effecting the migration of PEGylated proteins on SDS-PAGE gels and so the increase in apparent MW of the PEGylated

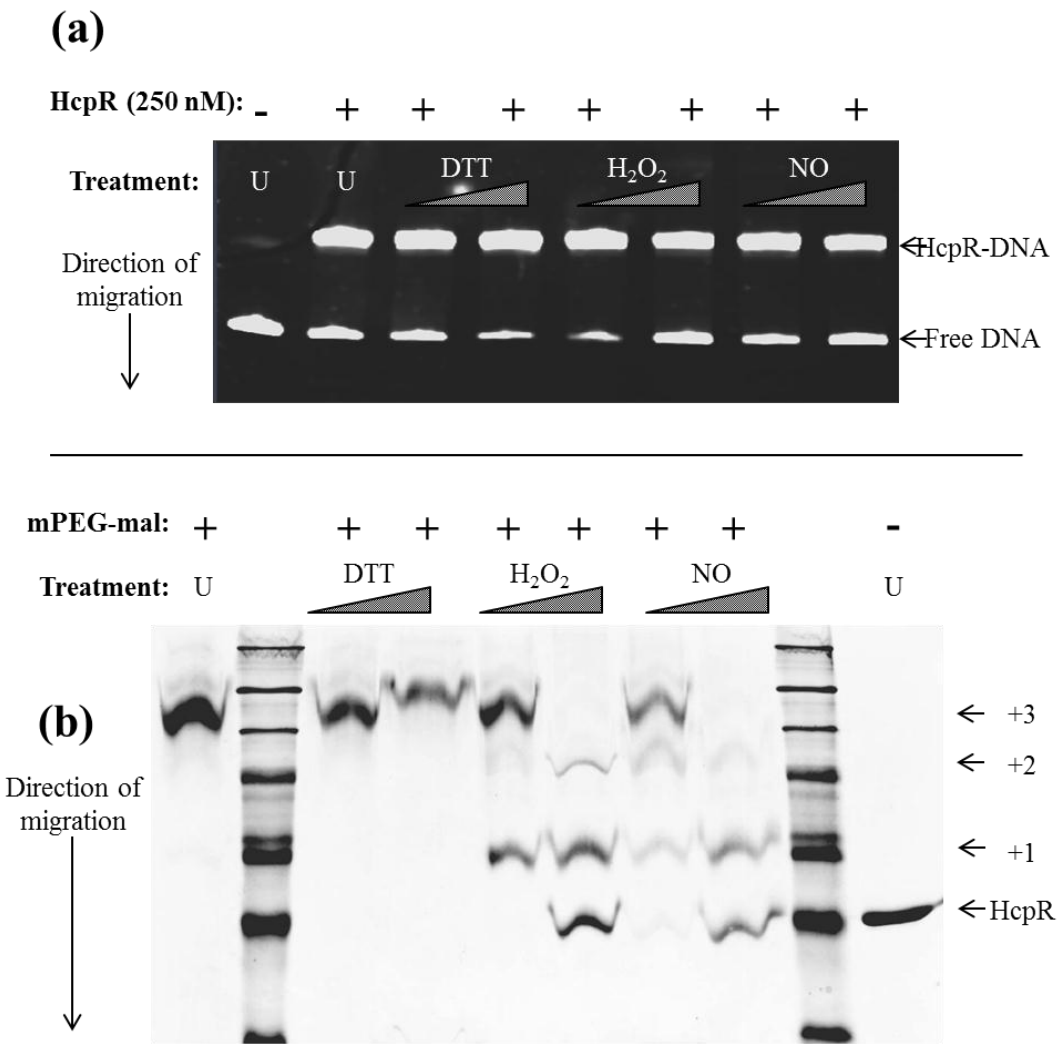


Figure 5.17: The effects of reducing or oxidising agents upon HcpR conformation and DNA binding activity. (a) Purified recombinant HcpR protein was treated with DTT, H_2O_2 or nitric oxide at 4 ºC overnight. Treated and untreated (U) protein was then used in an EMSA assay with the p*hcpR* promoter fragment. Free DNA fragment and DNA-HcpR complexes are indicated by arrows. **(b)** Treated and untreated HcpR was treated with mPEG-mal and then resolved by SDS-PAGE. mPEG-mal binds to free and accessible thiol groups resulting in a change in the apparent MW of a protein. +1, +2 and +3 indicate the number of mPEG-mal groups bound to HcpR thiols.

protein on the gel does not necessarily match the expected increments of 5 kDa (Zheng *et al.*, 2007).

Treatment of HcpR with the different redox agents did not affect its DNA binding affinity for the p*hcpR* fragment (Figure 5.17a). However, after treatment with mPEG-mal it was apparent that the purified HcpR seems to exist in the reduced form in solution (Figure 5.17b). This was indicated by the observation that DTT treated and non-treated PEGylated proteins migrated to the same position on the gel. As HcpR from *D. desulfuricans* has three cysteines this position represents the binding of three PEG molecules to each molecule of HcpR. Treatment of HcpR with nitric oxide caused the majority of HcpR to migrate to the same position as untreated protein. This would suggest that the presence of nitric oxide caused either disulphide bond formation or sequestration of thiol groups by S-nitrosylation. Potentially this modification of HcpR cysteines could function as a redox sensing mechanism for HcpR. Unfortunately attempts to test the thiol co-ordination of HcpR *in vivo* were unsuccessful so whether these *in vitro* observations translate to *in vivo* protein function remains unknown. Treatment of HcpR with DTT, H_2O_2 or NO had no effect upon its DNA binding affinities. Perhaps the activities of HcpR are not modulated by a change in its DNA binding affinities but by a switch in its activities whilst bound to targets.

5.10 The transcriptional partners of *hcpR*

The up-regulation of *hcpR* in response to nitric oxide suggests a role in coping with nitrosative stress. However, the various putative HcpR targets that were analysed by qRT-PCR suggest that most of these targets do not vary greatly in terms of transcript abundance. Those that did change significantly were *ssc*, which does not seem to have

an obvious role in dealing with nitric oxide, and *nap*. Furthermore, regulation of these two targets seems to require an additional factor and their expression does not always correlate with *hcpR* expression. The biggest change in expression levels for any HcpR regulon member happened to be *hcpR* itself. Why is a transcription regulator produced in what seem to be unnecessarily high levels? The HcpR response to nitric oxide does not make sense from an economical point of view. To determine why *hcpR* is produced at such levels the *hcpR* operon was re-considered.

The *D. desulfuricans hcpR* gene is immediately upstream of two genes that are similar to *wrbA* and *nimA*. WrbA, also known as the tryptophan repressor associated protein, is a flavin-binding protein that was thought to modulate the activity of the tryptophan repressor, TrpR, due to the observation that these two proteins co-purify together but is now thought to be involved in redox processes (Yang *et al.*, 1993; Patridge & Ferry, 2006). NimA proteins are involved in resistance to the antimicrobial prodrugs nitroimidazoles. The *wrbA* and *nimA*-like genes of *D. desulfuricans* will be discussed in detail in Chapter 6.

To investigate whether *hcpR*, *wrbA* and *nimA* form a single transcription unit, RNA was prepared from nitrate grown *D. desulfuricans*. The RNA purification included an optional DNase digest step to ensure removal of contaminating DNA. cDNA was generated with random hexamers and used in a series of PCRs using overlapping primers designed to map the *hcpR* transcript and ascertain whether *wrbA* and *nimA* are co-transcribed with *hcpR* (Figure 5.18). A schematic detailing the target PCR products used in the scheme are detailed in Figure 5.18a. A primer that anneals upstream of the putative *hcpR* promoter was included as a negative control for the cDNA samples.

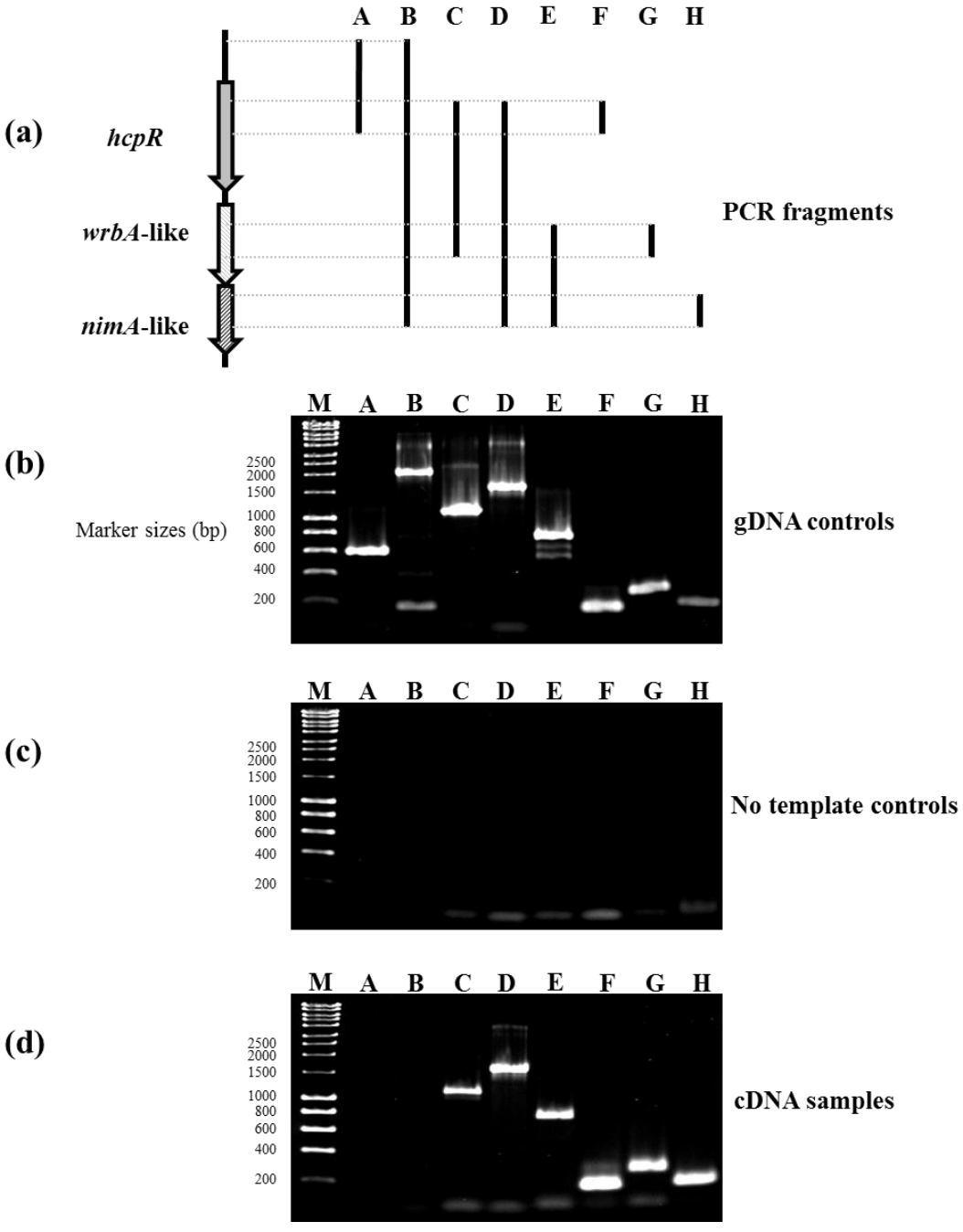

(a)
A B C D E F G H
hcpR
wrbA-like
nimA-like
PCR fragments
(b)
M A B C D E F G H
Marker sizes (bp)
2500
2000
1500
1000
800
600
400
200
gDNA controls
(c)
M A B C D E F G H
2500
2000
1500
1000
800
600
400
200
No template controls
(d)
M A B C D E F G H
2500
2000
1500
1000
800
600
400
200
cDNA samples

Figure 5.18 : Transcript mapping of the *hcpR* locus. (a) Primers were designed to amplify DNA fragments spanning the coding regions of *hcpR, wrbA* and *nimA*. An additional primer specific to DNA sequences upstream of the putative *hcpR* promoter was included. Combinations of these primers were expected to generate PCR fragments of different sizes and were allocated a letter A-H. These are represented by the cartoon. Primer combinations were used for a series of PCRs using either gDNA **(b)**, no template **(c)** or cDNA **(d)**. PCRs were resolved by agarose gel electrophoresis. Bioline Hyperladder II was used as a standard on the gel to assess PCR fragment size (M). Fragments of corresponding sizes were generated for all primer combinations when gDNA was used as the PCR template. No fragments were generated when no template was used. Fragments were generated for all primer combinations except those utilising the primer located upstream of the *hcpR* promoter **w**hen cDNA from *D. desulfuricans* was used as the template. **(M:** Bioline Hyperladder I DNA marker set).

gDNA was used in PCRs as positive controls for each primer pair. PCRs were also conducted with no template as negative controls. This strategy would indicate whether *hcpR* was co-transcribed with other genes, if the cDNA preparation and primers were indeed free from contaminating gDNA, and also whether the primers used will amplify the desired DNA fragments.

All primer combinations, including those utilising the upstream primer, provided the corresponding predicted products when gDNA was used as the PCR template (Figure 5.18b). No products were obtained when template was omitted from the PCR reaction (Figure 5.18c). No products were obtained with the upstream distal primer when cDNA was used as template (Figure 5.18d). This indicates that the cDNA preparation was free from contaminating gDNA and also that this position falls outside the *hcpR* transcript. Products were obtained with the other primer combinations. Short PCR products falling within *hpcR*, *nimA* and *wrbA* coding regions indicated that these putative genes are transcribed. PCR products overlapping these three coding regions were also obtained indicating that *hcpR* can be co-transcribed with these other genes and that they form a single transcriptional unit.

The results explain why *hcpR* is induced so profoundly, these other genes must encode proteins critical for dealing with nitric oxide. These co-localised genes are conserved in some other bacteria such as *D. desulfuricans* sp. 3_1_syn3 and *D. desulfuricans* sp 6_1_46AFAA. Indeed, it is possible that the *hcpR* transcript also includes additional downstream genes. However, in these other bacteria *hcp* is adjacent to *hcpR* whereas in *D. desulfuricans hcp* is at another locus. Presumably this is also part of the *hcpR* operon

in these species. However, *hcp* expression is not believed to be linked to the activities of HcpR in *D. desulfuricans* but instead requires HcpR2.

5.11 Differential expression at the *hcp* locus

The gene encoding Hcp is not co-localised with *hcpR* in *D. desulfuricans*. Instead it shares its locus with a *ylbA*-like gene and also the putative regulator *hcpR2*. In *E. coli* YlbA is involved in purine metabolism. The *ylbA*-like gene of *D. desulfuricans* will be discussed further in Chapter 6.

In Chapter 4, a contrasting pattern of expression was noted for *hcp* and *hcpR*. In *E. coli*, *hcp* is up-regulated in response to nitric oxide (Pullan *et al.*, 2007). To test whether this is also true for *D. desulfuricans*, RNA was prepared from sulphate-grown and nitric oxide treated *D. desulfuricans* and then used in qRT-PCR analysis to measure expression of *hcpR2*, *hcp* and the putative HcpR2 regulon member *dfx* (Figure 5.19). Expression of *hcp* and *dfx* was induced in the presence of nitric oxide (Figure 5.19b). However, expression of *hcpR2* did not change in response to nitric oxide. This suggests that both *hcp* and *dfx* are responsive to nitric oxide and are likely to be involved in dealing with its detoxification. Since both these genes are members of the HcpR2 regulon predicted in Chapter 3 this result supports the proposal that HcpR2 is concerned with regulating nitrosative stress response.

The observation that *hcp* and *hcpR2* are expressed differentially suggests that they are not part of the same operon and there must be a promoter between these two genes. The strategy of transcript mapping, as described earlier, was employed using primers spanning the neighbouring genes of *hcp* to test this hypothesis (Figure 5.20). When

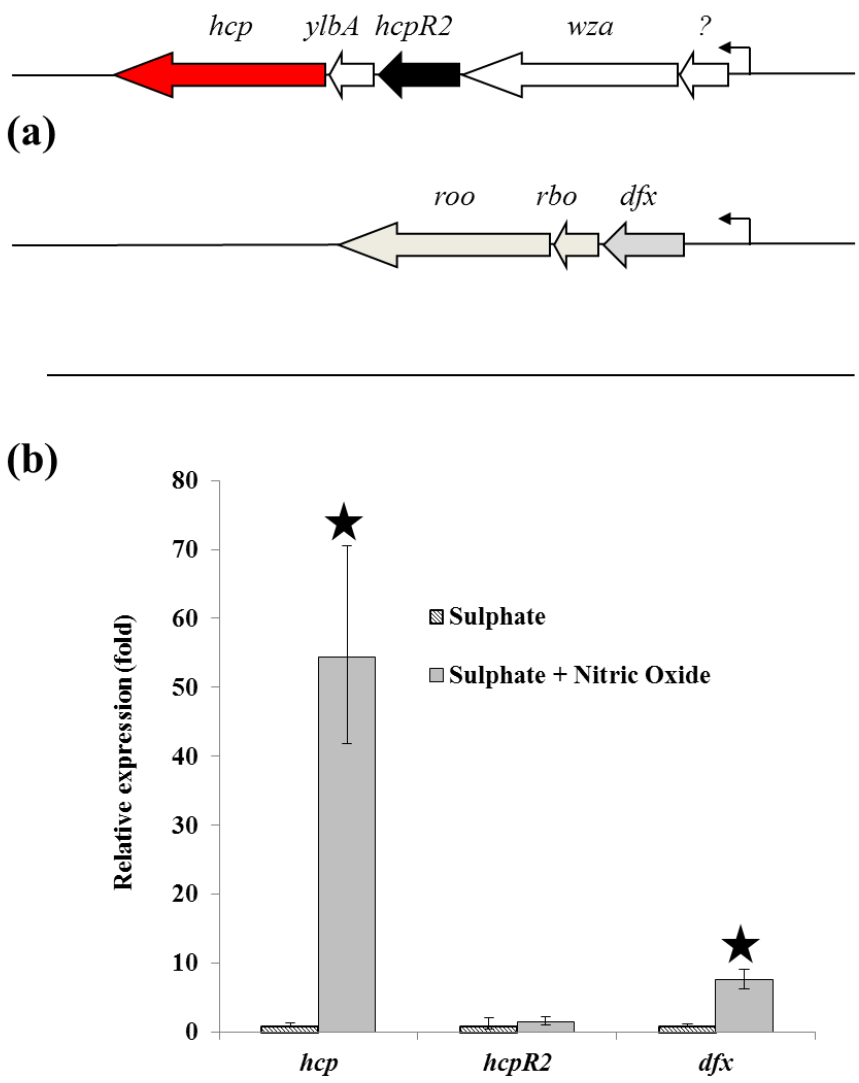


Figure 5.19: qRT-PCR analysis of *hcpr2, hcp* and *dfx* expression in response to nitric oxide. (a) Cartoon the *hcpR2-hcp* and *dfx* loci. **(b)** qRT-PCR analysis of *hcpR2, hcp* and *dfx*. Sulphate grown cells were used to inoculate medium supplemented with 10 mM sulphate. Cultures were treated with 10 µM nitric oxide or no treatment and grown for an additional 20 hours. Cells were harvested and used for RNA purification. RNA was reverse transcribed with random hexamer primers and then used for qRT-PCR with gene specific primers. Expression values were normalised to levels of the *polA* transcript. Error bars indicate the standard error of the relative expression levels. Stars indicate nitric oxide treated expression levels derived from ΔCt values that are significantly different from the corresponding untreated ΔCt values (P>0.05).

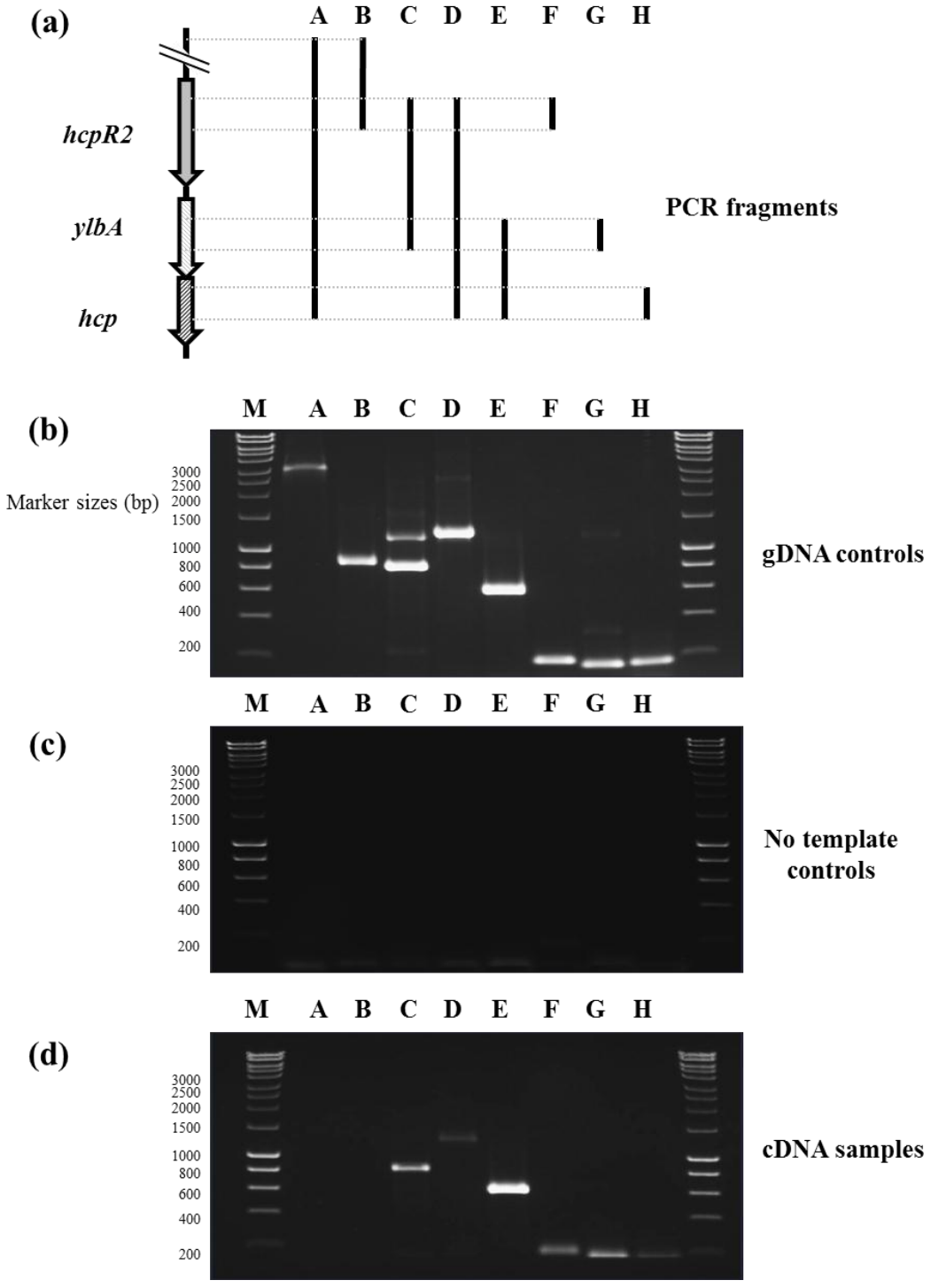

(a)
A B C D E F G H
hcpR2
ylbA
hcp
PCR fragments
(b)
M A B C D E F G H
Marker sizes (bp)
3000
2500
2000
1500
1000
800
600
400
200
gDNA controls
(c)
M A B C D E F G H
3000
2500
2000
1500
1000
800
600
400
200
No template controls
(d)
M A B C D E F G H
3000
2500
2000
1500
1000
800
600
400
200
cDNA samples

Figure 5.20: Transcript mapping of the *hcpR2* locus. (a) Primers were designed to amplify DNA fragments spanning the ORFs of *hcpR2, ylbA* and *hcp*. An additional primer specific to DNA sequences upstream of the putative *hcpR2* operon promoter was included. Combinations of these primers were expected to generate PCR fragments of different sizes and were allocated a letter A-H. These are represented by the cartoon. Primer combinations were used for a series of PCRs using either gDNA **(a)**, no template **(b)** or cDNA **(c)**. PCRs were resolved by agarose gel electrophoresis. Bioline Hyperladder I was used as a standard on the gel to assess PCR fragment size (M).

cDNA was used as the template, small products were obtained for primers internal to the *hcpR2*, *hcp* and *ylbA*-like coding regions indicating that all three of these genes are indeed transcribed. Products were also generated with the primer combinations overlapping the genes suggesting that these three genes may be co-transcribed as a single unit. The primer pair overlapping the *ylbA*-like and *hcp* coding regions produced a more intense PCR product than the other overlapping primer pairs when cDNA was the template. When gDNA was the template all three primer combinations giving overlapping products gave bands of similar intensities. The differences in band intensities could indicate that the *ylbA-hcp* transcript is expressed at higher levels than the *hcpR2-ylbA* or *hcpR-ylbA-hcp* transcripts.

These findings indicate that *hcpR2*, *ylbA* and *hcp* can be transcribed as a single operon. However, there must be an additional promoter between *hcpR2* and *hcp* to explain the differential expression witnessed in Figure 5.19. The intensities of the transcript mapping fragments provide some additional clues as to the whereabouts of this promoter. A promoter might be located between *hcpR2* and *ylbA* as predicted in Chapter 3. A putative HcpR2 binding site is situated at this location.

5.12 Overexpression and purification of HcpR2

To determine whether HcpR2 can bind to DNA, the HcpR2 coding region was cloned into the overexpression vector pET21a (Novagen) as described previously. *E. coli* strain BL21* was used to over-express the recombinant HcpR2 protein, which includes a His_6-tag, from the resulting plasmid, pETHcpR2. Small scale over-expressions were made in shake flasks to identify the optimal conditions for HcpR2 production (Figure 5.21). Optimal conditions were deemed as being with 500 µM IPTG and harvested at 24

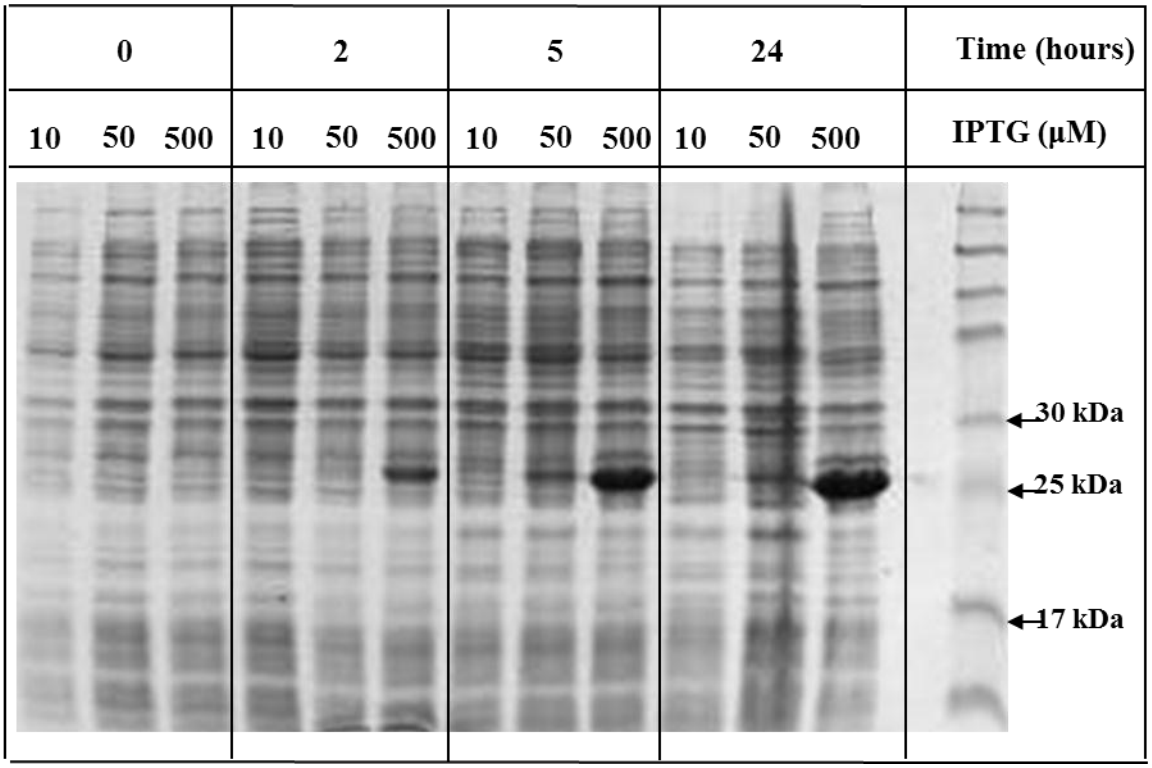


Figure 5.21: Overexpression of recombinant HcpR2 in *E. coli* strain BL21*. Over-expression of recombinant HcpR2 was achieved by treating cells harbouring plasmid pETHcpR2 with 10, 50 or 500 µM IPTG. Cells were harvested at 0, 2 , 5 and 24 post-induction and total cell proteins were separated by SDS-PAGE. The theoretical MW of His-tagged recombinant HcpR2 protein is 26 kDa. This position on the gel is marked with a black star.

hours. These growth conditions were used for producing large scale cultures for the purification process.

Recombinant HcpR2 was purified by nickel agarose affinity chromatography as described for HcpR. Protein containing fractions eluted from the nickel agarose column were analysed by SDS-PAGE (Figure 5.22a). Unlike HcpR, HcpR2 eluted from the column over a narrow range of imidazole concentrations in a comparatively small volume and at a high protein concentration. Fractions containing HcpR2 protein were supplemented with 2 mM EDTA as during trial purifications this additive was identified as useful for maintaining HcpR2 solubility and prevent precipitation. Fractions containing HcpR2 were pooled, dialysed, and subject to a cation-exchange purification step using an SP-FF column as described in Chapter 2. Proteins were eluted in a linear gradient of KCl. Fractions were collected and their protein content assessed by SDS-PAGE (Figure 5.22b). HcpR2 eluted as a single peak and was deemed to be pure. These peak fractions were pooled, transferred into Buffer C by buffer exchange and concentrated using a Vivaspin 10 kDa molecular cut off column. The concentrated HcpR2 protein was again assessed by SDS-PAGE (Figure 5.22c). Throughout the purification it was noted that fractions containing HcpR2 protein have a subtle pale yellow-straw colour to them (Figure 5.22d). To determine whether this colour was provided by a metal cofactor the protein was used in difference spectroscopy and in a TPTZ assay for iron quantification. As with HcpR, no clear peaks were identified in the spectra and no iron was detected in the TPTZ assay. It seems that HcpR2 lacks an iron cofactor when it has been produced in *E. coli.*

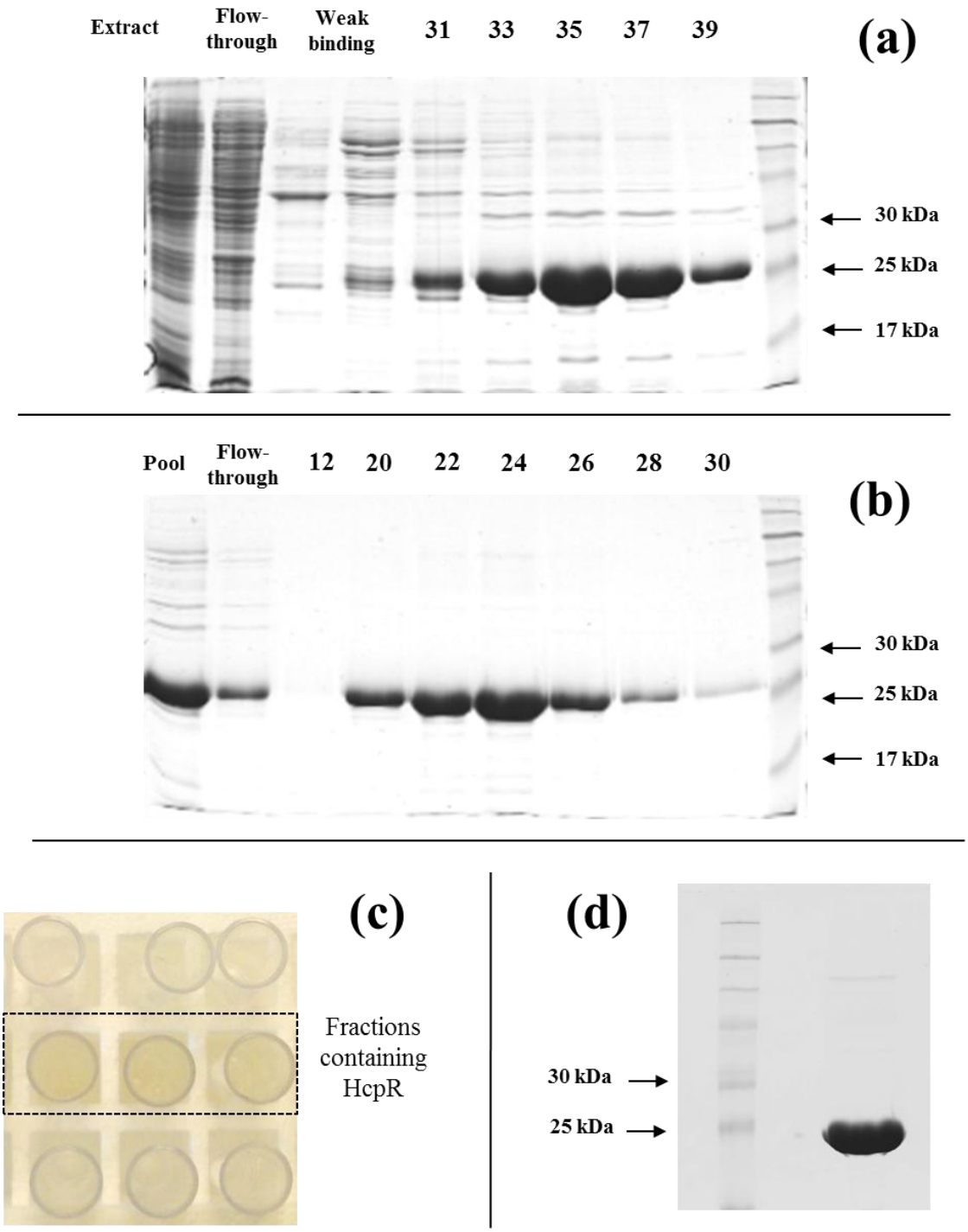

Extract
Flow-through
Weak binding
31
33
35
37
39
(a)
30 kDa
25 kDa
17 kDa
Pool
Flow-through
12
20
22
24
26
28
30
(b)
30 kDa
25 kDa
17 kDa
(c)
Fractions containing HcpR
(d)
30 kDa
25 kDa

Figure 5.22: Purification of recombinant HcpR2. (a) Cultures of *E. coli* strain BL21* expressing HcpR2 from plasmid pETHcpR2 were harvested by centrifugation. Cell pellets were lysed with lysozyme and sonication. Lysates were clarified by centrifugation and the loaded onto a 1 ml nickel agarose column fitted to an *Äkta prime* HPLC system (GE Healthcare). Proteins binding weakly to the column were eluted with a low concentration of imidazole. Proteins binding strongly to the column were eluted in a linear gradient of imidazole from 10-400 mM and collected in 2 ml fractions. Fractions were supplemented with 2 mM EDTA and analysed by SDS-PAGE. HcpR2 eluted in a narrow range of fractions with contaminating proteins. **(b)** Fractions containing HcpR2 protein were combined and dialysed against low salt Buffer C overnight at 4 ºC. The de-salted HcpR2 pool weas loaded onto a 5 ml SP-FF column fitted to an *Äkta prime* HPLC system (GE Healthcare). Proteins were eluted from the column in a linear gradient of KCl from 0.05-1 M. 1 ml fractions were collected and analysed by SDS-PAGE. HcpR2 eluted in a single peak of high purity. **(c)** HcpR2 containing fractions were slightly straw-coloured in appearance compared with fractions lacking HcpR2. **(d)** Fractions containing HcpR2 were pooled and concentrated on a Vivaspin 10 kDa spin-column. The purity of the concentrated HcpR2 protein was assessed by SDS-PAGE.

5.13 Sequence specific DNA binding by HcpR2

The purified HcpR2 protein was used in EMSAs with two different DNA fragments: p*ylbA* and p*dd1825*. The p*ylbA* fragment spans the gap between the 3' end of the coding region of *hcpR2* and the 5' end of the *ylbA*-like gene coding region and contains a putative HcpR2 binding site (Figure 5.23a). The *pdd1825* fragment contains sequences directly upstream of the coding region of Ddes_1825 and was identified as containing an HcpR binding site earlier in this chapter. Since it is similar in size to the p*ylbA* fragment but lacks a predicted HcpR2 binding site, the p*dd1825* fragment served as a control for assaying specific DNA binding by HcpR2 in an EMSA (Figure 5.23b). Titrating in HcpR2 protein resulted in a change in the migration pattern of the p*ylbA* fragment giving a band of higher apparent molecular weight. This band is discrete without blurring and so represents a single unit of HcpR2, either as a monomer or dimer, binding to a single position on the p*ylbA* fragment. No change in the migration pattern of the p*dd1825* fragment was witnessed in the presence of HcpR2 indicating that this protein requires a sequence specific to the p*ylbA* fragment for binding. To complete these investigations, the binding of HcpR2 to the p*ylbA* fragment was monitored in the presence of DTT, H_2O_2 and NO as described for HcpR. However, similar to HcpR, the DNA binding affinity of HcpR2 was not affected by these treatments.

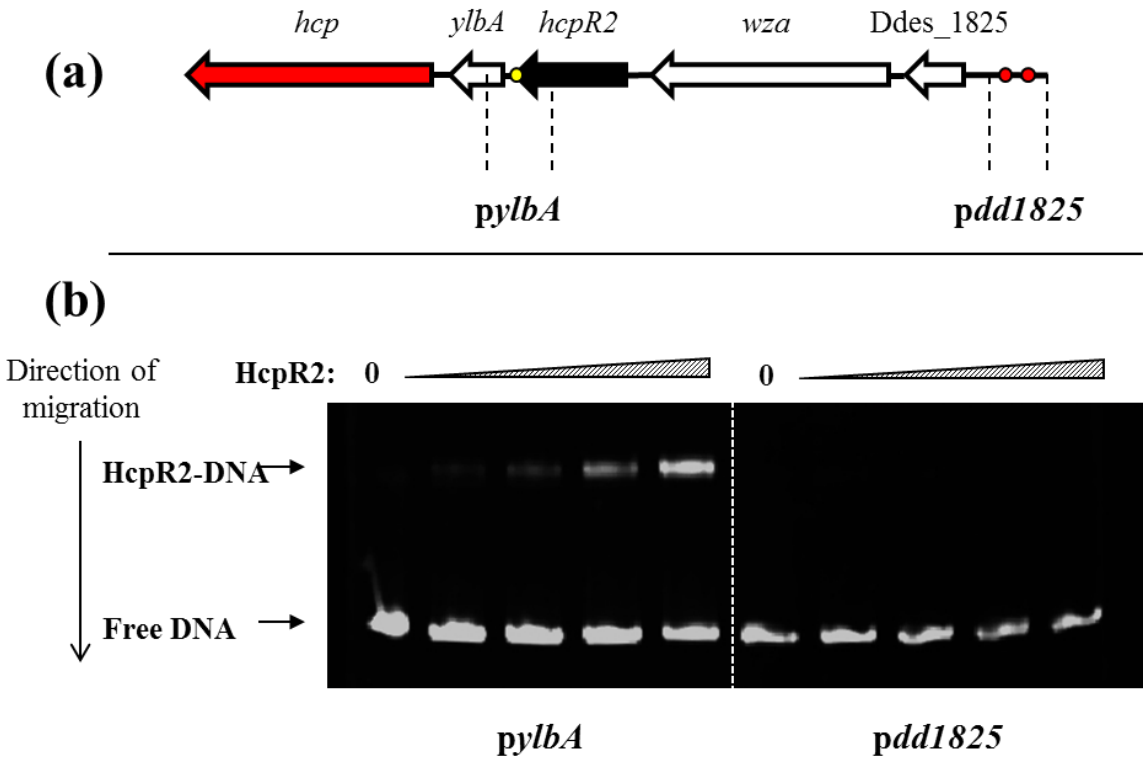


Figure 5.23: *In vitro* DNA binding activity of HcpR2. (a) Fragments containing DNA sequences upstream of *ylbA* and *Dd1825* were generated by PCR and their locations are indicated in the cartoon. The fragments contained either putative HcpR binding sites (p*dd1825* fragment, red circles) or a putative HcpR2 binding site (p*ylbA* fragment, yellow circle). **(b)** The p*ylbA* and p*dd1825* fragments were used in EMSAs with purified recombinant HcpR2. Promoter DNA fragments were incubated with increasing concentrations of HcpR2 and then resolved by non-denaturing PAGE. Free DNA and DNA-HcpR2 complexes are marked with arrows. Concentrations of HcpR2 used in the assay were 0, 62.5, 125, 250 and 500 nM.

5.14 Discussion

In this chapter the two HcpR proteins from *D. desulfuricans* have been characterised. The ability of HcpR to bind DNA target sites identical to those targeted by *E. coli* CRP was confirmed. HcpR can bind to elements upstream of the *nap*, *sat*, *hcpR* and Ddes_*1825* promoters *in vitro*. Furthermore, when expressed in *E. coli*, HcpR is able to bind to promoters containing CRP sites and repress transcription in a Δ*crp* background. CRP out-competes HcpR for binding to these sites when HcpR is co-expressed in these systems with CRP. This difference in apparent DNA binding affinities is supported by the results from EMSAs. Indeed, it was proposed in Chapter 3 that HcpR might have more stringent requirements for DNA site recognition than CRP since the DNA binding helix of HcpR contains the critical residues for CRP to bind DNA and also those required for DNA binding by FNR. The dimerization interface of HcpR must be sufficiently different from that of CRP to prevent the two proteins forming a heterodimer in an *E. coli* system. No transcription activation by HcpR was achieved in *E. coli*. This might be due to differences in the amino acid sequences between *E. coli* RNAP and that of *D. desulfuricans* meaning that favourable interactions cannot be formed between HcpR and *E. coli* RNAP. Also, the promoters screened in the *E. coli* system might require a particular sigma factor from *D. desulfuricans* to ensure favourable HcpR-RNAP interactions.

Since DNA binding by HcpR can be measured in an *E. coli* system utilising promoter::*lacZ* fusions this model was used to screen conditions that might trigger a change in the DNA binding affinity of HcpR. The advantage of using the *E. coli* model for this purpose rather than an *in vitro* system is that the side products and metabolites

produced by *E. coli* growing in a particular condition are also included in the screen. Contrastingly, in an EMSA it is only possible to screen a few different molecules at a time. Unfortunately, this *E. coli* screen did not provide any significant change in HcpR binding affinity when the bacteria were grown on nitrate, nitrite or DMSO. These conditions seemed likely to provide the necessary effector molecule to which HcpR responds. The consistent DNA binding by HcpR was also supported by the EMSAs employed with various effectors. Furthermore, a redox sensitive cofactor of HcpR could not be identified by measuring oxidised and reduced spectra and TPTZ assays indicated a lack of an iron cofactor. Potentially, the cofactor for HcpR might not be inserted when the protein is expressed in *E. coli*. The HcpR of *D. desulfuricans* contains cysteine residues which seem to be sensitive to redox state or S-nitrosylation *in vitro* but again this modification does not seem to have any effect upon DNA binding.

It is possible that HcpR does not respond to an effector molecule. However, it would be surprising if HcpR were to function independently of effector molecules as a large portion of the HcpR protein would then be functionally redundant fulfilling only a structural role. In purifying recombinant HcpR it was noted that the protein eluted from the column in a series of small peaks. This could suggest that HcpR existed in the lysates as two or more different species resulting in different affinities for the nickel agarose medium. Possibly this could be a reflection of structural isomerisation of HcpR.

Anti-HcpR antibodies provided a way to monitor the *in vivo* expression of HcpR. Levels of HcpR fluctuate in response to different terminal electron acceptors. Indeed, levels of the *hcpR* transcript indicated that *hcpR* expression varies from being effectively silent to highly up-regulated. Initially, it seemed that the regulation of HcpR is subject to induction by nitrite and repression by sulphate, sulphite and thiosulphate. However,

treatment of *D. desulfuricans* with nitric oxide stimulates expression of *hcpR*, with elevated levels of HcpR protein also being detected. These observations link *hcpR* to the nitrosative stress response of *D. desulfuricans*. Furthermore, HcpR seems to have a long half-life inside the cell as its presence was prolonged after entry into stationary phase. In *E. coli*, CRP was able to activate transcription from the *hcpR* promoter, presumably by a class I mechanism. It would be reasonable to expect CRP homologues to be able to activate from this promoter and position. Both FNR and CRP can activate transcription from sites centred at -41.5 and -61.5 (Wing *et al.*, 1995). Thus it seems probable that HcpR positively auto-regulates its own expression. This self-perpetuated auto-induction in response to nitrate reduction, nitrite and nitric oxide would explain the cascade of HcpR expression witnessed. Furthermore, HcpR levels were elevated in cultures inoculated with nitrate-grown cells, even in the absence of nitrate, nitrite or nitric oxide, probably due to auto-induction provided by a low level of HcpR present in the nitrate-grown inoculum. This would also suggest that if HcpR were to bind to an effector molecule then this binding may be strong or irreversible. Hence, HcpR perpetuates its own expression long after the stimulus triggering HcpR activity has been removed.

The DNA binding activity of HcpR seems to be constitutive. Other transcription regulators behave in this way, an example being SoxR from *E. coli*. SoxR, which is responsible for regulating superoxide response, senses redox state via two [2Fe-2S] clusters. Oxidised SoxR binds to specific operator sequences and enhances transcription of target genes. This transcriptional influence of SoxR is lost once the protein is exposed to reducing conditions. However, the DNA binding activity of SoxR remains unchanged between the oxidised and reduced states (Hidalgo & Demple, 1994; Gaudu & Weiss, 1996; Hidalgo *et al.*, 1995).

Potentially, HcpR from *D. desulfuricans* could function similarly to SoxR with respect to DNA binding activity but senses its signal, nitric oxide, via thiol-disulphide bond interchange similar to another *E. coli* regulator, OxyR. OxyR, a redox sensitive transcription factor, senses redox state via disulphide bond isomerisation. Oxidised OxyR actively influences transcription of target genes. The thiol groups of OxyR are sensitive to S-nitrosylation which also leads to OxyR exerting transcriptional influence (Hausladen *et al.*, 1996).

Since HcpR is co-transcribed with two other genes that are similar to *wrbA* and *nimA* it is likely that their activities provide an explanation for the large induction of the *hcpR* operon. Indeed, it was suggested earlier that the wave of HcpR expression seems uneconomical with cellular resources. Presumably these co-transcribed genes have some relevance to dealing with nitrosative stress. These genes and the possible activities of their products will be discussed in detail in the Chapter 6.

The second protein characterised in this chapter, HcpR2, also seems to be involved in the nitrosative stress response. Transcript mapping indicated that HcpR2 is co-localised with *ylbA* and *hcp*. These three genes may be co-transcribed as a single unit but *hcp* and, potentially, *ylbA* are also transcribed from another promoter downstream of *hcpR2*. This is clear from the differential expression of these genes in response to certain growth conditions. Like HcpR, *hcp* is up-regulated by nitrate reduction, nitrite and nitric oxide. Another putative HcpR2 regulon member, *dfx*, is also up-regulated by nitric oxide. A DNA binding site for HcpR2 between the coding regions of *hcpR2* and *ylbA* was confirmed by EMSA. It is possible that HcpR2 regulates expression of *ylbA* and *hcp* when bound to this position *in vivo.* Again, no cofactor or effector could be identified for this protein. In contrast with HcpR, HcpR2 expression seems to be constitutive and

does not fluctuate. Thus, *D. desulfuricans* has two HcpR family proteins that seem to respond to a common signal in different ways.

Chapter 6

Discussion

The regulation of gene expression in response to terminal electron acceptors and nitrosative stress

6.1 Introduction

Prior to this study, little was known about HcpR proteins. The seminal HcpR articles of Rodionov *et al*. (2004; 2005) have been referred to throughout this thesis but, more recently, additional papers investigating HcpR have been published. Thus, to begin this final chapter, a brief review of the literature detailing experimental analysis of HcpR will be presented. Since the *D. desulfuricans hcpR* gene is co-transcribed with at least two other genes, *wrbA* and *nimA*, the potential activities of these proteins will be discussed with reference to sequence and structure homologues. Similarly, the function of *ylbA*, which is co-transcribed with *hcp*, will be considered. With these assessments made, and with reference to the literature, the results of this thesis will be used to produce models explaining how *hcpR* and *hcpR2* could regulate transcription in response to nitrosative stress in *D. desulfuricans*. The importance of HcpR family proteins to the survival of SRB in response to stress will be discussed and a model explaining the current understanding of how terminal electron acceptor selection by *D. desulfuricans* is mediated will be presented.

6.2 HcpR proteins: insights from other studies

HcpR and its putative regulon were first identified *in silico* by Rodionov *et al.* (2004). The first experimental analysis of HcpR from *D. vulgaris* was the PhD work of Hemme (2004). In that thesis a mutant deficient for *hcpR*, then termed *hbaR* according to genome annotation, was generated. The only notable phenotype for the *hbaR* mutant strain was that it was unable to grow in medium supplemented with sulphate and ethanol suggesting an essential role for HcpR in utilising ethanol as a carbon source. However, the *adh* gene suggested to be responsible for ethanol metabolism in *D.*

vulgaris is not *adhE*, which is linked to *hcp*, but another *adh* gene located at a distant locus (Haveman *et al.*, 2003). Preliminary experiments in the current study indicated that expression of *hcpR* or *hcpR2* from *D. desulfuricans* is not influenced by ethanol. One would expect a change in the expression profile of *hcpR* in response to the switch to ethanol dependent growth if this protein were essential for ethanol utilisation. Indeed, a more recent publication by Hemme and colleagues describes an *hcpR* mutant of *D. vulgaris* but does not mention this phenotype, suggesting that this dependency upon HcpR for ethanol metabolism has either been discounted or attributed to a secondary effect (Zhou *et al*., 2012).

The next experimental investigation of HcpR was also a PhD thesis that attempted to characterise *D. desulfuricans* HcpR (Marietou, 2009). Since that particular article was published prior to the *D. desulfuricans* genome becoming widely available on-line, the *D. desulfuricans* genes encoding CRP family proteins were identified by Southern blotting using probes derived from *D. vulgaris* DNA sequences. Counterparts of the four *D. vulgaris* CRP encoding-genes were detected in *D. desulfuricans* and then cloned using a 'fishing-out' strategy employing the primers used for amplifying the *D. vulgaris* CRP probes. These four genes encoding putative CRP homologues were reported to have >98 % identity to those of *D. vulgaris*. Since these genes were seemingly identical in these two species the study proceeded with cloning, over-expression, purification and *in vitro* characterisation of *D. vulgaris* HcpR. Unfortunately, as detailed in Chapter 3 of this study which benefitted from the availability of the *D. desulfuricans* genome sequence, these levels of similarity reported between the *hcpR* genes of *D. desulfuricans* and *D. vulgaris* do not exist. It seems likely that the products of the 'fishing-out' strategy of Marietou (2009) were generated from contaminating *D. vulgaris* gDNA and

therefore that study was actually focussed exclusively upon the HcpR of *D. vulgaris.* Using a combination of EMSAs and DNase I footprinting assays the *in vitro* DNA binding abilities of *D. vulgaris* HcpR to the p*nap* fragment were assessed. Critically, HcpR binding was to CRP-like inverted repeat sequences and was cAMP dependent. Alas, attempts to recreate the experiments of Marietou (2009) were unsuccessful. Particularly, the concentrations of *D. vulgaris* HcpR protein required to provide equivalent migration patterns in EMSAs were approximately one thousand times greater than those reported in that study. The apparent experimental errors in that study combined with the lack of conserved cAMP binding residues in *D. vulgaris* HcpR make these results unreliable. Indeed, it is possible that these observations for *D. vulgaris* HcpR could possibly be from contaminating CRP in the HcpR preparations produced by over-expression in *E. coli.* However, what can be gleaned from Marietou (2009) is that the HcpR of *D. vulgaris* behaves differently *in vitro* to that of *D. desulfuricans*. The *D. vulgaris* HcpR has a significantly lower affinity for CRP-like inverted repeats, requiring µM concentrations of protein for noticeable shifts in EMSAs.

During the later stages of the current study two additional articles regarding HcpR were published. The HcpR of *Porphyromonas gingivalis*, characterised by Lewis *et al.* (2012), is believed to bind to the CRP-like sequence TGTCGC[N_4]GCGACA with binding being hemin dependent. Growth of an *hcpR* mutant of *P. gingivalis* was severely compromised in the presence of nitrite or nitric oxide and expression of *hcp* was abolished in this mutant. Furthermore, survival of the *hcpR* mutant in the presence of host cells was compromised. It seems that the HcpR of *P. gingivalis* is linked to the nitrosative stress response and is essential for expression of *hcp.*

Zhou *et al.* (2012) reported that the HcpR of *D. vulgaris* is up-regulated in response to nitrite stress or heat shock and down-regulated in response to elevated NaCl levels. Similar to the observations of Lewis *et al.* (2012), expression of *hcp* was significantly decreased in an *hcpR* mutant of *D. vulgaris.* Expression of *frdX*, which is part of an operon with *hcp*, was also down-regulated in the mutant. In total this mutant showed significant changes in the expression of 33 genes relative to wild-type cells. HcpR from *D. vulgaris* was claimed to be involved in alternative energy metabolism and chemotaxis. Lower expression of *hcp* and *frdX* was also noted for a mutant of *D. vulgaris* lacking the DVU3111 gene, which encodes a CRP family protein. There was no significant change in the levels of *aprAB* or *sat* transcripts in the *D. vulgaris hcpR* mutant. The findings of Lewis *et al.* (2012) and Zhou *et al*. (2012) indicate that HcpR is responsive to nitrite or nitrosative stress and is necessary for full induction of the *hcp* operon. Reference to these points will be made whilst discussing the results of the present study.

6.3 An assessment of DNA binding by HcpR

The DNA binding affinity of CRP has been extensively characterised. Oligonucleotides with substitutions to the CRP consensus sequence have been used in binding assays and indicate that a deviation from the symmetrical consensus sequence lowers the affinity of CRP for that site. Furthermore, different positions and nucleotides used in a substitution affect the affinity of CRP for a site in different ways (Jansen *et al.*, 1987).

The DNA binding activity of *D. desulfuricans* HcpR was assessed *in silico, in vitro* and, to a lesser extent, *in vivo.* The putative HcpR regulon, which was assembled using the *E. coli* PWM, is large and includes genes with a wide range of putative functions.

However, *in vitro* DNA binding assays with HcpR highlight that the initial estimation of the HcpR regulon is likely to be an over-estimation. Indeed, it is possible to create a list of those fragments tested *in vitro* and order them in terms of their affinity for HcpR (Figure 6.1). Of those tested, the p*hcpR* fragment, which contains a single site that is a perfect match to that of CRP, was bound by HcpR with the highest affinity. The p*nap*, AM4 and AM3 fragments, which contain site IR1, were also bound by HcpR with high affinity. The preferential binding of HcpR to IR1, which differs from the CRP consensus DNA binding site by a T>A substitution at position 1, highlights that position 1 of each HcpR half site is not particularly important for binding by HcpR. Nucleotide substitutions at positions 2 or 3 significantly decrease the affinity of HcpR for that site. Positions 4 and 5 are also of importance for site recognition by HcpR as the *sat* and Ddes_1825 fragments were bound with intermediate affinity. No HcpR binding could be detected by EMSA at the *apr*, fragment indicating that nucleotide substitutions at each position 2, 3 and 4 of one of the half sites is sufficient to abolish DNA binding by HcpR. Thus, half site positions 2, 3 and 4 are most important for recognition by HcpR with positions 1 and 5 also affecting DNA binding, but to a lesser extent. HcpR bound with greatest preference to a symmetrical site identical to that of the CRP consensus sequence.

In the case of CRP, position 4 of each target DNA half site is most important for site specificity but position 2 is also important. Substitutions at position 5 have only minor effects upon DNA binding by CRP (Jansen *et al*., 1987). These nucleotides in the CRP half sites are those that are involved in hydrogen bonding with the E and R residues of the CRP DNA-recognition helices (Parkinson *et al*., 1996). DNA binding by CRP and HcpR seems to be very similar with positions 2 and 4 being critical for both regulators.

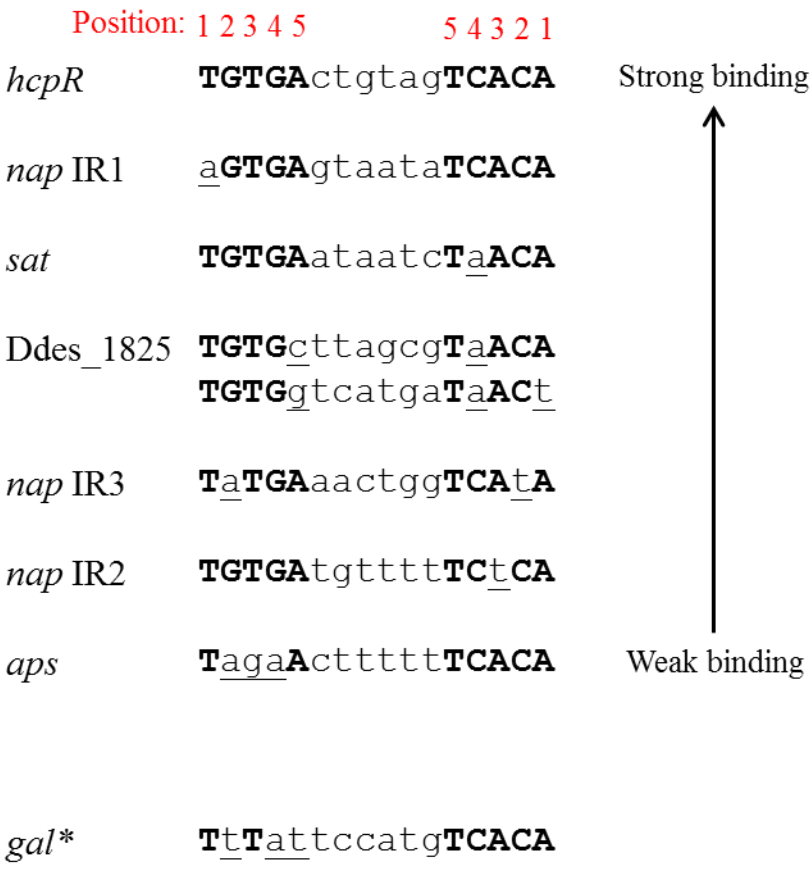


Figure 6.1: Hierarchical ranking of HcpR target sites tested by EMSA. Sequences of putative Sequences of HcpR sites are shown and the positions of nucleotides in each half-site are labelled. Nucleotides conforming to the CRP consensus sequence are in bold upper case whereas those not conforming are in lower case and underlined. * the *gal* promoter was not screened by EMSA but HcpR binding was confirmed by heterologous expression in *E. coli.*

The most obvious difference between the DNA binding activities of these two regulators is that position 3 of the half site also seems to be crucial for HcpR binding. It was suggested in Chapter 3 that, in addition to positions 2, 4 and 5 being contacted by the E and R residues of HcpR, an additional position contact could be made between the S residue of HcpR and position 3 of the DNA half-site. The observation of substitutions at position 3 leading to severely compromised binding by HcpR supports this suggestion.

Heterologous expression of HcpR in *E. coli* provides evidence that this protein can bind to the CRP site of the *E. coli gal* promoter with sufficient affinity to modulate transcription. This site differs at positions 2, 4 and 5 of one CRP half site and so provides some further indication that position 3 might be of importance for HcpR binding. Furthermore, this suggests that the *in vivo* DNA binding activity of HcpR could be stronger than that observed *in vitro*.

Assessment of the DNA binding activities of HcpR indicates that this regulator would bind to the sites of the *hcpR, nap* and *sat* promoters *in vivo*. From the putative HcpR regulon presented in Chapter 3, other putative targets that seem most likely to be genuine targets for HcpR would include: *cckA-drrA, adhE, sscC,* Ddes_1664-Ddes_1665, the Ddes_1237 operon, the Ddes_1252 operon, *echABCDEF, fldA* and *iscR-nsrR*. These targets would be ideal for further *in vitro* assays, β-galactosidase assays in *E. coli* heterologously expressing HcpR and transcription analysis.

The effectors of HcpR and HcpR2 are unknown. cAMP and a cocktail of other small molecules failed to change the DNA binding activity of HcpR. Specific mutations of CRP that alter effector binding by *E. coli* CRP have been identified (Kolb *et al.*, 1993;

Youn *et al.*, 2006). A T127L S128I mutant of CRP is able to bind DNA independently of cAMP (Youn *et al.*, 2006). Furthermore, this mutant showed decreased DNA binding activity in the presence of cGMP. Additionally, a D53S mutant of CRP binds a wider range of effectors than the wild-type protein (Kolb *et al.*, 1993). *D. desulfurcians* HcpR has these point mutations at corresponding positions indicating that this transcription factor is unlikely to bind cAMP having evolved to respond to some other effector molecule.

6.4 Potential roles for the transcriptional partners of *hcpR*

Since both *hcpR* and *hcp* are co-transcribed with other neighbouring genes it is highly likely that these genes are also up-regulated in response to growth in the presence of nitrate or in response to nitrosative stress. Thus, by considering sequence and structural homologues of the gene products of these neighbours it is possible to propose their functions or their response to these signals.

Immediately downstream of the *hcpR* ORF are the genes *wrbA* and *nimA.* Both *wrbA* and *nimA* are conserved at this locus in other bacteria, normally with *hcp* also, supporting the observation of co-transcription of these genes with *hcpR* and therefore their induction in times of nitrostative stress.

The *wrbA* gene is annotated as encoding a flavodoxin family protein. Structure prediction indicates that this gene encodes a protein that is extremely likely to resemble that of WrbA proteins. The WrbA, or tryptophan (W) repressor binding protein, of *E. coli* co-purifies with the *trp* repressor protein, TrpR, and was believed to influence the activities of this transcription regulator by enhancing the binding of TrpR to its target DNA sites (Yang *et al.*, 1993). Later studies indicated that the interactions between

WrbA and TrpR were non-specific and, since *wrbA* is part of the RpoS regulon, the function of WrbA is likely to be part of some stress response (Grandori *et al.*, 1998; Patridge & Ferry, 2006). Indeed, it was demonstrated that WrbA from *E. coli* and *Archaeoglobus fulgidus* has NAD(P)H:quinone oxidoreductase activity and that, via this activity, WrbA might function in cell signalling by reducing the quinone pool resulting in an indirect influence upon redox sensitive transcription regulators (Patridge & Ferry, 2006).

The structure of WrbA lacks any transmembrane domains and is therefore assumed to not have a role in proton pumping (Andrade *et al.*, 2007; Gorman & Shapiro, 2005). The reduction of quinones by WrbA is a process that has been suggested to limit the semiquinone dependent generation of superoxides from molecular oxygen or to contribute to oxygen reduction by the cytochrome *bd*-II oxidase (Partridge & Ferry, 2006; Shepherd *et al.*, 2010). The *bd* complex, a membrane bound haem-containing quinol oxidase, of *D. vulgaris* has been demonstrated to be involved in oxygen reduction (Lamrabet *et al*., 2011). Furthermore, in *E. coli* the *bd* complex has a high affinity for nitric oxide and has been proposed to be crucial for survival in the presence of nitric oxide and for pathogenicity (Hori *et al*., 1996; Mason *et al*., 2008; Giuffrè *et al*., 2012). The association between WrbA and the *bd* complex hints that a potential function of *D. desulfuricans* WrbA might be in the oxidative and/or nitrosative stress responses.

The structure of WrbA proteins are also very similar to a domain of FprA from *Moorella thermoacitica*, a protein that functions as a high affinity nitric oxide reductase (Silaghi-Dumitrescu *et al*., 2005). The FprA proteins of *Desulfovibrio* species are more commonly known as Roo. It is appealing to assign WrbA as an FprA nitric oxide

reductase, however, WrbA lacks the di-iron-containing domain necessary for catalysing this reductive process. Thus, the WrbA-like protein of *D. desulfuricans* seems likely to function in redox processes shuttling electrons, potentially to another protein that is responsible for direct enzymic catalysis of some redox reaction.

Also co-transcribed with *hcpR* and *wrbA* is *nimA*, a gene annotated as encoding an FMN-binding pyridoxamine 5'-phosphate oxidase-like protein. Pyridoxamine 5'-phosphate oxidases are involved in vitamin B6 synthesis. Structural modelling of this gene product indicates that the most similar putative structural homologues of this protein are uncharacterised. Those that have been characterised are proteins with varied roles. HutZ from *Vibrio cholerae* is a haem binding, rather than flavin binding, protein that has a role in utilising haem either as an iron source, for transferring haem to other proteins, or as a haem storage protein (Wyckoff *et al.*, 2004; Wyckoff *et al.*, 2007).

Another homologue, the FMN and FAD binding general stress protein of *Xanthomonas citri*, is up-regulated during infection and is believed to be involved in protection against oxidative stress imposed by the host defence systems (Hilario *et al.*, 2012). The NimA proteins, such as that of *Clostridium acetobutylicum*, are involved in nitroimidazole resistance. Nitroimidazoles are a class of antibacterial prodrugs that become active by the one electron reduction of the nitro group by bacterial ferredoxins, yielding a toxic nitro radical group (Vidakovic *et al*., 2003). Nim proteins convert the nitro group of nitroimidazoles into an amine group, preventing prodrug activation with electrons for this reduction being donated by ferredoxin (Leiros *et al.*, 2004).

The pyridoxamine-5'-phosphate oxidase-like proteins have varied functions, being involved in direct catalysis of redox reactions, stress response and alternative modes of

metabolism. Thus, it is plausible that the *D. desulfuricans nimA* gene product is the functional partner of WrbA, which would putatively function as the electron donor for NimA. The NimA amino-acid sequence is rich in H, D and E residues that could potentially confer haem, similar to HutZ, or non-haem iron binding ability. From examining homologues of these proteins it is plausible that they function either as a multi-component equivalent of FprA, as a nitro reductase similar to NimA, or as donors for membrane-bound respiratory components such as the *bd* complex. Considering the up-regulation of *hcpR* and, presumably, *wrbA-nimA* in response to nitric oxide, it seems highly likely that they function in coping with nitrosative stress and/or oxidative stress. This presumption seems all the more likely when reminded that these genes are linked to *hcp* in other *Desulfovibrio* species. It is also possible, due to its conservation at this locus, that the downstream *frdX2* is co-transcribed with these genes. Only short regions of the FrdX2 protein have any resemblance to known protein structures and so it is difficult to propose a function for this protein.

6.5 Potential roles for the transcriptional partner of *hcp*: *ylbA*

The *hcp* gene of *D. desulfuricans* can be co-transcribed constitutively with a series of other genes. However, when *hcp* is up-regulated by exposure to nitric oxide only one of these other genes, *ylbA*, is thought to be up-regulated also. This assumption stems from the observation that *ylbA-hcp* are co-localised in a range of other bacteria and that putative HcpR2 target DNA sites are always located upstream of this gene couple. Generally this arrangement of genes occurs in bacteria other than SRB with *D. desulfuricans* seemingly an exception. In *E. coli* the *hcp* gene is co-transcribed with its cognate reductase, *hcr*, and so an obvious role for the *D. desulfuricans ylbA* gene

product is to fulfil this role. In *E. coli* YlbA, also known as AllE and UghY, is a cupin protein involved in allantoin degradation (Werner *et al.*, 2009). The cupin superfamily has been described as being one of the most functionally diverse protein families identified yet (Dunwell *et al*., 2001; Dunwell *et al.*, 2004). The YlbA of *D. desulfuricans* is a short protein, 113 amino acids long, with no characterised homologues identified in blast searches. The majority of YlbA structural homologues identified are putative seed storage proteins, typical of the archetype cupin germin, or dioxygenase-like proteins. With diverse functions in the cupin family, the function of YlbA cannot be predicted with confidence from its sequence alone although a role as the cognate reductase of Hcp seems most likely.

6.6 Auto-regulation of the *hcpR* operon

The results presented in this study indicate a strong link between HcpR and coping with nitrosative stress. This link is supported by the predictions and findings of other groups (Zhou *et al.* 2012; Lewis *et al*., 2012; Rodionov *et al*., 2005; Marietou, 2009). Since *hcpR* mutants of *D. vulgaris* and *P. gingivalis* show decreased expression of the key regulon member, *hcp*, it seems that HcpR functions as a transcription activator at this locus. This function might not be conserved for the HcpR of *D. desulfuricans* since, as already discussed, the HcpR proteins of these species seem to be in different branches of the same family. However, the observation that CRP could activate transcription from the *hcpR* promoter in *E. coli* hints that HcpR is likely to positively influence its own expression. The activity of HcpR heterologously expressed in *E. coli* indicates the potential for HcpR to negatively influence transcription. Thus, we can assume that HcpR has the potential to regulate transcription of its targets by both activation and

repression. With these points in mind it is possible to form hypothetical regulatory circuits related to the actions of HcpR.

Expression of *hcpR* is triggered by nitric oxide. In the absence of this stimulus the rate of transcription from the *hcpR* promoter must be at a very low basal level (Figure 6.2a). As already discussed, HcpR probably senses nitric oxide directly, possibly via protein thiol groups. The results presented here suggest that DNA binding by *D. desulfuricans* HcpR is constitutive although that of *P. gingivalis* requires hemin. In either instance, when nitric oxide is absent HcpR is 'off' with respect to transcription activation (for clarity this is depicted as HcpR not binding to DNA in Figure 6.2a). Levels of the *wrbA-nimA* transcripts are correspondingly low. However, the small quantities of HcpR present in the cell are sufficient to sense the presence of nitric oxide and mediate an appropriate response (Figure 6.2b). This trigger causes HcpR to bind to its DNA target and to induce a cascade of expression *hcpR-wrbA-nimA*, probably by a class II mechanism. It is likely that these downstream genes mediate the detoxification of the nitric oxide signal or contribute to repair of nitrosative damage. In *Desulfovibrio* sp. 3_1_syn3 and *Desulfovibrio* sp. 6_4_6AFAA the *hcpR-wrbA-nimA* operon includes *hcp*, supporting this proposal and also indicating that a large up-regulation of *hcpR* in response to nitric oxide is also likely to occur in these species. The cascade of expression would have a saturating effect and ensure elimination of nitric oxide or repair of damage.

If DNA binding by HcpR is constitutive then once this nitric oxide was eliminated there would still be significant levels of HcpR being synthesised (Figure 6.2c). This newly synthesised, inactive HcpR could compete with active HcpR for DNA binding, decreasing the rate of *hcpR* transcription and resulting in a quenching effect upon the

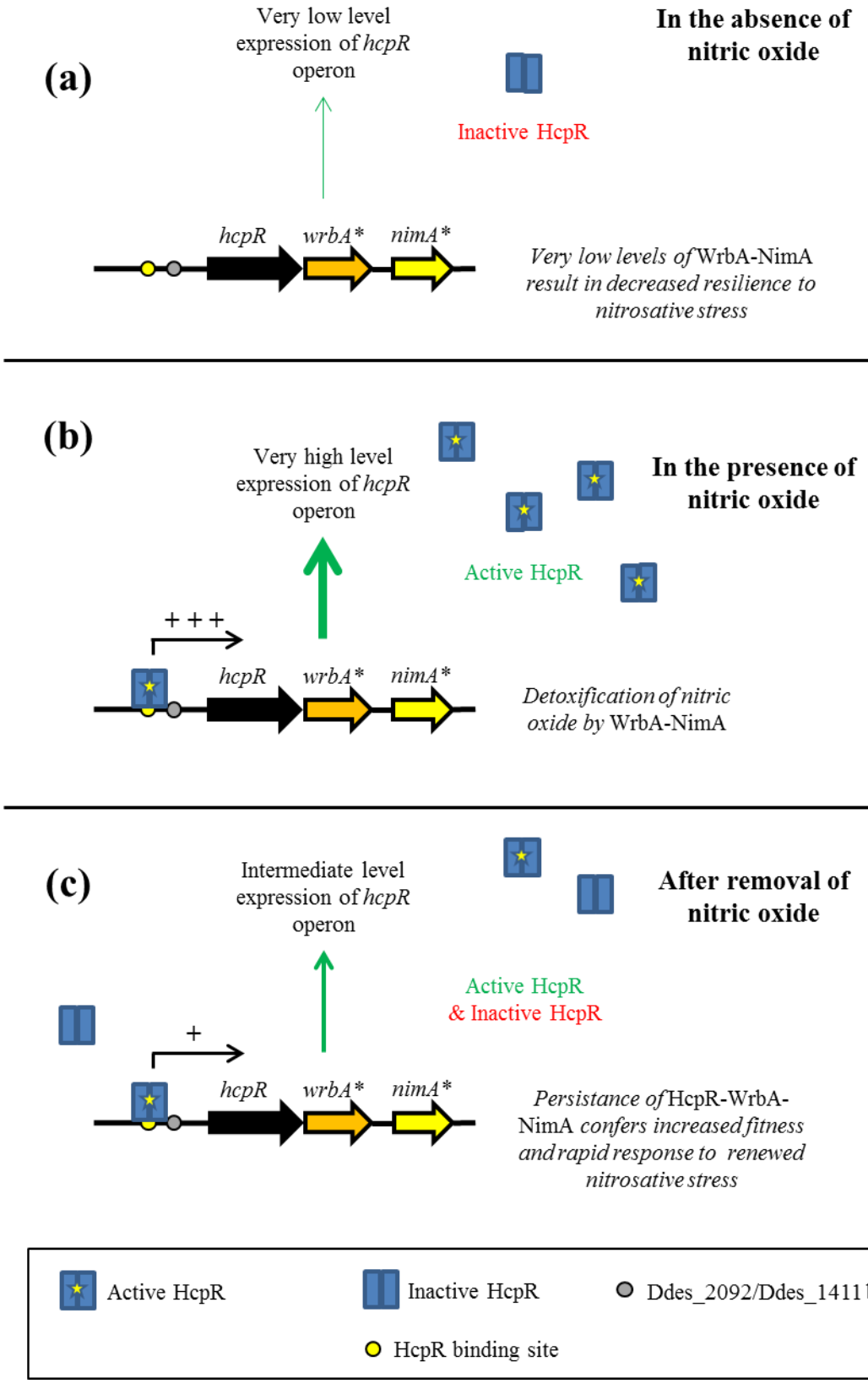

(a)
Very low level expression of hcpR operon
In the absence of nitric oxide
Inactive HcpR
hcpR
wrbA*
nimA*
Very low levels of WrbA-NimA result in decreased resilience to nitrosative stress
(b)
Very high level expression of hcpR operon
In the presence of nitric oxide
Active HcpR
+++
hcpR
wrbA*
nimA*
Detoxification of nitric oxide by WrbA-NimA
(c)
Intermediate level expression of hcpR operon
After removal of nitric oxide
Active HcpR & Inactive HcpR
+
hcpR
wrbA*
nimA*
Persistance of HcpR-WrbA-NimA confers increased fitness and rapid response to renewed nitrosative stress
Active HcpR
Inactive HcpR
Ddes_2092/Ddes_1411 binding site
HcpR binding site

Figure 6.2: Nitric oxide dependent regulation of the *hcpR* operon. A putative model of regulation. **(a)** In the absence of nitric oxide the *hcpR* operon is expressed at a very low rate. HcpR is inactive with respect to modulating transcription. **(b)** In the presence of nitric oxide any HcpR within the cell becomes active with respect to activating transcription and the *hcpR* operon is fully induced. The *wrbA* and *nimA* gene products putatively function to remove nitric oxide. **(c)** Expression of the *hcpR* operon decreases after elimination of nitric oxide. However, due to its long half-life, a mixture of active and inactive HcpR exists in the cell. This mixture of HcpR perpetuates transcription of the *hcpR* operon at an intermediate level for multiple generations ensuring that *D. desulfuricans* is able to cope with another bout of nitrosative stress.

remaining active HcpR. Alternatively, if inactive HcpR does not bind DNA, induction would continue until complete degradation of the active HcpR. The putative binding site for Ddes_1411/Ddes_2092 that occludes the *hcpR* promoter -35 element suggests that one or both of these regulators could repress transcription of *hcpR* in certain conditions providing an additional route to quelling *hcpR* expression. Alternatively one of these regulators could function as an activator providing, an alternative route to induction of the *hcpR* operon. Zhou *et al*. (2012) noted that deletion of the CRP homologue DVU3111 resulted in a down-regulation of the *hcp* operon in *D. vulgaris.* Since the *hcp* operon of *D. vulgaris* can be regarded as a counterpart of the *hcp-hcpR* loci of *Desulfovibrio sp. 3_1_syn3, Desulfovibrio sp. 6_4_6AFAA* and the *hcpR* locus of *D. desulfuricans* it can be speculated that the activity of multiple CRP family proteins at these loci might be a conserved regulatory feature.

Pre-exposure of *D. desulfuricans* to nitrate instils improved resilience to toxic nitrite. As indicated by western blot, pre-exposure to nitrate also leads to elevated levels of HcpR. This pre-induced HcpR persists even in an absence of effectors seemingly perpetuating its own synthesis in cells growing on sulphate or sulphite alone. Thus, in the model of HcpR expression, we have an after-effect of nitric oxide exposure (Figure 6.2c). An intermediate level of *hcpR-wrbA-nimA* expression seems to continue for many cell divisions, even in progeny cells. This provides an explanation for the improved nitric oxide resistance witnessed and also provides a rationale for the seemingly wasteful abundance of HcpR generated in response to nitric oxide. High level expression of *hcpR* functions as insurance against sustained or further nitrosative stress following the initial exposure. Thus, *D. desulfuricans* can be regarded as being in a state of alert. Indeed, in its natural environment, where nitrosative stress would be a common encounter, this

'alert' stage is probably normal with the low-expression state being an artificial product of unnatural laboratory culture. Expression of *hcpR-wrbA-nimA* could also be influenced by either Ddes_1411 or Ddes_2092 by an unknown mechanism.

6.7 Regulation of *hcp* by HcpR2

Expression of HcpR2 is constant regardless of terminal electron acceptor availability and nitrosative stress. Constitutive expression of HcpR2 ensures that this regulator is available to respond rapidly to transient changes in the levels of its effector. In contrast, expression of *hcp* is greatly up-regulated in response to nitric oxide. The binding of HcpR2 to an inverted repeat sequence upstream of the *ylbA-hcp* gene was confirmed by EMSA and indicates that HcpR2 exerts some influence over expression of these genes. The *hcpR2* transcript can be co-transcribed as a single unit with these genes and the preceding genes Ddes_1825 and *wrz*. Thus, it seems that the Ddes_1825-*wrz-hcpR2-ylbA-hcp* unit can be transcribed constitutively and that up-regulation of *hcp* is mediated from a position downstream of *hcpR2*. The prime candidate for regulating *hcp* expression is HcpR2. For HcpR2 to fulfil this role it must respond to nitric oxide since this is the inducer of *hcp*.

The *hcpR2-ylbA* intergenic region is relatively short. It is unknown whether HcpR2 binding to this region results in repression of *hcp* or recruitment of RNAP and transcription activation. Since the RNAP binding sites of the *hcp* promoter could not be identified it is unclear whether this is an extended -10 promoter. A simple model of *ylbA-hcp* regulation by HcpR2 can be assembled (Figure 6.3). In this model HcpR2 is synthesised constitutively as a component of the Ddes_1825-*wrz-hcpR2-ylbA-hcp* operon. The assumption that HcpR2 senses nitric oxide is supported by the observations

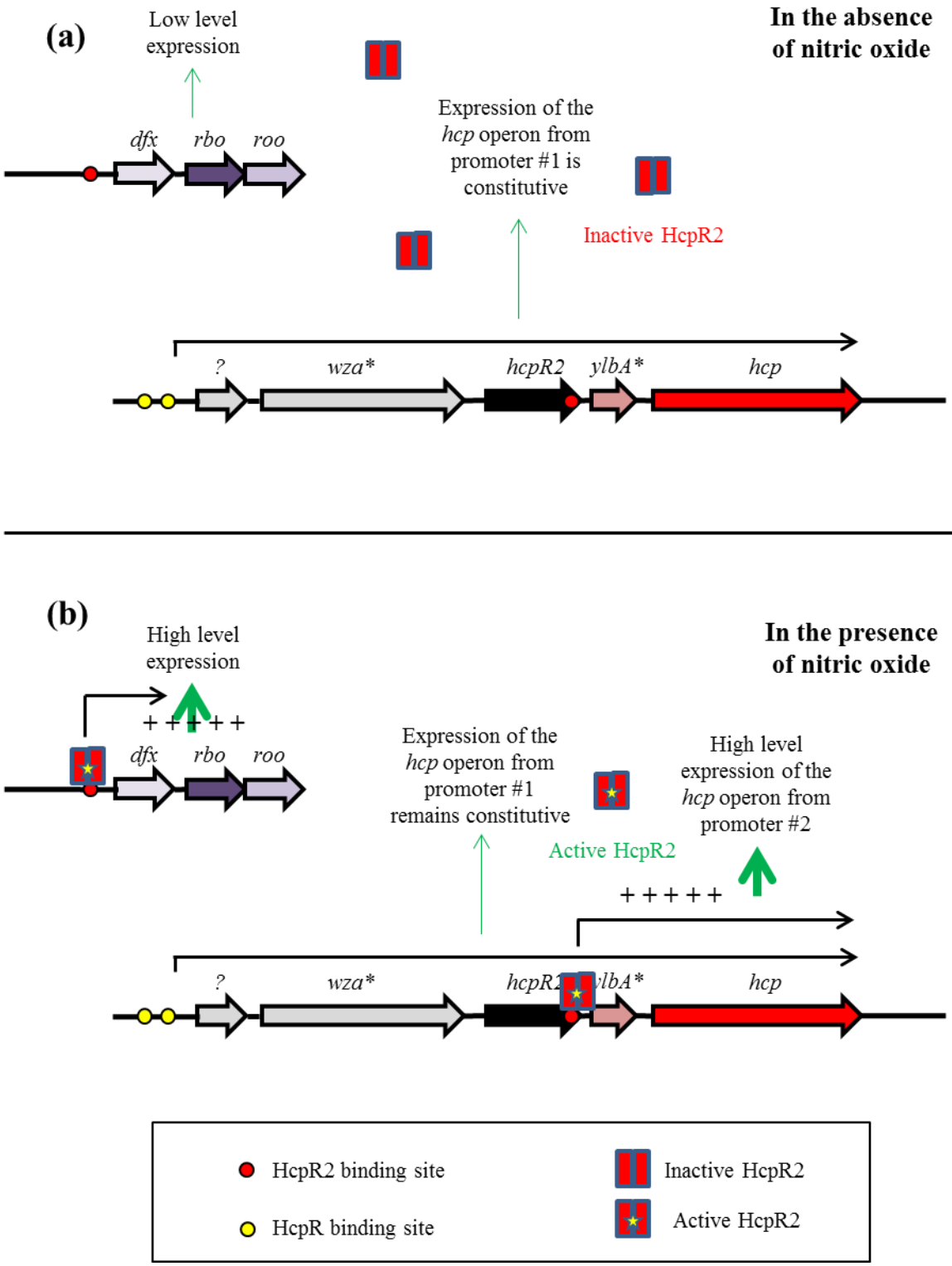

(a)
Low level expression
In the absence of nitric oxide
dfx
rbo
roo
Expression of the hcp operon from promoter #1 is constitutive
Inactive HcpR2
?
wza*
hcpR2
ylbA*
hcp
(b)
High level expression
In the presence of nitric oxide
+ + + + +
dfx
rbo
roo
Expression of the hcp operon from promoter #1 remains constitutive
High level expression of the hcp operon from promoter #2
Active HcpR2
+ + + + +
?
wza*
hcpR2
ylbA*
hcp
HcpR2 binding site
HcpR binding site
Inactive HcpR2
Active HcpR2

Figure 6.3: Regulation of *hcp and dfx-rbo-roo* by HcpR2. A putative model of regulation. **(a)** In the absence of nitric oxide, low level transcription of the *hcp* operon occurs from promoter #1. Similarly, expression of the *dfx* operon is low. Any HcpR2 protein in the cell is inactive with respect to DNA binding. **(b)** HcpR2 is activated when the levels of nitric oxide become elevated within the cell and binds to specific DNA sequences upstream of the *dfx* operon and the *hcp* promoter #2. HcpR2 activates transcription at these two loci leading to increased levels of Hcp and Dfx. These gene products function in coping with nitrosative stress.

that HcpR seems to be an activator of *hcp* expression in both *D. vulgaris* and *P. gingivalis* and that *hcp* expression is responsive to nitric oxide (Lewis *et al.*, 2012; Zhou *et al.*, 2012). Thus, in the absence of nitric oxide, HcpR2 is 'inactive' with respect to modulating transcription (depicted as no DNA binding in Figure 6.3a).

The constitutive presence of HcpR2 in the cell means that when nitric oxide becomes present, either as the result of nitrate/nitrite metabolism or exogenous sources, it is able to mediate a response immediately. Nitric oxide could be sensed by HcpR2 by a haem group similar to *P. gingivalis* triggering HcpR2 to assume the transcription influencing 'active' conformation (depicted as DNA binding in Figure 6.3b). Active HcpR2 would then bind to the HcpR2 binding site upstream of the *ylbA* gene and possibly to those upstream of other putative HcpR2 targets such as the *dfx-rbo-roo* operon which was shown to be up-regulated in response to nitric oxide and activate transcription of target genes. This activation is likely to involve recruitment of RNAP to the *hcp* promoter or possibly class II activation due to the close proximity of the HcpR2 binding site to the start of the *ylbA* ORF. Transcription of *ylbA-hcp* would now be from a previously silent promoter within the constitutively expressed Ddes_1825-*wrz-hcpR2-ylbA-hcp* operon. Thus, *ylbA-hcp* and *dfx-rbo-roo* would be able to contribute to detoxification of nitric oxide and protection against nitrosative stress.

It is possible that HcpR2 could alternatively function as a transcription repressor and lose DNA binding ability once nitric oxide is present in a manner similar to NsrR of *E. coli*. However, as already mentioned in both *D. vulgaris* and *P. gingivalis* HcpR is necessary for induction of *hcp* (Lewis, 2012; Zhou *et al.*, 2012). Transcript analysis indicates that the nitric oxide induced up-regulation of *hcp* and *dfx* persists for at least 20 hours after exposure to nitric oxide. Similar to *hcpR-wrbA-nimA*, the *hcp* and *dfx*

gene products could linger following the stress event and contribute to the increased resistance to nitrosative stress witnessed for pre-treated cultures. Once the nitrosative stress had been relinquished the active HcpR2 would eventually be degraded and replaced with the non-active form as part of on-going HcpR2 turnover in the cell.

6.8 Regulation of genes responsible for sulphate reduction

In Chapter 3 a simple model explaining the mechanism of nitrate-sulphate diauxie in *D. desulfuricans* was presented. This model was based primarily upon the activities of HcpR as the regulator of *sat*, *aprAB* and *nap*. According to the model, HcpR was responsible for activating expression of *nap* by a class III mechanism and repression of *sat* and *aprAB* by steric hindrance of RNAP. This model, based upon the findings of Marietou (2009) and the earlier *in silico* analysis, will now be revised with reference to the results presented in Chapters 4 and 5.

Expression of *sat* does not seem to vary much with terminal electron acceptor availability despite strong evidence indicating that HcpR can bind to sequences overlapping the -10 and -35 RNAP consensus sequences of the *sat* promoter. Strong binding of HcpR to this promoter was recorded *in vitro* but no changes in transcription of the downstream genes were detected. Whether or not HcpR does indeed bind this site, and that of the *aprAB* promoter, *in vivo* remains unknown. If HcpR does bind to these sites then its activity seems minor and obscure. Perhaps HcpR function at these promoters only occurs with the synergistic activity of another transcription factor under extreme conditions.

Similarly, although sulphite reduction seems to require a period of induction, the expression of *dsrAB* does not vary with different terminal electron acceptors. These

observations are supported by the fact that both *qmoABC* and *dsrMKJOP* are also expressed constitutively with regard to terminal electron acceptor. Thus, the findings of this study indicate that the sulphate reduction pathway is expressed constitutively (or within a narrow enough range to be regarded as constitutive) and so the regulation of these genes can be disregarded in the revised diauxie model. Sulphate and sulphite reduction might be inhibited by the presence of nitrite, which presumably functions as a competitive inhibitor of *dsrAB.*

6.9 Regulation of genes responsible for nitrate reduction

A model of *nap* regulation by HcpR

It is difficult to determine how HcpR influences the transcription of its other targets. Presumably HcpR activates transcription of *split-soret* which putatively shuttles electrons to the Nap complex. Binding to the *nap* promoter seems highly likely and, in accordance with the proposed model of *hcpR* auto-regulation, this binding or active state should be induced in the presence of nitric oxide. However, from qRT-PCR results, *nap* expression does not correlate exactly with *hcpR* expression. Highest levels of *hcpR* were detected in the presence of nitrite when the levels of the *nap* transcript were approximately 75 % lower than in the presence of nitrate. Furthermore, nitrate reduction is completely repressed in the presence of sulphate or sulphite even when high levels of HcpR were detected by western blot. We can assume that HcpR has a positive effect upon *nap* expression since high levels are present in nitrate reducing cultures and since some induction of *nap* occurs in the presence of nitrite. However, maximal expression of *nap* requires at least one other regulatory factor. This could either be an additional nitrate-specific activator or a sulphate specific repressor. Indeed, it seems

most likely that both would be required to explain the qRT-PCR and western blot results.

A prime candidate for this role could be an unidentified protein that putatively binds to the two tandem DNA motifs, each referred to as site A, overlapping IR3. This site is comparatively large and an almost identical sequence is located upstream of the *nrf* operon. The presence of these sites at these loci is conserved in other species so coincidence seems unlikely. Furthermore, when searching for a DNA motif in a genome one would expect to find false sites within the coding regions of genes. These two loci were the only locations at which these tandem repeats were discovered. It is possible that these sites could be the targets for one or more nitrate responsive regulators that modulate transcription of *nap* and *nrf*. This scenario is analogous to *nap* and *nrf* regulation by the NarXL-NarQP systems in *E. coli*. A hypothetical model of regulation would therefore rely primarily upon a homologue of the NarXL-NarQP systems for activation of *nap* expression in the presence of nitrate. HcpR would function as a co-activator. However, HcpR could also potentially provide balance to the expression of *nap* in response to nitric oxide. In the presence of low levels of nitric oxide HcpR could act as an enhancer of *nap* transcription by binding to a single site, IR1, of the *nap* promoter. If nitric oxide levels were to become critically high this would increase the levels of HcpR. Once a threshold of HcpR levels had been reached then this regulator would begin occupying the less preferable sites, IR2 and IR3, potentially displacing the putative NarL-NarP response regulator and reducing the frequency of *nap* transcription until nitrosative stress had been alleviated. This mechanism would function as a safeguard against producing high levels of nitrite too quickly.

This model of *nap* regulation requires a repressor that is specific to sulphate-sulphite metabolism. A factor most likely to function as a signalling molecule is sulphide. Marietou (2009) proposed that another CRP homologue could compete with HcpR for the CRP-like sites of the *nap* operon. Possibly Ddes_1411 or Ddes_2092 could fulfil this role. Alternatively, one could speculate that an additional regulator could compete for the site A motifs. The activities of the transcription factor SsuR of *Corynebacterium glutamicum* are modulated by sulphate, APS, sulphite and sulphide so the potential exists (Koch *et al.*, 2005). Thus, in this model, activation of *nap* would be subject to nitrate specific activation, sulphide specific repression and be counter-balanced against nitric oxide generation. An overview of this model of *nap* regulation is given in Figure 6.4.

An alternative model of *nap* regulation by sigma-54

A candidate for binding to the site A motifs upstream of *nap* is found divergent from the *nrf* operon. Genes encoding a two-component hybrid sensor kinase and response regulator are located upstream of *nrf* and the intergenic region between these two operons encodes two site A motifs almost identical to those upstream of *nap*. A common regulatory factor activating expression of both *nap* and *nrf* in the presence of nitrate would make sense since nitrate reduction will inevitably lead to nitrite reduction. Rajeev *et al.* (2006) reported that the sensor histidine kinase upstream of the *nrf* operon in *D. vulgaris* is a hybrid sensor histidine kinase with more than one receiver domain, a characteristic of sensor histidine kinase systems that are involved in multi-step phospho-relay. Hybrid sensor histidine kinases tend to have relaxed specificity for phosphorylating response regulators allowing for increased cross-talk between two-component systems (Townsend *et al.*, 2013). Thus, the action of this two-component

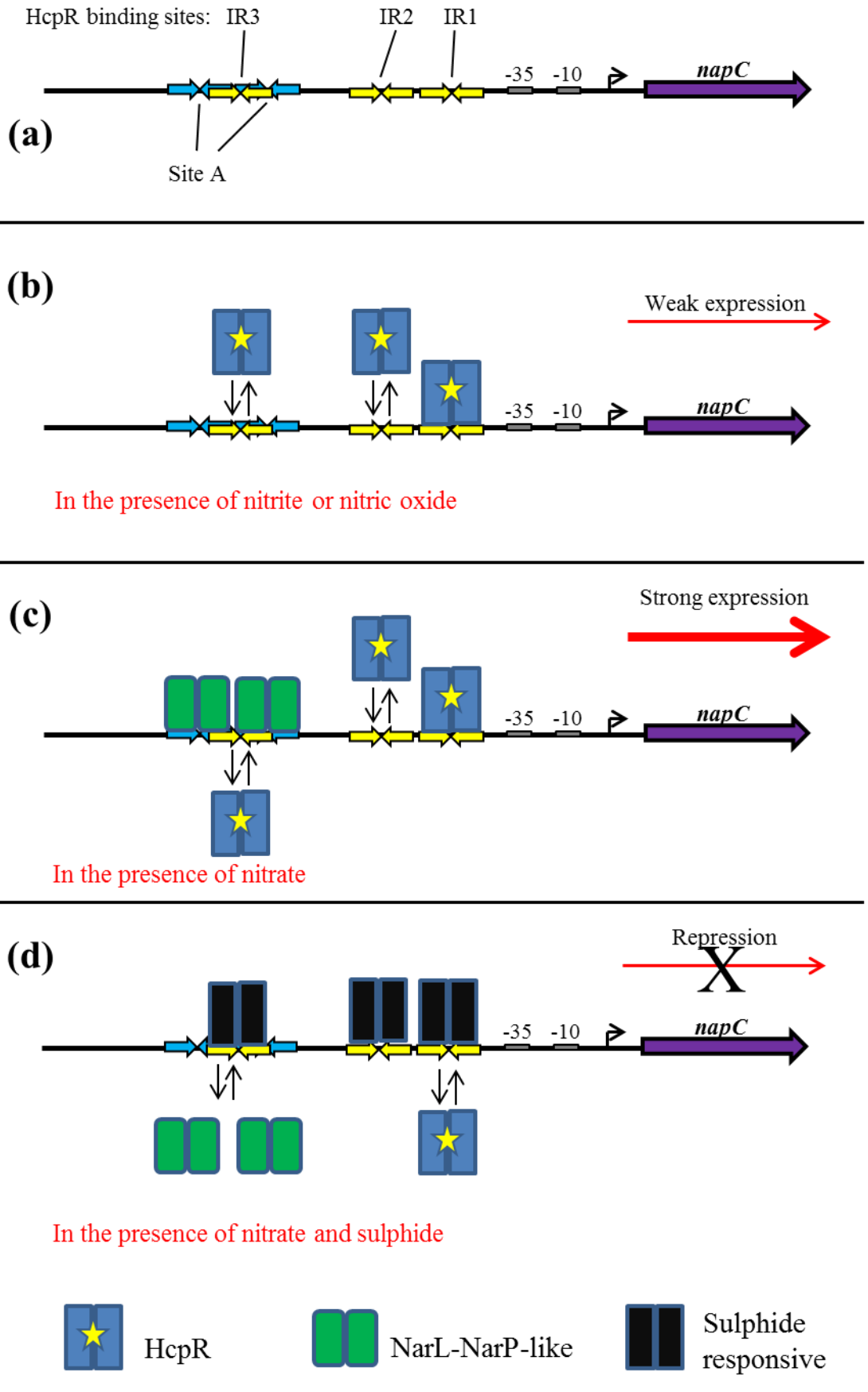

HcpR binding sites: IR3
IR2
IR1
-35
-10
napC
(a)
Site A
(b)
Weak expression
-35
-10
napC
In the presence of nitrite or nitric oxide
(c)
Strong expression
-35
-10
napC
In the presence of nitrate
(d)
Repression
X
-35
-10
napC
In the presence of nitrate and sulphide
HcpR
NarL-NarP-like
Sulphide responsive

Figure 6.4: Model of *nap* regulation dependent upon dual activation by HcpR and a NarL-NarP-like regulator with sigma-70 RNAP. (a) The architecture of the *nap* promoter. (b) In the presence of nitrite or nitric oxide alone HcpR is up-regulated and provides weak activation of *nap* expression. (c) In the presence of nitrate alone the NarL-NarP-like activator is present and active for influencing transcription. This binds to the *nap* promoter along with HcpR and activates transcription of *nap* by a class III mechanism. High levels of nitric oxide lead to increased HcpR production which then competes with NarL-NarP for binding. This competition for binding provides balance and prevents excessive *nap* expression. (d) In the presence of sulphide and nitrate an unidentified sulphide responsive regulator competes with HcpR for binding sites. This regulator, which functions as a repressor displaces both HcpR and the NarL-NarP-like regulator and competely represses *nap* expression in the presence of sulphide.

system seems likely to be complex but there is also the potential for it to exert regulatory control over both *nrf* and *nap* in response to different signals.

The cognate response regulator for this hybrid sensor kinase, Ddes_0084, has an AAA+ domain typical of sigma-54 dependent transcription activators. The *D. desulfuricans* genome encodes a sigma-54 subunit with 40 % identity to that of *E. coli* and sigma-54 dependent transcription activation of *D. vulgaris* genes has been demonstrated (Fiévet *et al.*, 2011). Previously, the *nap* promoter sequence had been considered with respect to the -35 and -10 promoter elements typical of sigma-70 promoters and consistent with those published by Marietou *et al.*, (2009). It seems that for Ddes_0084 to function as a transcription activator would require the activities of sigma-54. Indeed, examination of the *nap* and *nrf* promoters reveal the presence of sequences that are near perfect matches to the sigma-54 consensus sequence mrNrYTGGCACG[N_4]TTGCWNNNw (Barrios *et al.*, 1999). This putative sigma-54 promoter is perfectly positioned upstream of the experimentally proven transcription start site of the *nap* gene cluster (Figure 6.5). Thus, an alternative model can be created where expression of *nap* is dependent upon sigma-54, Ddes_0084 binding and a DNA bending transcription factor between the two (Figure 6.6).

Typically, in *E. coli*, the DNA bender at sigma-54 dependent promoters is IHF. Since it seems likely that HcpR bends DNA differently from CRP, as inferred from comparative EMSAs utilising these two proteins, HcpR could function by providing the necessary bend in the DNA between RNAP-sigma-54 and the two tandem Ddes_0084 units bound upstream. Repeats of TTTT, AAAA and TTAA have also been identified as being able to introduce DNA bends and have been linked to sigma-54 dependent transcription (Huo *et al.*, 2009). Alternatively, HcpR could again act as a repressor to balance the

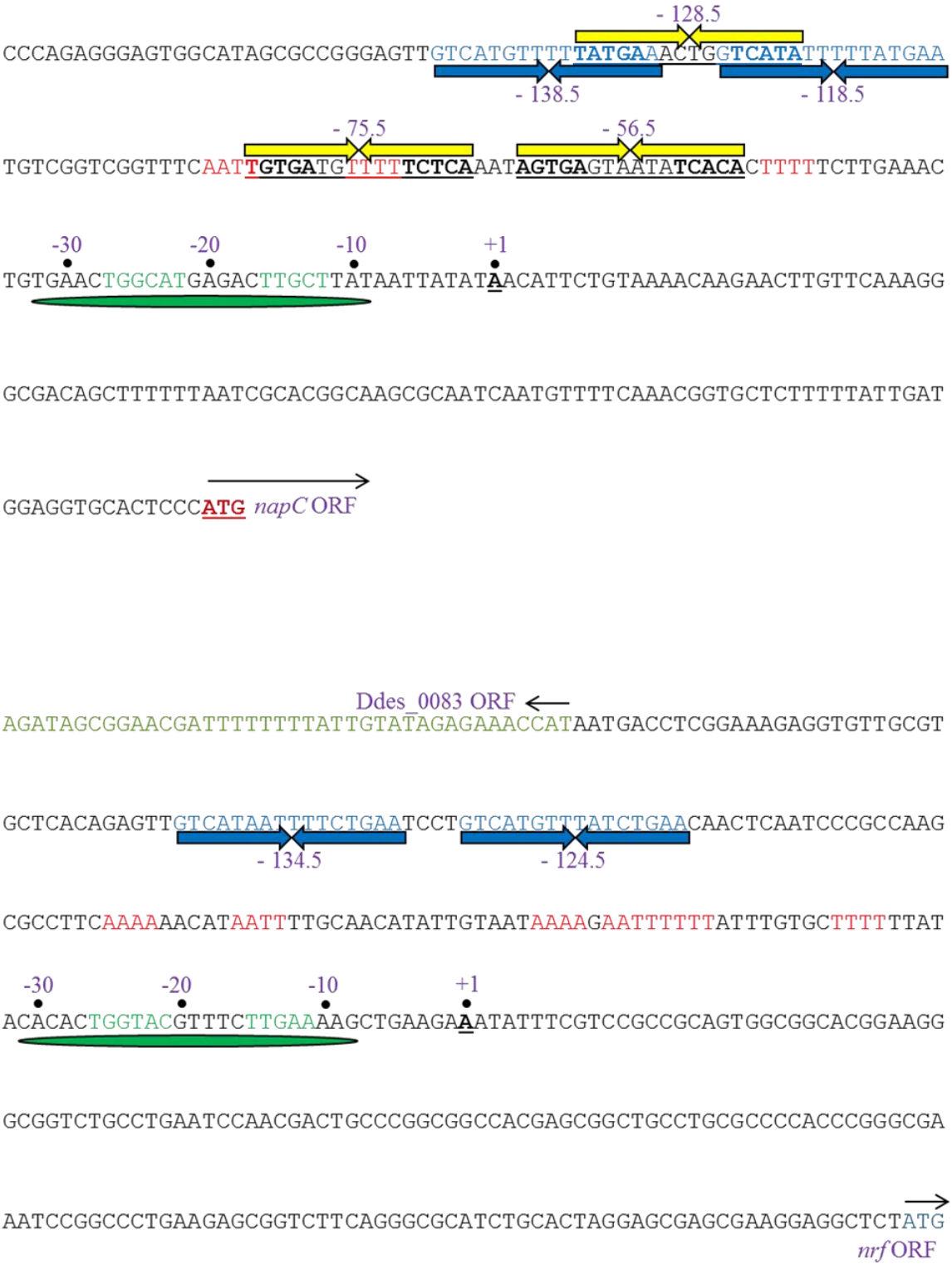

- 128.5
CCCAGAGGGAGTGGCATAGCGCCGGGAGTTGTCATGTTTTTATGAAACTGGTCATATTTTTATGAA
- 138.5
- 118.5
- 75.5
- 56.5
TGTCGGTCGGTTTCAATTGTGATGTTTTTCTCAAATAGTGAGTAATATCACACTTTTTCTTGAAAC
-30
-20
-10
+1
TGTGAACTGGCATGAGACTTGCTTATAATTATATAACATTCTGTAAAACAAGAACTTGTTCAAAGG
GCGACAGCTTTTTTAATCGCACGGCAAGCGCAATCAATGTTTTCAAACGGTGCTCTTTTTATTGAT
GGAGGTGCACTCCCATG napC ORF
Ddes_0083 ORF
AGATAGCGGAACGATTTTTTTTATTGTATAGAGAAACCATAATGACCTCGGAAAGAGGTGTTGCGT
GCTCACAGAGTTGTCATAATTTTCTGAATCCTGTCATGTTTATCTGAACAACTCAATCCCGCCAAG
- 134.5
- 124.5
CGCCTTCAAAAAACATAATTTTGCAACATATTGTAATAAAAGAATTTTTTATTTGTGCTTTTTTAT
-30
-20
-10
+1
ACACACTGGTACGTTTCTTGAAAAGCTGAAGAAATATTTCGTCCGCCGCAGTGGCGGCACGGAAGG
GCGGTCTGCCTGAATCCAACGACTGCCCGGCGGCCACGAGCGGCTGCCTGCGCCCCACCCGGGCGA
AATCCGGCCCTGAAGAGCGGTCTTCAGGGCGCATCTGCACTAGGAGCGAGCGAAGGAGGCTCTATG
nrf ORF

Figure 6.5: Sigma-54 elements at the *nap* and *nrf* promoters. (a) The *nap* promoter and (b) the Ddes_0083-*nrf* intergenic region. The ORFs are highlighted and labelled. The experimentally verified *nap* transcription start site and predicted *nrf* transcription start sites are labelled as +1. Sigma-54 consensus -12 and -24 sequences are highlighted green. HcpR sites are labelled with yellow arrows and are underlined. The putative Ddes_0084 binding sites are marked with blue arrows and sequences are highlighted blue. AAAA, TTTT and AATT sequences are highlighted red.

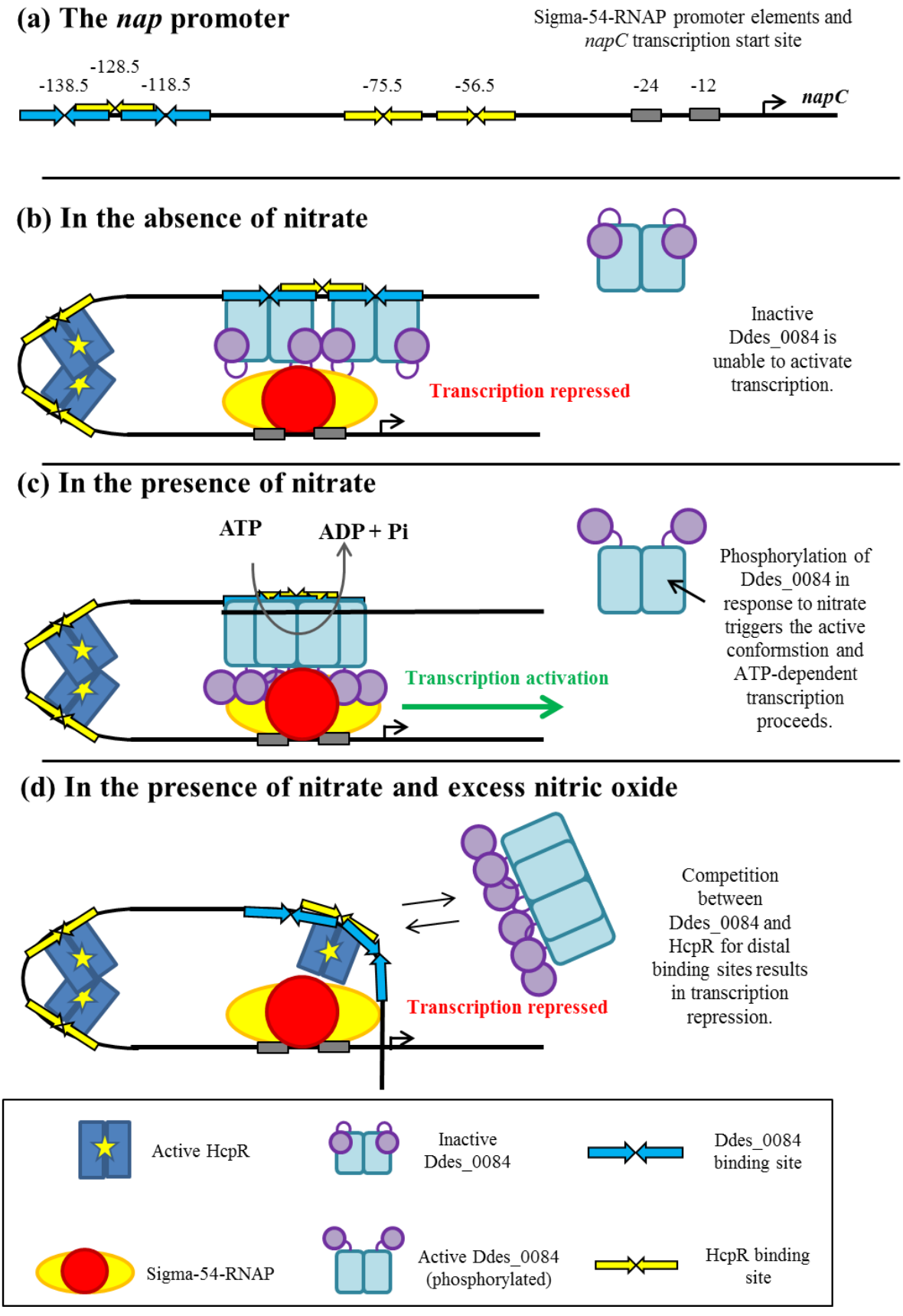

(a) The nap promoter
Sigma-54-RNAP promoter elements and napC transcription start site
-128.5
-138.5
-118.5
-75.5
-56.5
-24
-12
napC
(b) In the absence of nitrate
Transcription repressed
Inactive Ddes_0084 is unable to activate transcription.
(c) In the presence of nitrate
ATP
ADP + Pi
Transcription activation
Phosphorylation of Ddes_0084 in response to nitrate triggers the active conformstion and ATP-dependent transcription proceeds.
(d) In the presence of nitrate and excess nitric oxide
Transcription repressed
Competition between Ddes_0084 and HcpR for distal binding sites results in transcription repression.
Active HcpR
Inactive Ddes_0084
Ddes_0084 binding site
Sigma-54-RNAP
Active Ddes_0084 (phosphorylated)
HcpR binding site

Figure 6.6: A model of *nap* regulation by sigma-54. (a) The positioning of putative regulatory elements at the *nap* promoter. (b) In the absence of nitrate Ddes_0084 is inactive and, although able to bind its DNA target sites, is unable to activate transcription of *nap*. Two HcpR dimers bound to the *nap* promoter proximal region introduce a bend in the DNA of ~180º. (c) In the presence of nitrate, Ddes_0084 becomes phosphorylated by its cognate sensor kinase, Ddes_0083. Phosphorylation relieves intramolecular inhibition of Ddes_0084, permitting ATP hydrolysis by the Ddes_0084 AAA+ domain. Multimers of active Ddes_0084 promote sigma-54-dependent transcription of *nap*. (d) In the presence of excess nitric oxide the levels of HcpR reach a threshold and competition between Ddes_0084 and HcpR for DNA binding occurs and transcription is repressed. Of the three HcpR binding sites of the *nap* promoter, the distal site is bound with the lowest affinity. Thus, this feedback mechanism only occurs in the presence of high levels of HcpR.

generation of nitrite producd from nitrate reduction. The activity of Ddes_0084 at the *nrf* promoter would be the similar allowing for enhanced transcription in response to nitrate. Ddes_0084 would simultaneously repress transcription from its own promoter in a manner reminiscent to how NorR from *E. coli*, which both interacts with sigma-54 and also regulates its own expression and that of NorVW from intergenic sites between these two transcription units (Tucker *et al*., 2004).

Regulation of nitrite reductase

Previous controversies regarding nitrite reduction by *D. desulfuricans* have been addressed in this study. Nitrite reduction and expression of *nrf* may be regarded as constitutive in the sense that cells are able to reduce nitrite without a lengthy period of induction. However, levels of *nrf* and rates of nitrite reduction are up-regulated in response to nitrite. Being equipped with a basal level of nitrite reductase sufficient to reduce nitrite is likely to be important in surviving transient changes in nitrite levels. Nitrite is very toxic to *D. desulfuricans* with sulphate adapted cells being killed at relatively low concentrations. Growth of a *D. vulgaris nrfA* mutant was severely inhibited in the presence of sulphate and nitrite compared with wild-type cells indicating the importance of nitrite removal for survival (Haveman *et al*., 2004). As indicated in the present study, pre-adaptation to nitrate-nitrite dependant growth increases survival of *D. desulfuricans* in the presence of increased concentrations of nitrite. Thus, the constitutive reduction of nitrite is advantageous and represents a trade-off between cellular economy and survival. To express *nrf* at levels sufficient to survive severe nitrite shock constantly would be wasteful but to not express at all could be suicidal. Nitrite severely inhibits growth in the presence of sulphite and, to a lesser extent, sulphate so constitutive expression of *nrf* is important. Expression of *nrf* seems

to be independent of nitric oxide. This is perhaps surprising considering that it is a known nitric oxide reductase in *E. coli* (Poock *et al.*, 2002; van Wonderen *et al.*, 2008).

As already discussed, up-regulation of *nrf* is likely to be due to the activities of Ddes_0084 binding to the two upstream site A motifs. DNA binding by the divergent response regulator from *D. vulgaris* to the *nrfHA* intergenic region has been demonstrated *in vitro* but the specific location of binding has not been predicted or determined (Rajeev *et al*., 2011). The intergenic DNA fragment used in EMSAs in that study shifted twice in the presence of the response regulator supporting the hypothesis made in the current study that motif A is actually two binding sites (Rajeev *et al.*, 2011). For Ddes_0084 to mediate a nitrate specific response at the *nap* operon there must be some unidentified factor distinguishing the *nap* and *nrf* promoters.

6.9 HcpR proteins and the environment

The HcpR proteins of *D. desulfuricans* are distinctive from those of *D. vulgaris* and *D.* G20 and represent novel branches of the HcpR family. HcpR and its loci from *D. desulfuricans* are similar to those of the SRB *Desulfovibrio* sp. 3_1_syn3 and *Desulfovibrio* sp. 6_4_6AFAA whereas HcpR2 and its loci more closely resemble those of some *Clostridia* species. Thus, *D. desulfuricans* may be regarded as an intermediate between these groups of bacteria with respect to HcpR. These species reside within a common niche - the gastrointestinal tracts of higher organisms.

The genomes of *Desulfovibrio* sp. 3_1_syn3, *Desulfovibrio* sp. 6_4_6AFAA and several other species used for comparison in Chapter 3 were sequenced as reference genomes for the Human Microbiome Project (Peterson *et al.*, 2009). It seems likely that the operons encoding HcpR proteins and their corresponding transcription partners are

propagated in bacterial populations by a combination of vertical and horizontal gene transfer. If this idea is correct then those species possessing *hcpR* and the transmission of *hcpR* could be important in shaping the dynamic changes in the relative abundances of constituent bacterial species in communities of the human gut.

Since *hcpR* operons seem highly likely to confer increased resistance to nitric oxide, those bacteria that are able to obtain this cassette are likely to have improved fitness against the immune responses of the host organism. Although SRB have not been directly linked to human bowel diseases, numerous articles have hypothesised or posed the question that the levels, activities and metabolic products of SRB could be a contributory or causative factor in these diseases (Pitcher *et al.*, 1996; Rowan *et al.*, 2010; Jia *et al*., 2012; Sartor, 2008; McKay, 2001). Furthermore, if the *wrbA-nimA* gene products do indeed confer resistance to nitroimidazoles then these groups of bacteria would also have increased fitness in the face of imposed selective pressures in the human gut. Nitroimidazoles have been described as 'the drug of choice' for dealing with gut infections (Löfmark *et al.*, 2010).. In recent years the efficacy of these drugs has declined. Particularly, numerous cases of *C. difficile* infections have failed to clear following treatment with the nitroimidazole, metronidazole (Miller, 2007). The activities of NimA-type proteins have been highlighted as a major route to resistance (Löfmark *et al*., 2010). As highlighted in the current study, several *Clostridium* species have been identified as containing *ylbA-hcpR2* operons similar to that of *D. desulfuricans.* Potentially, HcpR proteins and their targets could aid in the resistance and proliferation of certain bacteria during following the devastation upon the gut microbiome following nitroimidazole treatment.

A recent study using high-throughput sequencing reported that the ratio of certain SRB and SiRB species changed in patients suffering from ulcerative colitis or Crohn's disease following treatment. Also, one unidentified SRB species was present only in certain patient groups (Jia *et al*., 2012). Individuals suffering from ulcerative colitis or Crohn's disease tend to have elevated levels of nitric oxide present in the bowels as a result of increased nitric oxide synthase activity by the patient (Rachmilewitz *et al.*, 1995). Drugs commonly used for treatment of these diseases resulted in a decrease in this nitric oxide synthase activity. Potentially, nitric oxide could be the driving force for selection of certain bacterial species, leading to disequilibrium of the microbiota in the bowels of patients suffering from these diseases. Nitroimidazoles drive selection in a similar way. Potentially, bacteria with resistance to host-derived nitric oxide could play a part in human gut diseases and dysfunction.

Another major niche occupied by SRB is in soils. Here too the NimA-WrbA gene products could an important role in survival since nitroimidazoles are produced in the environment by soil-dwelling *Streptomyces* species. Although *Streptomyces* are regarded as aerobes, interactions between them and anaerobic SRB are still extremely likely since the highest densities of SRB in a particular habitat are usually found at the aerobic-anaerobic interface. Could the gene products of the HcpR regulon play a role in co-habitation of SRB and other bacterial species? Since gene knock-outs of *hcpR* lead to compromised resilience to nitric oxide the importance of HcpR in survival seems certain (Lewis *et al.*, 2012; Zhou *et al*., 2012).

6.10 Final conclusions

For any bacterium to thrive it is imperative that it should be able to respond to its surroundings. Transient changes in the environment must be sensed and an appropriate response mediated. *D. desulfuricans* is able to utilise a range of terminal electron acceptors and the way in which these are selected is complex. Sulphate and sulphite reductases are expressed constitutively and utilisation of these terminal electron acceptors seems to be independent of the regulatory processes of selection. In stark contrast with this system, nitrate reduction by *D. desulfuricans* is subject to tight regulation. Superficially, from studying sequences upstream of the *nap* gene cluster, it would seem that nitrate reductase is regulated by HcpR in a manner reminiscent of how different carbon sources are selected by CRP in *E. coli*. However, HcpR, although able to bind its promoter, is not able to activate *nap* expression alone. It is proposed that expression of *nap* is primarily reliant upon the activities of the two component regulatory system Ddes_0083-Ddes_0084 and also sigma-54. These regulators are also believed to enhance the constitutive expression of *nrf* in a similar way. Despite all the clues, HcpR seems to be primarily involved in the regulation of genes responsible for a different, but related, process.

In addition to detecting and selecting nutrients it is crucial that *D. desulfuricans* and related bacteria that reside within the human gut be able to sense and resist nitrosative stress. Central to this resistance are the gene products of *hcp, dfx, rbo* and *roo*. These defence proteins are produced in abundance when nitric oxide is detected and must be crucial for its detoxification or related processes. In *D. desulfuricans* two additional proteins, homologues of WrbA and NimA, are also part of a cascade of expression in

response to nitric oxide. Their exact functions in the face of this stress are unknown. Mediating this cascade of expression are HcpR and HcpR2. These proteins are able to bind to discrete DNA motifs upstream of the aforementioned stress response genes. Their exact activities at these loci are likely to be activation of transcription in response to nitric oxide, directly sensing the stress signal and mediating response. The persistence of HcpR long after the initial stress provides circumstantial evidence that this factor could be central in protecting *D. desulfuricans* against sustained or repeated nitrosative stress.

The findings of this study indicate the importance and diversity of HcpR proteins and provide information with obvious relevance and applicability to a wide range of bacteria identified in the human microbiome project. Additionally, many new questions are proposed regarding the transcriptional networks of *D. desulfurcicans* and related bacteria. The cascade of *wrbA* and *nimA* expression has been identified as a prime candidate for further research exploring how bacteria are able to cope with nitrosative stress.

References

Abreu, I. A., Lourenço, A. I., Xavier, A. V., LeGall, J., Coelho, A. V., Matias, P. M. and Saraiva, L. M. (2003). A novel iron centre in the split-soret cytochrome *c* from *Desulfovibrio desulfuricans* ATCC 27774. *J Biol Inorg Chem* **8**: 360-370.

Afshar, S., Kim, C., Monbouquette, H. G. and Schröder, I. (1998). Effect of tungstate on nitrate reduction by the hyperthermophilic archaeon *Pyrobaculum aerophilum*. *Appl Environ Microb* **64**: 3004-3008.

Almeida, M. G., Macieira, S., Gonçalves, L. L., Huber, R., Cunha, C. A., Romão, M. J. and Moura, I. (2003). The isolation and characterization of cytochrome *c* nitrite reductase subunits (NrfA and NrfH) from *Desulfovibrio desulfuricans* ATCC 27774. *Eur J Biochem* **270**: 3904-3915.

Andrade, S. L., Patridge, E. V., Ferry, J. G. and Einsle, O. (2007). Crystal structure of the NADH: quinone oxidoreductase WrbA from *Escherichia coli*. *J Bacteriol* **189**: 9101-9107.

Antipov, A. N., Lyalikova, N. N., Khijniak, T. V. and L'vov, N. P. (1998). Molybdenum-free nitrate reductases from vanadate-reducing bacteria. *FEBS Lett* **441**: 257-260.

Aono, S., Takasaki, H., Unno, H., Kamiya, T. and Nakajima, H. (1999). Recognition of target DNA and transcription activation by the CO-sensing transcriptional activator CooA. *Biochem Bioph Res Co* **261**: 270-275.

Arendsen, A. F., Hadden, J., Card, G., McAlpine, A. S., Bailey, S., Zaitsev, V., Duke, E. H. M. and Hagen, W. R. (1998). The "prismane" protein resolved: X-ray structure at 1.7 Å and multiple spectroscopy of two novel 4Fe clusters. *J Biol Inorg Chem* **3**: 81-95.

Arnoux, P., Sabaty, M., Alric, J., Frangioni, B., Guigliarelli, B., Adriano, J. M. and Pignol, D. (2003). Structural and redox plasticity in the heterodimeric periplasmic nitrate reductase. *Nat Struct Mol Biol* **10**: 928-934.

Ascenso, C., Rusnak, F., Cabrito, I., Lima, M. J., Naylor, S., Moura, I. and Moura, J. J. (2000). Desulfoferrodoxin: a modular protein. *J Biol Inorg Chem* **5**: 720-729.

Attey, A., Belyaeva, T., Hoggett, J., Fujita, N., Ishihama, A. and Busby, S. (1994). Interactions between the cyclic AMP receptor protein and the alpha subunit of RNA polymerase at the *Escherichia coli* galactose operon P1 promoter. *Nucleic Acids Res* **22**: 4375-4380.

Auchère, F., Pauleta, S. R., Tavares, P., Moura, I. and Moura, J. J. (2006). Kinetics studies of the superoxide-mediated electron transfer reactions between rubredoxin-type proteins and superoxide reductases. *J Biol Inorg Chem* **11**: 433-444.

Bailey, T. L., Boden, M., Buske, F. A., Frith, M., Grant, C. E., Clementi, L. and Noble, W. S. (2009). MEME SUITE: tools for motif discovery and searching. *Nucleic Acids Res* **37**: 202-208.

Balsalobre, C., Johansson, J. and Uhlin, B. E. (2006). Cyclic AMP-dependent osmoregulation of *crp* gene expression in *Escherichia coli*. *J Bacteriol* **188**: 5935-5944.

Bamford, V. A., Angove, H. C., Seward, H. E., Thomson, A. J., Cole, J. A., Butt, J. N., Hemmings, A. M. and Richardson, D. J. (2002). Structure and spectroscopy of the periplasmic cytochrome *c* nitrite reductase from *Escherichia coli*. *Biochemistry* **41**: 2921-2931.

Barrios, H., Valderrama, B. and Morett, E. (1999). Compilation and analysis of σ54-dependent promoter sequences. *Nucleic Acids Res* **27**: 4305-4313.

Barton, L. L. and Fauque, G. D. (2009). Biochemistry, Physiology and Biotechnology of Sulfate-Reducing Bacteria. *Adv Appl Microbiol* **68**: 41-98.

Baumann, A. and Denk, V. (1950). Zur Physiologie der Sulfatreduktion. *Arch Mikrobiol* **15**: 283-307.

Baumgarten, A., Redenius, I., Kranczoch, J. and Cypionka, H. (2001). Periplasmic oxygen reduction by *Desulfovibrio* species. *Arch Microbiol* **176**: 306-309.

Beatty, C. M., Browning, D. F., Busby, S. J. and Wolfe, A. J. (2003). Cyclic AMP receptor protein-dependent activation of the *Escherichia coli acsP2* promoter by a synergistic class III mechanism. *J Bacteriol* **185**: 5148-5157.

Bell, A. I., Gaston, K. L., Cole, J. A. and Busby, S. J. W. (1989). Cloning of binding sequences for the *Escherichia coli* transcription activators, FNR and CRP: location of bases involved in discrimination between FNR and CRP. *Nucleic Acids Res* **17**: 3865-3874.

Bell, A., Gaston, K., Williams, R., Chapman, K., Kolb, A., Buc, H., Minchin, S., Williams, J. and Busby, S. (1990). Mutations that alter the ability of the *Escherichia coli* cyclic AMP receptor protein to activate transcription. *Nucleic Acids Res* **18**: 7243-7250.

Benoff, B., Yang, H., Lawson, C. L., Parkinson, G., Liu, J., Blatter, E., Ebright, Y. W., Berman, H. M. and Ebright, R. H. (2002). Structural basis of transcription activation: the CAP-αCTD-DNA complex. *Science* **297**: 1562-1566.

van den Berg, W. A., Hagen, W. R. and van Dongen, W. M. (2000). The hybrid-cluster protein ('prismane protein') from *Escherichia coli*. *Eur J Biochem* **267**: 666-676.

Bertero, M. G., Rothery, R. A., Palak, M., Hou, C., Lim, D., Blasco, F., Weiner, J. H. and Strynadka, N. C. (2003). Insights into the respiratory electron transfer pathway from the structure of nitrate reductase A. *Nat Struct Mol Biol* **10**: 681-687.

Beynon, J. D., MacRae, I. J., Huston, S. L., Nelson, D. C., Segel, I. H. and Fisher, A. J. (2001). Crystal structure of ATP sulfurylase from the bacterial symbiont of the hydrothermal vent tubeworm *Riftia pachyptila*. *Biochemistry* **40**: 14509-14517.

Blasco, F., Iobbi, C., Ratouchniak, J., Bonnefoy, V. and Chippaux, M. (1990). Nitrate reductases of *Escherichia coli*: sequence of the second nitrate reductase and comparison with that encoded by the *narGHJI* operon. *Mol Gen Genet* **222**: 104-111.

Blasco, F., Dos Santos, J. P., Magalon, A., Frixon, C., Guigliarelli, B., Santini, C. L. and Giordano, G. (1998). NarJ is a specific chaperone required for molybdenum cofactor assembly in nitrate reductase A of *Escherichia coli*. *Mol Microbiol* **28**: 435-447.

Boopathy, R. (2009). Anaerobic Metabolism and Bioremediation of Explosives-Contaminated Soil. In *Advances in Applied Bioremediation* (pp. 151-172). Springer Berlin Heidelberg.

Bradley, M. E., Rest, J. S., Li, W. H. and Schwartz, N. B. (2009). Sulfate activation enzymes: phylogeny and association with pyrophosphatase. *J Mol Evol* **68**: 1-13.

Brigé, A., Leys, D., Meyer, T. E., Cusanovich, M. A. and Van Beeumen, J. J. (2002). The 1.25 Å resolution structure of the diheme NapB subunit of soluble nitrate reductase reveals a novel cytochrome *c* fold with a stacked heme arrangement. *Biochemistry* **41**: 4827-4836.

Brioukhanov, A., Pieulle, L. and Dolla, A. (2010). Antioxidative Defence Systems of Anaerobic Sulfate-Reducing Microorganisms. *Current Research, Technology and Education Topics in Applied Microbiology and Microbial Biotechnology* **1**: 148-159.

Brondijk, T., Nilavongse, A., Filenko, N., Richardson, D. and Cole, J. (2004). NapGH components of the periplasmic nitrate reductase of *Escherichia coli* K-12: location, topology and physiological roles in quinol oxidation and redox balancing. *Biochem. J* **379**: 47-55.

Browning, D. F. and Busby, S. J. (2004). The regulation of bacterial transcription initiation. *Nat Rev Microbiol* **2**: 57-65.

Browning, D. F., Grainger, D. C., Beatty, C. M., Wolfe, A. J., Cole, J. A. and Busby, S. J. (2005). Integration of three signals at the *Escherichia coli nrf* promoter: a role for Fis protein in catabolite repression. *Mol Microbiol* **57**: 496-510.

Brumlik, M. J. and Voordouw, G. (1989). Analysis of the transcriptional unit encoding the genes for rubredoxin (*rub*) and a putative rubredoxin oxidoreductase (*rbo*) in *Desulfovibrio vulgaris* Hildenborough. *J Bacteriol* **171**: 4996-5004.

Brune, A., Frenzel, P. and Cypionka, H. (2000). Life at the oxic–anoxic interface: microbial activities and adaptations. *FEMS Microbiol Rev* **24**: 691-710.

Busby, S., Kotlarz, D. and Buc, H. (1983). Deletion mutagenesis of the *Escherichia coli* galactose operon promoter region. *J Mol Biol* **167**: 259-274.

Busby, S. and Ebright, R. H. (1997). Transcription activation at Class II CAP-dependent promoters. *Mol Microbiol* **23**: 853-859.

Busby, S. and Ebright, R. H. (1999). Transcription activation by catabolite activator protein (CAP). *J Mol Biol* **293**: 199-213.

Bush, M., Ghosh, T., Tucker, N., Zhang, X. and Dixon, R. (2011). Transcriptional regulation by the dedicated nitric oxide sensor, NorR: a route towards NO detoxification. *Biochem Soc T* **39**: 289.

Cartron, M., Roldan, M., Ferguson, S., Berks, B. and Richardson, D. (2002). Identification of two domains and distal histidine ligands to the four haems in the bacterial *c*-type cytochrome NapC; the prototype connector between quinol/quinone and periplasmic oxido-reductases. *Biochem J* **368**: 425-432.

Casadaban, M. J. and Cohen, S. N. (1980). Analysis of gene control signals by DNA fusion and cloning in *Escherichia coli*. *J Mol Biol* **138**: 179-207.

Caffrey, S. M. and Voordouw, G. (2010). Effect of sulfide on growth physiology and gene expression of *Desulfovibrio vulgaris* Hildenborough. *Antonie van Leeuwenhoek* **97**: 11-20.

Chen, L., Liu, M. Y., Legall, J., Fareleira, P., Santos, H. and Xavier, A. V. (1993). Rubredoxin oxidase, a new flavo-hemo-protein, is the site of oxygen reduction to water by the" strict anaerobe" *Desulfovibrio gigas*. *Biochem Bioph Res Co* **193**: 100-105.

Chen, L., Sharma, P., Gall, J., Mariano, A. M., Teixeira, M. and Xavier, A. V. (1994). A Blue Non-Heme Iron Protein from *Desulfovibrio gigas*. *Eur J Biochem* **226**: 613-618.

Chiang, Y. L., Hsieh, Y. C., Fang, J. Y., Liu, E. H., Huang, Y. C., Chuankhayan, P., Jeyakathan, J., Liu, M. Y., Chan, S. I. and Chen, C. J. (2009). Crystal structure of adenylylsulfate reductase from *Desulfovibrio gigas* suggests a potential self-regulation mechanism involving the C terminus of the β-subunit. *J Bacteriol* **191**: 7597-7608.

Chin, K. H., Lee, Y. C., Tu, Z. L., Chen, C. H., Tseng, Y. H., Yang, J. M., ... and Chou, S. H. (2010). The cAMP Receptor-Like Protein CLP Is a Novel c-di-GMP Receptor Linking Cell–Cell Signaling to Virulence Gene Expression in *Xanthomonas campestris*. *J Mol Biol* **396**: 646-662.

Coelho, C., González, P. J., Moura, J. G., Moura, I., Trincão, J. and João Romão, M. (2011). The Crystal Structure of *Cupriavidus necator* Nitrate Reductase in Oxidized and Partially Reduced States. *J Mol Biol* **408**: 932-948.

Cole, J. (1996). Nitrate reduction to ammonia by enteric bacteria: redundancy, or a strategy for survival during oxygen starvation? *FEMS Microbiol Lett* **136**: 1-11.

Constantinidou, C., Hobman, J. L., Griffiths, L., Patel, M. D., Penn, C. W., Cole, J. A. and Overton, T. W. (2006). A reassessment of the FNR regulon and transcriptomic analysis of the effects of nitrate, nitrite, NarXL, and NarQP as *Escherichia coli* K12 adapts from aerobic to anaerobic growth. *J Biol Chem* **281**: 4802-4815.

Corker, H. and Poole, R. K. (2003). Nitric Oxide Formation by *Escherichia coli* dependence on nitrite reductase, the no-sensing regulator Fnr, and flavohemoglobin Hmp. *J Biol Chem* **278**: 31584-31592.

Crack, J., Jervis, A., Gaskell, A., White, G., Green, J., Thomson, A. and Lebrun, N. (2008). Signal perception by FNR: the role of the iron-sulfur cluster. *Biochem Soc T* **36**: 1144.

Crack, J. C., Gaskell, A. A., Green, J., Cheesman, M. R., Le Brun, N. E. and Thomson, A. J. (2008). Influence of the environment on the [4Fe-4S] $^{2+}$ to [2Fe-2S] $^{2+}$ cluster switch in the transcriptional regulator FNR. *J Am Chem Soc* **130**: 1749-1758.

Crane, B. R., Siegel, L. M. and Getzoff, E. D. (1995). Sulfite reductase structure at 1.6 Å: Evolution and catalysis for reduction of inorganic anions. *Science* **270**: 59-67.

Crane, B. R. and Getzoff, E. D. (1996). The relationship between structure and function for the sulfite reductases. *Curr Opin Struc Biol* **6**: 744-756.

de Crombrugghe, B., Busby, S. and Buc, H. (1984). Activation of transcription by the cyclic AMP receptor protein. *Biological regulation and development* **3**: 129-167.

Cypionka, H. (1986). Sulfide-controlled continuous culture of sulfate-reducing bacteria. *J Microbiol Meth* **5**: 1-9.

Cypionka, H. (2000). Oxygen Respiration by *Desulfovibrio Species*. *Ann Rev Microbiol* **54**: 827-848.

Cypionka, H. and Pfennig, N. (1986). Growth yields of *Desulfotomaculum orientis* with hydrogen in chemostat culture. *Arch Microbiol* **143**: 396-399.

Dalsgaard, T. and Bak, F. (1994). Nitrate reduction in a sulfate-reducing bacterium, *Desulfovibrio desulfuricans*, isolated from rice paddy soil: sulfide inhibition, kinetics, and regulation. *Appl Environ Microb* **60**: 291-297.

Darwin, A., Tormay, P., Page, L., Griffiths, L. and Cole, J. (1993). Identification of the formate dehydrogenases and genetic determinants of formate-dependent nitrite reduction by *Escherichia coli* K12. *J Gen Microbiol* **139**: 1829-1840.

D'Autréaux, B., Tucker, N. P., Dixon, R. and Spiro, S. (2005). A non-haem iron centre in the transcription factor NorR senses nitric oxide. *Nature* **437**: 769-772.

Devreese, B., Costa, C., Demol, H., Papaefthymiou, V., Moura, I., Moura, J. J. and Beeumen, J. (1997). The Primary Structure of the Split-Soret Cytochrome *c* from *Desulfovibrio desulfuricans* ATCC 27774 Reveals an Unusual Type of Diheme Cytochrome *c*. *Eur J Biochem* **248**: 445-451.

Dias, J. M., Than, M. E., Humm, A., Huber, R., Bourenkov, G. P., Bartunik, H. D., Bursakov, S. and Romão, M. J. (1999). Crystal structure of the first dissimilatory nitrate reductase at 1.9 Å solved by MAD methods. *Structure* **7**: 65-79.

Dolla, A., Fournier, M. and Dermoun, Z. (2006). Oxygen defense in sulfate-reducing bacteria. *J Biotechnol* **126**: 87-100.

Don, R. H., Cox, P. T., Wainwright, B. J., Baker, K. and Mattick, J. S. (1991). 'Touchdown' PCR to circumvent spurious priming during gene amplification. *Nucleic Acids Res* **19**: 4008.

Dunwell, J. M., Culham, A., Carter, C. E., Sosa-Aguirre, C. R. and Goodenough, P. W. (2001). Evolution of functional diversity in the cupin superfamily. *Trends Biochem Sci* **26**: 740-746.

Dunwell, J. M., Purvis, A. and Khuri, S. (2004). Cupins: the most functionally diverse protein superfamily? *Phytochemistry* **65**: 7-17.

Ebright, R. H. (1993). Transcription activation at Class I CAP-dependent promoters. *Mol Microbiol* **8**: 797-802.

Evans, C. L. (1967). The toxicity of hydrogen sulphide and other sulphides. *Exp Physiol* **52**: 231-248.

Fang, J. Y., Chiang, Y. L., Hsieh, Y. C., Wang, V. C. C., Huang, Y. C., Chuankhayan, P. and Chen, C. J. (2011). Crystallization of adenylylsulfate reductase from *Desulfovibrio gigas*: a strategy based on controlled protein oligomerization. *Cryst Growth Des* **11**: 2127-2134.

Fauque, G. D. and Barton, L. L. (2012). Hemoproteins in Dissimilatory Sulfate-and Sulfur-Reducing Prokaryotes. *Adv Microb Physiol* **60**, 2.

Fava, F. and Danese, S. (2011). Intestinal microbiota in inflammatory bowel disease: friend of foe? *World Journal of Gastroenterology: WJG* **17**: 557.

Fiévet, A., Cascales, E., Ansaldi, M., Pauleta, S. R., Moura, I., Dermoun, Z. and Aubert, C. (2011). The Anaerobe-Specific Orange Protein Complex of *Desulfovibrio vulgaris* Hildenborough Is Encoded by Two Divergent Operons Coregulated by σ54 and a Cognate Transcriptional Regulator. *J Bacteriol* **193**: 3207-3219.

Figueiredo, M. C., Lobo, S. A., Carita, J. N., Nobre, L. S. and Saraiva, L. M. (2012). Bacterioferritin protects the anaerobe *Desulfovibrio vulgaris* Hildenborough against oxygen. *Anaerobe* **18**: 454-458.

Filenko, N. A., Browning, D. F. and Cole, J. A. (2005). Transcriptional regulation of a hybrid cluster (prismane) protein. *Biochem Soc T* **33**: 195-197.

Filenko, N., Spiro, S., Browning, D. F., Squire, D., Overton, T. W., Cole, J. and Constantinidou, C. (2007). The NsrR regulon of *Escherichia coli* K-12 includes genes encoding the hybrid cluster protein and the periplasmic, respiratory nitrite reductase. *J Bacteriol* **189**: 4410-4417.

Fisher, D. S. and Price, D. C. (1964). Iron determination with TPTZ (tripyriyltriazine: acid labile iron) in protein. *Clin. Chem* **10**: 21-31.

Forrester, M. T. and Foster, M. W. (2012). Protection from nitrosative stress: A central role for microbial flavohemoglobin. *Free Radical Bio Med* **52**: 1620-1633.

Frazão, C., Silva, G., Gomes, C. M., Matias, P., Coelho, R., Sieker, L., ... and Le Gall, J. (2000). Structure of a dioxygen reduction enzyme from *Desulfovibrio* gigas. *Nat Struct Mol Biol* **7**: 1041-1045.

Gallagher, D. T., Smith, N., Kim, S. K., Robinson, H. and Reddy, P. T. (2009). Profound asymmetry in the structure of the cAMP-free cAMP receptor protein (CRP) from *Mycobacterium tuberculosis*. *J Biol Chem* **284**: 8228-8232.

Gardner, P. R., Costantino, G., Szabó, C. and Salzman, A. L. (1997). Nitric oxide sensitivity of the aconitases. *J Biol Chem* **272**: 25071-25076.

Gardner, A. M. and Gardner, P. R. (2002). Flavohemoglobin detoxifies nitric oxide in aerobic, but not anaerobic, *Escherichia coli* evidence for a novel inducible anaerobic nitric oxide-scavenging activity. *J Biol Chem* **277**: 8166-8171.

Gardner, A. M., Helmick, R. A. and Gardner, P. R. (2002). Flavorubredoxin, an inducible catalyst for nitric oxide reduction and detoxification in *Escherichia coli*. *J Biol Chem* **277**: 8172-8177.

Gardner, P. R. (2012). Hemoglobin: A Nitric-Oxide Dioxygenase. *Scientifica, 2012*.

Gaston, K., Bell, A., Kolb, A., Buc, H. and Busby, S. (1990). Stringent spacing requirements for transcription activation by CRP. *Cell* **62**: 733-743.

Gaudu, P. and Weiss, B. (1996). SoxR, a [2Fe-2S] transcription factor, is active only in its oxidized form. *Proc Natl Acad Sci* **93**: 10094-10098.

Gibson, G. R. (1990). Physiology and ecology of the sulphate-reducing bacteria. *J Appl Microbiol* **69**: 769-797.

Giel, J. L., Rodionov, D., Liu, M., Blattner, F. R. and Kiley, P. J. (2006). IscR-dependent gene expression links iron-sulphur cluster assembly to the control of O_2-regulated genes in *Escherichia coli*. *Mol Microbiol* **60**: 1058-1075.

Giuffrè, A., Borisov, V. B., Mastronicola, D., Sarti, P. and Forte, E. (2012). Cytochrome *bd* oxidase and nitric oxide: From reaction mechanisms to bacterial physiology. *FEBS Lett* **586**: 622-629.

Gomes, C. M., Silva, G., Oliveira, S., LeGall, J., Liu, M. Y., Xavier, A. V., ... and Teixeira, M. (1997). Studies on the redox centers of the terminal oxidase from *Desulfovibrio gigas* and evidence for its interaction with rubredoxin. *J Biol Chem* **272**: 22502-22508.

Gomes, C. M., Giuffrè, A., Forte, E., Vicente, J. B., Saraiva, L. M., Brunori, M. and Teixeira, M. (2002). A novel type of nitric-oxide reductase *Escherichia coli* flavorubredoxin. *J Biol Chem* **277**: 25273-25276.

Gorman, J. and Shapiro, L. (2005). Crystal structures of the tryptophan repressor binding protein WrbA and complexes with flavin mononucleotide. *Protein sci* **14**: 3004-3012.

Grainger, D. C., Hurd, D., Harrison, M., Holdstock, J. and Busby, S. J. (2005). Studies of the distribution of *Escherichia coli* cAMP-receptor protein and RNA polymerase along the *E. coli* chromosome. *Proc Natl Acad Sci U S A* **102**: 17693-17698.

Grainger, D. C., Aiba, H., Hurd, D., Browning, D. F. and Busby, S. J. (2007). Transcription factor distribution in *Escherichia coli*: studies with FNR protein. *Nucleic Acids Res*, **35**: 269-278.

Grandori, R., Khalifah, P., Boice, J. A., Fairman, R., Giovanielli, K. and Carey, J. (1998). Biochemical characterization of WrbA, founding member of a new family of multimeric flavodoxin-like proteins. *J Biol Chem* **273**: 20960-20966.

Green, J., Scott, C. and Guest, J. R. (2001). Functional versatility in the CRP-FNR superfamily of transcription factors: FNR and FLP. *Adv Microb Physiol* **44**: 1-34.

Grimm, F., Dobler, N. and Dahl, C. (2010). Regulation of *dsr* genes encoding proteins responsible for the oxidation of stored sulfur in *Allochromatium vinosum*. *Microbiology* **156**: 764-773.

Gusarov, I., Shatalin, K., Starodubtseva, M. and Nudler, E. (2009). Endogenous nitric oxide protects bacteria against a wide spectrum of antibiotics. *Science* **325**: 1380-1384.

Hamilton, W. A. (1995). Biofilms and microbially influenced corrosion. *Microbial Biofilms*, 171-182.

Hamilton, W. A. (2003). Microbially influenced corrosion as a model system for the study of metal microbe interactions: a unifying electron transfer hypothesis. *Biofouling* **19**: 65-76.

Han, S. W., Lee, S. W., Bahar, O., Schwessinger, B., Robinson, M. R., Shaw, J. B., ... and Ronald, P. C. (2012). Tyrosine sulfation in a Gram-negative bacterium. *Nature Communications* **3**: 1153.

Harman, J. G. (2001). Allosteric regulation of the cAMP receptor protein. *BBA-Protein Struct M* **1547**: 1-17.

Hausladen, A., Privalle, C. T., Keng, T., DeAngelo, J. and Stamler, J. S. (1996). Nitrosative stress: activation of the transcription factor OxyR. *Cell* **86**: 719-729.

Haveman, S. A., Brunelle, V., Voordouw, J. K., Voordouw, G., Heidelberg, J. F. and Rabus, R. (2003). Gene expression analysis of energy metabolism mutants of *Desulfovibrio vulgaris* Hildenborough indicates an important role for alcohol dehydrogenase. *J Bacteriol* **185**: 4345-4353.

Haveman, S. A., Greene, E. A., Stilwell, C. P., Voordouw, J. K. and Voordouw, G. (2004). Physiological and gene expression analysis of inhibition of *Desulfovibrio vulgaris* Hildenborough by nitrite. *J Bacteriol* **186**: 7944-7950.

He, Q., Huang, K. H., He, Z., Alm, E. J., Fields, M. W., Hazen, T. C., ... and Zhou, J. (2006). Energetic consequences of nitrite stress in *Desulfovibrio vulgaris* Hildenborough, inferred from global transcriptional analysis. *Appl Environ Microb* **72**: 4370-4381.

Hemme, C. L. (2004). Examination of metabolic and regulatory networks of *Desulfovibrio* species. *PhD thesis, University of Missouri-Columbia.*

Hidalgo, E. and Demple, B. (1994). An iron-sulfur center essential for transcriptional activation by the redox-sensing SoxR protein. *EMBO J* **13**: 138.

Hidalgo, E., Bollinger, J. M., Bradley, T. M., Walsh, C. T. and Demple, B. (1995). Binuclear 2Fe-2S Clusters in the *Escherichia coli* SoxR Protein and Role of the Metal Centers in Transcription. *J Biol Chem* **270**: 20908-20914.

Hilario, E., Li, Y., Niks, D. and Fan, L. (2012). The structure of a *Xanthomonas* general stress protein involved in citrus canker reveals its flavin-binding property. *Acta Crystallogr D* **68**: 846-853.

Hill, B. G., Dranka, B. P., Bailey, S. M., Lancaster, J. R. and Darley-Usmar, V. M. (2010). What part of NO don't you understand? Some answers to the cardinal questions in nitric oxide biology. *J Biol Chem* **285**: 19699-19704.

Hori, H., Tsubaki, M., Mogi, T. and Anraku, Y. (1996). EPR study of NO complex of *bd*-type ubiquinol oxidase from *Escherichia coli* the proximal axial ligand of heme D is a nitrogenous amino acid residue. *J Biol Chem* **271**: 9254-9258.

Hudson, B. P., Quispe, J., Lara-González, S., Kim, Y., Berman, H. M., Arnold, E., Ebright, R. H. and Lawson, C. L. (2009). Three-dimensional EM structure of an intact activator-dependent transcription initiation complex. *Proc Natl Acad Sci* **106**: 19830-19835.

Hudson, B. P., Turo, K., Birktoft, J. J., Ebright, R. H. and Lawson, C. L. (2012). Crystal structure of *T. thermophiles* catabolite activator protein. To be published. PDB entry: 4EV0.

Huo, Y. X., Nan, B. Y., You, C. H., Tian, Z. X., Kolb, A. and Wang, Y. P. (2006). FIS activates *glnAp2* in *Escherichia coli*: role of a DNA bend centered at− 55, upstream of the transcription start site. *FEMS Microbiol Lett* **257**: 99-105.

Huo, Y. X., Zhang, Y. T., Xiao, Y., Zhang, X., Buck, M., Kolb, A. and Wang, Y. P. (2009). IHF-binding sites inhibit DNA loop formation and transcription initiation. *Nucleic Acids Res* **37**: 3878-3886.

Hwang, S., Kim, M., Ryu, S. and Jeon, B. (2011). Regulation of oxidative stress response by CosR, an essential response regulator in *Campylobacter jejuni*. *PloS one* **6**: e22300.

Jackson, D. W., Simecka, J. W. and Romeo, T. (2002). Catabolite repression of *Escherichia coli* biofilm formation. *J Bacteriol* **184**: 3406-3410.

Jansen, C., Gronenborn, A. M. and Clore, G. M. (1987). The binding of the cyclic AMP receptor protein to synthetic DNA sites containing permutations in the consensus sequence TGTGA. *Biochem. J* **246**: 227-232.

Jennings, M. P. and Beacham, I. R. (1993). Co-dependent positive regulation of the *ansBF* promoter of *Escherichia coli* by CRP and the FNR protein: a molecular analysis. *Mol Microbiol* **9**: 155-164.

Jepson, B. J., Mohan, S., Clarke, T. A., Gates, A. J., Cole, J. A., Butler, C. S.,Butt, J. N., Hemmings, A. M. and Richardson, D. J. (2007). Spectropotentiometric and structural analysis of the periplasmic nitrate reductase from *Escherichia coli*. *J Biol Chem* **282**: 6425-6437.

Ji, X. B. and Hollocher, T. C. (1988). Reduction of nitrite to nitric oxide by enteric bacteria. *Biochem Bioph Res Co* **157**: 106-108.

Jia, W., Whitehead, R. N., Griffiths, L., Dawson, C., Bai, H., Waring, R. H., Ramsden, D. B. and Cole, J. A. (2012). Diversity and distribution of sulphate-reducing bacteria in human faeces from healthy subjects and patients with inflammatory bowel disease. *FEMS Immunol Med Mic* **65**: 55-68.

Johnston, S., Lin, S., Lee, P., Caffrey, S. M., Wildschut, J., Voordouw, J. K., ... and Voordouw, G. (2009). A genomic island of the sulfate-reducing bacterium *Desulfovibrio vulgaris* Hildenborough promotes survival under stress conditions while decreasing the efficiency of anaerobic growth. *Environ Microbiol* **11**: 981-991.

Justino, M. C., Almeida, C. C., Gonçalves, V. L., Teixeira, M. and Saraiva, L. M. (2006). *Escherichia coli* YtfE is a di-iron protein with an important function in assembly of iron–sulphur clusters. *FEMS Microbiol Lett* **257**: 278-284.

Katouzian-Safadi, M., Blazy, B., Cremet, J. Y., Le Caer, J. P., Rossier, J. and Charlier, M. (1993). Photo-cross-linking of CRP to nonspecific DNA in the absence of cAMP, DNA interacts with both the N-and C-terminal parts of the protein. *Biochemistry* **32**: 1770-1773.

Keller, K. L. and Wall, J. D. (2011). Genetics and molecular biology of the electron flow for sulfate respiration in *Desulfovibrio*. *Frontiers in Microbiology, 2*.

Kelley, L.A. and Sternberg, M.J.E. (2009). Protein structure prediction on the web: a case study using the Phyre server. *Nat Protoc* **4**: 363 – 371.

Kern, M. and Simon, J. (2009). Periplasmic nitrate reduction in Wolinella succinogenes: cytoplasmic NapF facilitates NapA maturation and requires the menaquinol dehydrogenase NapH for membrane attachment. *Microbiology* **155**: 2784-2794.

Kern, M. and Simon, J. (2008). Characterization of the NapGH quinol dehydrogenase complex involved in Wolinella succinogenes nitrate respiration. *Mol Microbiol* **69**: 1137-1152.

Khankal, R., Chin, J. W., Ghosh, D. and Cirino, P. C. (2009). Transcriptional effects of CRP* expression in *Escherichia coli*. *Journal of Biological Engineering* **3**: 13.

Khoroshilova, N., Popescu, C., Münck, E., Beinert, H. and Kiley, P. J. (1997). Iron-sulfur cluster disassembly in the FNR protein of *Escherichia coli* by O_2:[4Fe-4S] to [2Fe-2S] conversion with loss of biological activity. *Proc Natl Acad Sci* **94**: 6087-6092.

Kirstein, K. and Bock, E. (1993). Close genetic relationship between Nitrobacter hamburgensis nitrite oxidoreductase and *Escherichia coli* nitrate reductases. *Arch Microbiol* **160**: 447-453.

Koch, D. J., Rückert, C., Albersmeier, A., Hüser, A. T., Tauch, A., Pühler, A. and Kalinowski, J. (2005). The transcriptional regulator SsuR activates expression of the *Corynebacterium glutamicum* sulphonate utilization genes in the absence of sulphate. *Mol Microbiol* **58**: 480-494.

Kolb, A., Busby, S., Buc, I. I., Garges, S. and Adhya, S. (1993). Transcriptional regulation by cAMP and its receptor protein. *Ann Rev Biochem* **62**: 749-797.

Lamrabet, O., Pieulle, L., Aubert, C., Mouhamar, F., Stocker, P., Dolla, A. and Brasseur, G. (2011). Oxygen reduction in the strict anaerobe *Desulfovibrio vulgaris* Hildenborough: characterization of two membrane-bound oxygen reductases. *Microbiology* **157**: 2720-2732.

Larkin, M. A., Blackshields, G., Brown, N. P., Chenna, R., McGettigan, P. A., McWilliam, H., ... and Higgins, D. G. (2007). Clustal W and Clustal X version 2.0. *Bioinformatics* **23**: 2947-2948.

Lazazzera, B. A., Beinert, H., Khoroshilova, N., Kennedy, M. C. and Kiley, P. J. (1996). DNA binding and dimerization of the Fe-S-containing FNR protein from *Escherichia coli* are regulated by oxygen. *J Biol Chem* **271**: 2762-2768.

Lee, D. J., Minchin, S. D. and Busby, S. J. (2012). Activating transcription in bacteria. *Ann Rev Microbiol* **66**: 125-152.

Lee, S. J., Moulakakis, C., Koning, S. M., Hausner, W., Thomm, M. and Boos, W. (2005). TrmB, a sugar sensing regulator of ABC transporter genes in *Pyrococcus furiosus* exhibits dual promoter specificity and is controlled by different inducers. *Mol Microbiol* **57**: 1797-1807.

Leiros, H. K. S., Kozielski-Stuhrmann, S., Kapp, U., Terradot, L., Leonard, G. A. and McSweeney, S. M. (2004). Structural basis of 5-nitroimidazole antibiotic resistance the crystal structure of NimA from *Deinococcus radiodurans*. *J Biol Chem* **279**: 55840-55849.

Lewis, J. P., Yanamandra, S. S. and Anaya-Bergman, C. (2012). HcpR of *Porphyromonas gingivalis* is required for growth under nitrosative stress and survival within host cells. *Infect Immun* **80**: 3319-3331.

Li, B., Wing, H., Lee, D., Wu, H. C. and Busby, S. (1998). Transcription activation by *Escherichia coli* FNR protein: similarities to, and differences from, the CRP paradigm. *Nucleic Acids Res* **26**: 2075-2081.

Liamleam, W. and Annachhatre, A. P. (2007). Electron donors for biological sulfate reduction. *Biotechnol Adv* **25**: 452-463.

Liochev, S. I. and Fridovich, I. (1997). A Mechanism for Complementation of the SodA SodB Defect in *Escherichia coli* by Overproduction of therbo Gene Product (Desulfoferrodoxin) from *Desulfoarculus baarsii*. *J Biol Chem* **272**: 25573-25575.

Liu, M. C. and Peck, H. D. (1981). The isolation of a hexaheme cytochrome from *Desulfovibrio desulfuricans* and its identification as a new type of nitrite reductase. *J Biol Chem* **256**: 13159-13164.

Liu, M. C., Costa, C., Coutinho, I. B., Moura, J. J., Moura, I., Xavier, A. V. and LeGall, J. (1988). Cytochrome components of nitrate-and sulfate-respiring *Desulfovibrio desulfuricans* ATCC 27774. *J Bacteriol* **170**: 5545-5551.

Livak, K. J. and Schmittgen, T. D. (2001). analysis of relative gene expression data using real-time quantitative PCR and the $^{2-}\Delta\Delta$Ct method. *Methods* **25**: 402-408.

Lobo, S. A., Melo, A. M., Carita, J. N., Teixeira, M. and Saraiva, L. M. (2007). The anaerobe *Desulfovibrio desulfuricans* ATCC 27774 grows at nearly atmospheric oxygen levels. *FEBS Lett* **581**: 433-436.

Lockwood, C., Butt, J., Clarke, T. and Richardson, D. (2011). Molecular interactions between multihaem cytochromes: probing the protein:protein interactions between pentahaem cytochromes of a nitrite reductase complex. *Biochem Soc T* **39**: 263.

Lodge, J., Fear, J., Busby, S., Gunasekaran, P. and Kamini, N. R. (1992). Broad host range plasmids carrying the Escherichia coli lactose and galactose operons. *FEMS Microbiol Lett* **74**: 271-276.

Löfmark, S., Edlund, C. and Nord, C. E. (2010). Metronidazole is still the drug of choice for treatment of anaerobic infections. *Clin Infect Dis* **50**: S16-23.

Lombard, M., Fontecave, M., Touati, D. and Nivière, V. (2000). Reaction of the desulfoferrodoxin from *Desulfoarculus baarsii* with superoxide anion evidence for a superoxide reductase activity. *J Biol Chem* **275**: 115-121.

Lovley, D. R. (1995). Bioremediation of organic and metal contaminants with dissimilatory metal reduction. *J Ind Microbiol* **14**: 85-93.

Lovley, D. R. and Phillips, E. J. (1992). Reduction of uranium by *Desulfovibrio desulfuricans*. *Appl Environ Microb* **58**: 850-856.

Lovley, D. R. and Phillips, E. J. (1994). Reduction of chromate by *Desulfovibrio vulgaris* and its *c3* cytochrome. *Appl Environ Microb* **60**: 726-728.

Macfarlane, G. T., Blackett, K. L., Nakayama, T., Steed, H. and Macfarlane, S. (2009). The gut microbiota in inflammatory bowel disease. *Curr Pharm Design* **15**: 1528-1536.

MacRae, I. J., Segel, I. H. and Fisher, A. J. (2001). Crystal structure of ATP sulfurylase from *Penicillium chrysogenum*: insights into the allosteric regulation of sulfate assimilation. *Biochemistry* **40**: 6795-6804.

Maillard, J., Spronk, C. A., Buchanan, G., Lyall, V., Richardson, D. J., Palmer, T., Vuister, G. V. and Sargent, F. (2007). Structural diversity in twin-arginine signal peptide-binding proteins. *Proc Natl Acad Sci* **104**: 15641-15646.

Malojčić, G. and Glockshuber, R. (2010). The PAPS-independent aryl sulfotransferase and the alternative disulfide bond formation system in pathogenic bacteria. *Antioxid Redox Sign* **13**: 1247-1259.

Marietou, A., Richardson, D., Cole, J. and Mohan, S. (2005). Nitrate reduction by *Desulfovibrio desulfuricans*: A periplasmic nitrate reductase system that lacks NapB, but includes a unique tetraheme *c*-type cytochrome, NapM. *FEMS Microbiol Lett* **248**: 217-225.

Marietou, A. (2009). Nitrate reduction in *Desulfovibrio desulfuricans* 27774. *PhD thesis, University of Birmingham.*

Marietou, A., Griffiths, L. and Cole, J. (2009). Preferential reduction of the thermodynamically less favorable electron acceptor, sulfate, by a nitrate-reducing strain of the sulfate-reducing bacterium *Desulfovibrio desulfuricans* 27774. *J Bacteriol* **191**: 882-889.

Mason, M. G., Shepherd, M., Nicholls, P., Dobbin, P. S., Dodsworth, K. S., Poole, R. K. and Cooper, C. E. (2008). Cytochrome *bd* confers nitric oxide resistance to *Escherichia coli*. *Nat Chem Biol* **5**: 94-96.

Maxam, A. M. and Gilbert, W. (1977). A new method for sequencing DNA. *Proc Natl Acad Sci* **74**: 560-564.

McKay, D. M. (2001). Bacterial superantigens: provocateurs of gut dysfunction and inflammation? *Trends Immunol* **22**: 497-501.

Mesa, S., Bedmar, E. J., Chanfon, A., Hennecke, H. and Fischer, H. M. (2003). *Bradyrhizobium japonicum* NnrR, a denitrification regulator, expands the FixLJ-FixK2 regulatory cascade. *J Bacteriol* **185**: 3978-3982.

Meyer, B. and Kuever, J. (2007). Phylogeny of the alpha and beta subunits of the dissimilatory adenosine-5′-phosphosulfate (APS) reductase from sulfate-reducing prokaryotes–origin and evolution of the dissimilatory sulfate-reduction pathway. *Microbiology* **153**: 2026-2044.

Miller, J. (1972) Experiments in Molecular Genetics. Cold Spring Harbor, NY: Cold Spring Harbor Laboratory Press.

Miller, M. A. (2007). Clinical management of *Clostridium difficile*-associated disease. *Clin Infect Dis* **45**: S122-S128.

Minailiuc, O. M., Ekiel, I., Cheng, J., Milad, M., Gandhi, S., Larocque, R., Cygler, M. and Matte, A. (2007). Solution structure of NapD, a private chaperone of periplasmic nitrate reductase NapA/B, in complex with NapA1-35 signal peptide. PDB ID: 2PQ4.

Mitchell, P. (1976). Possible molecular mechanisms of the protonmotive function of cytochrome systems. *Journal of Theoretical Biology* **62**: 327-367.

Monod, J. (1966). From enzymatic adaptation to allosteric transitions. *Science* **154**: 475-483.

Moore, L. J. and Kiley, P. J. (2001). Characterization of the dimerization domain in the FNR transcription factor. *J Biol Chem* **276**: 45744-45750.

Moreno-Vivián, C., Cabello, P., Martínez-Luque, M., Blasco, R. and Castillo, F. (1999). Prokaryotic nitrate reduction: molecular properties and functional distinction among bacterial nitrate reductases. *J Bacteriol* **181**: 6573-6584.

Motteram, P. A. S., McCarthy, J. E. G., Ferguson, S. J., Jackson, J. B. and Cole, J. A. (1981). Energy conservation during the formate-dependent reduction of nitrite by *Escherichia coli*. *FEMS Microbiol Lett* **12**: 317-320.

Mougous, J. D., Lee, D. H., Hubbard, S. C., Schelle, M. W., Vocadlo, D. J., Berger, J. M. and Bertozzi, C. R. (2006). Molecular basis for G protein control of the prokaryotic ATP sulfurylase. *Mol Cell* **21**: 109-122.

Moura, I., Tavares, P., Moura, J. J., Ravi, N., Huynh, B. H., Liu, M. Y. and LeGall, J. (1990). Purification and characterization of desulfoferrodoxin. A novel protein from *Desulfovibrio desulfuricans* (ATCC 27774) and from *Desulfovibrio vulgaris* (strain Hildenborough) that contains a distorted rubredoxin center and a mononuclear ferrous center. *J Biol Chem* **265**: 21596-21602.

Moura, I., Bursakov, S., Costa, C. and Moura, J. J. (1997). Nitrate and nitrite utilization in sulfate-reducing bacteria. *Anaerobe* **3**: 279-290.

Moura, J. J., Gonzalez, P., Moura, I. and Fauque, G. (2007). Dissimilatory nitrate and nitrite ammonification by sulphate-reducing eubacteria. *Sulphate-reducing bacteria. Environmental and engineered systems*, 241-264.

Münch, R., Hiller, K., Grote, A., Scheer, M., Klein, J., Schobert, M. and Jahn, D. (2005). Virtual Footprint and PRODORIC: an integrative framework for regulon prediction in prokaryotes. *Bioinformatics* **21**: 4187-4189.

Muyzer, G. and Stams, A. J. (2008). The ecology and biotechnology of sulphate-reducing bacteria. *Nat Rev Microbiol* **6**: 441-454.

Natarajan, K. A. (2008). Microbial aspects of acid mine drainage and its bioremediation. *T Nonferr Metal Soc* **18**: 1352-1360.

Neretin, L. N., Schippers, A., Pernthaler, A., Hamann, K., Amann, R. and Jørgensen, B. B. (2003). Quantification of dissimilatory (bi) sulphite reductase gene expression in *Desulfobacterium autotrophicum* using real-time RT-PCR. *Environ Microbiol* **5**: 660-671.

Nilavongse, A., Brondijk, T. H. C., Overton, T. W., Richardson, D. J., Leach, E. R. and Cole, J. A. (2006). The NapF protein of the *Escherichia coli* periplasmic nitrate reductase system: demonstration of a cytoplasmic location and interaction with the catalytic subunit, NapA. *Microbiology* **152**: 3227-3237.

Nishino, K., Senda, Y. and Yamaguchi, A. (2008). CRP regulator modulates multidrug resistance of *Escherichia coli* by repressing the *mdtEF* multidrug efflux genes. *J Antibiot* **61**: 120-127.

Niu, W., Kim, Y., Tau, G., Heyduk, T. and Ebright, R. H. (1996). Transcription activation at class II CAP-dependent promoters: two interactions between CAP and RNA polymerase. *Cell* **87**: 1123-1134.

Noriega, C. E., Lin, H. Y., Chen, L. L., Williams, S. B. and Stewart, V. (2010). Asymmetric cross-regulation between the nitrate-responsive NarX–NarL and NarQ–NarP two-component regulatory systems from *Escherichia coli* K-12. *Mol Microbiol* **75**: 394-412.

Odom, J. M. and Peck, H. D. (1981). Hydrogen cycling as a general mechanism for energy coupling in the sulfate-reducing bacteria, *Desulfovibrio* sp. *FEMS Microbiol Lett* **12**: 47-50.

Okabe, S., Nielsen, P. H., Jones, W. L. and Characklis, W. G. (1995). Sulfide product inhibition of *Desulfovibrio desulfuricans* in batch and continuous cultures. *Water research* **29**: 571-578.

Oliveira, T. F., Vonrhein, C., Matias, P. M., Venceslau, S. S., Pereira, I. A. and Archer, M. (2008). Purification, crystallization and preliminary crystallographic analysis of a dissimilatory DsrAB sulfite reductase in complex with DsrC. *J Struct Biol* **164**: 236-239.

Oliveira, T. F., Vonrhein, C., Matias, P. M., Venceslau, S. S., Pereira, I. A. and Archer, M. (2008). The crystal structure of *Desulfovibrio vulgaris* dissimilatory sulfite reductase bound to DsrC provides novel insights into the mechanism of sulfate respiration. *J Biol Chem* **283**: 34141-34149.

Parkinson, G., Wilson, C., Gunasekera, A., Ebright, Y. W., Ebright, R. E. and Berman, H. M. (1996). Structure of the CAP-DNA complex at 2.5 Å resolution: a complete picture of the protein-DNA interface. *J Mol Biol* **260**: 395-408.

Patridge, E. V. and Ferry, J. G. (2006). WrbA from *Escherichia coli* and *Archaeoglobus fulgidus* is an NAD (P) H: quinone oxidoreductase. *J Bacteriol* **188**: 3498-3506.

Pereira, I. C., Abreu, I. A., Xavier, A. V., LeGall, J. and Teixeira, M. (1996). Nitrite reductase from *Desulfovibrio desulfuricans* (ATCC 27774) - A heterooligomer heme protein with sulfite reductase activity. *Biochem Bioph Res Co* **224**: 611-618.

Peterson, J., Garges, S., Giovanni, M., McInnes, P., Wang, L., Schloss, J. A., ... and Guyer, M. (2009). The NIH human microbiome project. *Genome Res* **19**: 2317-2323.

Pietzsch, K. and Babel, W. (2003). A sulfate-reducing bacterium that can detoxify U (VI) and obtain energy via nitrate reduction. *J Basic Microb* **43**: 348-361.

Pinto, A. F., Rodrigues, J. V. and Teixeira, M. (2010). Reductive elimination of superoxide: Structure and mechanism of superoxide reductases. *BBA-Proteins Proteom* **1804**: 285-297.

Pires, R. H., Lourenço, A. I., Morais, F., Teixeira, M., Xavier, A. V., Saraiva, L. M. and Pereira, I. A. (2003). A novel membrane-bound respiratory complex from *Desulfovibrio desulfuricans* ATCC 27774. *BBA-Biophysics* **1605**: 67-82.

Pires, R. H., Venceslau, S. S., Morais, F., Teixeira, M., Xavier, A. V. and Pereira, I. A. (2006). Characterization of the *Desulfovibrio desulfuricans* ATCC 27774 DsrMKJOP complex: A membrane-bound redox complex involved in the sulfate respiratory pathway. *Biochemistry* **45**: 249-262.

Pitcher, M. C. and Cummings, J. H. (1996). Hydrogen sulphide: a bacterial toxin in ulcerative colitis? *Gut* **39**: 1-4.

Plate, L. and Marletta, M. A. (2012). Nitric oxide modulates bacterial biofilm formation through a multicomponent cyclic-di-GMP signaling network. *Mol Cell*.

Poock, S. R., Leach, E. R., Moir, J. W., Cole, J. A. and Richardson, D. J. (2002). Respiratory detoxification of nitric oxide by the cytochromec nitrite reductase of *Escherichia coli*. *J Biol Chem* **277**: 23664-23669.

Popovych, N., Tzeng, S. R., Tonelli, M., Ebright, R. H. and Kalodimos, C. G. (2009). Structural basis for cAMP-mediated allosteric control of the catabolite activator protein. *Proc Natl Acad Sci* **106**: 6927-6932.

Postgate, J. R. (1984). FRS."The Sulphate-reducing bacteria". *Cambridge University Press* 17-18.

Postma, P. (2000) PEP:Carbohydrate Phosphotransferase Systems. In *Encyclopedia of Microbiology*. Vol. 3. Lederberg, J. London: Academic Press: 580-593.

Potter, L. and Cole, J. (1999). Essential roles for the products of the *napABCD* genes, but not napFGH, in periplasmic nitrate reduction by *Escherichia coli* K-12. *Biochem. J* **344**: 69-76.

Potter, L., Millington, P., Griffiths, L., Thomas, G. and Cole, J. (1999). Competition between *Escherichia coli* strains expressing either a periplasmic or a membrane-bound nitrate reductase: does Nap confer a selective advantage during nitrate-limited growth? *Biochem. J* **344**: 77-84.

Predicala, B., Nemati, M., Stade, S. and Laguë, C. (2008). Control of H_2S emission from swine manure using Na-nitrite and Na-molybdate. *J Hazard Matar* **154**: 300-309.

Pullan, S. T., Gidley, M. D., Jones, R. A., Barrett, J., Stevanin, T. M., Read, R. C., Green, J. and Poole, R. K. (2007). Nitric oxide in chemostat-cultured *Escherichia coli* is

sensed by Fnr and other global regulators: unaltered methionine biosynthesis indicates lack of S nitrosation. *J Bacteriol* **189**: 1845-1855.

Rabin, R. S. and Stewart, V. (1993). Dual response regulators (NarL and NarP) interact with dual sensors (NarX and NarQ) to control nitrate-and nitrite-regulated gene expression in *Escherichia coli* K-12. *J Bacteriol* **175**: 3259-3268.

Rachmilewitz, D., Stamler, J. S., Bachwich, D., Karmeli, F., Ackerman, Z. and Podolsky, D. K. (1995). Enhanced colonic nitric oxide generation and nitric oxide synthase activity in ulcerative colitis and Crohn's disease. *Gut* **36**: 718-723.

Rajeev, L., Luning, E. G., Dehal, P. S., Price, M. N., Arkin, A. P. and Mukhopadhyay, A. (2011). Systematic mapping of two component response regulators to gene targets in a model sulfate reducing bacterium. *Genome Biol* **12**: R99.

Ramos, A. R., Venceslau, S. S. and Pereira, I. A. Interaction Studies of a conserved membrane-bound complex in SRB: the QmoABC complex from *Desulfovibrio desulfuricans* ATCC. *Book of Abstracts of MicroBiotec* **9**: 19.

Rhodius, V. A., West, D. M., Webster, C. L., Busby, S. J. and Savery, N. J. (1997). Transcription activation at class II CRP-dependent promoters: the role of different activating regions. *Nucleic Acids Res* **25**: 326-332.

Rice, P., Longden, I. and Bleasby, A. (2000). EMBOSS: the European molecular biology open software suite. *Trends Genet* **16**: 276-277.

Richardson, A. R., Payne, E. C., Younger, N., Karlinsey, J. E., Thomas, V. C., Becker, L. A., Navarre, W. W., Castor, M. E., Libby, S. J. and Fang, F. C. (2011). Multiple Targets of Nitric Oxide in the Tricarboxylic Acid Cycle of *Salmonella enterica Serovar Typhimurium*. *Cell Host Microbe* **10**: 33-43.

Richardson, D. J. and Watmough, N. J. (1999). Inorganic nitrogen metabolism in bacteria. *Curr Opin Chem Biol* **3**: 207-219.

Richardson, D. J., Berks, B. C., Russell, D. A., Spiro, S. and Taylor, C. J. (2001). Functional, biochemical and genetic diversity of prokaryotic nitrate reductases. *Cell Mol Life Sci* **58**: 165-178.

Riebe, O., Fischer, R. J. and Bahl, H. (2007). Desulfoferrodoxin of *Clostridium acetobutylicum* functions as a superoxide reductase. *FEBS Lett* **581**: 5605-5610.

Rinaldo, S., Giardina, G., Brunori, M. and Cutruzzola, F. (2006). N-oxide sensing and denitrification: the DNR transcription factors. *Biochem Soc T* **34**: 185-187.

Rodionov, D. A., Dubchak, I. L., Arkin, A. P., Alm, E. J. and Gelfand, M. S. (2005). Dissimilatory metabolism of nitrogen oxides in bacteria: comparative reconstruction of transcriptional networks. *PLoS Computational Biology* **1**: e55.

Rodionov, D. A., Dubchak, I., Arkin, A., Alm, E. and Gelfand, M. S. (2004). Reconstruction of regulatory and metabolic pathways in metal-reducing delta-proteobacteria. *Genome Biol* **5**: R90.

Römling, U., Galperin, M. Y. and Gomelsky, M. (2013). Cyclic di-GMP: the first 25 years of a universal bacterial second messenger. *Microbiol Mol Biol Rev* **77**: 1-52.

Rowan, F. E., Docherty, N. G., Coffey, J. C. and O'Connell, P. R. (2009). Sulphate-reducing bacteria and hydrogen sulphide in the aetiology of ulcerative colitis. *Brit J Surg* **96**: 151-158.

Rowan, F., Docherty, N. G., Murphy, M., Murphy, B., Coffey, J. C. and O'Connell, P. R. (2010). *Desulfovibrio* bacterial species are increased in ulcerative colitis. *Dis Colon Rectum*, **53**: 1530-1536.

Rozen, S. and Skaletsky, H. (1999). Primer3 on the WWW for general users and for biologist programmers. In *Bioinformatics methods and protocols* (pp. 365-386). Humana Press.

Sartor, R. B. (2008). Microbial influences in inflammatory bowel diseases. *Gastroenterology*, **134**: 577-594.

Schiffer, A., Fritz, G., Kroneck, P. M. and Ermler, U. (2006). Reaction mechanism of the iron-sulfur flavoenzyme adenosine-5'-phosphosulfate reductase based on the structural characterization of different enzymatic states. *Biochemistry* **45**: 2960-2967.

Schiffer, A., Parey, K., Warkentin, E., Diederichs, K., Huber, H., Stetter, K. O., Kroneck, P. M. H. and Ermler, U. (2008). structure of the dissimilatory sulfite reductase from the hyperthermophilic Archaeon *Archaeoglobus fulgidus*. *J Mol Biol* **379**: 1063-1074.

Schmid, A. K., Reiss, D. J., Pan, M., Koide, T. and Baliga, N. S. (2009). A single transcription factor regulates evolutionarily diverse but functionally linked metabolic pathways in response to nutrient availability. *Mol Syst Biol* **5**

Schmidt, A., Hagen, M., Schütze, E., Schmidt, A. and Kothe, E. (2010). In silico prediction of potential metallothioneins and metallohistins in actinobacteria. *J Basic Microb* **50**: 562-569.

Schultz, S. C., Shields, G. C. and Steitz, T. A. (1991). Crystal structure of a CAP-DNA complex: the DNA is bent by 90 degrees. *Science* **253**: 1001-1007.

Seitz, H. J. and Cypionka, H. (1986). Chemolithotrophic growth of *Desulfovibrio desulfuricans* with hydrogen coupled to ammonification of nitrate or nitrite. *Arch Microbiol*, **146**: 63-67.

Seth, D., Hausladen, A., Wang, Y. J. and Stamler, J. S. (2012). Endogenous protein S-Nitrosylation in E. coli: regulation by OxyR. *Science* **336**: 470-473.

Sharma, H., Yu, S., Kong, J., Wang, J. and Steitz, T. A. (2009). Structure of apo-CAP reveals that large conformational changes are necessary for DNA binding. *Proc Natl Acad Sci* **106**: 16604-16609.

Shelver, D., Thorsteinsson, M. V., Kerby, R. L., Chung, S. Y., Roberts, G. P., Reynolds, M. F., ... and Burstyn, J. N. (1999). Identification of two important heme site residues (cysteine 75 and histidine 77) in CooA, the CO-sensing transcription factor of *Rhodospirillum rubrum*. *Biochemistry* **38**: 2669-2678.

Shen, Y., Buick, R. and Canfield, D. E. (2001). Isotopic evidence for microbial sulphate reduction in the early Archaean era. *Nature* **410**: 77-81.

Shepherd, M., Sanguinetti, G., Cook, G. M. and Poole, R. K. (2010). Compensations for diminished terminal oxidase activity in *Escherichia coli* cytochrome *bd-II*-mediated respiration and glutamate metabolism. *J Biol Chem* **285**: 18464-18472.

Silaghi-Dumitrescu, R., Coulter, E. D., Das, A., Ljungdahl, L. G., Jameson, G. N., Huynh, B. H. and Kurtz, D. M. (2003). A flavodiiron protein and high molecular weight rubredoxin from *Moorella thermoacetica* with nitric oxide reductase activity. *Biochemistry* **42**: 2806-2815.

Silaghi-Dumitrescu, R., Ng, K. Y., Viswanathan, R. and Kurtz, D. M. (2005). A flavo-diiron protein from *Desulfovibrio vulgaris* with oxidase and nitric oxide reductase activities. Evidence for an in vivo nitric oxide scavenging function. *Biochemistry* **44**: 3572-3579.

Silaghi-Dumitrescu, R., Kurtz, D. M., Ljungdahl, L. G. and Lanzilotta, W. N. (2005). X-ray crystal structures of *Moorella thermoacetica* FprA. Novel diiron site structure and mechanistic insights into a scavenging nitric oxide reductase. *Biochemistry* **44**: 6492-6501.

da Silva, S. M., Pacheco, I. and Pereira, I. A. C. (2012). Electron transfer between periplasmic formate dehydrogenase and cytochromes *c* in *Desulfovibrio desulfuricans* ATCC 27774. *J Biol Inorg Chem* **17**: 831-838.

Simm, R., Morr, M., Kader, A., Nimtz, M. and Römling, U. (2004). GGDEF and EAL domains inversely regulate cyclic di-GMP levels and transition from sessility to motility. *Mol Microbiol* **53**: 1123-1134.

Søgaard-Andersen, L. and Valentin-Hansen, P. (1993). Protein-protein interactions in gene regulation: the cAMP-CRP complex sets the specificity of a second DNA-binding protein, the CytR repressor. *Cell* **75**: 557-566.

Spiro, S., Gaston, K. L., Bell, A. I., Roberts, R. E., Busby, S. J. W. and Guest, J. R. (1990). Interconversion of the DNA-binding specificities of two related transcription regulators, CRP and FNR. *Mol Microbiol* **4**: 1831-1838.

Spreadbury, C. L., Pallen, M. J., Overton, T., Behr, M. A., Mostowy, S., Spiro, S.,Busby, S. J. W. and Cole, J. A. (2005). Point mutations in the DNA-and cNMP-binding domains of the homologue of the cAMP receptor protein (CRP) in *Mycobacterium bovis* BCG: implications for the inactivation of a global regulator and strain attenuation. *Microbiology* **151**: 547-556.

Stallings, C. L., Stephanou, N. C., Chu, L., Hochschild, A., Nickels, B. E. and Glickman, M. S. (2009). CarD Is an Essential Regulator of rRNA Transcription Required for *Mycobacterium tuberculosis* Persistence. *Cell* **138**: 146-159.

Stewart, V. (1993). Nitrate regulation of anaerobic respiratory gene expression in *Escherichia coli*. *Mol Microbiol* **9**: 425-434.

Stewart, V., Bledsoe, P. J., Chen, L. L. and Cai, A. (2009). Catabolite repression control of *napF* (periplasmic nitrate reductase) operon expression in *Escherichia coli* K-12. *J Bacteriol* **191**: 996-1005.

Studier, F. W. and Moffatt, B. A. (1986). Use of bacteriophage T7 RNA polymerase to direct selective high-level expression of cloned genes. *J Mol Biol* **189**: 113-130.

Taguchi, Y., Sugishima, M. and Fukuyama, K. (2004). Crystal structure of a novel zinc-binding ATP sulfurylase from *Thermus thermophilus* HB8. *Biochemistry* **43**: 4111-4118.

Todorovic, S., Justino, M. C., Wellenreuther, G., Hildebrandt, P., Murgida, D. H., Meyer-Klaucke, W. and Saraiva, L. M. (2008). Iron–sulfur repair YtfE protein from *Escherichia coli*: structural characterization of the di-iron center. *J Biol Inorg Chem* **13**: 765-770.

Tosques, I. E., Shi, J. and Shapleigh, J. P. (1996). Cloning and characterization of *nnrR*, whose product is required for the expression of proteins involved in nitric oxide metabolism in *Rhodobacter sphaeroides*. *J Bacteriol* **178**: 4958-4964.

Townsend, G. E., Raghavan, V., Zwir, I. and Groisman, E. A. (2013). Intramolecular arrangement of sensor and regulator overcomes relaxed specificity in hybrid two-component systems. *Proc Natl Acad Sci* **110**: E161-E169.

Tucker, N. P., D'autreaux, B., Studholme, D. J., Spiro, S. and Dixon, R. (2004). DNA binding activity of the *Escherichia coli* nitric oxide sensor NorR suggests a conserved target sequence in diverse proteobacteria. *J Bacteriol* **186**: 6656-6660.

Tucker, N. P., D'autréaux, B., Spiro, S. and Dixon, R. (2006). Mechanism of transcriptional regulation by the *Escherichia coli* nitric oxide sensor NorR. *Biochem Soc T* **34**: 191.

Tucker, N. P., D'Autréaux, B., Yousafzai, F. K., Fairhurst, S. A., Spiro, S. and Dixon, R. (2008). Analysis of the nitric oxide-sensing non-heme iron center in the NorR regulatory protein. *J Biol Chem* **283**: 908-918.

Tucker, N. P., Ghosh, T., Bush, M., Zhang, X. and Dixon, R. (2010). Essential roles of three enhancer sites in σ54-dependent transcription by the nitric oxide sensing regulatory protein NorR. *Nucleic Acids Res* **38**: 1182-1194.

Turinsky, A. J., Grundy, F. J., Kim, J. H., Chambliss, G. H. and Henkin, T. M. (1998). Transcriptional activation of the *Bacillus subtilis ackA* gene requires sequences upstream of the promoter. *J Bacteriol* **180**: 5961-5967.

Tyson, K. L., Bell, A. I., Cole, J. A. and Busby, S. J. W. (1993). Definition of nitrite and nitrate response elements at the anaerobically inducible *Escherichia coli nirB* promoter: interactions between FNR and NarL. *Mol Microbiol* **7**: 151-157.

Ullrich, T. C. and Huber, R. (2001). The complex structures of ATP sulfurylase with thiosulfate, ADP and chlorate reveal new insights in inhibitory effects and the catalytic cycle. *J Mol Biol* **313**: 1117-1125.

Ullmann, A. and Monod, J. (1968). Cyclic AMP as an antagonist of catabolite repression in *Escherichia coli*. *FEBS Lett* **2**: 57-60.

Valentin-Hansen, P., Søgaard-Andersen, L. and Pedersen, H. (1996). A flexible partnership: the CytR anti-activator and the cAMP–CRP activator protein, comrades in transcription control. *Mol Microbiol* **20**: 461-466.

Venceslau, S. S., Lino, R. R. and Pereira, I. A. (2010). The Qrc membrane complex, related to the alternative complex III, is a menaquinone reductase involved in sulfate respiration. *J Biol Chem* **285**: 22774-22783.

Vidakovic, M., Crossnoe, C. R., Neidre, C., Kim, K., Krause, K. L. and Germanas, J. P. (2003). Reactivity of reduced [2Fe-2S] ferredoxins parallels host susceptibility to nitroimidazoles. *Antimicrob Agents Ch* **47**: 302-308.

Villarreal, J. M., Hernández-Lucas, I., Gil, F., Calderón, I. L., Calva, E. and Saavedra, C. P. (2011). cAMP receptor protein (CRP) positively regulates the *yihU–yshA* operon in *Salmonella enterica serovar Typhi*. *Microbiology* **157**: 636-647.

Vicente, J. B., Scandurra, F. M., Rodrigues, J. V., Brunori, M., Sarti, P., Teixeira, M. and Giuffre, A. (2007). Kinetics of electron transfer from NADH to the *Escherichia coli* nitric oxide reductase flavorubredoxin. *FEBS J* **274**: 677-686.

Vine, C. E. and Cole, J. A. (2011). Unresolved sources, sinks, and pathways for the recovery of enteric bacteria from nitrosative stress. *FEMS Microbiol Lett* **325**: 99-107.

Vine, C. and Cole, J. (2011). Nitrosative stress in *Escherichia coli*: reduction of nitric oxide. *Biochem Soc T* **39**: 213.

Vine, C. E., Purewal, S. K. and Cole, J. A. (2011). NsrR-dependent method for detecting nitric oxide accumulation in the *Escherichia coli* cytoplasm and enzymes involved in NO production. *FEMS Microbiol Lett* **325**: 108-114.

Vine, C. E. (2012) *Escherichia coli* response to nitrosative stress. *PhD thesis, University of Birmingham.*

Voordouw, G. (1995). The genus *Desulfovibrio*: the centennial. *Appl Environ Microb* **61**: 2813.

Voordouw, J. K. and Voordouw, G. (1998). Deletion of the *rbo* gene increases the oxygen sensitivity of the sulfate-reducing bacterium *Desulfovibrio vulgaris* Hildenborough. *Appl Environ Microb* **64**: 2882-2887.

Voordouw, G. (2011). Production-related petroleum microbiology: progress and prospects. *Curr Opin Biotechnol* **22**: 401-405.

Wang, H., Tseng, C. P. and Gunsalus, R. P. (1999). The *napF* and *narG* nitrate reductase operons in *Escherichia coli* are differentially expressed in response to submicromolar concentrations of nitrate but not nitrite. *J Bacteriol* **181**: 5303-5308.

Wang, H. and Gunsalus, R. P. (2000). The *nrfA* and *nirB* nitrite reductase operons in *Escherichia coli* are expressed differently in response to nitrate than to nitrite. *J Bacteriol* **182**: 5813-5822.

Weiss, B. (2006). Evidence for mutagenesis by nitric oxide during nitrate metabolism in *Escherichia coli*. *J Bacteriol* **188**: 829-833.

Werner, A. K., Romeis, T. and Witte, C. P. (2009). Ureide catabolism in *Arabidopsis thaliana* and *Escherichia coli*. *Nat Chem Biol* **6**: 19-21.

Wing, H. J., Williams, S. M. and Busby, S. J. (1995). Spacing requirements for transcription activation by *Escherichia coli* FNR protein. *J Bacteriol* **177**: 6704-6710.

Wolfe, B. M., Lui, S. M. and Cowan, J. A. (1994). Desulfoviridin, a multimeric-dissimilatory sulfite reductase from *Desulfovibrio vulgaris* (Hildenborough) Purification, characterization, kinetics and EPR studies. *Eur J Biochem* **223**: 79-89.

van Wonderen, J. H., Burlat, B., Richardson, D. J., Cheesman, M. R. and Butt, J. N. (2008). The nitric oxide reductase activity of cytochrome *c* nitrite reductase from *Escherichia coli*. *J Biol Chem* **283**: 9587-9594.

Wyckoff, E. E., Schmitt, M., Wilks, A. and Payne, S. M. (2004). HutZ is required for efficient heme utilization in *Vibrio cholerae*. *J Bacteriol* **186**: 4142-4151.

Wyckoff, E. E., Mey, A. R. and Payne, S. M. (2007). Iron acquisition in *Vibrio cholerae*. *Biometals* **20**: 405-416.

Yang, W., Ni, L. and Somerville, R. L. (1993). A stationary-phase protein of *Escherichia coli* that affects the mode of association between the trp repressor protein and operator-bearing DNA. *Proc Natl Acad Sci* **90**: 5796-5800.

Yong, P., Rowson, N. A., Farr, J. P. G., Harris, L. R. and Macaskie, L. E. (2003). A novel electrobiotechnology for the recovery of precious metals from spent automotive catalysts. *Environ Tech* **24**: 289-297.

Youn, H., Kerby, R. L., Conrad, M. and Roberts, G. P. (2006). Study of highly constitutively active mutants suggests how cAMP activates cAMP receptor protein. *J Biol Chem* **281**: 1119-1127.

Yu, Z., Lansdon, E. B., Segel, I. H. and Fisher, A. J. (2007). Crystal structure of the bifunctional ATP sulfurylase-APS kinase from the chemolithotrophic thermophile *Aquifex aeolicus*. *J Mol Biol* **365**: 732-743.

Yurkiw, M. A., Voordouw, J. and Voordouw, G. (2012). Contribution of rubredoxin: oxygen oxidoreductases and hybrid cluster proteins of *Desulfovibrio vulgaris* Hildenborough to survival under oxygen and nitrite stress. *Environ Microbiol* **14**: 2711-2725.

Zane, G. M., Yen, H. C. B. and Wall, J. D. (2010). Effect of the deletion of *qmoABC* and the promoter-distal gene encoding a hypothetical protein on sulfate reduction in *Desulfovibrio vulgaris* Hildenborough. *Appl Environ Microb* **76**: 5500-5509.

Zhang, W., Culley, D. E., Wu, G. and Brockman, F. J. (2006). Two-component signal transduction systems of *Desulfovibrio vulgaris*: structural and phylogenetic analysis and deduction of putative cognate pairs. *J Mol Evol* **62**: 473-487.

Zheng, C. Y., Ma, G. and Su, Z. (2007). Native PAGE eliminates the problem of PEG–SDS interaction in SDS-PAGE and provides an alternative to HPLC in characterization of protein PEGylation. *Electrophoresis* **28**: 2801-2807.

Zhou, A., Chen, Y. I., Zane, G. M., He, Z., Hemme, C. L., Joachimiak, M. P., Baumohl, J. K. and Zhou, J. (2012). Functional characterization of Crp/Fnr-type global transcriptional regulators in *Desulfovibrio vulgaris* Hildenborough. *Appl Environ Microb* **78**: 1168-1177.

Zhou, J., He, Q., Hemme, C. L., Mukhopadhyay, A., Hillesland, K., Zhou, A., He, Z., Nostrand, J. D. V., Hazen, T. C., Stahl, D. A., Wall, J. D. and Arkin, A. P. (2011). How sulphate-reducing microorganisms cope with stress: lessons from systems biology. *Nat Rev Microbiol* **9**: 452-466.

Zhou, Y., Zhang, X. and Ebright, R. H. (1993). Identification of the activating region of catabolite gene activator protein (CAP): isolation and characterization of mutants of CAP specifically defective in transcription activation. *Proc Natl Acad Sci* **90**: 6081-6085.

Zhou, Y., Merkel, T. J. and Ebright, R. H. (1994). Characterization of the activating region of *Escherichia coli* catabolite gene activator protein (CAP) II. Role at class I and class II CAP-dependent promoters. *J Mol Biol* **243**: 603-610.

Zinoni, F., Beier, A., Pecher, A., Wirth, R. and Böck, A. (1984). Regulation of the synthesis of hydrogenase (formate hydrogen-lyase linked) of *E. coli*. *Arch Microbiol* **139**: 299-304.

Zumft, W. G. (1997). Cell biology and molecular basis of denitrification. *Microbiol Mol Biol Rev* **61**: 533-616.